Studies of ionic liquid modified materials for adsorption of organic pollutants from aqueous media

by

Isiaka Ayobamidele Lawal

Submitted in fulfilment of the academic requirements of

Doctor of Philosophy

in Chemistry

School of Chemistry and Physics

College of Agriculture, Engineering and Science

University of KwaZulu-Natal

Westville

South Africa

(December, 2015)

PREFACE

The research contained in this thesis was completed by the candidate while based in the Discipline of Chemistry, School of Chemistry and Physics of the College of Agriculture, Engineering and Science, University of KwaZulu-Natal, Westville, South Africa.

The contents of this work have not been submitted in any form to another university and, except where the work of others is acknowledged in the text, the results reported are due to investigations by the candidate.

_____

Signed: **Dr Brenda Moodley**

Date:

DECLARATION 1: PLAGIARISM

I, **Isiaka Ayobamidele**, **Lawal** declare that:

1. the research reported in this dissertation, except where otherwise indicated or acknowledged, is my original work;

2. this dissertation has not been submitted in full or in part for any degree or examination to any other university;

3. this dissertation does not contain other persons' data, pictures, graphs or other information, unless specifically acknowledged as being sourced from other persons;

4. this dissertation does not contain other persons' writing, unless specifically acknowledged as being sourced from other researchers. Where other written sources have been quoted, then:

   a. their words have been re-written but the general information attributed to them has been referenced;

   b. where their exact words have been used, their writing has been placed inside quotation marks, and referenced;

5. where I have used material for which publications followed, I have indicated in detail my role in the work;

6. this dissertation is primarily a collection of material, prepared by myself, published as journal articles or presented as a poster and oral presentations at conferences. In some cases, additional material has been included;

7. this dissertation does not contain text, graphics or tables copied and pasted from the Internet, unless specifically acknowledged, and the source being detailed in the dissertation and in the References sections.

_____

Signed: **Isiaka Ayobamidele Lawal**

Date:

DECLARATION 2: PUBLICATIONS

My role in each paper and presentation is indicated. The * indicates corresponding author.

Chapter 4

Isiaka A. Lawal and Brenda Moodley* **Synthesis, characterisation and application of imidazolium based long chain ionic liquid modified montmorillonite sorbents for the removal of amaranth dye** *(published –RSC Advances 2015,5,6191. DOI: 10.1039/c5ra09483f)*

My contribution: I synthesized, characterized, executed the experiments to investigate the adsorption behaviour of the material, and I wrote the article. These were done under the supervision of my supervisor.

Chapter 5

Isiaka A. Lawal and Brenda Moodley* **Column, kinetic and isotherm studies of PAH (phenanthrene) and dye (acid red) on kaolin modified with 1-hexyl, 3-decahexyl imidazolium ionic liquid** *Manuscript ready for submission*

My contribution: I designed the experiments and wrote the manuscript under the guidance of my supervisor.

Chapter 6

Isiaka A. Lawal and Brenda Moodley* **Kinetics, isotherm and sorption studies of emerging contaminant (pharmaceuticals) on ionic liquid modified montmorillonite** *Manuscript ready for submission*

My contribution: This work was designed and executed by me and I wrote the manuscript under the guidance of my supervisor.

Chapter 7

Isiaka A. Lawal, Darren Chetty and Brenda Moodley* **Sorption of Congo red and reactive blue on peanut shell and activated carbon derived from peanut shell modified by ionic liquid** *Manuscript ready for submission*

My contribution: This work was done in collaboration with Darren Chetty (Hons. student), I wrote the proposal, designed the work, synthesized the ionic liquid, and actively participated in the adsorption experiments under the guidance of my supervisor.

Chapter 8

Isiaka A. Lawal, and Brenda Moodley* **Sorption of personal care products from aqueous medium on raw *kigelia pinnata* and *kigelia pinnata* modified with ionic liquid** *Manuscript ready for submission*

My contribution: The experiment was done by me under the guidance of my supervisor.

_____

Signed: **Isiaka A. Lawal**

Date:

LIST OF PUBLICATIONS

1. <u>Isiaka A. Lawal</u> and Brenda Moodley* **Synthesis, characterisation and application of imidazolium based long chain ionic liquid modified montmorillonite sorbents for the removal of amaranth dye** *(published – RSC Advances 2015, 5,6191. DOI: 10.1039/c5ra09483f)*

2. <u>Isiaka A. Lawal</u> and Brenda Moodley[a]* **Column, kinetic and isotherm studies of PAH (phenanthrene) and dye (acid red) on kaolin modified with 1-hexyl, 3-decahexyl imidazolium ionic liquid** *Manuscript ready for submission*

3. <u>Isiaka A. Lawal</u> and Brenda Moodley[a]* **Kinetics, isotherm and sorption studies of emerging contaminant (pharmaceuticals) on ionic liquid modified montmorillonite** *Manuscript ready for submission*

4. <u>Isiaka A. Lawal</u>, Darrel Chetty and Brenda Moodley[a]* **Sorption of Congo red and reactive blue on peanut shell and activated carbon derived from peanut shell modified by ionic liquid** *Manuscript ready for submission*

5. <u>Isiaka A. Lawal</u>, and Brenda Moodley[a]* **Sorption of personal care products from aqueous medium on raw *kigelia pinnata* and *kigelia pinnata* modified with ionic liquid** *Manuscript ready for submission*

CONFERENCE PARTICIPATION

1. <u>Isiaka A. Lawal</u>, and Brenda Moodley **Column, kinetic and isotherm studies of PAH (phenanthrene) and dye (acid red) on kaolin modified with 1-hexyl, 3-decahexyl** (Poster presented at the 5th International Colloids Conference, 21st - 24th 2015,– Amsterdam).

2. <u>Isiaka A. Lawal</u>, and Brenda Moodley **Synthesis, characterisation and application of ionic liquid modified kaolin sorbent for column and batch adsorption of PAH (phenanthrene) and dye (acid red)** (Poster presented at the College of Agriculture, Engineering and Science research day, 22nd September 2015, Pietermaritzburg Campus UKZN).

3. <u>Isiaka A. Lawal</u>, and Brenda Moodley **Kinetics, isotherm and sorption studies of emerging contaminant (pharmaceuticals) on ionic liquid modified montmorillonite** (Oral presented at the 42nd National Convention of the South African Chemical Institute 29th November – 4th December 2015).

LIST OF ABBREVIATIONS

Full name	Abbreviations
Acid red	ARD
Activated carbon	AC
Activated carbon modified with ionic liquid	ILAC
Ampicillin	AMP
Brunauer−Emmett−Teller	BET
Cation exchange capacity	CEC
Cetrimonium bromide	CTAB
Chloramphenicol	CHL
Congo red	CR
Critical micelle concentration	CMC
Diclofenac	DCL
Dimethyl sulphuroxide	DMSO
Energy dispersive X-ray analyzer	EDX
Fourier transform infrared	FT-IR
Gram molecular weight	GMW
High-pressure liquid chromatography	HPLC
High-resolution mass spectroscopy	HR-MS
Ibuprofen	IBU
Ionic liquid	IL
Kaolin	K
Kaolin modified with ionic liquid	K-IL
Ketoprofen	KET
Kigelia pinnata	*KP*
Kigelia pinnata modified with ionic liquid	KP–IL
Montmorillonite	Mt
Montmorillonite modified with ionic liquid	Mt–IL
Nalidixic acid	NAD

Nuclear magnetic resonance	NMR
Pharmaceuticals Personal care products	PPCPs
Phenanthrene	PHN
Polyaromatic hydrocarbons	PAHs
Potassium hydroxide	KOH
Peanut shell	NS
Peanut shell modified with ionic liquid	ILNS
Reactive Blue 4	RB
Scanning electron microscopy	SEM
Sodium dodecylsulfate	SDS
Sodium modify with ionic liquid montmorillonite	Na^+–Mt
Sulfamethoxazole	SMZ
Tetracycline	TC
Thermal gravimetric analysis and differential thermal	TGA/DCS
Ultra-Violent −Visible	UV−Vis
X-ray diffraction	XRD

ABSTRACT

Adsorption has been one of the most used methods for the removal of organic pollutants from wastewater owing to its low economic costs, availability and simplicity in application. Different surfactants have however been used for the modification of these materials to improve their adsorptive capacities. Ionic liquids (IL) have recently been considered as a replacement of many surfactants due to its environmentally friendly properties. The aim of this study was to synthesize new ILs that could be used as a replacement for known surfactants in the area of material modification and application for removal of organic pollutants from aqueous media. Two new ILs (1-methyl, 3-decahexyl imidazolium and 1-hexyl, 3-decahexyl) were synthesised, and characterised by various instrumental techniques. The ILs were thereafter used to modify different types of materials which included: clay (montmorillonite (Mt) and kaolin (K)), biomass (peanut shell (NS) and *kigelia pinnata* (KP) plant species, and activated carbon derived from peanut shell (AC)). Instrumental and titrimetric standard techniques were used to characterise the unmodified and modified materials. The different modified materials were used in batch and column adsorption studies, for different organic pollutants. These pollutants include pharmaceuticals (tetracycline (TC), sulfamethoxazole (SMZ), nalidixic acid (NAD), chloramphenicol (CHL), ibuprofen (IBU), ketoprofen (KET), ampicillin (AMP), and diclofenac (DCL)), dyes (amaranth, acid red (AR), congo red (CR) and reactive blue (RB)) and polyaromatic hydrocarbon (phenanthrene). Ionic liquid (1-methyl, 3-decahexyl imidazolium) was used to modify montmorillonite (Mt-IL), and was used for the adsorption of amaranth dye. Pseudo-second-order kinetics and the Langmuir adsorption isotherm best described the adsorption process, with a maximum adsorption capacity (q_e) of 263.2 mg g^{-1} at pH 2. Adsorption studies of Mt-IL with TC, SMZ, NAD and CHL showed q_e values of 765.7, 504.1, 150.3 and 30.9 mg g^{-1} respectively and an optimum pH of between 3 and 10. Kaolin intercalated with 1-hexyl, 3-decahexyl (K-IL) was also studied and used for both column and batch adsorption studies of phenanthrene and AR. The q_e of phenanthrene and AR on K-IL were 188.9 and 842.7 mg g^{-1}. The q_e for column studies at the same flow rate and different concentrations (50, 100, 200 mg L^{-1}) for phenanthrene were 222.9, 611.8 and 1093.5 mg g^{-1}, while AR were 877.0, 1337.4 and 1350.7 mg g^{-1}. IL (1-methyl, 3-decahexyl imidazolium) was used in the modification of NS (ILNS) and AC (IL-AC) and were used in the adsorption of CR and RB. ILNS and IL-AC had q_e values of 136.4 and 150.0 mg g^{-1} for CR and 290.0 and 364.4 mg g^{-1} for RB respectively. Adsorption was pH dependant, with optimum

adsorption of CR and RB onto ILAC at pH 1 – 6, while CR and RB onto ILNS was optimum at pH 7 – 9. Adsorption of pharmaceuticals on 1-methyl, 3-decahexyl imidazolium modified kigelia pinnata (IL-KP) was studied. Optimum adsorption was obtained at pH 2.5 for AMP and pH 5 for IBU, KET and DCL. The values for q_e were 251.2, 197.1, 276.8 and 73 mg g^{-1} for KET, DCL, IBU and AMP respectively. The q_e of all the materials investigated were higher compared with the corresponding unmodified materials as well as some materials modified with other surfactants as reported in literature. The use of IL modified adsorbents has potential for the adsorption of organic pollutants from aqueous media.

ACKNOWLEDGMENTS

I also appreciate my research colleagues and friends, Adebola, Samson, Oluwaseun, Imrana, Habeebah, Gbadebo, Tracey, Emmanuel, Ekemena, Zainab, Oluleye, Tomi, Dr. Abafe, Osadolor, Akpan, and others who in a way contributed to the successful completion of the program.

TABLE OF CONTENTS

LIST OF TABLES

LIST OF FIGURES

CHAPTER 1: INTRODUCTION

1.1 BACKGROUND

Environmental issues such as climate change, carbon emission, green environment and organic pollutants e.g. dyes, pharmaceuticals, polycyclic aromatic hydrocarbons and other harmful pollutants have, in recent times, received increasing global attention. Water is fundamental to the existence of all living creatures, and contamination of water bodies with organic chemicals remains a pervasive risk. High concentrations of organic wastes which include industrial chemicals, pesticides, dyes, polycyclic aromatic hydrocarbons and pharmaceuticals, are discharged, either intentionally or unintentionally, on a daily basis into water ways, leading to accumulation of these contaminants in the aquatic environment (Luo et al., 2011; Kümmerer, 2009). Most of these organic pollutants are man-made chemicals and are found in ecosystems globally far away from point of manufacture (Ericson Jogsten et al., 2012). These pollutants have been shown to have many adverse health effects on living organisms, hence for remediation of polluted water.

Dyes are discharged into water bodies through several industrial usages. They are also an integral part of many manufacturing processes sources include, leather tanning (Kabdaşli et al., 1999), textile (Sokolowska-Gajda et al., 1996), printing and dye, food processing, plastics, cosmetics, rubber (Bensalah et al., 2009; Wróbel et al., 2001; Dawood et al., 2014) and the paper and pulp industry (Ivanov et al., 1996). Dyes have been reported to be a source of chemical pollution and have been listed in Annex C of the Stockholm Convention along with polychlorinated dibenzo-*p*-dioxins (PCDD) and polychlorinated dibenzofurans (PCDF) (Salthammer et al., 1995; Halling-Sørensen et al., 1998). Dyes are highly coloured compounds which are visible even at very low concentrations (Banat et al., 1996; Mittal and Gupta, 1996; Fu and Viraraghavan, 2001; Chu and Chen, 2002; Clarke and Anliker, 1980). They are generally complex in nature, carcinogenic, mutagenic and cause kidney dysfunction; may affect the reproductive system, cause damage to the liver, brain and the central nervous system (Kadirvelu et al., 2003; Mishra and Tripathy, 1993; Banat et al., 1996; Clarke and Anliker, 1980). Aquatic organisms are generally the first line of exposure to dyes in the environment and they are affected by the dyes ability to prevent light

penetrating to the bottom of the sea or river bed. In addition, the metals or aromatic components of the dye can also have negative effects on some aquatic life (Yagub et al., 2014).

Pharmaceutical compounds are used globally in medical service deliveries, human healthcare and in livestock rearing as veterinary drugs in treating animals. Over 3,000 compounds have been approved as constituents of pharmaceuticals and medicinal products (Löffler and Ternes, 2003). The presence of pharmaceuticals in the environment has recently drawn much attention due to an increase in its reported toxicity (Murray et al., 2010; Xie and Ebinghaus, 2008). Pharmaceuticals and other personal care products have been categorised as part of emerging organic contaminants (EOCs), because they have not been classified as risk prone compounds. Some of their potential adverse effects are resistance to antibiotics, sterility, and feminization of aquatic animals, as well as drug resistance of pathogenic organisms amongst others (Carucci et al., 2006; Bolong et al., 2009; Schriks et al., 2010).

There has also been global concern about polycyclic aromatic hydrocarbons, PAHs. The US EPA has listed some PAHs as priority pollutants, some of which are suspected to be possible human carcinogens (Van Metre et al., 2006). Their detection in the environment and potential risks to human health have been the focus of much attention (Registry, 1995). PAHs find their way into the environment through atmospheric fallout, urban run-off, municipal effluents, industrial effluents, and oil spillage or leakage (Manoli and Samara, 1999).

Due to the toxicity and the risk of the presence of these organic pollutants (dyes, pharmaceuticals and PAHs), frantic efforts have been made by the global scientific community to remove these harmful pollutants from the environment. Several methods have been used in the removal of these pollutants from water-bodies. They include chemical treatment (coagulating and flocculating agents) (Shi et al., 2007; Zhou et al., 2008; Mishra et al., 2006; Mishra and Bajpai, 2006; Hai et al., 2007; Wang et al., 2007; Yue et al., 2008), oxidation (Gupta et al., 2007; Lin and Peng, 1994; Doğan and Türkdemir, 2005; Faouzi et al., 2007; Lopes et al., 2004), and ultrasonic irradiation. Photo degradation, coagulation, precipitation, biodegradation, membrane separation and adsorption (Crini and Badot, 2008; Peternel et al., 2007; Eckenfelder, 2000). Of all of these, adsorption is widely applied for the removal of organic compounds in wastewater due to its high

removal efficiencies, availability, relative cheapness and simplicity in application (Eckenfelder, 2000).

Activated carbon has been the most widely used adsorbent because of its high capacity for adsorption of heavy metals and organic pollutants. However, due to difficulties in regeneration and affordability, clays and biomasses are now being considered as alternative low cost adsorbents.

Studies showed that the adsorption capabilities of clays are due to a net negative charge on the silicate mineral which is neutralized by the adsorption of positively charged cations such as cationic dyes, heavy metals and some organic pollutants like phenyls or alkylphenyl groups. Another reason for the high adsorption capacity of clays is the large surface area which can be as high as 800 $m^2 g^{-1}$ (Boyd et al., 2001). These all enhance the adsorption process because the sorption mechanism of organics includes electrostatic attraction, and hydrophobic interaction (Zhou et al., 2010).

Generally clay has a lower affinity for hydrophobic organic compounds due to its hydrophilic surface (Hassett and Banwart, 1989). However, clays can be activated for hydrophobic sorption *via* simple ion exchange reactions using organic cations which convert it to organo-clays (Boyd et al., 1988; El-Nahhal et al., 1998). The adsorption of organic cations on clays (organo-clays) transforms the clay-mineral surface from hydrophilic to hydrophobic, thereby enhancing its affinity for neutral organic molecules of hydrophobic characteristics (Xu et al., 1997). When the loading of the organic cations exceeds the cation exchange capacity (CEC) of the clay, it becomes positively charged and potentially suitable for the adsorption of certain anions, such as triazolinones, sulfonylurea, aromatic carboxylic acids, humic acid or fulvic acid, antibiotics or their mixtures (Nir et al., 2006), nitrobenzene, phenol, and *m*-nitrophenol (Borisover et al., 2008). Organo-clays are powerful adsorbents of organic pollutants and are thus useful for the remediation of wastewater and are capable of removing oil and grease at 5–7 times the rate of activated carbon or at 50% of its dry weight (Alther, 1995). The adsorption of organic molecules (ionic and non-ionic) on organo-clays has been extensively studied (Theng, 1974; Boyd et al., 1988).

Biomasses are also currently used for biosorption processes of both organic and inorganic pollutants, and are able to replace conventional treatment methods of pollutants removal from aqueous solutions (Vijayaraghavan and Yun, 2008; Daneshvar et al., 2012). Bacteria, fungi, algae, byproducts of food, beverage or pharmaceutical production, are all examples of biomass that may be viable alternatives for the development of inexpensive adsorption processes (Reddad et al., 2002; Yun et al., 2001). Low sorption capacity has been the drawback of native biomass due its poor mechanical strength (Pagnanelli et al., 2000; Skowronski et al., 2001). Therefore researchers have improved the sorption capacity of these biomasses by modifying the surface of the biomass with surfactants.

Surfactants known to activate surfaces, do not exist in nature but are manufactured by chemical reactions (Aksu et al., 2010). Surfactants have both hydrophilic and hydrophobic components in one molecule and can be classified into four groups depending on the charge of the hydrophilic part: non-ionic (0), anionic (−), cationic (+) and zwitterionic (±) (Aksu et al., 2010). Researchers have reported an increase in sorption capacity after modification of biomass with different types of surfactants for the adsorption of both organic and inorganic pollutants (Bingol et al., 2009; Loukidou et al., 2003; Xi and Chen, 2014; Montazer-Rahmati et al., 2011; Li et al., 2010; Feng et al., 2011; Brandão et al., 2010; Ansari et al., 2012; Zhou et al., 2011; Ibrahim et al., 2010; Ibrahim et al., 2012; Zhou et al., 2012b; Zhou et al., 2012a; Akar et al., 2015; Aksu et al., 2010; Deng and Ting, 2005; Akar and Divriklioglu, 2010).

Ionic liquids (ILs) have attracted an increasing amount of interest, due to their low volatility, non-flammability, high chemical and thermal stabilities, high ionic conductivity and broad electrochemical windows (Zhang et al., 2006). Ionic liquids are low-melting-point salts, thus forming liquids that consist only of cations and anions. Ionic liquids are often considered as green solvents capable of replacing traditional organic solvents and have been extensively studied in materials chemistry, electrochemistry, and catalysis (Welton, 1999). IL's uniqueness is due to its constituents, where it has molecular ions as its building blocks. ILs (molten salts) are also known as liquids that are composed of only ions, either at room temperature or at elevated temperatures but below 100 °C (Shukla et al., 2011).

In this research ionic liquids (ILs) were synthesized and used to modify clays, biomasses and activated carbon from biomass for the adsorption of organic pollutants.

1.2 STATEMENT OF PROBLEM/JUSTIFICATION

The US EPA's Science Advisory Board suggested that pharmaceuticals, one of the classes of compounds regarded as emerging organic contaminants (EOC), are possible human carcinogens, liver toxicant and also exerts hormonal effects including alteration of thyroid hormone levels (Lau et al., 2007; Takagi et al., 2008). Likewise, PAHs and dyes have been reported to be possible human carcinogens as well (Van Metre et al., 2006).

Most developing countries import these organic pollutants either directly or as products made from them. Organic pollutant wastes are normally not disposed off in environmentally friendly ways. They are at most times dumped in waterways or open waste dumps without proper control. Furthermore, these organic pollutants often make their way into waterbodies *via* runoff and as leachates from dump sites which seep into ground water. This constitutes a very serious environmental pollution nuisance that jeopardizes the health of humans and other animals dwelling within the vicinities of these dumps.

There is also a global shortage of water which has led to a need for water recycling (Falkenmark et al., 1989). Recycled water must be rid of organic pollutants if it is to be considered safe for human consumption. If these pollutants are not removed by wastewater treatment plant processes and make their way back into rivers and lakes, as well as contaminate water sources, they will eventually lead to poor quality of drinking water. In addition, these pollutants may travel several thousands of miles away from the source posing a danger to populations that use the water directly without proper treatment. Efforts have been made within the scientific community to clean up these compounds from polluted water bodies, but the existing methods seem to be exorbitantly expensive. It has therefore become critically important to develop sustainable methods that can reduce the concentrations of these pollutants by removing them from polluted water. Therefore, this study aims to develop sorbents that are effective, cheap and readily able to adsorb organic pollutants from aqueous media.

1.3 HYPOTHESIS

Ionic liquids have the characteristic of a surfactant owing to their molecular arrangement (hydrophilic and hydrophobic) (Maclay, 1956). Ionic liquids are able to modify a specific type of clay, biomass and activated carbon from biomass, and can improve the adsorption capacities for some selected organic pollutants.

1.4 OBJECTIVES OF THE STUDY

The general aim of this research was to investigate the suitability of ionic liquid modified materials for adsorption of organic pollutants from aqueous media.
The specific objectives were:

(i)   To synthesize and characterize two ionic liquids (1-methyl, 3-decahexyl imidazolium and 1-hexyl, 3-decahexyl)

(ii)   To prepare and characterize ionic liquid modified sorbents - clays (montmorillonite and kaolin), biomass (*kigelia pinnata* and peanut shell) and activated carbon derived from peanut shell.

(iii)   To optimize the adsorption of organic pollutants, such as, pharmaceuticals (tetracycline (TC), sulfamethoxazole (SMZ), nalidixic acid (NAD), chloramphenicol (CHL), ibuprofen (IBU), ketoprofen (KET), ampicillin (AMP), and diclofenac (DCL)), dyes (amaranth, acid red (AR), congo red (CR) and reactive blue (RB)) and a polyaromatic hydrocarbon (phenanthrene) onto the sorbents by varying adsorbent dose, initial concentration, pH and temperature.

(iv)   To study the mechanism of adsorption based on existing models (Langmuir, Freundlich, Dubinin-Radushkevich, and Temkin models).

(v)   To use the Adams-Bohart, Yoon-Nelson model flow and Thomas sorption model to determine adsorption capacities.

1.5 REFERENCES

Akar, S. T., Yilmazer, D., Celik, S., Balk, Y. Y. & Akar, T. 2015. Effective biodecolorization potential of surface modified lignocellulosic industrial waste biomass. *Chemical Engineering Journal,* 259(1)**,** pp 286-292.

Akar, T. & Divriklioglu, M. 2010. Biosorption applications of modified fungal biomass for decolorization of Reactive Red 2 contaminated solutions: Batch and dynamic flow mode studies. *Bioresource Technology,* 101(19)**,** pp 7271-7277.

Aksu, Z., Ertuğrul, S. & Dönmez, G. 2010. Methylene Blue biosorption by Rhizopus arrhizus: Effect of SDS (sodium dodecylsulfate) surfactant on biosorption properties. *Chemical Engineering Journal,* 158(3)**,** pp 474-481.

Alther, G. R. 1995. Organically modified clay removes oil from water. *Waste Management,* 15(8)**,** pp 623-628.

Ansari, R., Seyghali, B., Mohammad-khah, A. & Zanjanchi, M. A. 2012. Application of Nano Surfactant Modified Biosorbent as an Efficient Adsorbent for Dye Removal. *Separation Science and Technology,* 47(12)**,** pp 1802-1812.

Banat, I. M., Nigam, P., Singh, D. & Marchant, R. 1996. Microbial decolorization of textile-dyecontaining effluents: A review. *Bioresource Technology,* 58(3)**,** pp 217-227.

Bensalah, N., Alfaro, M. Q. & Martínez-Huitle, C. 2009. Electrochemical treatment of synthetic wastewaters containing Alphazurine A dye. *Chemical Engineering Journal,* 149(1)**,** pp 348-352.

Bingol, A., Aslan, A. & Cakici, A. 2009. Biosorption of chromate anions from aqueous solution by a cationic surfactant-modified lichen (Cladonia rangiformis (L.)). *Journal of Hazardous Materials,* 161(2)**,** pp 747-752.

Bolong, N., Ismail, A., Salim, M. R. & Matsuura, T. 2009. A review of the effects of emerging contaminants in wastewater and options for their removal. *Desalination,* 239(1)**,** pp 229-246.

Borisover, M., Gerstl, Z., Burshtein, F., Yariv, S. & Mingelgrin, U. 2008. Organic Sorbate− Organoclay Interactions in Aqueous and Hydrophobic Environments: Sorbate− Water Competition. *Environmental Science & Technology,* 42(19)**,** pp 7201-7206.

Boyd, S. A., Mortland, M. M. & Chiou, C. T. 1988. Sorption characteristics of organic compounds on hexadecyltrimethylammonium-smectite. *Soil Science Society of America Journal,* 52(3)**,** pp 652-657.

Boyd, S. A., Sheng, G., Teppen, B. J. & Johnston, C. T. 2001. Mechanisms for the adsorption of substituted nitrobenzenes by smectite clays. *Environmental Science & Technology,* 35(21)**,** pp 4227-4234.

Brandão, P. C., Souza, T. C., Ferreira, C. A., Hori, C. E. & Romanielo, L. L. 2010. Removal of petroleum hydrocarbons from aqueous solution using sugarcane bagasse as adsorbent. *Journal of Hazardous Materials,* 175(1–3)**,** pp 1106-1112.

Carucci, A., Cappai, G. & Piredda, M. 2006. Biodegradability and toxicity of pharmaceuticals in biological wastewater treatment plants. *Journal of Environmental Science and Health Part A,* 41(9)**,** pp 1831-1842.

Chu, H. C. & Chen, K. M. 2002. Reuse of activated sludge biomass: I. Removal of basic dyes from wastewater by biomass. *Process Biochemistry,* 37(6)**,** pp 595-600.

Clarke, E. A. & Anliker, R. 1980. Organic Dyes and Pigments. *Anthropogenic Compounds.* Switzerland: Springer Berlin Heidelberg.

Crini, G. & Badot, P.-M. 2008. Application of chitosan, a natural aminopolysaccharide, for dye removal from aqueous solutions by adsorption processes using batch studies: A review of recent literature. *Progress in Polymer Science,* 33(4)**,** pp 399-447.

Daneshvar, E., Kousha, M., Sohrabi, M. S., Khataee, A. & Converti, A. 2012. Biosorption of three acid dyes by the brown macroalga Stoechospermum marginatum: Isotherm, kinetic and thermodynamic studies. *Chemical Engineering Journal,* 195(1)**,** pp 297-306.

Dawood, S., Sen, T. K. & Phan, C. 2014. Synthesis and characterisation of novel-activated carbon from waste biomass pine cone and its application in the removal of congo red dye from aqueous solution by adsorption. *Water, Air, & Soil Pollution,* 225(1)**,** pp 1-16.

Deng, S. & Ting, Y.-P. 2005. Characterization of PEI-modified biomass and biosorption of Cu(II), Pb(II) and Ni(II). *Water Research,* 39(10)**,** pp 2167-2177.

Doğan, D. & Türkdemir, H. 2005. Electrochemical oxidation of textile dye indigo. *Journal of Chemical Technology and Biotechnology,* 80(8)**,** pp 916-923.

Eckenfelder, W. W. 2000. *Industrial Water Pollution Control*, third ed., New York: McGraw-Hill.

El-Nahhal, Y., Nir, S., Polubesova, T., Margulies, L. & Rubin, B. 1998. Leaching, phytotoxicity, and weed control of new formulations of alachlor. *Journal of Agricultural and Food Chemistry,* 46(8)**,** pp 3305-3313.

Ericson Jogsten, I., Nadal, M., van Bavel, B., Lindström, G. & Domingo, J. L. 2012. Per- and polyfluorinated compounds (PFCs) in house dust and indoor air in Catalonia, Spain: Implications for human exposure. *Environment International,* 39(1)**,** pp 172-180.

Falkenmark, M., Lundqvist, J. & Widstrand, C. Macro-scale water scarcity requires micro-scale approaches. Natural resources forum, 1989. Blackwell Publishing Ltd, 258-267.

Faouzi, A. M., Nasr, B. & Abdellatif, G. 2007. Electrochemical degradation of anthraquinone dye Alizarin Red S by anodic oxidation on boron-doped diamond. *Dyes and Pigments,* 73(1)**,** pp 86-89.

Feng, N., Guo, X., Liang, S., Zhu, Y. & Liu, J. 2011. Biosorption of heavy metals from aqueous solutions by chemically modified orange peel. *Journal of Hazardous Materials,* 185(1)**,** pp 49-54.

Fu, Y. & Viraraghavan, T. 2001. Fungal decolorization of dye wastewaters: a review. *Bioresource Technology,* 79(3)**,** pp 251-262.

Gupta, V. K., Jain, R. & Varshney, S. 2007. Electrochemical removal of the hazardous dye Reactofix Red 3 BFN from industrial effluents. *Journal of Colloid and Interface Science,* 312(2)**,** pp 292-296.

Hai, F. I., Yamamoto, K. & Fukushi, K. 2007. Hybrid treatment systems for dye wastewater. *Critical Reviews in Environmental Science and Technology,* 37(4)**,** pp 315-377.

Halling-Sørensen, B., Nielsen, S. N., Lanzky, P., Ingerslev, F., Lützhøft, H. H. & Jørgensen, S. 1998. Occurrence, fate and effects of pharmaceutical substances in the environment-A review. *Chemosphere,* 36(2)**,** pp 357-393.

Ibrahim, S., Ang, H.-M. & Wang, S. 2012. Adsorptive separation of emulsified oil in wastewater using biosorbents. *Asia-Pacific Journal of Chemical Engineering,* 7(2)**,** pp S216-S221.

Ibrahim, S., Wang, S. & Ang, H. M. 2010. Removal of emulsified oil from oily wastewater using agricultural waste barley straw. *Biochemical Engineering Journal,* 49(1)**,** pp 78-83.

Ivanov, K., Gruber, E., Schempp, W. & Kirov, D. 1996. Possibilities of using zeolite as filler and carrier for dyestuffs in paper. *Papier,* 50(7-8)**,** pp 456-&.

J.J. Hassett & L.W. Banwart 1989. Front Matter. *In:* Sawhney, B. L. & Brown, K. (eds.) *Reactions and Movement of Organic Chemicals in Soils.* Soil Science Society of America and American Society of Agronomy.

Kabdaşli, I., Tünay, O. & Orhon, D. 1999. Wastewater control and management in a leather tanning district. *Water Science and Technology,* 40(1)**,** pp 261-267.

Kadirvelu, K., Kavipriya, M., Karthika, C., Radhika, M., Vennilamani, N. & Pattabhi, S. 2003. Utilization of various agricultural wastes for activated carbon preparation and application for the removal of dyes and metal ions from aqueous solutions. *Bioresource Technology,* 87(1)**,** pp 129-132.

Kümmerer, K. 2009. Antibiotics in the aquatic environment – A review – Part I. *Chemosphere,* 75(4)**,** pp 417-434.

Lau, C., Anitole, K., Hodes, C., Lai, D., Pfahles-Hutchens, A. & Seed, J. 2007. Perfluoroalkyl acids: a review of monitoring and toxicological findings. *Toxicological Sciences,* 99(2)**,** pp 366-394.

Li, Y., Chen, B. & Zhu, L. 2010. Enhanced sorption of polycyclic aromatic hydrocarbons from aqueous solution by modified pine bark. *Bioresource Technology,* 101(19)**,** pp 7307-7313.

Lin, S. H. & Peng, C. F. 1994. Treatment of textile wastewater by electrochemical method. *Water Research,* 28(2)**,** pp 277-282.

Löffler, D. & Ternes, T. A. 2003. Determination of acidic pharmaceuticals, antibiotics and ivermectin in river sediment using liquid chromatography–tandem mass spectrometry. *Journal of Chromatography A,* 1021(1)**,** pp 133-144.

Lopes, A., Martins, S., Morao, A., Magrinho, M. & Gonçalves, I. 2004. Degradation of a textile dye CI Direct Red 80 by electrochemical processes. *Portugaliae Electrochimica Acta,* 22(3)**,** pp 279-294.

Loukidou, M. X., Matis, K. A., Zouboulis, A. I. & Liakopoulou-Kyriakidou, M. 2003. Removal of As (V) from wastewaters by chemically modified fungal biomass. *Water Research,* 37(18)**,** pp 4544-4552.

Luo, Y., Xu, L., Rysz, M., Wang, Y., Zhang, H. & Alvarez, P. J. 2011. Occurrence and transport of tetracycline, sulfonamide, quinolone, and macrolide antibiotics in the Haihe River Basin, China. *Environmental Science & Technology,* 45(5)**,** pp 1827-1833.

Maclay, W. N. 1956. Factors affecting the solubility of nonionic emulsifiers. *Journal of Colloid Science,* 11(3)**,** pp 272-285.

Manoli, E. & Samara, C. 1999. Polycyclic aromatic hydrocarbons in natural waters: sources, occurrence and analysis. *TrAC Trends in Analytical Chemistry,* 18(6)**,** pp 417-428.

Mishra, A. & Bajpai, M. 2006. The flocculation performance of Tamarindus mucilage in relation to removal of vat and direct dyes. *Bioresource Technology,* 97(8)**,** pp 1055-1059.

Mishra, A., Bajpai, M. & Pandey, S. 2006. Removal of dyes by biodegradable flocculants: a lab scale investigation. *Separation Science and Technology,* 41(3)**,** pp 583-593.

Mishra, G. & Tripathy, M. 1993. A critical review of the treatments for decolourization of textile effluent. *Colourage,* 40(35-35.

Mittal, A. K. & Gupta, S. K. 1996. Biosorption of cationic dyes by dead macro fungus Fomitopsis carnea: Batch studies. *Water Science and Technology,* 34(10)**,** pp 81-87.

Montazer-Rahmati, M. M., Rabbani, P., Abdolali, A. & Keshtkar, A. R. 2011. Kinetics and equilibrium studies on biosorption of cadmium, lead, and nickel ions from aqueous solutions by intact and chemically modified brown algae. *Journal of Hazardous Materials,* 185(1)**,** pp 401-407.

Murray, K. E., Thomas, S. M. & Bodour, A. A. 2010. Prioritizing research for trace pollutants and emerging contaminants in the freshwater environment. *Environmental Pollution,* 158(12)**,** pp 3462-3471.

Nir, S., Rubin, B., Mishael, Y. G., Zadaka, D., Polubesova, T., Wakshal, E. & Rabinovitz, O. 2006. *Removal Of Organic Pollutants From Contaminated Water*. WO 2006/077583 A1, USA patent application.

Pagnanelli, F., Petrangeli Papini, M., Toro, L., Trifoni, M. & Veglio, F. 2000. Biosorption of metal ions on Arthrobacter sp.: biomass characterization and biosorption modeling. *Environmental Science & Technology,* 34(13)**,** pp 2773-2778.

Peternel, I. T., Koprivanac, N., Božić, A. M. L. & Kušić, H. M. 2007. Comparative study of UV/TiO2, UV/ZnO and photo-Fenton processes for the organic reactive dye degradation in aqueous solution. *Journal of Hazardous Materials,* 148(1–2)**,** pp 477-484.

Reddad, Z., Gerente, C., Andres, Y. & Le Cloirec, P. 2002. Adsorption of several metal ions onto a low-cost biosorbent: kinetic and equilibrium studies. *Environmental Science & Technology,* 36(9)**,** pp 2067-2073.

Registry, A. f. T. S. a. D., 1995. Toxicological profile for Polycyclic Aromatic Hydrocarbons (PAHs), Registry, A. f. T. S. a. D.

Salthammer, T., Klipp, H., Peek, R. D. & Marutzky, R. 1995. Formation of polychlorinated dibenzo-p-dioxins (PCDD) and polychlorinated dibenzofurans (PCDF) during the combustion of impregnated wood. *Chemosphere,* 30(11)**,** pp 2051-2060.

Schriks, M., Heringa, M. B., van der Kooi, M. M., de Voogt, P. & van Wezel, A. P. 2010. Toxicological relevance of emerging contaminants for drinking water quality. *Water Research,* 44(2)**,** pp 461-476.

Shi, B., Li, G., Wang, D., Feng, C. & Tang, H. 2007. Removal of direct dyes by coagulation: The performance of preformed polymeric aluminum species. *Journal of Hazardous Materials,* 143(1)**,** pp 567-574.

Shukla, M., Srivastava, N. & Saha, S. 2011. *Interactions and transitions in imidazolium cation based ionic liquids*, India: Intech Open Access Publisher.

Skowronski, T., Pirszel, J. & Pawlik-Skowronska, B. 2001. Heavy metal removal by the waste biomass of Penicillium chrysogenum. *Water Quality Research Journal of Canada,* 36(4)**,** pp 793-803.

Sokolowska-Gajda, J., Freeman, H. S. & Reife, A. 1996. Synthetic dyes based on environmental considerations. Part 2: Iron complexes formazan dyes. *Dyes and Pigments,* 30(1)**,** pp 1-20.

Takagi, S., Adachi, F., Miyano, K., Koizumi, Y., Tanaka, H., Mimura, M., Watanabe, I., Tanabe, S. & Kannan, K. 2008. Perfluorooctanesulfonate and perfluorooctanoate in raw and treated tap water from Osaka, Japan. *Chemosphere,* 72(10)**,** pp 1409.

Theng, B. K. 1974. *The chemistry of clay-organic reactions*, London: Adam Hilger Ltd., Rank Precision Industries.

Van Metre, P., Mahler, B. J., Scoggins, M. & Hamilton, P. A. 2006. *Parking lot sealcoat: A major source of polycyclic aromatic hydrocarbons (pahs) in urban and suburban environments*, US Department of the Interior, US Geological Survey.

Vijayaraghavan, K. & Yun, Y.-S. 2008. Bacterial biosorbents and biosorption. *Biotechnology Advances,* 26(3)**,** pp 266-291.

Wang, J.-P., Chen, Y.-Z., Ge, X.-W. & Yu, H.-Q. 2007. Optimization of coagulation–flocculation process for a paper-recycling wastewater treatment using response surface methodology. *Colloids and Surfaces A: Physicochemical and Engineering Aspects,* 302(1)**,** pp 204-210.

Welton, T. 1999. Room-temperature ionic liquids. Solvents for synthesis and catalysis. *Chemical Reviews,* 99(2)**,** pp 2071-2084.

Wróbel, D., Boguta, A. & Ion, R. M. 2001. Mixtures of synthetic organic dyes in a photoelectrochemical cell. *Journal of Photochemistry and Photobiology A: Chemistry,* 138(1)**,** pp 7-22.

Xi, Z. & Chen, B. 2014. Removal of polycyclic aromatic hydrocarbons from aqueous solution by raw and modified plant residue materials as biosorbents. *Journal of Environmental Sciences,* 26(4)**,** pp 737-748.

Xie, Z. & Ebinghaus, R. 2008. Analytical methods for the determination of emerging organic contaminants in the atmosphere. *Analytica Chimica Acta,* 610(2)**,** pp 156-178.

Xu, S., Sheng, G. & Boyd, S. A. 1997. Use of organoclays in pollution abatement. *Advances in Agronomy,* 59(1)**,** pp 25-62.

Yagub, M. T., Sen, T. K., Afroze, S. & Ang, H. M. 2014. Dye and its removal from aqueous solution by adsorption: A review. *Advances in Colloid and Interface Science,* 209(1)**,** pp 172-184.

Yue, Q., Gao, B., Wang, Y., Zhang, H., Sun, X., Wang, S. & Gu, R. R. 2008. Synthesis of polyamine flocculants and their potential use in treating dye wastewater. *Journal of Hazardous Materials,* 152(1)**,** pp 221-227.

Yun, Y.-S., Park, D., Park, J. M. & Volesky, B. 2001. Biosorption of trivalent chromium on the brown seaweed biomass. *Environmental Science & Technology,* 35(21)**,** pp 4353-4358.

Zhang, Y., Shen, Y., Yuan, J., Han, D., Wang, Z., Zhang, Q. & Niu, L. 2006. Design and Synthesis of Multifunctional Materials Based on an Ionic-Liquid Backbone. *Angewandte Chemie International Edition,* 45(35)**,** pp 5867 –5870.

Zhou, Q., Deng, S., Zhang, Q., Fan, Q., Huang, J. & Yu, G. 2010. Sorption of perfluorooctane sulfonate and perfluorooctanoate on activated sludge. *Chemosphere,* 81(4)**,** pp 453-458.

Zhou, Y., Chen, L., Lu, P., Tang, X. & Lu, J. 2011. Removal of bisphenol A from aqueous solution using modified fibric peat as a novel biosorbent. *Separation and Purification Technology,* 81(2)**,** pp 184-190.

Zhou, Y., Chen, L., Wang, X., Xu, Y. & Lu, J. 2012a. Adsorption of phenanthrene by quaternary ammonium surfactant modified peat and the mechanism involved. *Water Science & Technology,* 66(4)**,** pp 810-815.

Zhou, Y., Liang, Z. & Wang, Y. 2008. Decolorization and COD removal of secondary yeast wastewater effluents by coagulation using aluminum sulfate. *Desalination,* 225(1)**,** pp 301-311.

Zhou, Y., Lu, P. & Lu, J. 2012b. Application of natural biosorbent and modified peat for bisphenol a removal from aqueous solutions. *Carbohydrate Polymers,* 88(2)**,** pp 502-508.

CHAPTER 2: LITERATURE REVIEW

2.1 INTRODUCTION

Adsorption has been reported as one of the most viable means for removal of pollutants in virtually all known matrices such as drying air, water treatment, air purification, removal of odours, or for the separation of components from mixtures (Ritter, 2008). Many materials have been used to adsorb organic and inorganic compounds from wastewater, ranging from clay, activated carbon, biomass, silica, nano materials, Mobil Catalytic Materials (MCM)-family and so on. These materials are applicable because of their high surface area and porosity that enhances its ability to trap contaminants, which is the reason activated carbon is widely used as an adsorbent. However, these materials also have their limitations, especially when applied to adsorption of organic pollutants, due to the complex nature of these pollutants. Surface area and porosity alone, can only support physical adsorption but not chemical adsorption.

Activated carbon is not efficient in removing oil, grease, natural organic matter, and other large organic molecules because the pores of activated carbon are easily blocked by oil and large organic molecules which results in reduced adsorption of organic molecules (Alther, 1995). Therefore, modification of these porous materials (organo-materials) is essential to make them more suitable for the adsorption of organic pollutants. Many organo-materials have been prepared and applied in the removal of organic pollutants such as pharmaceuticals, dyes, phenols, polyaromatic hydrocarbons (PAHs), polychlorinated biphenyls (PCBs), and so on. Several modifiers, such as, cetylpyridinium chloride (CPC), hexadecyltrimethyl ammonium bromide (HTAB) and dodecyltrimethyl ammonium bromide (DTAB) have been found to be suitable modifiers. Ionic liquids are another type of modifier that has the potential to improve the efficiency of adsorbents. They are green solvents that are capable of replacing traditional organic solvents and have been extensively studied in materials chemistry, electrochemistry and catalysis (Welton, 1999). The aim of this review is to show the efficiency of ionic liquids in substituting the traditional known modifiers for the purpose of adsorption of organic pollutants.

2.2 IONIC LIQUIDS

Ionic liquids (ILs) have attracted an increasing amount of interest, owing to their low volatility, non-flammability, high chemical and thermal stabilities, high ionic conductivity and broad electrochemical windows (Zhang et al., 2006). ILs are low-melting-point salts, thus forming liquids that consist only of cations and anions. Ionic liquids can be used as green solvents with the potential of substituting traditional organic solvents in materials chemistry, electrochemistry, catalysis (Welton, 1999), spectroscopy, as well as extraction and separation processes. The defining characteristic of ILs is based on its constituent makeup where it has molecular ions as its building blocks as opposed to molecules in the traditional solvents. In other words, ILs or molten salts in general are defined as liquids composed of ions only, either at room temperature or at elevated temperatures but below 100 °C. ILs are also unique in the sense that in addition to ionic and covalent interactions, there are relatively weaker interactions such as H-bonding, and π-stacking, which are not commonly found in conventional solvents (Shukla et al., 2011).

Ionic liquids are composed of an organic cation and an inorganic anion, and their properties, such as melting point, density, viscosity, and miscibility with other substances, can be adjusted by selecting specific anions and/or cations (Turner et al., 2003). The cations in some ionic liquids are organic-based moieties such as imidazolium, N-alkyl pyridinium, tetraalkyl ammonium, and tetraalkyl phosphonium ions. The anions can be organic or inorganic, such as halides, nitrates, acetates, hexafluorophosphate, tetrafluroborate, trifluoromethylsulfonate and bis (trifluoromethanesulfonyl) imide (Balasubramanian and Venkatesan, 2012). The anion mainly controls their water miscibility (Huddleston et al., 2001), whereas the length of the alkyl chain of the cation influences all the other properties (Jess et al., 2005). Over two hundred ionic liquids are known and a significant number are commercially available (Poole, 2004; Forsyth et al., 2004). There are many types of ILs but the main types are alkyl ammonium, tetraalkyl ammonium, tetraalkyl phosphonium, 1,3-dialkyl imidazolium, and N-alkyl pyridinium salts formed with weak nucleophilic anions such as bis(trifluoromethylsulfonyl) imide, hexafluorophosphate, tetrafluoroborate, perfluoroalkylsulfonate and many more (Poole, 2004). Researchers believe that 1 trillion ILs could be possible because of its flexibility in cation and anion combinations (Holbrey and Seddon, 1999).

ILs have attracted interest as green solvents for chemical processes, for minimizing solvent waste, reducing exposure to hazardous vapors, and are considered environmentally friendly (low toxicity) (Poole and Poole, 2010). They are also considered to be highly solvating (Welton, 1999). They are referred to as "designer solvents" because their physical properties, such as melting point, density, viscosity, and hydrophobicity, can be varied by changing the cation and anion to tailor it for a given end use (Earle and Seddon, 2000). These adjustable physical properties have led to the application of ILs as solvents for synthesis (Chiappe et al., 2001; Stark et al., 1999) and catalysis (Sheldon, 2001; Carmichael et al., 1999), biocatalytic transformation (Sheldon et al., 2002; van Rantwijk and Sheldon, 2007; Park and Kazlauskas, 2003; Reetz et al., 2002; Lozano et al., 2014), electrochemical device designs (MacFarlane et al., 2007), analytical and separation processes (Pandey, 2006; Pei et al., 2007) and as an alternative medium for extractions (Chun et al., 2001; Pei et al., 2009) and purifications (Fadeev and Meagher, 2001; Wasserscheid and Keim, 2000). They are also used as templates or stabilizers for nanostructures (Antonietti et al., 2004; Zhang et al., 2006), and as supported catalysts for organic and electrochemical reactions.

Their negligible vapor pressure minimizes environmental contamination through evaporation which is a major concern of conventional organic solvents. In addition their specificity, yield and rate has made them very good replacements for conventional organic surfactants (Olivier-Bourbigou and Magna, 2002; Dupont and Suarez, 2006; Mallakpour and Kolahdoozan, 2008; Leclercq and Schmitzer, 2009).

ILs can be divided into different groups such as imidazolium, pyridinium, tetraalkyl ammonium, tetraalkyl phosphonium, and so on (Wasserscheid and Waffenschmidt, 2000; Welton, 1999). Imidazolium ILs are the most stable, most commonly used, and most studied. Hydrophilicity and hydrophobicity of ILs are determined by the type and structure of anions and cations. Shorter alkyl side chains result in stronger hydrophilicity of ILs, while longer alkyl side chains result in stronger hydrophobicity (Zheng et al., 2014).

2.3 METHODS OF REMOVING ORGANIC POLLUTANTS

Organic pollutants have been removed from aqueous solutions by several methods which include, sedimentation (Cheremisinoff, 2002b), filtration, microfiltration, ultrafiltration, (nanofiltration, and reverse osmosis) (Cheremisinoff, 2002a; Avlonitis et al., 2008; Marmagne and Coste, 1996; Al-Bastaki, 2004; Marcucci et al., 2001; Šostar-Turk et al., 2005), chemical treatment such as use of coagulating and flocculating agents (Shi et al., 2007; Zhou et al., 2008; Mishra et al., 2006; Mishra and Bajpai, 2006; Hai et al., 2007; Wang et al., 2007; Yue et al., 2008), oxidation and ozonation (Hsu et al., 2001; Omura, 1994; Hage and Lienke, 2006; Wang, 2008; Kim et al., 2004; Gregor, 1993; Perkins et al., 1996; Soares et al., 2006; Wu et al., 2008), electrochemical oxidation/reduction (Gupta et al., 2007; Lin and Peng, 1994; Doğan and Türkdemir, 2005; Faouzi et al., 2007; Lopes et al., 2004), advanced oxidation processes (AOPs) (Bandala et al., 2008; Muruganandham and Swaminathan, 2004; Aguedach et al., 2005; Akyol et al., 2004; Arslan-Alaton, 2003; Behnajady et al., 2006; Aarthi and Madras, 2007; Chen, 2009; Kansal et al., 2007) and biological treatment (Barragán et al., 2007; Bromley-Challenor et al., 2000; dos Santos et al., 2007; Frijters et al., 2006; Van der Zee and Villaverde, 2005; Zhang et al., 1998; Rai et al., 2005; Przystaś et al., 2012; Knapp et al., 1995; Wesenberg et al., 2003; Bumpus and Brock, 1988; Radha et al., 2005; Husain, 2006; Stolz, 2001; Pandey et al., 2007; Senan and Abraham, 2004; Brown and Laboureur, 1983; Bhattacharyya and Sarma, 2003; Crini, 2006; Robinson et al., 2001; Razo-Flores et al., 1997).

Adsorption is presently widely used for the removal of organic pollutants from wastewaters. Adsorption refers to a process whereby a substance is transferred from a liquid or gaseous phase onto a solid surface, or a surface phenomenon where adsorbate molecules or ions (liquid or gas) are concentrated on the surface of a solid (adsorbent) (Gupta and Suhas, 2009). Adsorption processes can be classified as physisorption or chemisorption depending on how the adsorbate species are adsorbed onto the adsorbent surface (Gupta and Suhas, 2009). In adsorption processes, dye molecules may be adsorbed on the surface of an adsorbent through several forces such as hydrogen bonding, electrostatic interactions, van der Waals forces, hydrophobic interactions etc. (Kumar et al., 2014; Ahmad et al., 2015).

Adsorption as a means of water purification was used as early as 1550 B.C as documented in an ancient Egyptian papyrus and later by Hippocrates and Pliny the Elder, mainly for medicinal purposes. In the 18th century purification of liquids was achieved by using carbon from blood, wood and animal materials (Cheremisinoff, 2001). There are several absorbents in use today, which include alumina, fly ash, silica gel, zeolites, sludge, red mud, biomass, chitosan, clay, activated carbon, etc. The most used adsorbents are clays (Alkan et al., 2005), activated carbon (McKay et al., 1998; Walker and Weatherley, 2001), chitosan and chitin (Juang et al., 1997; Longhinotti et al., 1998), as well as cellulosic materials (Bousher et al., 1997). The commonly used adsorbent for the removal of organic pollutants from water is activated carbon (AC), but its drawback is the high regeneration cost and the generation of activated carbon fines, owing to the brittle nature of carbon used for the removal of organic compounds (Alther, 1995). Also, AC has little ability to adsorb oil, grease, natural organic matter, and other large organic molecules (Alther, 2002). Meanwhile, surfactants or organic-modified materials have been reported to adsorb oil and grease at 5–7 times that of unmodified AC (Alther, 1995).

2.4 SURFACTANTS

The primary objective of the adsorbent is to remove pollutants thus cleaning-up the environmental matrix. Many traditional organic surfactants are often used for the modification of absorbents to increase their adsorptive capacity. Most of these surfactants are hazardous, flammable, and toxic to the environment (Esrafili et al., 2011).

Surfactant or surface-active agents have been in existence for a long time (Moradi and Yamini, 2012) and their uses span across a wide range of industries (Doren and Goldfarb, 1970; Schott et al., 1984). Surfactants are chemicals that are active at surfaces, or interfaces of two physical phases and are made up of two parts or groups; the water liking end (hydrophilic) and the oil-liking or lipophilic or water-hating end (hydrophobic) (Maclay, 1956). These make them soluble in both organic solvents and water. Ionic liquids possess all these characteristics which make them good surfactants. Ionic surfactants adsorb onto oppositely-charged materials through electrostatic interaction between the surfaces. Adsorption of ionic surfactants on a like-charged material is less understood, but can occur through hydrogen bonding or attractive dispersion forces (Rosen and

Kunjappu, 2012; Buckley, 1998). Surfactants are classified into four groups depending on the charge of the hydrophilic part: non-ionic (0), anionic (−), cationic (+) and zwitterionic (±).

Many organic surfactants have been used for the modification of materials for the purpose of adsorption of organics where the cationic surface-active bonding agent may be quaternary ammonium, phosphonium and arsonium bases, or primary, secondary or tertiary organic amines or salts. Dimethyl dihydrogenated tallow ammonium was used for the modification of montmorillonite (Ho et al., 2001); ammonium surfactant and phosphonium surfactant were used to modify montmorillonite (Calderon et al., 2008; Singla et al., 2012); polypropylene was used to modify bentonite (Du et al., 2009); hexadecyltrimethyl ammonium (HDTMA) was used to modify montmorillonite and smectite (Boyd et al., 1988; Kim et al., 1996) and many more. ILs have been recently used for the modification of montmorillonite (Takahashi et al., 2013), nanoparticles (Sajjadi et al., 2013), Fe3O4 magnetic nanoparticles for removal of reactive red 141 and reactive yellow 81 (Kamran et al., 2014b) and the removal of phenolic compounds from aqueous solutions by emulsion liquid membrane containing ionic liquids (Balasubramanian and Venkatesan, 2012).

2.5 DIFFERENT TYPES OF ADSORBENTS AND MODIFIERS USED

Several surfactants have been used to modify different materials for the removal of organic compounds.

2.5.1 Activated Carbon

Activated carbon (AC) has been studied by many researchers for the adsorption of both anionic and cationic surfactants (Wu and Pendleton, 2001; Xiao et al., 2005; Gonzalez-Garcia et al., 2001; Gonzalez-Garcia et al., 2004a; Gonzalez-Garcia et al., 2004b). However, application of surfactant modified AC for adsorption of organic pollutants from aqueous solution has been reported to a lesser extent. In the work of Choi and co-workers, reactive black 5 was adsorbed from aqueous solution using activated carbon modified by cetylpyridinium chloride (CPC) and their results showed that modification of AC using surfactants enhanced the sorption of reactive black 5 (Choi et al., 2008). Cota-Espericueta (2003) modified AC with hexadecyltrimethyl ammonium bromide (HTAB) dodecylethyldimethyl ammonium bromide (DEDAB) cetyl pyridium bromide (CPB), dimethyl-dioctadecyl ammonium bromide (DDOAB) and dodecyltrimethyl ammonium bromide

(DTAB) for the adsorption of 2,4-dinitrophenol (2,4-DNP) and 2,4-dinitrotoluene (2,4-DNT). An increase in adsorption capacity of AC was observed when modified with DTAB, DEDAB or HTAB. Meanwhile, the adsorptive capacity of AC decreased when modified with CPB or DEDAB.

2.5.2 Clay

Clay is currently one of the most used adsorbents and is considered as one of the potential alternatives to activated carbon because of its adsorption capabilities which comes from its high surface-area and exchange capacity. Clay can be classified by the differences in its layered structures. There are several classes of clays such as smectites (montmorillonite, saponite), mica (illite), kaolinite, serpentine, pylophyllite (talc), vermiculite and sepiolite (Shichi and Takagi, 2000). Raw clay cannot adsorb organic compounds efficiently as it is hydrophilic in nature, whereas organics are generally hydrophobic (Shen et al., 2009). Surfactants are therefore used as a modifier to alter the surface property of the clay from hydrophilic to hydrophobic (Estevinho et al., 2007) thus increasing the affinity of clays for organics (Ralston and Kitchener, 1975; Van Olphen and Fripiar, 1981; Manne and Gaub, 1995). Modification of different types of clay with different modifiers (surfactants) has yielded a significant increase in adsorption capacity towards organic compounds. The surfactant modified clay is also known as organo-clay, which transforms an organophobic clay surface to strongly organophilic, thus increasing its adsorption capacity toward organic compounds (Li and Bowman, 2001). Organo-clays are able to hold on to their low permeability in the presence of nonpolar liquids (Li et al., 1996), and are also stronger and less compressible than unmodified clay (Soule and Burns, 2001). These characteristics has made them good additives to waste containment facilities, landfill liners (Smith and Jaffe, 1994), slurry walls, and wastewater treatment processes (Sheng and Boyd, 2000; Park and Jaffe, 1993) and as adsorbents for air sampling of airborne organic contaminants (Harper and Purnell, 1990).

These organically modified clays are mostly modified with quaternary amines (Mortland, 1970), where the nitrogen end of the quaternary amine, which has a positive charge, is exchanged onto the clay surface for sodium and calcium (Mortland, 1970). This results in ionic bonding with the free chloride ions from the amines, forming salts which are washed out during the initial washing of the material (Mortland et al., 1986). The amine chains extend into the water, removing the oils

and other nonpolar or slightly polar organics by a partition phenomenon (Alther, 1999; Street and White, 1963; Stockmeyer, 1991).

Most organically modified clays adsorb nonionic organic compounds more strongly than unmodified clay with the molecular structure of the organic cation influencing adsorption capacity and its mechanism. Studies have shown high adsorption capacities for clays modified with quaternary ammonium cations that have one or more long-chain alkyl functional groups (e.g., hexadecyltrimethyl ammonium) (Smith and Jaffe, 1994; Smith et al., 1990; Smith and Jaffé, 1994; Deitsch et al., 1998; Jaynes and Boyd, 1991; Jaynes and Vance, 1999; Smith and Jaffe, 1991).

Sepiolite modified with dodecyl ethyl dimethyl ammonium (DEDMA) bromide showed a very high adsorption capacity of 425.0 mg g^{-1} as reported by Ozcan and Ozcan for the adsorption of acid red 57 (AR57) (Özcan and Özcan, 2005), compared to the adsorption capacity of Na–bentonite and DTMA–bentonite (dodecyltrimethyl ammonium bromide-modified bentonite). The latter showed an adsorption capacity of 740.5 mg g^{-1}, while the former had an adsorption capacity of 67.1 mg g^{-1} for the adsorption of acid blue 193 (Özcan et al., 2004). Sorption of benzene, trichloroethene, and 1,2-dichlorobenzene onto hexadecyltrimethyl ammonium bentonite (HDTMA bentonite) and benzyltriethyl ammonium bentonite (BTEA bentonite) were investigated and showed that the adsorption capacity increased as the total organic-carbon content of quaternary ammonium cation on the clay increased (Bartelt-Hunt et al., 2003).

Adsorption of acid dye onto organo-bentonite was reported by Baskarakingam and co-workers, who used cetyldimethylbenzyl ammonium chloride and cetylpyridinium chloride to modify bentonite resulting in adsorption capacities of 357.14 and 416.66 mg g^{-1} for the cetyldimethylbenzyl ammonium chloride-bentonite (CDBA-bent) and cetylpyridinium chloride-bentonite (CP-bent), respectively (Baskaralingam et al., 2006).

Smectite modified with benzyltrimethyl ammonium (BTMA) and hexadecyltrimethyl ammonium (HDTMA) ion was used in the removal of phenol (Shen, 2004). This study showed that exchanged organic cations affected the adsorptive behavior of smectite based on the size and molecular arrangement of the exchanged organic cations in the clay. Tetraphenylphosphonium chloride (TPP) and crystal violet (CV) modified montmorillonite was used for the adsorption of 2,4,5-

trichlorophenol, 2-chlorophenol, picric acid, 4-nitrophenol, phenol, and naphthalene, which proved to be more efficient absorbers of these organic pollutants compared to unmodified montmorillonite (Rytwo et al., 2007). Rytwo and co-workers showed the efficiency of montmorillonite modified with crystal violet as an absorber of fast green and erythrosin-B (Rytwo et al., 2006).

Adsorption of phenol and dichlorophenols (2,5 DCP and 3,4 DCP) from water by a porous clay heterostructure (hexadecyltrimethyl ammonium bromide (HDTMA), dodecylamine (PCH)) was reported High adsorption capacities of 14.5 mg g^{-1} for phenol, 48.7 mg g^{-1} for 3,4-DCP and 45.5 mg g^{-1} for 2,5-DCP onto PCH were observed for both phenol and DCPs from water (Arellano-Cárdenas et al., 2005). Similarly, Lawrence and co-workers studied the adsorption of phenol, 2-,3- and 4-chlorophenol from water onto smectite modified by tetramethyl ammonium (TMA) and tetramethyl phosphonium (TMP) (Lawrence et al., 1998).

Adsorption of phenols onto 1,1′-dimethyl-4,4′-bipyridinium-smectites (Okada and Ogawa, 2002), mono, bis and tris(2,2′-bipyridine) nickel(II)- and tris(ethylenediamine)nickel(II)-saponite intercalated compounds from aqueous solution were examined by Okada and co-workers (Okada et al., 2004). The adsorption of alkylbenzenes and phenols on aliphatic ammonium smectite was also reported (Barrer, 1989; Xu et al., 1997). Organo-bentonites prepared by modifying natural bentonite by quaternary amines which included tetramethyl ammonium bromide (TMAB), hexadecyltrimethyl ammonium bromide (HDTMAB), benzyltriethyl ammonium bromide (BTEAB), tetraethyl ammonium bromide (TEAB) and cetylpyridinium bromide (CPB) were used to investigate the adsorption of phenol and m-chlorophenol (Brosillon et al., 2000). Bentonite modified by polyhydroxy ferric solution was used to adsorb pentachlorophenol from aqueous solutions (Bouras et al., 2001). Cationic surfactant modified Al-pillared montmorillonite also showed high adsorption capacity for the adsorption of chlorophenolic derivatives (Bouras et al., 1999; Srinivasan and Fogler, 1990; Srinivasan and Scott, 1990).

Na-montmorillonite modified with monoalkyl-(dodecyltrimethyl ammonium and octadecyltrimethyl ammonium), and dialkyl ammonium (didodecyldimethyl ammonium and ioctade-cyldimethyl ammonium) bromides was used to adsorb 2,4-dichlorophenol (DCP) (Witthuhn et al., 2005). Studies by Mortland and co-workers used hexadecylpyridinium (HDPY+),

hexadecyltrimethyl ammonium (HDTMA+), trimethylphenyl ammonium (TMPA+) and tetramethyl ammonium (TMA+) to modify clay (smectite) for the adsorption of phenol and several of its chlorinated congeners (Mortland et al., 1986). It was further established that the complexes containing alkyl long-chains (hexadecyl) were the most hydrophobic and adsorbed the phenolics from water in proportion to their hydrophobicities, which increased with the number of chlorines (phenol < chlorophenol < dichloropohenol < trichlorophenol). Bentonite modified dodecylammonium (DDAB) was also studied for the adsorption of p-chlorophenol (p-CP) and p-nitrophenol (p-NP) (Akçay and Akçay, 2004).

The adsorption of phenols from aqueous solutions was studied using three different adsorbents, clinoptilolite, montmorillonite and hydrotalcite (HT) (Yapar and Yilmaz, 2005). Clinoptilolite was modified using cetyltrimethyl ammonium bromide (CTAB) and hydrotalcite was calcined by heating to 550 °C. The comparison of five different modified bentonite adsorbents with unmodified bentonite showed that CTAB/Al-bentonite had the highest adsorption capacity followed by Al-bentonite, CTAB bentonite, thermal-treated bentonite, cyclohexane-treated bentonite and natural bentonite (Al-Asheh et al., 2003). Barhoumi and co-workers worked on kaolinite and montmorillonite modified with parateroctyl benzene polyethoxy (TX100) and paranonyl benzene polyethoxy (TN101) (Barhoumi et al., 2003). An increase in adsorption capacity was observed compared to the unmodified kaolinite and montmorillonite. Organo-clays made from the modification with hexadecyltrimethyl ammonium (HDTMA) and didodecyldimethyl ammonium (DDDMA) were also studied for the adsorption of trichloroethylene and showed a high affinity for trichloroethylene (Zhao and Vance, 1998).

Four different surfactants were used in the modification of bentonite. Hexadecyltrimethyl ammonium (HDTMA) modified bentonite showed the highest adsorption capacity for the adsorption of 2,4-dichlorophenol (2,4-D) from aqueous solution with a removal efficiency of 97.0% compared with raw bentonite that had a removal efficiency of less than 60% (Ruan et al., 2014). Also, adsorption of phenol from wastewater by organo-bentonite was investigated by Anirudhan and Ramachandran (2014). Their results showed that adsorption of 2,4,6-trichlorophenol (TCP) on to Na-bentonite modified by exchanging Na^+ ions with the cationic surfactant, hexadecyltrimethyl ammonium (HDTMA) chloride, was significantly enhanced (2.3 times) through surfactant treatment of bentonite. Cao et al. (2013) reported an increase in

adsorption capacity when Na–bentonite was modified with hexadecyl trimethyl ammonium bromide (CTAB) and used in the adsorption of phenol. Improved adsorption capacity of organo-clay (montmorillonite modified hexadecyltrimethyl ammonium) compared to Na-montmorillonite was observed in the sorption of nitrobenzene, phenol, and m-nitrophenol from water and n-hexadecane (Borisover et al., 2008). Zhu and co-workers investigated a series of dual-cation organo-bentonites synthesized by replacing the metal ions in bentonite with both long-chain alkyl quaternary ammonium cations (dodecyltrimethyl ammonium (DTMA), benzyl dimethyl tetradecyl ammonium (BDTDA), cetyltrimethyl ammonium (CTMA), octodecyltrimethyl ammonium (OTMA)), and short-chain alkyl quaternary ammonium cations, such as tetramethyl ammonium (TMA) (Zhu et al., 2000). They reported that sorption of organic compounds onto dual-cation organo-bentonite was dominated by adsorption at low concentrations and by partitioning at high concentrations, making the organo-bentonites powerful sorbents for organic contaminants over a wide range of concentrations.

Lee and co-workers studied a high-charged smectite and a low-charged smectite modified with tetramethyl ammonium (TMA), to form a TMA-clay complex (Lee et al., 1989; Lee et al., 1990). The adsorption of benzene, toluene, and o-xylene as vapors by the dry TMA-clays and as solutes from water by the wet TMA-clays showed potential versatility for the removal of organic compounds in aqueous systems. Eight organo-clays were prepared and used for the adsorption of naphthalene and phenanthrene. The organo-clays were made from sodium-rich bentonite and dodecylpyridinium chloride, with loading levels ranging from 0.25–2.00 times the cation exchange capacity (CEC) of bentonite (Changchaivong and Khaodhiar, 2009). The sorption of benzene to bentonite, on two organo-clays synthesized from quaternary ammonium organic cations hexadecyltrimethyl ammonium (HDTMA) and benzyltriethyl ammonium (BTEA) were investigated. It was discovered that organo-clays adsorbed more benzene than the unmodified bentonite (Redding et al., 2002). Seven organo-clays were reportedly prepared by modification of bentonite with benzyl triethyl ammonium chloride (BTEA) at 50, 75, and 100% and with hexadecyl trimethyl ammonium bromide (HDTMA) at 25, 50, 75, and 100% of the bentonite's cation exchange capacity (Upson and Burns, 2006). It was reported that the organo-clays absorbed more 2,4,6-trinitrotoluene (TNT), 2-amino-4,6-dinitrotoluene (2-A-4,6-DNT) and 4-amino-2,6-dinitrotoluene (4-A-2,6-DNT) than the unmodified bentonite. Kaolinite and montmorillonite modified with aromatic organic constituents have higher adsorption capacities to adsorb

naphthalene and phenanthrene than those modified with aliphatic organic compounds (Huang et al., 2005).

Batch and column experiments investigated the efficiency of the adsorption of chlorobenzenes on cationic surfactant (dodecylpyridinium (DP)) modified soil (Wagner et al., 1994). Wagner and co-workers concluded that treatment of surfaces with cationic surfactants showed potential as a suitable adsorber in both batch and column experiments. Adsorption of naphthalene, p-nitrotoluene, nitrobenzene and m-dinitrobenzene from water onto bentonite, bentonite modified by KCl solutions and organo-bentonite (i.e., 100 CTMAB) were also investigated. The affinities of these sorbates with bentonite were extremely weak and similar compared with 100 CTMAB (Chen et al., 2008). The enhancement in the adsorption capacity was said to be due to strong retention of the CTMA+-derived organic phase and the exposed-siloxane surfaces. The K_d values increased 5360, 780, 200 and 40 times, respectively, for naphthalene, p-nitrotoluene, m-dinitrobenzene and nitrobenzene (Chen et al., 2008). Sheng et al. (1998) investigated smectitic modified with hydrophobic cationic surfactants (hexadecyl trimethyl ammonium (HDTMA)) which showed that at higher loadings of HDTMA the material adsorbed trichloroethylene and chlorobenzene by both ion exchange and hydrophobic bonding. Sorption coefficients for trichloroethylene and chlorobenzene on HDTMA-modified soils (0.7 CEC) were 20 - 60 and 100 - 350 times higher, respectively, than those on the corresponding unmodified soils.

A series of organo-bentonites synthesized by exchanging organic cations such as dodecyl tri-methyl ammonium (DTMA), benzyl dimethyl tetradecyl ammonium (BDTDA), cetyltrimethyl-ammonium (CTMA) and octodecyl trimethyl ammonium (OTMA) on bentonite was also investigated by Chen and Zhu (Chen and Zhu, 2001). They reported that the K_{oc} values of phenanthrene, anthracene, naphthalene and acenaphthene were 2.621×10^5, 2.106×10^5, 2.247×10^4 and 5.085×10^4, respectively. They further suggested that, since the K_{oc} values for the organo-bentonites were about ten to twenty times larger than the values on the soils and sediments, organo-bentonite was good for remediation of polluted soil and groundwater. Inorgano–organo-bentonite (IOB) synthesised from bentonite modified with both Fe polycations and cetyltrimethyl ammonium bromide (CTMAB) was studied for the simultaneous removal of phosphate and phenanthrene from water (Ma and Zhu, 2006). Ma and Zhu found that IOB had a strong affinity for both phosphate and phenanthrene in water compared to unmodified bentonite. It was further

reported that more than 95% phosphate and 99% phenanthrene were removed from water within 30 minutes. They concluded that IOB was a favorable sorbent that could simultaneously remove non-biodegradable organic pollutants such as phenanthrene and phosphate after the bioprocessing of wastewater (Ma and Zhu, 2006).

Bentonite was modified with cetyltrimethyl ammonium bromide (CTMAB), and used for the adsorption of benzene, toluene, ethylbenzene, nitrobenzene, aniline, phenol, and p-nitrophenol in water (Zhu et al., 1998). Removal efficiencies and sorption capacities of organo-bentonites for organic compounds in water increased with increasing amounts of associated quaternary ammonium cations in the bentonite.

Tetramethyl ammonium (TMA+) ion was used to modify bentonite, which resulted in an increase in the adsorptive properties of the TMA-bentonite in direct proportion to the exchange reaction below 60% of the CEC of the clay (Cadena, 1989). Cadena's studies showed that the ability of the modified clay to remove benzene decreased at doses higher than 150% of the CEC of the clay (Cadena, 1989). Organo-clay sorbents were also prepared by modifying montmorillonite with four different quaternary ammonium compounds (tetramethyl ammonium chloride (TMA), hexadacecyl benzyl dimethyl ammonium chloride (HDBDMA), hexadecyl trimethyl ammonium bromide (HDTMA) and dioctodecyl dimethyl ammonium bromide (DDDMA)) (Dentel et al., 1998). The researchers concluded that the use of these organo-clays for removal of 1,2,4-trichlorobenzene from water was satisfactory as a result of its enhanced sorption capacity. Phenanthrene adsorption on different organo-clay complexes was investigated (El-Nahhal and Safi, 2004). The adsorbed amounts of phenanthrene on this montmorillonite modified with tetraheptyl ammonium, benzyl trimethyl ammonium, hexadecyl trimethyl ammonium and tetraphenylphosphonium were several times higher than those obtained using montmorillonite clay without surface modification. Cetyltrimethyl ammonium chloride (CTAC) modified bentonite was used in the adsorption of petroleum hydrocarbons emulsified in aqueous solution. Emam (2013) discovered that modified bentonite was an excellent alternative for the removal of hydrocarbons from oil-water emulsions.

Modified bentonite (bentonite-dimethyl dihydrogenated) has been used for the sorption of benzene, toluene, ethylbenzene, and o-xylene (BTEX compounds) in contaminated liquids.

Sorption isotherms and column leach tests were performed to assess the efficiency of the clay in adsorbing organics from liquid solutions. The efficiencies of the clays in removing BTEX compounds were 75%, 87%, 89%, and 89%, respectively (Gitipour et al., 1997). Gitipour and co-workers further suggested that the modified bentonite can be used as a practical organic adsorbent for wastewater treatment systems, landfill liners, slurry walls, and underground storage tank barriers.

2.5.3 Biosorbents

Biosorbents, which include bark and wood chips, chitosan, peat, sugarcane bagasse, straw and rice husks, activated bamboo and many more, are one of the recent low-cost materials used for the removal of pollutants from water bodies because they are cheap, easy to use and readily available compared to other techniques such as ion exchange, reverse osmosis, electrochemical treatment, evaporation recovery, solvent extraction, and adsorption (Olu-Owolabi et al., 2012). Low adsorption capacity has been the limitation of biosorption being used industrially for cleaning up of toxic pollutants in wastewater (Deng and Ting, 2005). This has led to the modification of biosorbents to enhance its adsorption capacity. Treatments range from acid treatment (Montazer-Rahmati et al., 2011; Li et al., 2010), base, acetone and ethanol treatments (Feng et al., 2011) as well as formaldehyde treatment (Feng et al., 2011; Montazer-Rahmati et al., 2011).

Recent trends in the modification of biosorbent with surfactants has increased (Brandão et al., 2010). It was confirmed that surfactant-modified solid surfaces improved removal of some organic contaminants from aqueous solutions (Adak et al., 2006). Ansari and co-workers investigated batch and fixed-bed column sorption of methylene blue dye (MB) from aqueous solutions, using sawdust modified with surfactant (sodium dodecyl sulfate (SDS/SD)) (Ansari et al., 2012). They obtained breakthrough from continuous sorption experiments, with the highest column capacity of 129.68 mg g^{-1} (Ansari et al., 2012). Their results also showed that surfactant-modified sawdust is much more effective for basic MB dye removal compared to untreated sawdust (SD). The sorption capacity of peat increased significantly after modification with quaternary ammonium surfactant (hexadecyltrimethyl ammonium bromide (HTAB)), for the sorption of bisphenol (Zhou et al., 2011). They further observed that hydrophobic interaction between the modified peat and bisphenol played a significant role during the process. They concluded that sorption capacity of natural peat can be significantly improved by surfactant modification (Zhou et al., 2011).

Barley straw was chemically modified using a cationic surfactant hexadecylpyridinium chloride monohydrate (CPC) to obtain a biosorbent for removal of emulsified mineral oil from aqueous solution. It was also found that addition of CPC created a non-polar layer on barley straw surface thus giving surfactant modified barley straw a much better adsorption capacity for oil removal from water than unmodified barley straw (Ibrahim et al., 2010). Barley straw was modified with cetylpyridinium chloride and used for the adsorption of acid blue 40 and reactive black 5 in aqueous solution. Surfactant modified barley straw exhibited higher adsorption of acid blue 40 and reactive black 5 than the unmodified barley straw (Oei et al., 2009). Removal of phenanthrene (PHE) from aqueous solution by adsorption onto quaternary ammonium surfactant modified peat (MP) was also studied (Zhou et al., 2012). Three different quaternary ammonium surfactants, tetrabutyl ammonium bromide (TBAB), hexadecylpyridinium bromide (HPB) and hexadecyl trimethyl ammonium bromide (HTAB) were used in the modification. The results showed that surfactant modification improved the PHE adsorption capacity of peat and that peat modified with long carbon chain surfactants performed better than peat modified with short carbon chain surfactants. The magnitude of PHE adsorption capacity followed the order of MP-HPB > MP-HTAB > MP-TBAB > raw fibric peat.

Sugar-beet pulp's potential application in decolorization of wastewater was reportedly improved by modification with quaternary ammonium-salts. Acid red 1 (AR1) dye biosorption performance onto quaternary ammonium-salt (cetrimonium bromide) modified sugar-beet pulp was investigated. Their results showed that AR1 biosorption onto surfactant modified sugar-beet pulp could also be successfully used for remediation of wastewater in continuous systems (Akar et al., 2015). The biosorption characteristics of a surfactant modified macro fungus were also investigated for the removal of reactive red 2 contaminated solutions (Akar and Divriklioglu, 2010). Biosorption efficiency was improved with a small amount of fungal biomass after the modification process. Akar and Divriklioglu concluded from the overall, batch and continuous mode data that the CTAB-modified fungal biomass is better than that of unmodified dried biomass, and that the biosorbent may be useful for the removal of reactive dyes from aqueous media (Akar and Divriklioglu, 2010). The biosorption of methylene blue onto dried *Rhizopus arrhizus,* a filamentous fungus, was investigated in the absence and in the presence of increasing concentrations of sodium dodecylsulfate (SDS) (Aksu et al., 2010). Literature reported that it

followed a Langmuir model with a maximum adsorption capacity of 370.3 mg g^{-1} of dried biomass in the absence of the surfactant. However the addition of 1 mM (288.4 mg L^{-1}) of SDS increased the adsorption capacity to 1666.6 mg g^{-1} leading to a 4.5-fold increase in the adsorption capacity.

2.5.4 Alumina

Alumina modified with anionic surfactants has also been used for the adsorption of organic pollutants. Anionic surfactants behave as normal electrolytes in very dilute aqueous solutions, but at higher concentrations its behavior changes. This behavior is explained in terms of the formation of organized aggregates of large molecules called micelles, in which the hydrophobic parts of the surfactant face inwards leaving the hydrophilic portion to face the aqueous medium. The surfactant concentration at which micelles are formed is called the critical micelle concentration (CMC). The micelles have the ability to preferentially absorb organic solutes from the solution. This process is called solubilization. The adsorption of ionic surfactants on oppositely charged surfaces is generally different from the ordinary adsorption process. At low surfactant concentrations monolayer and bilayer structures are formed. These structures act as micelles and have the potential to solubilize the organics into the three dimensional structures. The process is called adsolubilization which is the surface phenomenon analogous to solubilization with adsorbed surfactant bilayers playing the role of the micelles. The monolayer structure is called the hemimicelle and the bilayer structure is called the admicelle. Fig. 2.1 shows a cationic surfactant adsorbed gradually on the negatively charged material through electrostatic attraction to form a monolayer (hemimicelle). After the formation of the monolayer on the surface of the material, additional cationic surfactant forms a second layer due to the hydrophobic attraction between their organic tails (admicelles).

The adsolubilization process can be efficiently used for the removal of different organic pollutants such as dyes, phenolic compounds, and so on from the water environment (Adak and Pal, 2006). At high anionic surfactant concentration, the adsorption of the surfactant on the alumina surface occurs *via* electrostatic attraction between the anionic head group of the surfactant and the positively charged alumina surface as well as the interaction between the hydrocarbon chains, which is responsible for the formation of micelle-like aggregates on the alumina surface (Adak and Pal, 2006; Adak et al., 2006).
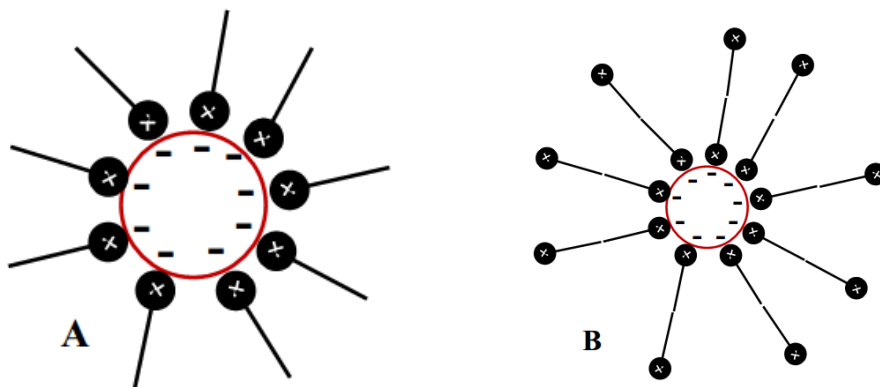
Fig. 2.1a Hemimicelle and 1b admicelle structures of the cationic surfactant aggregates formed on the surface of a negatively charged material

Batch and fixed bed studies of alumina modified with anionic surfactant (AS) as an efficient adsorbent for the removal of phenol from aqueous solutions, showed that surfactant-modified alumina (SMA) possessed the ability to remove organic solutes from aquatic environments (Adak and Pal, 2006). Adak and co-workers also reported fixed bed column studies for the removal of crystal violet (CV), known as basic violet 3, from wastewater using surfactant-modified alumina (SMA) as an adsorbing medium (Adak et al., 2006). The SMA was found to be a very efficient medium for the removal of dye from wastewater.

Prepared surfactant-modified alumina (SMA) was used to remove malachite green (MG) from aqueous media. Sodium dodecyl sulfate (SDS) was used as the modifier, and batch and fixed bed column studies were carried out with surfactant-modified alumina (SMA) for MG removal from aqueous environments. SMA was found to be an efficient adsorbent of MG compared to the unmodified alumina (Das et al., 2009a; Das et al., 2009b).

2.5.5 Natural Zeolites

Natural zeolites are highly porous hydrated alumina silicate materials with three dimensional crystal structures. There are more than 40 natural zeolites identified in the world (Crini, 2006). Natural zeolite modified with hexamethylenediamine (HMDA) was found to be a good adsorbent

for the removal of reactive red 239 (RR-239) and reactive blue 250 (RB-250). Batch adsorption experiments showed a substantial improvement in adsorption of reactive dyes on modified zeolites (HMDA-Z) compared to natural zeolites (Alver and Metin, 2012). Surfactant-modified zeolite (SMZ) was used to remove remazol brillant blue R and remazol yellow reactive dyes from aqueous solutions. SMZ was prepared by allowing the hexadecyltrimethyl ammonium bromide (HDTMA) adsorbed onto the negatively charged surface of the zeolite to form a monolayer (Kuleyin and Aydin, 2011). As the concentration of the surfactant solution increased, the surfactant molecules with large tail groups adsorbed through hydrophobic (tail–tail) interactions, forming a bilayer or admicelles. The study showed that SMZ was an effective sorbent for the removal of remazol brilliant blue R and remazol yellow from aqueous solutions.

Two zeolites synthesized from coal fly ash (ZFA) were prepared and then modified using hexadecyl trimethyl ammonium (HDTMA). Both ZFAs and surfactant modified ZFAs (SMZFAs) were investigated for their ability to adsorb humic acid (HA) from water. The results indicated that, while ZFA had little affinity for HA, SMZFA showed a greatly enhanced adsorption capacity for humic acid (Li et al., 2011). The adsorption of HA by SMZFA was primarily attributed to HDTMA loading onto the zeolite surface. Surfactant-modified zeolite (SMZ) was also studied for the adsorption of BTEX with batch and column experiments (Ranck et al., 2005; Altare et al., 2007). Bowman worked on the application of surfactant-modified zeolites for environmental remediation (Bowman, 2003). Their results indicated that SMZ was able to adsorb all major classes of water contaminants (anions, cations, organics, and pathogens), thus making it amenable to a variety of water treatment applications.

2.5.6 Nanomaterials

2.5.6.1 Titanate nanotubes (TNT)

Titanate nanotubes (TNT) have also been modified with surfactants for the purpose of adsorption. The potential of adsorptive removal of acid dyes from aqueous solutions using surfactant modified TNT was investigated by Juang and co-workers (Juang et al., 2008). The modified material was prepared by the hydrothermal method and subsequently washed with a 10^{-4} N HCl aqueous solution. The prepared TNT was then modified with a quaternary amine, hexadecyl trimethyl ammonium chloride (HDTMA), through the cation exchange process. It was found that

hydrophobic bonding by conglomeration of large C_{16} alkyl groups associated with HDTMA produced a dense packing of HDTMA with positively charged hydrophobic tails, which adsorbed 14 times higher than that of unmodified TNT (Juang et al., 2008). Adsorptive removal of basic dyes and acid dyes by TNTs modified with hexadecyl trimethyl ammonium chloride (HDTMA) were also investigated (Lee et al., 2007). Lee and co-workers noted an improved adsorptive capacity in modified TNT and suggested that surfactant modified TNT may be a good adsorbent for the removal of basic dyes and acid dyes from aqueous solution through the cation and anion exchange mechanism, respectively.

2.5.6.2 Carbon nanotubes

Carbon nanotubes (CNTs) are highly popular due to their novel properties such as high aspect ratio, high thermal, electrical and mechanical properties. Its large surface area, high porosity and layered structure make it suitable for adsorption of harmful pollutants (Ghobadi et al., 2013) such as cationic, anionic and other organic and inorganic impurities including 1,2-dichlorobenzene, trihalomethanes, dyes, microcystins, fluoride, nickel, arsenate and so on (Lu et al., 2005; Gong et al., 2009; Yan et al., 2006; Li et al., 2002; Iijima, 1991). Modification of multi-walled carbon nanotubes (MWCNTs) with a cationic surfactant, cetyl trimethyl ammonium bromide (CTAB) and its application for removal of direct red 80 (DR80) and direct red 23 (DR23) dyes were investigated (Ghobadi et al., 2013). The results showed that CTAB was efficiently immobilized on the surface of the MWCNT. The Langmuir adsorption capacities of surfactant-functionalized carbon nanotubes (SF-CNTs) for DR23 and DR80 were found to be 188.68 and 120.48 mg g^{-1}, respectively. Ghobadi and co-workers concluded that the adsorption capacity of SF-CNT was more significant than unmodified-CNT (Ghobadi et al., 2013).

Magnetic adsorbent nanoparticles (zinc ferrite nanoparticles) were modified using cetyl trimethyl ammonium bromide for the removal of direct green 6 (DG6), direct red 31 (DR31) and direct red 23 (DR23) (Mahmoodi et al., 2014). Mahmoodi and co-workers concluded that zinc ferrite nanoparticles modified with cetyl trimethyl ammonium bromide, being a magnetic adsorbent with high dye adsorption capacity, may be a suitable alternative for the removal of dyes from colored aqueous solutions (Mahmoodi et al., 2014).

2.5.7 Other Adsorbents

Fly ash modified with surfactants has also been studied. Pansuk and Vinitnantharat (2011) studied unmodified fly ash (Un-G) and surfactant modified granules (Mo-G) for the adsorption of acid brown 75 (AB 75) and direct yellow 162 (DY 162) from aqueous solutions. Preparation was by wet granulation of fly ash powder which was agglomerated into porous granules and modified with hexadecyl trimethyl ammonium bromide (HDTMA-Br). The adsorption of the aqueous anionic dyes onto Mo-G's was significantly increased compared with the unmodified granule (Un-G).

2.6 IONIC LIQUIDS AS A SURFACTANT

Lesser work has been reported on the usage of ILs as surfactants, but the few reports published have shown ILs as a promising potential replacement for commonly used surfactants. Kamran et al. (2014b) studied Fe_3O_4 magnetic nanoparticles modified with 1-octyl-3-methylimidazolium bromide ([C_8MIM]-Fe_3O_4) and used it for the removal of reactive red 141 (RR141) and reactive yellow 81 (RY81) from aqueous solutions. The maximum adsorption capacity of [C_8MIM]-Fe_3O_4 for the Langmuir model was 71.4 mg g^{-1} and 62.5 mg g^{-1} for RR141 and RY81, respectively. Their results indicated that magnetic nanoparticles of [C_8MIM]-Fe_3O_4 have potential application in the removal of RR141 and RY81 from wastewaters compared to the unmodified nanoparticles. Short contact time, high adsorption capacity, stability and reusability of the adsorbent were attributed to the surface electrostatic and/or hydrophobic interactions between dyes and adsorbent (Kamran et al., 2014b). An experimental study on the removal of phenolic compounds from aqueous solutions using ionic liquid mixed carrier (ILMC) containing 1-butyl 3 methylimidazolium hexafluorophosphate [BMIM]$^+$[PF6]$^-$ dissolved in tributyl phosphate (TBP) in an emulsion liquid membrane (ELM) was also carried out (Balasubramanian and Venkatesan, 2012). It was found that addition of 0.02% (v/v) of [BMIM]$^+$[PF6]$^-$ in the membrane phase enhanced the emulsion stability 5 times.

Adsorption of reactive red-120 (RR) and 4-(2-pyridylazo) resorcinol (PAR) from aqueous solutions by Fe_3O_4 magnetic nanoparticles using ionic liquid as a modifier was studied in a batch reactor (Absalan et al., 2011). The results indicated that the IL-Fe_3O_4 nanoparticles had removed more than 98% of both dyes. The maximum adsorption capacity of IL-Fe_3O_4 was 166.67 and 49.26

mg g^{-1} for RR-120 and PAR, respectively. The IL-Fe$_3$O$_4$ nanoparticles were quite efficient as a magnetic nano-adsorbent for the fast removal of dyes from aqueous solutions compared to the unmodified form. Adsorption of folic acid, riboflavin, and ascorbic acid from aqueous samples by Fe$_3$O$^+$ magnetic nanoparticles using ionic liquid as a modifier was also investigated (Kamran et al., 2014a). Maximum adsorption capacities of folic acid, riboflavin and ascorbic acid were 22.5, 4.8 and 6.9 mg g^{-1} of the adsorbent, respectively.

In this research two novel ionic liquids were synthesized and used in the modification of clay (montmorillonite and kaolin), biomass (*kigelia pinnata* and peanut shell) and activated carbon derived from peanut shell. The modified adsorbents were thereafter used in the adsorption of some selected organic pollutants and the optimization and kinetic studies of the adsorption were undertaken. This work is novel in that these two ionic liquids have not been previously synthesized and characterized and this is the first report of these newly synthesized surfactants. No previous reports of ionic liquid modified clay and biomass used for the purpose of removal of organic pollutants have been identified. This work is therefore novel in that this is the first experimental work and discussion of results obtained showing the adsorption of IL modified clay, biomass and activated carbon from biomass as well as the optimization and kinetic studies of the adsorption of selected organic pollutants using these materials. This work provides important knowledge and results in the field of developing new adsorbents for the removal of organic pollutants.

2.7 REFERENCES

Aarthi, T. & Madras, G. 2007. Photocatalytic degradation of rhodamine dyes with nano-TiO2. *Industrial & Engineering Chemistry Research,* 46(1)**,** pp 7-14.

Absalan, G., Asadi, M., Kamran, S., Sheikhian, L. & Goltz, D. M. 2011. Removal of reactive red-120 and 4-(2-pyridylazo) resorcinol from aqueous samples by Fe3O4 magnetic nanoparticles using ionic liquid as modifier. *Journal of Hazardous Materials,* 192(2)**,** pp 476-484.

Adak, A., Bandyopadhyay, M. & Pal, A. 2006. Fixed bed column study for the removal of crystal violet (CI basic violet 3) dye from aquatic environment by surfactant-modified alumina. *Dyes and Pigments,* 69(3)**,** pp 245-251.

Adak, A. & Pal, A. 2006. Removal of phenol from aquatic environment by SDS-modified alumina: Batch and fixed bed studies. *Separation and Purification Technology,* 50(2)**,** pp 256-262.

Aguedach, A., Brosillon, S., Morvan, J. & Lhadi, E. K. 2005. Photocatalytic degradation of azo-dyes reactive black 5 and reactive yellow 145 in water over a newly deposited titanium dioxide. *Applied Catalysis B: Environmental,* 57(1)**,** pp 55-62.

Ahmad, A., Mohd-Setapar, S. H., Chuong, C. S., Khatoon, A., Wani, W. A., Kumar, R. & Rafatullah, M. 2015. Recent advances in new generation dye removal technologies: novel search for approaches to reprocess wastewater. *RSC Advances,* 5(39)**,** pp 30801-30818.

Akar, S. T., Yilmazer, D., Celik, S., Balk, Y. Y. & Akar, T. 2015. Effective biodecolorization potential of surface modified lignocellulosic industrial waste biomass. *Chemical Engineering Journal,* 259(1)**,** pp 286-292.

Akar, T. & Divriklioglu, M. 2010. Biosorption applications of modified fungal biomass for decolorization of Reactive Red 2 contaminated solutions: Batch and dynamic flow mode studies. *Bioresource Technology,* 101(19)**,** pp 7271-7277.

Akçay, M. & Akçay, G. 2004. The removal of phenolic compounds from aqueous solutions by organophilic bentonite. *Journal of Hazardous Materials,* 113(1–3)**,** pp 189-193.

Aksu, Z., Ertuğrul, S. & Dönmez, G. 2010. Methylene blue biosorption by rhizopus arrhizus: Effect of SDS (sodium dodecylsulfate) surfactant on biosorption properties. *Chemical Engineering Journal,* 158(3)**,** pp 474-481.

Akyol, A., Yatmaz, H. & Bayramoglu, M. 2004. Photocatalytic decolorization of remazol red RR in aqueous ZnO suspensions. *Applied Catalysis B: Environmental,* 54(1)**,** pp 19-24.

Al-Asheh, S., Banat, F. & Abu-Aitah, L. 2003. Adsorption of phenol using different types of activated bentonites. *Separation and Purification Technology,* 33(1)**,** pp 1-10.

Al-Bastaki, N. 2004. Removal of methyl orange dye and Na_2SO_4 salt from synthetic waste water using reverse osmosis. *Chemical Engineering and Processing: Process Intensification,* 43(12)**,** pp 1561-1567.

Alkan, M., Çelikçapa, S., Demirbaş, Ö. & Doğan, M. 2005. Removal of reactive blue 221 and acid blue 62 anionic dyes from aqueous solutions by sepiolite. *Dyes and Pigments,* 65(3)**,** pp 251-259.

Altare, C. R., Bowman, R. S., Katz, L. E., Kinney, K. A. & Sullivan, E. J. 2007. Regeneration and long-term stability of surfactant-modified zeolite for removal of volatile organic compounds from produced water. *Microporous and Mesoporous Materials,* 105(3)**,** pp 305-316.

Alther, G. 1999. Organoclays remove oil, grease, solvents, and surfactants from water. *CleanTech 99 Proceedings,* 2)**,** pp 72-79.

Alther, G. 2002. Using organoclays to enhance carbon filtration. *Waste Management,* 22(5)**,** pp 507-513.

Alther, G. R. 1995. Organically modified clay removes oil from water. *Waste Management,* 15(8)**,** pp 623-628.

Alver, E. & Metin, A. Ü. 2012. Anionic dye removal from aqueous solutions using modified zeolite: Adsorption kinetics and isotherm studies. *Chemical Engineering Journal,* 200–202(1)**,** pp 59-67.

Anirudhan, T. & Ramachandran, M. 2014. Removal of 2, 4, 6-trichlorophenol from water and petroleum refinery industry effluents by surfactant-modified bentonite. *Journal of Water Process Engineering,* 1(2)**,** pp 46-53.

Ansari, R., Seyghali, B., Mohammad-khah, A. & Zanjanchi, M. A. 2012. Application of nano surfactant modified biosorbent as an efficient adsorbent for dye removal. *Separation Science and Technology,* 47(12)**,** pp 1802-1812.

Antonietti, M., Kuang, D., Smarsly, B. & Zhou, Y. 2004. Ionische flüssigkeiten für die synthese funktioneller nanopartikel und anderer anorganischer Nanostrukturen. *Angewandte Chemie,* 116(38)**,** pp 5096-5100.

Arellano-Cárdenas, S., Gallardo-Velázquez, T., Osorio-Revilla, G., López-Cortéz, M. & Gómez-Perea, B. 2005. Adsorption of phenol and dichlorophenols from aqueous solutions by porous clay heterostructure (PCH). *Journal of the Mexican Chemical Society,* 49(3)**,** pp 287-291.

Arslan-Alaton, I. 2003. A review of the effects of dye-assisting chemicals on advanced oxidation of reactive dyes in wastewater. *Coloration Technology,* 119(6)**,** pp 345-353.

Avlonitis, S. A., Poulios, I., Sotiriou, D., Pappas, M. & Moutesidis, K. 2008. Simulated cotton dye effluents treatment and reuse by nanofiltration. *Desalination,* 221(1–3)**,** pp 259-267.

Balasubramanian, A. & Venkatesan, S. 2012. Removal of phenolic compounds from aqueous solutions by emulsion liquid membrane containing Ionic Liquid [BMIM]$^+$[PF6]$^-$ in tributyl phosphate. *Desalination,* 289(1)**,** pp 27-34.

Bandala, E. R., Peláez, M. A., García-López, A. J., Salgado, M. d. J. & Moeller, G. 2008. Photocatalytic decolourisation of synthetic and real textile wastewater containing benzidine-based azo dyes. *Chemical Engineering and Processing: Process Intensification,* 47(2)**,** pp 169-176.

Barhoumi, M., Beurroies, I., Denoyel, R., Saıd, H. & Hanna, K. 2003. Coadsorption of phenol and nonionic surfactants onto clays. *Colloids and Surfaces A: Physicochemical and Engineering Aspects,* 223(1)**,** pp 63-72.

Barragán, B. E., Costa, C. & Carmen Marquez, M. 2007. Biodegradation of azo dyes by bacteria inoculated on solid media. *Dyes and Pigments,* 75(1)**,** pp 73-81.

Barrer, R. 1989. Shape-selective sorbents based on clay minerals: a review. *Clays and Clay Minerals,* 37(5)**,** pp 385-395.

Bartelt-Hunt, S. L., Burns, S. E. & Smith, J. A. 2003. Nonionic organic solute sorption onto two organobentonites as a function of organic-carbon content. *Journal of Colloid and Interface Science,* 266(2)**,** pp 251-258.

Baskaralingam, P., Pulikesi, M., Elango, D., Ramamurthi, V. & Sivanesan, S. 2006. Adsorption of acid dye onto organobentonite. *Journal of Hazardous Materials,* 128(2)**,** pp 138-144.

Behnajady, M., Modirshahla, N. & Hamzavi, R. 2006. Kinetic study on photocatalytic degradation of CI acid yellow 23 by ZnO photocatalyst. *Journal of Hazardous Materials,* 133(1)**,** pp 226-232.

Bhattacharyya, K. G. & Sarma, A. 2003. Adsorption characteristics of the dye, brilliant green, on neem leaf powder. *Dyes and Pigments,* 57(3)**,** pp 211-222.

Borisover, M., Gerstl, Z., Burshtein, F., Yariv, S. & Mingelgrin, U. 2008. Organic sorbate−organoclay interactions in aqueous and hydrophobic environments: sorbate− water competition. *Environmental Science & Technology,* 42(19)**,** pp 7201-7206.

Bouras, O., Houari, M. & Khalaf, H. 1999. Adsorption of some phenolic derivatives by surfactant treated al-pillared Algerian bentonite. *Toxicological & Environmental Chemistry,* 70(1-2)**,** pp 221-227.

Bouras, O., Houari, M. & Khalaf, H. 2001. Using of surfactant modified Fe-pillared bentonite for the removal of pentachlorophenol from aqueous stream. *Environmental Technology,* 22(1)**,** pp 69-74.

Bousher, A., Shen, X. & Edyvean, R. G. 1997. Removal of coloured organic matter by adsorption onto low-cost waste materials. *Water Research,* 31(8)**,** pp 2084-2092.

Bowman, R. S. 2003. Applications of surfactant-modified zeolites to environmental remediation. *Microporous and Mesoporous Materials,* 61(1–3)**,** pp 43-56.

Boyd, S. A., Mortland, M. M. & Chiou, C. T. 1988. Sorption characteristics of organic compounds on hexadecyltrimethylammonium-smectite. *Soil Science Society of America Journal,* 52(3)**,** pp 652-657.

Brandão, P. C., Souza, T. C., Ferreira, C. A., Hori, C. E. & Romanielo, L. L. 2010. Removal of petroleum hydrocarbons from aqueous solution using sugarcane bagasse as adsorbent. *Journal of Hazardous Materials,* 175(1–3)**,** pp 1106-1112.

Bromley-Challenor, K., Knapp, J., Zhang, Z., Gray, N., Hetheridge, M. & Evans, M. 2000. Decolorization of an azo dye by unacclimated activated sludge under anaerobic conditions. *Water Research,* 34(18)**,** pp 4410-4418.

Brosillon, S., Manero, M. H. & Foussard, J. N. 2000. Adsorption of acetone / heptane gaseous mixtures on zeolite co-adsorption equilibria and selectivities. *Environmental Technology,* 21(4)**,** pp 457-465.

Brown, D. & Laboureur, P. 1983. The aerobic biodegradability of primary aromatic amines. *Chemosphere,* 12(3)**,** pp 405-414.

Buckley, J. S. 1998. Evaluation of reservoir wettability and its effect on oil recovery. DE-FC22-96ID13421. Oklahoma, USA: Petroleum Recovery Research Center.,

Bumpus, J. A. & Brock, B. J. 1988. Biodegradation of crystal violet by the white rot fungus Phanerochaete chrysosporium. *Applied and Environmental Microbiology,* 54(5)**,** pp 1143-1150.

Cadena, F. 1989. Use of tailored bentonite for selective removal of organic pollutants. *Journal of Environmental Engineering,* 115(4)**,** pp 756-767.

Calderon, J. U., Lennox, B. & Kamal, M. R. 2008. Thermally stable phosphonium-montmorillonite organoclays. *Applied Clay Science,* 40(1)**,** pp 90-98.

Cao, C.-Y., Meng, L.-K. & Zhao, Y.-H. 2013. Adsorption of phenol from wastewater by organo-bentonite. *Desalination and Water Treatment,* 2(1)**,** pp 1-6.

Carmichael, A. J., Earle, M. J., Holbrey, J. D., McCormac, P. B. & Seddon, K. R. 1999. The heck reaction in ionic liquids: A multiphasic catalyst system. *Organic Letters,* 1(7)**,** pp 997-1000.

Changchaivong, S. & Khaodhiar, S. 2009. Adsorption of naphthalene and phenanthrene on dodecylpyridinium-modified bentonite. *Applied Clay Science,* 43(3)**,** pp 317-321.

Chen, B.-l. & Zhu, L.-z. 2001. Partition of polycyclic aromatic hydrocarbons on organobentonites. *Journal of Environmental Sciences,* 13(2)**,** pp 129-136.

Chen, B., Huang, W., Mao, J. & Lv, S. 2008. Enhanced sorption of naphthalene and nitroaromatic compounds to bentonite by potassium and cetyltrimethylammonium cations. *Journal of Hazardous Materials,* 158(1)**,** pp 116-123.

Chen, C.-Y. 2009. Photocatalytic degradation of azo dye reactive orange 16 by TiO2. *Water, Air, and Soil Pollution,* 202(1-4)**,** pp 335-342.

Cheremisinoff, N. P. 2001. *Handbook of Water and Wastewater Treatment Technologies*, USA: Butterworth-Heinemann.

Cheremisinoff, N. P. 2002a. Chapter 2 - What Filtration is All About. *In:* Cheremisinoff, N. P. (ed.) *Handbook of Water and Wastewater Treatment Technologies.* Woburn: Butterworth-Heinemann.

Cheremisinoff, N. P. 2002b. Chapter 8 - Sedimentation, Clarification, Flotation, and Coalescence. *In:* Cheremisinoff, N. P. (ed.) *Handbook of Water and Wastewater Treatment Technologies.* Woburn: Butterworth-Heinemann.

Chiappe, C., Capraro, D., Conte, V. & Pieraccini, D. 2001. Stereoselective halogenations of alkenes and alkynes in ionic liquids. *Organic Letters,* 3(7)**,** pp 1061-1063.

Choi, H.-D., Shin, M.-C., Kim, D.-H., Jeon, C.-S. & Baek, K. 2008. Removal characteristics of reactive black 5 using surfactant-modified activated carbon. *Desalination,* 223(1–3)**,** pp 290-298.

Chun, S., Dzyuba, S. V. & Bartsch, R. A. 2001. Influence of structural variation in room-temperature ionic liquids on the selectivity and efficiency of competitive alkali metal salt extraction by a crown ether. *Analytical Chemistry,* 73(15)**,** pp 3737-3741.

Cota-Espericueta, A. D. 2003. *Removal of 2, 4-dinitrophenol and 2, 4-dinitrotoluene from Water Using Surfactant Modified Activated Carbon.* PhD thesis, New Mexico State University.

Crini, G. 2006. Non-conventional low-cost adsorbents for dye removal: a review. *Bioresource Technology,* 97(9)**,** pp 1061-1085.

Das, A., Pal, A., Saha, S. & Maji, S. K. 2009a. Behaviour of fixed-bed column for the adsorption of malachite green on surfactant-modified alumina. *Journal of Environmental Science and Health, Part A,* 44(3)**,** pp 265-272.

Das, A. K., Saha, S., Pal, A. & Maji, S. K. 2009b. Surfactant-modified alumina: An efficient adsorbent for malachite green removal from water environment. *Journal of Environmental Science and Health, Part A,* 44(9)**,** pp 896-905.

Deitsch, J. J., Smith, J. A., Arnold, M. B. & Bolus, J. 1998. Sorption and desorption rates of carbon tetrachloride and 1,2-dichlorobenzene to three organobentonites and a natural peat soil. *Environmental Science & Technology,* 32(20)**,** pp 3169-3177.

Deng, S. & Ting, Y.-P. 2005. Characterization of PEI-modified biomass and biosorption of Cu(II), Pb(II) and Ni(II). *Water Research,* 39(10)**,** pp 2167-2177.

Dentel, S. K., Jamrah, A. I. & Sparks, D. L. 1998. Sorption and cosorption of 1, 2, 4-trichlorobenzene and tannic acid by organo-clays. *Water Research,* 32(12)**,** pp 3689-3697.

Doğan, D. & Türkdemir, H. 2005. Electrochemical oxidation of textile dye indigo. *Journal of Chemical Technology and Biotechnology,* 80(8)**,** pp 916-923.

Doren, A. & Goldfarb, J. 1970. Electrolyte effects on micellar solutions of nonionic detergents. *Journal of Colloid and Interface Science,* 32(1)**,** pp 67-72.

dos Santos, A. B., Cervantes, F. J. & van Lier, J. B. 2007. Review paper on current technologies for decolourisation of textile wastewaters: perspectives for anaerobic biotechnology. *Bioresource Technology,* 98(12)**,** pp 2369-2385.

Du, B., Guo, Z., Song, P. a., Liu, H., Fang, Z. & Wu, Y. 2009. Flame retardant mechanism of organo-bentonite in polypropylene. *Applied Clay Science,* 45(3)**,** pp 178-184.

Dupont, J. & Suarez, P. A. Z. 2006. Physico-chemical processes in imidazolium ionic liquids. *Physical Chemistry Chemical Physics,* 8(21)**,** pp 2441-2452.

Earle, M. J. & Seddon, K. R. 2000. Ionic liquids. Green solvents for the future. *Pure and Applied Chemistry,* 72(7)**,** pp 1391-1398.

El-Nahhal, Y. Z. & Safi, J. M. 2004. Adsorption of phenanthrene on organoclays from distilled and saline water. *Journal of Colloid and Interface Science,* 269(2)**,** pp 265-273.

Emam, E. A. 2013. Modified activated carbon and bentonite used to adsorb petroleum hydrocarbons emulsified in aqueous solution. *American Journal of Environmental Protection,* 2(6)**,** pp 161-169.

Esrafili, A., Yamini, Y., Ghambarian, M. & Moradi, M. 2011. Dynamic three-phase hollow fiber microextraction based on two immiscible organic solvents with automated movement of the acceptor phase. *Journal of Separation Science,* 34(1)**,** pp 98-106.

Estevinho, B. N., Martins, I., Ratola, N., Alves, A. & Santos, L. 2007. Removal of 2, 4-dichlorophenol and pentachlorophenol from waters by sorption using coal fly ash from a Portuguese thermal power plant. *Journal of Hazardous Materials,* 143(1)**,** pp 535-540.

Fadeev, A. G. & Meagher, M. M. 2001. Opportunities for ionic liquids in recovery of biofuels. *Chemical Communications,* 4(3)**,** pp 295-296.

Faouzi, A. M., Nasr, B. & Abdellatif, G. 2007. Electrochemical degradation of anthraquinone dye alizarin red S by anodic oxidation on boron-doped diamond. *Dyes and Pigments,* 73(1)**,** pp 86-89.

Feng, N., Guo, X., Liang, S., Zhu, Y. & Liu, J. 2011. Biosorption of heavy metals from aqueous solutions by chemically modified orange peel. *Journal of Hazardous Materials,* 185(1)**,** pp 49-54.

Forsyth, S. A., Pringle, J. M. & MacFarlane, D. R. 2004. Ionic Liquids : An Overview. *Australian Journal of Chemistry,* 57(2)**,** pp 113-119.

Frijters, C., Vos, R., Scheffer, G. & Mulder, R. 2006. Decolorizing and detoxifying textile wastewater, containing both soluble and insoluble dyes, in a full scale combined anaerobic/aerobic system. *Water Research,* 40(6)**,** pp 1249-1257.

Ghobadi, J., Arami, M., Bahrami, H. & Mahmoodi, N. M. 2013. Modification of carbon nanotubes with cationic surfactant and its application for removal of direct dyes. *Desalination and Water Treatment,* 52(22-24)**,** pp 4356-4368.

Gitipour, S., Bowers, M. T., Huff, W. & Bodocsi, A. 1997. The efficiency of modified bentonite clays for removal of aromatic organics from oily liquid wastes. *Spill Science & Technology Bulletin,* 4(3)**,** pp 155-164.

Gong, J.-L., Wang, B., Zeng, G.-M., Yang, C.-P., Niu, C.-G., Niu, Q.-Y., Zhou, W.-J. & Liang, Y. 2009. Removal of cationic dyes from aqueous solution using magnetic multi-wall carbon nanotube nanocomposite as adsorbent. *Journal of Hazardous Materials,* 164(2)**,** pp 1517-1522.

Gonzalez-Garcia, C. M., Gonzalez-Martin, M. L., Denoyel, R., Gallardo-Moreno, A. M., Labajos-Broncano, L. & Bruque, J. M. 2004a. Ionic surfactant adsorption onto activated carbons. *Jounranl of Colloid Interface Science,* 278(2)**,** pp 257–264.

Gonzalez-Garcia, C. M., Gonzalez-Martin, M. L., Gomez-Serrano, V., Bruque, J. M. & Labajos-Broncano, L. 2001. Analysis of the adsorption isotherms of a non-ionic surfactant from aqueous solution onto activated carbons. *Carbon,* 39(1)**,** pp 849–855.

Gonzalez-Garcia, C. M., Gonzalez-Martin, M. L., Gonzalez, J. F., Sabio, E., Ramiro, A. & Ganan, J. 2004b. Nonionic surfactants adsorption onto activated carbon: influence of the polar chain length. *Powder Technology,* 148(2)**,** pp 32–37.

Gregor, K. H. 1993. Oxidative decolourisation of textile wastewater with advanced oxidation processes. *Chemical Oxidation: Technologies for the Nineties,* 2(3)**,** pp 161-193.

Gupta, V. K., Jain, R. & Varshney, S. 2007. Electrochemical removal of the hazardous dye reactofix red 3 BFN from industrial effluents. *Journal of Colloid and Interface Science,* 312(2)**,** pp 292-296.

Gupta, V. K. & Suhas 2009. Application of low-cost adsorbents for dye removal – A review. *Journal of Environmental Management,* 90(8)**,** pp 2313-2342.

Hage, R. & Lienke, A. 2006. Applications of transition-metal catalysts to textile and wood-pulp bleaching. *Angewandte Chemie International Edition,* 45(2)**,** pp 206-222.

Hai, F. I., Yamamoto, K. & Fukushi, K. 2007. Hybrid treatment systems for dye wastewater. *Critical Reviews in Environmental Science and Technology,* 37(4)**,** pp 315-377.

Harper, M. & Purnell, C. J. 1990. Alkylammonium montmorillonites as adsorbents for organic vapors from air. *Environmental Science & Technology,* 24(1)**,** pp 55-62.

Ho, D. L., Briber, R. M. & Glinka, C. J. 2001. Characterization of organically modified clays using scattering and microscopy techniques. *Chemistry of Materials,* 13(5)**,** pp 1923-1931.

Holbrey, J. D. & Seddon, K. R. 1999. Ionic liquids. *Clean Products and Processes,* 1(4)**,** pp 223-236.

Hsu, Y.-C., Chen, J.-T., Yang, H.-C. & Chen, J.-H. 2001. Decolorization of dyes using ozone in gas-induced a reactor. *AIChE Journal,* 47(1)**,** pp 169-176.

Huang, H.-C., Lee, J.-F., Chao, H.-P., Yeh, P.-W., Yang, Y.-F. & Liao, W.-L. 2005. The influences of solid-phase organic constituents on the partition of aliphatic and aromatic organic contaminants. *Journal of Colloid and Interface Science,* 286(1)**,** pp 127-133.

Huddleston, J. G., Visser, A. E., Reichert, W. M., Willauer, H. D., Broker, G. A. & Rogers, R. D. 2001. Characterization and comparison of hydrophilic and hydrophobic room temperature ionic liquids incorporating the imidazolium cation. *Green Chemistry,* 3(4)**,** pp 156-164.

Husain, Q. 2006. Potential applications of the oxidoreductive enzymes in the decolorization and detoxification of textile and other synthetic dyes from polluted water: a review. *Critical Reviews in Biotechnology,* 26(4)**,** pp 201-221.

Ibrahim, S., Wang, S. & Ang, H. M. 2010. Removal of emulsified oil from oily wastewater using agricultural waste barley straw. *Biochemical Engineering Journal,* 49(1)**,** pp 78-83.

Iijima, S. 1991. Helical microtubules of graphitic carbon. *Nature,* 354(6348)**,** pp 56-58.

Jaynes, W. & Vance, G. 1999. Sorption of benzene, toluene, ethylbenzene, and xylene (BTEX) compounds by hectorite clays exchanged with aromatic organic cations. *Clays and Clay Minerals,* 47(3)**,** pp 358-365.

Jaynes, W. F. & Boyd, S. A. 1991. Clay mineral type and organic compound sorption by hexadecyltrimethlyammonium-exchanged clays. *Soil Science Society of America Journal,* 55(1)**,** pp 43-48.

Jess, A., Große Böwing, A. & Wasserscheid, P. 2005. Kinetik und reaktionstechnik der synthese ionischer flüssigkeiten. *Chemie Ingenieur Technik,* 77(9)**,** pp 1430-1439.

Juang, L.-C., Lee, C.-K., Wang, C.-C., Hung, S.-H. & Lyu, M.-D. 2008. Adsorptive removal of acid red 1 from aqueous solution with surfactant modified titanate nanotubes. *Environmental Engineering Science,* 25(4)**,** pp 519-528.

Juang, R. S., Tseng, R. L., Wu, F. C. & Lee, S. H. 1997. Adsorption behavior of reactive dyes from aqueous solutions on chitosan. *Journal of Chemical Technology and Biotechnology,* 70(4)**,** pp 391-399.

Kamran, S., Asadi, M. & Absalan, G. 2014a. Adsorption of folic acid, riboflavin, and ascorbic acid from aqueous samples by Fe3O4 magnetic nanoparticles using ionic liquid as modifier. *Analytical Methods,* 6(3)**,** pp 798-806.

Kamran, S., Hossein Tavallali & Azad, A. 2014b. Fast removal of reactive red 141 and reactive yellow 81 from aqueous solution by Fe3O4 magnetic nanoparticles modified with ionic liquid 1-octyl-3-methylimidazolium bromide. *Iranian Journal of Analytical Chemistry,* 1(1)**,** pp 78-86.

Kansal, S., Singh, M. & Sud, D. 2007. Studies on photodegradation of two commercial dyes in aqueous phase using different photocatalysts. *Journal of Hazardous Materials,* 141(3)**,** pp 581-590.

Kim, T.-H., Park, C., Yang, J. & Kim, S. 2004. Comparison of disperse and reactive dye removals by chemical coagulation and Fenton oxidation. *Journal of Hazardous Materials,* 112(1)**,** pp 95-103.

Kim, Y. S., Song, D. I., Jeon, Y. W. & Choi, S. J. 1996. Adsorption of organic phenols onto hexadecyltrimethylammonium-treated montmorillonite. *Separation Science and Technology,* 31(20)**,** pp 2815-2830.

Knapp, J., Newby, P. & Reece, L. 1995. Decolorization of dyes by wood-rotting basidiomycete fungi. *Enzyme and Microbial Technology,* 17(7)**,** pp 664-668.

Kuleyin, A. & Aydin, F. 2011. Removal of reactive textile dyes (remazol brillant blue R and remazol yellow) by surfactant-modified natural zeolite. *Environmental Progress & Sustainable Energy,* 30(2)**,** pp 141-151.

Kumar, R., Rashid, J. & Barakat, M. A. 2014. Synthesis and characterization of a starch-AlOOH-FeS$_2$ nanocomposite for the adsorption of Congo red dye from aqueous solution. *RSC Advances,* 4(72)**,** pp 38334-38340.

Lawrence, M. A. M., Kukkadapu, R. K. & Boyd, S. A. 1998. Adsorption of phenol and chlorinated phenols from aqueous solution by tetramethylammonium- and tetramethylphosphonium-exchanged montmorillonite. *Applied Clay Science,* 13(1)**,** pp 13-20.

Leclercq, L. & Schmitzer, A. R. 2009. Supramolecular effects involving the incorporation of guest substrates in imidazolium ionic liquid networks: Recent advances and future developments. *Supramolecular Chemistry,* 21(3-4)**,** pp 245-263.

Lee, C.-K., Liu, S.-S., Juang, L.-C., Wang, C.-C., Lyu, M.-D. & Hung, S.-H. 2007. Application of titanate nanotubes for dyes adsorptive removal from aqueous solution. *Journal of Hazardous Materials,* 148(3)**,** pp 756-760.

Lee, J.-F., Mortland, M. M., Boyd, S. A. & Chiou, C. T. 1989. Shape-selective adsorption of aromatic molecules from water by tetramethylammonium–smectite. *Journal of the Chemical Society, Faraday Transactions 1: Physical Chemistry in Condensed Phases,* 85(9)**,** pp 2953-2962.

Lee, J.-F., Mortland, M. M., Chiou, C. T., Kile, D. E. & Boyd, S. A. 1990. Adsorption of benzene, toluene, and xylene by two tetramethylammonium-smectites having different charge densities. *Clays and Clay Minerals,* 38(2)**,** pp 113-120.

Li, C., Dong, Y., Wu, D., Peng, L. & Kong, H. 2011. Surfactant modified zeolite as adsorbent for removal of humic acid from water. *Applied Clay Science,* 52(4)**,** pp 353-357.

Li, J., Smith, J. A. & Winquist, A. S. 1996. Permeability of earthen liners containing organobentonite to water and two organic liquids. *Environmental Science & Technology,* 30(10)**,** pp 3089-3093.

Li, Y.-H., Wang, S., Wei, J., Zhang, X., Xu, C., Luan, Z., Wu, D. & Wei, B. 2002. Lead adsorption on carbon nanotubes. *Chemical Physics Letters,* 357(3)**,** pp 263-266.

Li, Y., Chen, B. & Zhu, L. 2010. Enhanced sorption of polycyclic aromatic hydrocarbons from aqueous solution by modified pine bark. *Bioresource Technology,* 101(19)**,** pp 7307-7313.

Li, Z. & Bowman, R. S. 2001. Retention of inorganic oxyanions by organo-kaolinite. *Water Research,* 35(16)**,** pp 3771-3776.

Lin, S. H. & Peng, C. F. 1994. Treatment of textile wastewater by electrochemical method. *Water Research,* 28(2)**,** pp 277-282.

Longhinotti, E., Pozza, F., Furlan, L., Sanchez, M. d. N. d. M., Klug, M., Laranjeira, M. & Fávere, V. T. 1998. Adsorption of anionic dyes on the biopolymer chitin. *Journal of the Brazilian Chemical Society,* 9(5)**,** pp 435-440.

Lopes, A., Martins, S., Morao, A., Magrinho, M. & Gonçalves, I. 2004. Degradation of a textile dye CI direct red 80 by electrochemical processes. *Portugaliae Electrochimica Acta,* 22(3)**,** pp 279-294.

Lozano, P., Bernal, J. M., García-Verdugo, E., Vaultier, M. & Luis, S. V. 2014. *Biocatalysis in Ionic Liquids*, USA: CRC press.

Lu, C., Chung, Y.-L. & Chang, K.-F. 2005. Adsorption of trihalomethanes from water with carbon nanotubes. *Water Research,* 39(6)**,** pp 1183-1189.

Ma, J. & Zhu, L. 2006. Simultaneous sorption of phosphate and phenanthrene to inorgano–organo-bentonite from water. *Journal of Hazardous Materials,* 136(3)**,** pp 982-988.

MacFarlane, D. R., Forsyth, M., Howlett, P. C., Pringle, J. M., Sun, J., Annat, G., Neil, W. & Izgorodina, E. I. 2007. Ionic liquids in electrochemical devices and processes: managing interfacial electrochemistry. *Accounts of Chemical Research,* 40(11)**,** pp 1165-1173.

Maclay, W. N. 1956. Factors affecting the solubility of nonionic emulsifiers. *Journal of Colloid Science,* 11(3)**,** pp 272-285.

Mahmoodi, N., Abdi, J. & Bastani, D. 2014. Direct dyes removal using modified magnetic ferrite nanoparticle. *Journal of Environmental Health Science and Engineering,* 12(1)**,** pp 96.

Mallakpour, S. & Kolahdoozan, M. 2008. Room temperature ionic liquids as replacements for organic solvents: direct preparation of wholly aromatic polyamides containing phthalimide and S-valine moieties. *Polymer Journal,* 40(6)**,** pp 513-519.

Manne, S. & Gaub, H. E. 1995. Molecular organization of surfactants at solid-liquid interfaces. *Science,* 270(5241)**,** pp 1480-1482.

Marcucci, M., Nosenzo, G., Capannelli, G., Ciabatti, I., Corrieri, D. & Ciardelli, G. 2001. Treatment and reuse of textile effluents based on new ultrafiltration and other membrane technologies. *Desalination,* 138(1–3)**,** pp 75-82.

Marmagne, O. & Coste, C. 1996. Color removal from textile plant effluents. *American Dyestuff Reporter,* 85(4)**,** pp 6.

McKay, G., Al-Duri, B., Allen, S. J. & Thomson, A. 1998. Adsorption for liquid process effluents. *Ich. E. Semp. Pap,* 17(1)**,** pp 1-17.

Mishra, A. & Bajpai, M. 2006. The flocculation performance of Tamarindus mucilage in relation to removal of vat and direct dyes. *Bioresource Technology,* 97(8)**,** pp 1055-1059.

Mishra, A., Bajpai, M. & Pandey, S. 2006. Removal of dyes by biodegradable flocculants: a lab scale investigation. *Separation Science and Technology,* 41(3)**,** pp 583-593.

Montazer-Rahmati, M. M., Rabbani, P., Abdolali, A. & Keshtkar, A. R. 2011. Kinetics and equilibrium studies on biosorption of cadmium, lead, and nickel ions from aqueous solutions

by intact and chemically modified brown algae. *Journal of Hazardous Materials,* 185(1)**,** pp 401-407.

Moradi, M. & Yamini, Y. 2012. Surfactant roles in modern sample preparation techniques: A review. *Journal of Separation Science,* 35(18)**,** pp 2319-2340.

Mortland, M. 1970. Clay-organic complexes and interactions. *Advances in Agronomy,* 22(75)**,** pp 117.

Mortland, M. M., Shaobai, S. & Boyd, S. A. 1986. Clay-organic complexes as adsorbents for phenol and chlorophenols. *Clays and Clay Minerals,* 34(5)**,** pp 581-585.

Muruganandham, M. & Swaminathan, M. 2004. Decolourisation of reactive orange 4 by Fenton and photo-Fenton oxidation technology. *Dyes and Pigments,* 63(3)**,** pp 315-321.

Oei, B. C., Ibrahim, S., Wang, S. & Ang, H. M. 2009. Surfactant modified barley straw for removal of acid and reactive dyes from aqueous solution. *Bioresource Technology,* 100(18)**,** pp 4292-4295.

Okada, T., Morita, T. & Ogawa, M. 2004. Adsorption behavior of phenol for mono, bis and tris(2,2'-bipyridine)nickel(ii)- and tris(ethylenediamine)nickel(ii)-saponette intercalation compounds from aqueous solution. *Clay Science,* 12(5)**,** pp 277-284.

Okada, T. & Ogawa, M. 2002. Adsorption of Phenols onto 1, 1'-Dimethyl-4, 4'-bipyridinium-smectites. *Chemistry Letters,* 2(8)**,** pp 812-813.

Olivier-Bourbigou, H. & Magna, L. 2002. Ionic liquids: perspectives for organic and catalytic reactions. *Journal of Molecular Catalysis A: Chemical,* 182–183(0)**,** pp 419-437.

Olu-Owolabi, B. I., Diagboya, P. N. & Ebaddan, W. C. 2012. Mechanism of Pb^{2+} removal from aqueous solution using a nonliving moss biomass. *Chemical Engineering Journal,* 195–196(1)**,** pp 270-275.

Omura, T. 1994. Design of chlorine-fast reactive dyes: Part 4: degradation of amino-containing azo dyes by sodium hypochlorite. *Dyes and Pigments,* 26(1)**,** pp 33-50.

Özcan, A. & Özcan, A. S. 2005. Adsorption of acid red 57 from aqueous solutions onto surfactant-modified sepiolite. *Journal of Hazardous Materials,* 125(1–3)**,** pp 252-259.

Özcan, A. S., Erdem, B. & Özcan, A. 2004. Adsorption of acid blue 193 from aqueous solutions onto Na–bentonite and DTMA–bentonite. *Journal of Colloid and Interface Science,* 280(1)**,** pp 44-54.

Pandey, A., Singh, P. & Iyengar, L. 2007. Bacterial decolorization and degradation of azo dyes. *International Biodeterioration & Biodegradation,* 59(2)**,** pp 73-84.

Pandey, S. 2006. Analytical applications of room-temperature ionic liquids: A review of recent efforts. *Analytica Chimica Acta,* 556(1)**,** pp 38-45.

Pansuk, C. & Vinitnantharat, S. A comparative study of the adsorption of acid brown 75 and direct yellow 162 onto unmodified and surfactant modified granule developed from coal fly ash. Proceedings of the Second International Conference on Environmental Science and Technology VI, 2011. IACSIT Press Singapore, pp 49-53.

Park, J. W. & Jaffe, P. R. 1993. Partitioning of three nonionic organic compounds between adsorbed surfactants, micelles, and water. *Environmental Science & Technology,* 27(12)**,** pp 2559-2565.

Park, S. & Kazlauskas, R. J. 2003. Biocatalysis in ionic liquids–advantages beyond green technology. *Current Opinion in Biotechnology,* 14(4)**,** pp 432-437.

Pei, Y., Wang, J., Wu, K., Xuan, X. & Lu, X. 2009. Ionic liquid-based aqueous two-phase extraction of selected proteins. *Separation and Purification Technology,* 64(3)**,** pp 288-295.

Pei, Y. C., Wang, J. J., Xuan, X. P., Fan, J. & Fan, M. 2007. Factors affecting ionic liquids based removal of anionic dyes from water. *Environmental Science & Technology,* 41(14)**,** pp 5090-5095.

Perkins, W. S., Walsh, W., Reed, I. & Namboodri, C. 1996. A demonstration of reuse of spent dyebath water following color removal with ozone. *Textile Chemist and Colorist,* 28(8)**,** pp 31-37.

Poole, C. F. 2004. Chromatographic and spectroscopic methods for the determination of solvent properties of room temperature ionic liquids. *Journal of Chromatography A,* 1037(1–2)**,** pp 49-82.

Poole, C. F. & Poole, S. K. 2010. Extraction of organic compounds with room temperature ionic liquids. *Journal of Chromatography A,* 1217(16)**,** pp 2268-2286.

Przystaś, W., Zabłocka-Godlewska, E. & Grabińska-Sota, E. 2012. Biological removal of azo and triphenylmethane dyes and toxicity of process by-products. *Water, Air, & Soil Pollution,* 223(4)**,** pp 1581-1592.

Radha, K. V., Regupathi, I., Arunagiri, A. & Murugesan, T. 2005. Decolorization studies of synthetic dyes using phanerochaete chrysosporium and their kinetics. *Process Biochemistry,* 40(10)**,** pp 3337-3345.

Rai, H. S., Bhattacharyya, M. S., Singh, J., Bansal, T., Vats, P. & Banerjee, U. 2005. Removal of dyes from the effluent of textile and dyestuff manufacturing industry: a review of emerging techniques with reference to biological treatment. *Critical Reviews in Environmental Science and Technology,* 35(3)**,** pp 219-238.

Ralston, J. & Kitchener, J. A. 1975. The surface chemistry of amosite asbestos, an amphibole silicate. *Journal of Colloid and Interface Science,* 50(2)**,** pp 242-249.

Ranck, J. M., Bowman, R. S., Weeber, J. L., Katz, L. E. & Sullivan, E. J. 2005. BTEX removal from produced water using surfactant-modified zeolite. *Journal of Environmental Engineering,* 131(3)**,** pp 434-442.

Razo-Flores, E., Luijten, M., Donlon, B., Lettinga, G. & Field, J. 1997. Biodegradation of selected azo dyes under methanogenic conditions. *Water Science and Technology,* 36(6)**,** pp 65-72.

Redding, A., Burns, S., Upson, R. & Anderson, E. 2002. Organoclay sorption of benzene as a function of total organic carbon content. *Journal of Colloid and Interface Science,* 250(1)**,** pp 261-264.

Reetz, M. T., Wiesenhöfer, W., Franciò, G. & Leitner, W. 2002. Biocatalysis in ionic liquids: batchwise and continuous flow processes using supercritical carbon dioxide as the mobile phase. *Chemical Communications,* 3(9)**,** pp 992-993.

Ritter, J. A. Adsorption processes-history and recent developments. The 2008 Annual Meeting, November 15-17 2008 Philadelphia. pp 175.

Robinson, T., McMullan, G., Marchant, R. & Nigam, P. 2001. Remediation of dyes in textile effluent: a critical review on current treatment technologies with a proposed alternative. *Bioresource Technology,* 77(3)**,** pp 247-255.

Rosen, M. J. & Kunjappu, J. T. 2012. *Surfactants and Interfacial Phenomena*, USA: John Wiley & Sons.

Ruan, X., Liu, H., Chang, C.-Y. & Fan, X.-y. 2014. Preparation of organobentonite by a novel semidry-method and its adsorption of 2, 4–dichlorophenol from aqueous solution. *International Biodeterioration & Biodegradation,* 95(1)**,** pp 212-218.

Rytwo, G., Huterer-Harari, R., Dultz, S. & Gonen, Y. 2006. Adsorption of fast green and erythrosin-B to montmorillonite modified with crystal violet. *Journal of Thermal Analysis and Calorimetry,* 84(1)**,** pp 225-231.

Rytwo, G., Kohavi, Y., Botnick, I. & Gonen, Y. 2007. Use of CV- and TPP-montmorillonite for the removal of priority pollutants from water. *Applied Clay Science,* 36(1–3)**,** pp 182-190.

Sajjadi, H., Modaressi, A., Magri, P., Domańska, U., Sindt, M., Mieloszynski, J.-L., Mutelet, F. & Rogalski, M. 2013. Aggregation of nanoparticles in aqueous solutions of ionic liquids. *Journal of Molecular Liquids,* 186(1)**,** pp 1-6.

Schott, H., Royce, A. E. & Han, S. K. 1984. Effect of inorganic additives on solutions of nonionic surfactants: VII. Cloud point shift values of individual ions. *Journal of Colloid and Interface Science,* 98(1)**,** pp 196-201.

Senan, R. C. & Abraham, T. E. 2004. Bioremediation of textile azo dyes by aerobic bacterial consortium aerobic degradation of selected azo dyes by bacterial consortium. *Biodegradation,* 15(4)**,** pp 275-280.

Sheldon, R. 2001. Catalytic reactions in ionic liquids. *Chemical Communications,* 11(23)**,** pp 2399-2407.

Sheldon, R. A., Lau, R. M., Sorgedrager, M. J., van Rantwijk, F. & Seddon, K. R. 2002. Biocatalysis in ionic liquids. *Green Chemistry,* 4(2)**,** pp 147-151.

Shen, X.-E., Shan, X.-Q., Dong, D.-M., Hua, X.-Y. & Owens, G. 2009. Kinetics and thermodynamics of sorption of nitroaromatic compounds to as-grown and oxidized multiwalled carbon nanotubes. *Journal of Colloid and Interface Science,* 330(1)**,** pp 1-8.

Shen, Y.-H. 2004. Phenol sorption by organoclays having different charge characteristics. *Colloids and Surfaces A: Physicochemical and Engineering Aspects,* 232(2–3)**,** pp 143-149.

Sheng, G. & Boyd, S. A. 2000. Polarity effect on dichlorobenzene sorption by hexadecyltrimethylammonium-exchanged clays. *Clays and Clay Minerals,* 48(1)**,** pp 43-50.

Sheng, G., Wang, X., Wu, S. & Boyd, S. A. 1998. Enhanced sorption of organic contaminants by smectitic soils modified with a cationic surfactant. *Journal of Environmental Quality,* 27(4)**,** pp 806-814.

Shi, B., Li, G., Wang, D., Feng, C. & Tang, H. 2007. Removal of direct dyes by coagulation: The performance of preformed polymeric aluminum species. *Journal of Hazardous Materials,* 143(1)**,** pp 567-574.

Shichi, T. & Takagi, K. 2000. Clay minerals as photochemical reaction fields. *Journal of Photochemistry and Photobiology C: Photochemistry Reviews,* 1(2)**,** pp 113-130.

Shukla, M., Srivastava, N. & Saha, S. 2011. *Interactions and transitions in imidazolium cation based ionic liquids*, India: Intech Open Access Publisher.

Singla, P., Mehta, R. & Upadhyay, S. N. 2012. Clay modification by the use of organic cations. *Green and Sustainable Chemistry,* 2(3)**,** pp 21-25.

Smith, J. & Jaffé, P. 1994. Adsorptive selectivity of organic-cation-modified bentonite for nonionic organic contaminants. *Water, Air, and Soil Pollution,* 72(1-4)**,** pp 205-211.

Smith, J. A. & Jaffe, P. R. 1991. Comparison of tetrachloromethane sorption to an alkylammonium-clay and an alkyldiammonium-clay. *Environmental Science & Technology,* 25(12)**,** pp 2054-2058.

Smith, J. A. & Jaffe, P. R. 1994. Benzene transport through landfill liners containing organophilic bentonite. *Journal of Environmental Engineering,* 120(6)**,** pp 1559-1577.

Smith, J. A., Jaffe, P. R. & Chiou, C. T. 1990. Effect of ten quaternary ammonium cations on tetrachloromethane sorption to clay from water. *Environmental Science & Technology,* 24(8)**,** pp 1167-1172.

Soares, O. S. G., Orfao, J. J., Portela, D., Vieira, A. & Pereira, M. F. R. 2006. Ozonation of textile effluents and dye solutions under continuous operation: Influence of operating parameters. *Journal of Hazardous Materials,* 137(3)**,** pp 1664-1673.

Šostar-Turk, S., Simonič, M. & Petrinić, I. 2005. Wastewater treatment after reactive printing. *Dyes and Pigments,* 64(2)**,** pp 147-152.

Soule, N. M. & Burns, S. E. 2001. Effects of organic cation structure on behavior of organobentonites. *Journal of Geotechnical and Geoenvironmental Engineering,* 127(4)**,** pp 363-370.

Srinivasan, K. R. & Fogler, H. S. 1990. Use of inorgano-organo-clays in the removal of priority pollutants from industrial wastewaters: adsorption of benzo (a) pyrene and chlorophenols from aqueous solutions. *Clays and Clay Minerals,* 38(3)**,** pp 287-293.

Srinivasan, K. R. & Scott, H. 1990. Use of inorgano-organo-clays in the removal of priority pollutants from industrial wastewaters: structural aspects. *Clays and Clay Minerals,* 38(3)**,** pp 277-286.

Stark, A., L. MacLean, B. & D. Singer, R. 1999. 1-Ethyl-3-methylimidazolium halogenoaluminate ionic liquids as solvents for Friedel-Crafts acylation reactions of ferrocene. *Journal of the Chemical Society, Dalton Transactions,* 2(1)**,** pp 63-66.

Stockmeyer, M. 1991. Adsorption of organic compounds on organophilic bentonites. *Applied Clay Science,* 6(1)**,** pp 39-57.

Stolz, A. 2001. Basic and applied aspects in the microbial degradation of azo dyes. *Applied Microbiology and Biotechnology,* 56(1-2)**,** pp 69-80.

Street, G. B. & White, D. 1963. Adsorption by organo-clay derivatives. *Journal of Applied Chemistry,* 13(7)**,** pp 288-291.

Takahashi, C., Shirai, T., Hayashi, Y. & Fuji, M. 2013. Study of intercalation compounds using ionic liquids into montmorillonite and their thermal stability. *Solid State Ionics,* 241(3)**,** pp 53-61.

Turner, E. A., Pye, C. C. & Singer, R. D. 2003. Use of ab initio calculations toward the rational design of room temperature ionic liquids. *The Journal of Physical Chemistry A,* 107(13)**,** pp 2277-2288.

Upson, R. & Burns, S. 2006. Sorption of nitroaromatic compounds to synthesized organoclays. *Journal of Colloid and Interface Science,* 297(1)**,** pp 70-76.

Van der Zee, F. P. & Villaverde, S. 2005. Combined anaerobic–aerobic treatment of azo dyes—a short review of bioreactor studies. *Water Research,* 39(8)**,** pp 1425-1440.

Van Olphen, H. & Fripiar, J. 1981. Data handbook for clay materials and other non-metallic minerals. *Soil Science,* 131(1)**,** pp 62.

van Rantwijk, F. & Sheldon, R. A. 2007. Biocatalysis in ionic liquids. *Chemical Reviews,* 107(6)**,** pp 2757-2785.

Wagner, J., Chen, H., Brownawell, B. J. & Westall, J. C. 1994. Use of cationic surfactants to modify soil surfaces to promote sorption and retard migration of hydrophobic organic compounds. *Environmental Science & Technology,* 28(2)**,** pp 231-237.

Walker, G. & Weatherley, L. 2001. Adsorption of dyes from aqueous solution—the effect of adsorbent pore size distribution and dye aggregation. *Chemical Engineering Journal,* 83(3)**,** pp 201-206.

Wang, J.-P., Chen, Y.-Z., Ge, X.-W. & Yu, H.-Q. 2007. Optimization of coagulation–flocculation process for a paper-recycling wastewater treatment using response surface methodology. *Colloids and Surfaces A: Physicochemical and Engineering Aspects,* 302(1)**,** pp 204-210.

Wang, S. 2008. A comparative study of Fenton and Fenton-like reaction kinetics in decolourisation of wastewater. *Dyes and Pigments,* 76(3)**,** pp 714-720.

Wasserscheid, P. & Keim, W. 2000. Ionic liquids-new" solutions" for transition metal catalysis. *Angewandte Chemie,* 39(21)**,** pp 3772-3789.

Wasserscheid, P. & Waffenschmidt, H. 2000. Ionic liquids in regioselective platinum-catalysed hydroformylation. *Journal of Molecular Catalysis A: Chemical,* 164(1–2)**,** pp 61-67.

Welton, T. 1999. Room-temperature ionic liquids. Solvents for synthesis and catalysis. *Chemical Reviews,* 99(2)**,** pp 2071-2084.

Wesenberg, D., Kyriakides, I. & Agathos, S. N. 2003. White-rot fungi and their enzymes for the treatment of industrial dye effluents. *Biotechnology Advances,* 22(1)**,** pp 161-187.

Witthuhn, B., Pernyeszi, T., Klauth, P., Vereecken, H. & Klumpp, E. 2005. Sorption study of 2,4-dichlorophenol on organoclays constructed for soil bioremediation. *Colloids and Surfaces A: Physicochemical and Engineering Aspects,* 265(1–3)**,** pp 81-87.

Wu, J., Doan, H. & Upreti, S. 2008. Decolorization of aqueous textile reactive dye by ozone. *Chemical Engineering Journal,* 142(2)**,** pp 156-160.

Wu, S. H. & Pendleton, P. 2001. Adsorption of anionic surfactant by activated carbon: effect of surface chemistry, ionic strength, and hydrophobicity. *Journal of Colloid and Interface Science,* 243(2)**,** pp 306-315.

Xiao, J. X., Zhang, Y., Wang, C., Zhang, J., Wang, C. M., Bao, Y. X. & Zhao, Z. G. 2005. Adsorption of cationic–anionic surfactant mixtures on activated carbon. *Carbon,* 43(2)**,** pp 1032–1038.

Xu, S., Sheng, G. & Boyd, S. A. 1997. Use of organoclays in pollution abatement. *Advances in Agronomy,* 59(1)**,** pp 25-62.

Yan, H., Gong, A., He, H., Zhou, J., Wei, Y. & Lv, L. 2006. Adsorption of microcystins by carbon nanotubes. *Chemosphere,* 62(1)**,** pp 142-148.

Yapar, S. & Yilmaz, M. 2005. Removal of phenol by using montmorillonite, clinoptilolite and hydrotalcite. *Adsorption,* 10(4)**,** pp 287-298.

Yue, Q., Gao, B., Wang, Y., Zhang, H., Sun, X., Wang, S. & Gu, R. R. 2008. Synthesis of polyamine flocculants and their potential use in treating dye wastewater. *Journal of Hazardous Materials,* 152(1)**,** pp 221-227.

Zhang, F.-m., Knapp, J. S. & Tapley, K. N. 1998. Decolourisation of cotton bleaching effluent in a continuous fluidized-bed bioreactor using wood rotting fungus. *Biotechnology Letters,* 20(8)**,** pp 717-723.

Zhang, Y., Shen, Y., Yuan, J., Han, D., Wang, Z., Zhang, Q. & Niu, L. 2006. Design and synthesis of multifunctional materials based on an ionic-Liquid backbone. *Angewandte Chemie International Edition,* 45(35)**,** pp 5867 –5870.

Zhao, H. & Vance, G. F. 1998. Sorption of trichloroethylene by organo-clays in the presence of humic substances. *Water Research,* 32(12)**,** pp 3710-3716.

Zheng, D., Dong, L., Huang, W., Wu, X. & Nie, N. 2014. A review of imidazolium ionic liquids research and development towards working pair of absorption cycle. *Renewable and Sustainable Energy Reviews,* 37(1)**,** pp 47-68.

Zhou, Y., Chen, L., Lu, P., Tang, X. & Lu, J. 2011. Removal of bisphenol A from aqueous solution using modified fibric peat as a novel biosorbent. *Separation and Purification Technology,* 81(2)**,** pp 184-190.

Zhou, Y., Chen, L., Wang, X., Xu, Y. & Lu, J. 2012. Adsorption of phenanthrene by quaternary ammonium surfactant modified peat and the mechanism involved. *Water Science & Technology,* 66(4)**,** pp 810-815.

Zhou, Y., Liang, Z. & Wang, Y. 2008. Decolorization and COD removal of secondary yeast wastewater effluents by coagulation using aluminum sulfate. *Desalination,* 225(1)**,** pp 301-311.

Zhu, L., Chen, B. & Shen, X. 2000. Sorption of phenol, p-nitrophenol, and aniline to dual-cation organobentonites from water. *Environmental Science & Technology,* 34(3)**,** pp 468-475.

Zhu, L., Ren, X. & Yu, S. 1998. Use of cetyltrimethylammonium bromide-bentonite to remove organic contaminants of varying polar character from water. *Environmental Science & Technology,* 32(21)**,** pp 3374-3378.

CHAPTER 3: MATERIALS AND METHODOLOGY

This study is divided into three parts which include: (i) synthesis and characterization of two ionic liquids (ii) modification of different materials with ionic liquids and its characterization (iii) adsorption studies of pharmaceuticals, a polyaromatic hydrocarbon and dyes with the modified materials

3.1 REAGENTS AND MATERIALS

Methyl-imidazole, 1-bromodecahexane (CAS Number 1318-93-0), imidazole (CAS Number 288-32-4), 1-bromohexane (CAS Number 111-25-1), benzyl bromide (CAS Number 602-057-002) and phenanthrene (CAS Number 85-01-8) were purchased from Merck. Montmorillonite powder (CAS Number: 1318-93-0), kaolin (CAS Number 1318-747), DMSO (CAS Number 67-68-5), amaranth (CAS Number 915-67-3), congo red (CAS Number 573-58-0) and reactive blue (CAS Number 13324-20-4), and NaCl, ketoprofen (CAS Number 22071-15-4), diclofenac sodium salt (CAS number 15307-79-6), ibuprofen (CAS Number 15687-27-1), sulfamethoxazole (CAS Number: 723-46-6), tetracycline (CAS Number: 60-54-8), nalidixic acid (CAS Number 389-08-2), chloramphenicol (CAS Number: 56-75-7) and ampicillin (CAS Number 69-53-4) were all purchased from Sigma Aldrich. Double distilled deionized water was used for all sample preparation. Raw peanut shell (species *Arachis hypogaea*), and mature sausage fruit (*Kigelia pinnata*) were sourced in Durban.

3.2 SYNTHESIS OF IONIC LIQUIDS (IL)

3.2.1 Synthesis of 1-hexyl, 3-decahexyl Imidazolium Ionic Liquids
1-hexyl, 3-decahexyl imidazolium is a salt consisting of imidazolium (a five ring compound with two nitrogen atom with one of them a quaternary ammonium) at the center with a hexyl group and decahexyl alkyl (16 carbon) chain attached to the ammonium and the quaternary ammonium in the ring respectively. The preparation was in two stages, formation of the 1-hexyl imidazole and thereafter formation of the salt.

The formation of the 1-hexyl imidazole was prepared by modification of the method used by Starikova and co-workers (Starikova et al., 2003). Briefly, KOH (0.84 g, 0.015 mmol) was added to the solution of imidazole (0.01 mol) in DMSO (30 mL) and stirred at room temperature for 2 hours. Freshly distilled alkyl halide (0.01 mol) was added drop wise to the mixture with vigorous stirring and thereafter cooled in a water bath. After 5 h the mixture was diluted with distilled water and extracted with dichloromethane (10 x 10 mL), the organic layers were washed with distilled water to pH 7, and dried over $MgSO_4$. After removal of chloroform the residue was distilled under vacuum. Column chromatography was used for product purification. Before formation of the salt, the product was characterised by ^1H and ^{13}C NMR to ascertain its purity. (Spectral data can be found in Appendix C 2.0).

Formation of the salt was achieved using the Dzyuba and Bartsch (2001) method. An oil bath with a stirred flask containing equimolar amounts of 1-hexyl imidazole and the primary alkyl bromide (bromodecahexane) was heated at 140 °C for 10-15 min and thereafter cooled. The solution was heated again in the oil bath at 140 °C for another 10-15 min, followed by drying under vacuum at 100-120 °C to give the desired product of a highly viscous golden liquid that solidified at room temperature. Characterization and spectral data are reported in chapter 5.4.1.
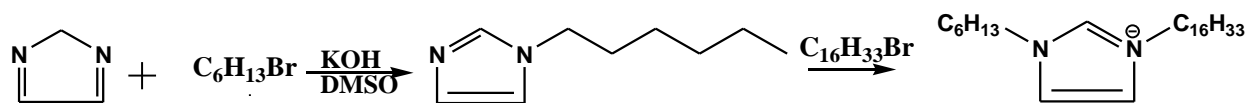
Scheme 1. Synthesis of 1-hexyl, 3-decahexyl imidazolium

3.2.2 Synthesis of 1-methyl, 3-decahexyl Imidazolium

1-methyl, 3-decahexyl imidazolium is a salt which consists of imidazolium (a five ring compound of two ammonium with one of them a quaternary ammonium) at the centre and a methyl group and decahexyl alkyl chain attached to the ammonium and the quaternary ammonium in the ring respectively. The method used by Dzyuba and Bartsch (2001) was modified for the synthesis of the salt. An oil bath with a stirred flask containing equimolar amounts of N-imidazole and the primary alkyl bromide (bromodecahexane) was heated at 140 °C for 10-15 min and thereafter cooled. The solution was heated again in the oil-bath at 140 °C for another 10-15 min, followed by drying under vacuum at 100-120 °C to give the desired product of a highly viscous golden

liquid that solidified at room temperature. Characterization and spectral data are reported in chapter 4.4.1.
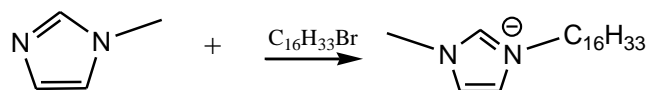
Scheme 2. Synthesis of 1-hexyl, 3-decahexyl imidazolium

3.3 PREPARATION OF THE ADSORBENT

3.3.1 Preparation of the Sodium-clay and Modification with IL

Montmorillonite was soaked in deionised water for 24 h and thereafter centrifuged. The upper layer having very fine clay, was decanted and converted to sodium–clay using the method employed by Zaghouane-Boudiaf and Boutahala (Zaghouane-Boudiaf and Boutahala, 2011). Briefly, 10 g of clay was mixed with 1 M NaCl solution and stirred for 24 h. Thereafter, it was dialyzed in deionized water until it was free of chloride and dried at 80 °C. The sodium–clay was further passed through a 53 μm sieve allowing for the fine sodium–clay (Na^+-clay) particles to be collected. The cation exchange capacity (CEC) of clay and clay modified ionic liquid were determined using the Gillman and Sumpter method (Gillman and Sumpter, 1986).

The Na^+–clay was then modified by adding IL in excess of the CEC of the clay to form clay-IL. Newman (1987) reported that clay can adsorb more than its CEC, and in the work of Xu and Boyd (1995) and Zhao et al. (1996) addition of organic cations greater than the CEC of clay, led to the adsorption of the organic cations on the external surface of the material through cation exchange and hydrophobic bonding, which generated positive charges on the surface. The mass of IL required was calculated and explained in chapters 4 and 5.

3.3.2 Preparation of Nut Shell (NS)

The peanut was removed from the shell and the shell was washed successively with tap water and double distilled deionized water to remove any unwanted particles and membranes. Thereafter, the shell was dried in an oven at 85 °C till dryness, ground in an Angstrom TE250 ring and puck pulveriser and sieved through a 120 micron sieve. A mass of 50 g powdered peanut shell was mixed with 100 mL of 1 M sodium hydroxide and then stirred for approximately 3 h at room

temperature. Thereafter, it was filtered off and washed repeatedly with double distilled deionised water until a neutral pH was achieved. The material was then dried in an oven at 85 $^{\circ}$C until dry and was labelled NS and stored in a desiccator until further use.

3.3.3 Preparation of Activated Carbon from NS

NS was calcined in a furnace under constant nitrogen flow, at a heating rate of 10 $^{\circ}$C min^{-1} until a temperature of 500 $^{\circ}$C was reached. The temperature was then maintained for a further 2 h. After 2 h the calcined material was activated by increasing the temperature to 800 $^{\circ}$C (under nitrogen) for a further 1 h 30 mins. The activated carbon obtained from the calcination was stored in a desiccator and labelled AC.

3.3.4 Modification of NS and AC

The AC was modified with the same ionic liquid in the same manner as ILNS. The modification of NS and AC by ionic liquid was done by adding ionic liquid in excess of its CMC (critical micelle concentration). A desired portion (in grams) of NS or AC powder was added into a known amount of ionic liquid already dissolved in methanol. The mixture was stirred at room temperature for 24 h, and thereafter, dried in an oven at 80 $^{\circ}$C overnight. The resulting modified material was cooled and washed several times with double distilled deionized water and dried in an oven. The resulting materials were labelled ILNS and ILAC respectively and stored in a desiccator until ready for use.

3.3.5 Preparation of KP-IL

Mature sausage fruit (*Kigelia pinnata*), KP, collected from a number of sausage trees in Durban, KwaZulu-Natal, was washed with distilled water to remove impurities and thereafter dried in an air circulating oven at 70 $^{\circ}$C till dry. The dried KP was ground, sieved through a 53 μm sieve and labeled KP. Modification with ionic liquid (IL) was achieved using the procedure by Ibrahim et al. (2010). Briefly, KP (5 g) was soaked in 200 mL of 1-methyl, 3-decahexyl imidazolium (0.25 mmol L^{-1}) in a methanol solution. The suspension was shaken on an orbital shaker for 24 h at room temperature (25 $^{\circ}$C). The modified KP was separated from the aqueous solution by vacuum filtration and thereafter washed with distilled water several times to remove surface retained IL. It was oven dried at 70 $^{\circ}$C overnight and was labelled as KP-IL.

3.4 ADSORPTION EXPERIMENTS

3.4.1 Batch Adsorption

All the experiments were carried out in glassware. To prevent sample contamination, all the containers were rinsed once with methanol and thrice with double distilled deionized water before use.

Adsorption experiments were performed in batch mode to investigate the effects of various process parameters such as pH, adsorbent and initial dye concentrations, contact time, and temperature on different materials. The effect of adsorbent dose was carried out with varying masses (g) of the adsorbents in constant volume (mL) of organic sample and constant concentration. Subsequent parameters (effect of concentration, pH, and temperature) were carried out using the same concentration and volume as in the case of dose. A blank was also determined under the same conditions but without the adsorbent. The concentration of the sample was measured using a UV−Vis−NIR spectrophotometer or LC-UV before and after the adsorption. All experiments were run for 24 h, to allow sufficient time for the adsorption to reach equilibrium conditions and were carried out in duplicate. The equilibrium adsorption capacities of the materials were calculated from the following relationship:

$$q_e = \frac{C_o - C_e}{W} V ...3.1$$

Where q_e is the equilibrium adsorption capacity (mg g^{-1}), C_0 and C_e are the sample initial and equilibrium concentrations respectively (in mg L^{-1}), V is the volume of solution (L), and W is the weight of adsorbent (g).

3.4.1.1 Kinetic study

Adsorption kinetics were determined by analysing the adsorptive uptake of samples from its aqueous solution of different concentrations (mg L^{-1}) at different times. The equilibrium data for developing the isotherms were obtained at different temperatures (20, 30, and 40 °C) by mixing a known mass (g) of adsorbent with pollutants for 36 h. After equilibrium, the aqueous phase

concentration of dye in the solution was determined by a double beam UV−Vis−NIR spectrophotometer or LC-UV.

In order to determine the mechanism and potential rate-controlling steps involved in the process of adsorption, the data obtained was fitted into pseudo first order (Lagergren, 1898) and pseudo second order (Ho and McKay, 1999) models. The pseudo first order kinetic model equation is:

$$In\ (q_e - q_t) = \ln q_e - K_1\,t ...3.2$$

Where q_t is the amount of adsorption at time t in (mg g^{-1}), k_1 is the rate constant of the equation in (min^{-1}), and q_e is the amount of adsorption equilibrium in (mg g^{-1}). The adsorption rate constant (k_1) can be determined experimentally by plotting ln (q_e-q_t) *versus* t.

The pseudo second order kinetic model is expressed as:

$$\frac{t}{q_t} = \frac{1}{(k_2 q_e^2)} + \frac{t}{q_e} ...3.3$$
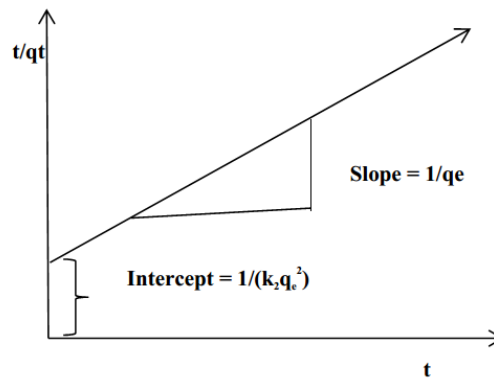
Fig. 3.1 Relation of constants in pseudo-second-order model

Where k_2 is the equilibrium rate constant of pseudo second order adsorption in (g mg^{-1} min^{-1}). The values of k_2 and q_e can be determined from the slope and intercept of the plot t/q_t *versus* t, respectively.

The data were also fitted into the Weber–Morris model, to evaluate the possibility of intra-particle diffusion as the rate limiting step; it is given by (Weber and Morris, 1963):

$$q_t = k_{id}t^{1/2} + C \text{...3.4}$$

Where k_{id} (mg g^{-1} h$^{-1/2}$) is the intra-particle diffusion rate constant.

3.4.1.2 Isotherm study

Adsorption data were fitted to Freundlich, (Freundlich, 1906) Langmuir, (Langmuir, 1916) Temkin and Dubinin–Raduskevich, (Dubinin and Radushkevich, 1947) isotherms. Linear equations of all the applied models are explained in chapters 4-8.

3.4.2 Column Studies

Column studies were conducted using glass columns of 1.5 cm internal diameter and 55 cm length. The columns were packed with a known quantity of the modified adsorbent between two supporting layers of glass wool to prevent the adsorbent floating from the outlet. The mass of the adsorbent was kept constant throughout the experiment. The flow rate was varied from 2 mL min^{-1} to 8.4 mL min^{-1} and influent concentration from 50 to 200 ppm. At different intervals, aliquots were removed from the effluent collected from the column for quantification.

3.4.2.1 Analysis of column data

Shape and time for breakthrough curve are very important characteristics for determining the operation and the dynamic response of adsorption in a column. The loading behavior of solute to be removed from solution in a column is shown by its breakthrough curve and is expressed in terms of adsorbed solute concentration (Cad), influent concentration of solute (Co), effluent concentration of solute (Ct) or normalized concentration defined as the ratio of effluent of solute concentration to influent solute concentration (Ct/Co) as a function of time or volume of effluent for a given bed height (Guo and Lua, 2003).

Total adsorbed quantity of solute q_{total} (mg) in the column, for a given influent concentration and flow rate, is calculated as described by Aksu and Gönen (2004). The equation and its parameters are explained in chapters 4 and 5.

3.4.2.2 Column models

Thomas model

The data obtained were fitted into the Thomas model (Thomas, 1944) in order to predict the adsorptive curve of breakthrough of the effluent and the determination of the maximum adsorption capacity of the adsorbent in the column. The linearized form and parameters are explained in chapters 4 and 5.

Adams–Bohart model

The data were also fitted into Adams-Bohart model (Bohart and Adams, 1920). This model assumes that the concentration of the adsorbing species and residual capacity of the adsorbent are both proportional to the adsorption rate. The Adams–Bohart model is used for the description of the initial part of the breakthrough curve. The linearized equation of the Adams-Bohart model is explained in chapters 4 and 5.

Yoon–Nelson model

The Yoon–Nelson model is straight forward unlike other models and also requires no detailed data concerning the characteristics of the adsorbate, the type of adsorbent, and the physical properties of the adsorption bed. The Yoon–Nelson is based on the assumption that the rate of decrease in the probability of adsorption for each adsorbate molecule is proportional to the probability of adsorbate adsorption and the probability of adsorbate breakthrough on the adsorbent (Yoon and Nelson, 1984). The linearized Yoon–Nelson equation is explained in chapters 4 and 5.

The data from the column was fitted into Thomas model (Thomas, 1944), Adams–Bohart model (Bohart and Adams, 1920) and Yoon–Nelson model (Yoon and Nelson, 1984)

3.5 PREPARATION OF STANDARDS, SAMPLE PRETREATMENT AND ANALYSIS OF INSTRUMENT

3.5.1 Standards

A 1000 mg L^{-1} stock solution of pharmaceuticals, PAH (phenanthrene)and dye standards were prepared by transferring 1 g of each standard to a 1000 mL volumetric flask and dissolving it in a small amount of methanol or double distilled deionized water as the case may be. After complete dissolution, the solution was made up to the mark with double distilled deionized water and homogenised by capping the flask and inverting a few times. The stock solution was stored in an amber glass bottle (to prevent degradation) and kept in a fridge at 4 °C prior to use. Thereafter, desired working concentrations were made from the stock solution using appropriate dilutions.

3.5.1.1 Preparation of working standard solutions

From the stock solution (1000 mg L^{-1}) the desired working standards were prepared using the dilution factor. The dilution factor is represented by the following equation:

$$C_1V_1 = C_2V_2...3.5$$

For example, a 50 mg L^{-1} solution of dye was prepared from a stock solution of 1000 mg L^{-1} by transferring a 1.50 mL aliquot of the stock solution to a 30 mL volumetric flask and making it up to mark with double distilled deionized water.

From equation 5

1000 mg L^{-1} x V$_1$ = 50 mg L^{-1} x 0.03 L

$$V_1 = \frac{50 \frac{mg}{L} X\ 0.03\ L}{1000\ mg/L}$$

V$_1$ = 0.0015 L

V$_1$ = 1.50 mL

Therefore, 1.50 mL of stock solution was required to prepare a 50 mg L^{-1} solution of dye in a 30 mL volumetric flask. Similarly, calibration standards in the range 0.50 – 200.00 mg L^{-1} were prepared and used to obtain a calibration graph.

3.5.2 Sample Pretreatment

Samples collected from the experiment as filtered through a 0.45 μm filter. The filtrates were further diluted with double distilled deionized water where necessary to fit in the range of the UV-Vis or the LC-UV.

3.5.3 Instrumental Analyses

Pharmaceuticals and polyaromatic hydrocarbon concentrations were determined by HPLC equipped with a UV detector. The summarized conditions used in the LC-UV instrument are presented in Table 3.1 and the concentrations of dyes and some pharmaceuticals (TC and NAD) were determined by double beam UV−Vis−NIR spectrophotometer (Shimadzu Model UV 3600, Japan) at λ_{max} ranging from 600 nm to 200 nm. The calibration curves with correlation coefficients (R^2) larger than 0.995 were used for the study as shown in Appendix A

Table 3.1 HPLC- UV method parameters for IBU, KET, DCL, AMP, SMZ, PHN and CHL

Parameters	IBU	KET	DCL	AMP	SMZ	PHN	CHL
Column type		Agilent C18,4.6 x 150 mm, 5 μm					
Injection volume (μL)		10.00					
Elution solvent system (Volume in %)	Methanol: acetonitrile : H$_2$O (85:15:5)	Aq. acetic acid:acetonitrile (57:43)	acetonitrile: H$_2$O (40:60)		0.05 M phosphoric acid : acetonitrile (83: 17, V : V)	acetonitrile: H$_2$O (40:60)	acetonitrile: H$_2$O (40:60)
Wave length (nm)	230	260	277	230	265	254	230
Flow rate (mL min^{-1})	1.00	1.00	1.00	1.00	1.00	1.00	1.00
Retention time (min)	9.89	8.36	3.10	3.04	11.20	4.45	2.81

3.6 CALCULATIONS

3.6.1 Determination of the Actual Concentrations of the Analytes

In calculating the actual concentration (mg L^{-1}) of the samples based on UV-Vis analysis, the absorbance (see Appendix B 3 for all absorbance spectra) obtained from the instrument (UV-Vis) was used.

From the calibration graph obtained from analysis of the standards, a straight line equation is obtained (see Appendix A1-A3).

$$y = mx + c...3.6$$

Where m = slope

X = concentration

Y = absorbance or peak area from the instrument

C = intercept

For example if the absorbance from the instrument is 50 and slope is 0.9997 (see Fig. 3.2) the actual sample concentration is calculated to be 1.576 mg L^{-1}.

$50 = x31.722$

$X = 1.576$ mg L^{-1}

$C = 0$

In the same way the actual concentration for all the samples were calculated.

While for LC-UV the peak area (see Appendix B 1 for samples) obtained from the instrument was used to determine the concentration of the analyte using the equation of the straight line as described in UV-vis. The dilution factors were taken into account where necessary and an average of the duplicate results was taken as the concentration.
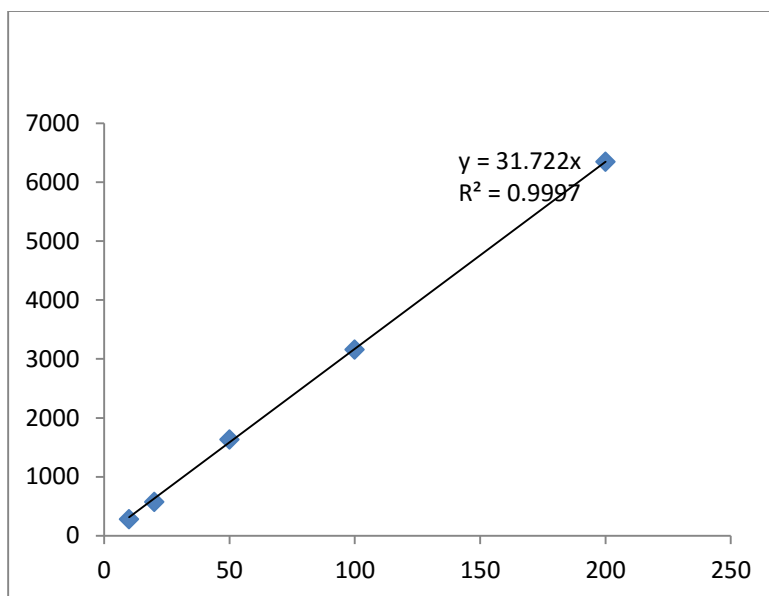
Fig. 3.2 Calibration curve for sulfamethoxazole

3.7 CHARACTERIZATION OF ADSORBENTS

3.7.1 Cation Exchange Capacity (CEC)

CEC of montmorillonite and kaolin were determined using the Gillman and Sumpter method (Gillman and Sumpter, 1986).

Procedure:

A centrifuge tube (30 mL) was weighed to the nearest mg, 2.00 g of the clay and 20 mL of 0.1 M BaCl$_2$.2H$_2$O was added, capped and shaken for 2 h. The mixture was centrifuged at about 10 000 rpm and decanted carefully. A 20 mL aliquot of 2 mM BaCl$_2$.2H$_2$O was added, capped, and shaken for an additional 1 h. It was centrifuged and the supernatant discarded.

These steps (adding 20 mL of 2 mM BaCl$_2$.2H$_2$O, capped, shaken for an additional 1 h, centrifuged and the supernatant discarded) were repeated twice. The slurry pH was obtained before the third centrifugation. After the third decantation of supernatant, 10.00 mL of 5 mM MgSO$_4$ was add and gently shaken for 1 h. Conductivity of the 1.5 mM MgSO$_4$ solution was determined (~300 μmhos),

and the conductivity of the sample solution was adjusted to make it approximately 1.5 times the value of 1.5 mM $MgSO_4$, with the addition of 0.100 mL increments of 0.1 M $MgSO_4$ (keeping track of the amount of 0.1 M $MgSO_4$ added). The pH of the solution was determined and adjusted with 0.05 M H_2SO_4 drop-wise until the pH was approximately 0.1 unit away from the previous measure. Double distilled deionized water was added and the solution mixed until the solution conductivity was equal to that of 1.5 mM $MgSO_4$. The solution pH and conductivity were adjusted alternately until the endpoint was reached. The outside of the tube was wiped dry and weighed.

CEC was calculated using this equation:

$$CEC \left(\frac{meq}{100\ g} \right) = (c - b)\ X\ 50...3.7$$

Where

b = total solution (mL) x 0.003 (meq mL^{-1}) [1.5 mM $MgSO_4$ had 0.003 meq mL^{-1}]

   [total solution (mL) = final tube weight (g) - tube tare weight (g) - 2 g (weight of soil used)]

c = Total Mg added (meq) = 0.1 meq (meq in 10 mL of 5 mM $MgSO_4$) + meq added in 0.1 M

   $MgSO_4$ (mL of 0.1 M $MgSO_4$) x 0.2 meq mL^{-1} (0.1 M$MgSO_4$ has 0.2 meq mL^{-1})

Example:

If a tube weighed 15.258 g, the final weight of the tube was 50.591 g, and 11.20 mL of 0.1 M $MgSO_4$ was added.

Total solution (mL)

   = 50.591 (final tube wt.) - 15.258 (tube wt.) - 2.00 g (clay wt.) = 33.333 mL

b = Mg in solution (meq)

   = 33.333 mL x 0.003 meq mL^{-1} [1.5 mM $MgSO_4$] = 0.100 meq

c = Total Mg added (meq)

   = 0.1 meq (10 mL of 5 mM $MgSO_4$) + 11.20 mL x 0.2 meq mL^{-1} (0.1 M $MgSO_4$)

   = 2.340 meq

CEC (meq 100 g^{-1}) = 2.340 meq (added) - 0.100 meq (final) x 50 = 112 meq 100 g^{-1}

3.7.2 Critical Micelle Concentration (CMC)

The CMC of 1-hexyl, 3-decahexyl imidazolium ionic liquids and 1-methyl, 3-decahexyl imidazolium ionic liquids were determined using a conductometric method described by Mandavi et al. (2008). Varying concentrations from 0.5×10^{-4} to 0.1 mol dm^{-3} of the ionic liquids were prepared and were plotted against their respective conductivities. The CMC value is the point where the intercept of two linear functions with mutually different slopes occurs (see sample graph in Appendix F 2.2).

3.7.3 Instrumentation

All the instruments used in this work are explained in detail in chapters 4 – 8.

3.8 REFERENCES

Aksu, Z. & Gönen, F. 2004. Biosorption of phenol by immobilized activated sludge in a continuous packed bed: prediction of breakthrough curves. *Process Biochemistry,* 39(5)**,** pp 599-613.

Bohart, G. & Adams, E. 1920. Some aspects of the behavior of charcoal with respect to chlorine. 1. *Journal of the American Chemical Society,* 42(3)**,** pp 523-544.

Dubinin, M. & Radushkevich, L. 1947. Equation of the characteristic curve of activated charcoal. *Chemisches Zentralblatt,* 1(1)**,** pp 875.

Dzyuba, S. V. & Bartsch, R. A. 2001. Efficient synthesis of 1-alkyl (aralkyl)-3-methyl (ethyl) imidazolium halides: precursors for room-temperature ionic liquids. *Journal of Heterocyclic Chemistry,* 38(1)**,** pp 265-268.

Freundlich, H. 1906. Über die Adsorption in Lösungen. *Zeitschrift fur Physikalische Chemie,* 57(A)**,** pp 385-470.

Gillman, G. & Sumpter, E. 1986. Modification to the compulsive exchange method for measuring exchange characteristics of soils. *Soil Research,* 24(1)**,** pp 61-66.

Guo, J. & Lua, A. C. 2003. Textural and chemical properties of adsorbent prepared from palm shell by phosphoric acid activation. *Materials Chemistry and Physics,* 80(1)**,** pp 114-119.

Ho, Y.-S. & McKay, G. 1999. Pseudo-second order model for sorption processes. *Process Biochemistry,* 34(5)**,** pp 451-465.

Ibrahim, S., Wang, S. & Ang, H. M. 2010. Removal of emulsified oil from oily wastewater using agricultural waste barley straw. *Biochemical Engineering Journal,* 49(1)**,** pp 78-83.

Lagergren, S. 1898. About the theory of so-called adsorption of soluble substances. *Kungliga Svenska Vetenskapsakademiens Handlingar,* 24(4)**,** pp 1-39.

Langmuir, I. 1916. The constitution and fundamental properties of solids and liquids. *Journal of the American Chemical Society,* 38(11)**,** pp 2221-2295.

Mandavi, R., Sar, S. K. & Rathore, N. 2008. Critical micelle concentration of surfactant, mixed–surfactant and polymer by different method at room temperature and its importance. *Oriental Journal of Chemistry,* 24(2)**,** pp 559-564.

Newman, A. C. 1987. *Chemistry of Clays and Clay Minerals*, USA: Wiley-Interscience.

Starikova, O., Dolgushin, G., Larina, L., Komarova, T. & Lopyrev, V. 2003. Synthesis of new stable carbenes from the corresponding 1, 3-dialkylimidazolium and benzimidazolium salts. *Arkivoc,* 13(2)**,** pp 119-124.

Thomas, H. C. 1944. Heterogeneous Ion Exchange in a Flowing System. *Journal of the American Chemical Society,* 66(10)**,** pp 1664-1666.

Weber, W. J. & Morris, J. C. 1963. Kinetics of adsorption on carbon from solution. *Journal of the Sanitary Engineering Division. ASCE,,* 89(1)**,** pp 31.

Xu, S. & Boyd, S. A. 1995. Cationic surfactant sorption to a vermiculitic subsoil via hydrophobic bonding. *Environmental Science & Technology,* 29(2)**,** pp 312-320.

Yoon, Y. H. & Nelson, J. H. 1984. Application of gas adsorption kinetics I. A theoretical model for respirator cartridge service life. *The American Industrial Hygiene Association Journal,* 45(8)**,** pp 509-516.

Zaghouane-Boudiaf, H. & Boutahala, M. 2011. Preparation and characterization of organo-montmorillonites. Application in adsorption of the 2, 4, 5-trichlorophenol from aqueous solution. *Advanced Powder Technology,* 22(6)**,** pp 735-740.

Zhao, H., Jaynes, W. F. & Vance, G. F. 1996. Sorption of the ionizable organic compound, dicamba (3, 6-dichloro-2-methoxy benzoic acid), by organo-clays. *Chemosphere,* 33(10)**,** pp 2089-2100.

CHAPTER 4: SYNTHESIS, CHARACTERISATION AND APPLICATION OF IMIDAZOLIUM BASED IONIC LIQUID MODIFIED MONTMORILLONITE SORBENTS FOR THE REMOVAL OF AMARANTH DYE

Isiaka A. Lawal[a] and Brenda Moodley[a]*

[a]School of Chemistry and Physics, College of Agriculture, Engineering and Science, University of KwaZulu-Natal, P/Bag X45001, Westville Campus, Durban, 4000, South Africa

*corresponding author email: moodleyb3@ukzn.ac.za

Tel: +27 31 2602796; Fax: +27 31 2603091

First author: lawalishaq000123@yahoo.com

Synthesis, characterisation and application of imidazolium based ionic liquid modified montmorillonite sorbents for the removal of amaranth dye†

Isiaka A. Lawal and Brenda Moodley*

The removal of amaranth dye using montmorillonite modified with an ionic liquid (IL) was investigated. An ionic liquid (1-methyl, 3-decahexyl imidazolium) was synthesised, and characterised by nuclear magnetic resonance (^{1}H and ^{13}C NMR), Fourier transform infrared (FT-IR) spectroscopy, high resolution mass spectroscopy (HR-MS) as well as thermal gravimetric analysis and differential thermal (TGA/DCS) analysis. The ionic liquid was thereafter used to modify sodium montmorillonite (Na⁺-Mt) to form a hydrophobic montmorillonite that has a positively charged surface, by adding IL in excess of the cation exchange capacity (CEC) of Na⁺-Mt. Energy dispersive X-ray analyser (EDX) was used to determine the chemical composition of Na⁺-Mt. Modified montmorillonite (Mt-IL) and Na⁺-Mt was characterised using FT-IR, scanning electron microscopy (SEM), X-ray diffraction (XRD) and Brunauer–Emmett–Teller (BET) method, and used in the adsorption study of an anionic amaranth dye. A higher CEC of the Mt-IL (112 meq per 100 g) than Na⁺-Mt (89 meq per 100 g) was observed. The effects of sorbent dosage, dye concentration, solution pH and contact time were investigated in order to determine optimal experimental conditions. Optimum adsorption was obtained at pH 2 and adsorption data was better described by the pseudo-second-order kinetics and Langmuir adsorption isotherm. A maximum adsorption capacity of 263.2 mg g⁻¹ was calculated. The thermodynamic parameters $\Delta G°$, $\Delta H°$ and $\Delta S°$ were also investigated at temperatures of 313, 303 and 293 K. Column studies were performed on the modified material and the data generated was applied to the Thomas model where high column adsorption capacities of 393.7, 580.9 and 603.6 mg g⁻¹ at different concentrations were obtained.

4.1 ABSTRACT

The removal of amaranth dye using montmorillonite modified with an ionic liquid (IL) was investigated. An ionic liquid (1-methyl, 3-decahexyl imidazolium) was synthesised, and characterised by nuclear magnetic resonance (1H and 13C NMR), fourier transform infrared (FT-IR) spectroscopy, high resolution mass spectroscopy (HR-MS) as well as thermal gravimetric analysis and differential thermal (TGA/DCS) analysis. The ionic liquid was thereafter used to modify sodium montmorillonite (Na^+–Mt) to form a hydrophobic montmorillonite that has a positively charged surface, by adding IL in excess of the cation exchange capacity (CEC) of Na^+–Mt. Energy dispersive X-ray analyser (EDX) was used to determine the chemical composition of Na^+–Mt. Modified montmorillonite (Mt–IL) and Na^+–Mt was characterised using FT-IR, scanning electron microscopy (SEM), x-ray diffraction (XRD) and Brunauer−Emmett−Teller (BET) method, and used in the adsorption study of an anionic amaranth dye. A higher CEC of the Mt–IL (112 meq per 100 g) than Na^+-Mt (89 meq per 100 g) was observed. The effects of sorbent dosage, dye concentration, solution pH and contact time were investigated in order to determine optimal experimental conditions. Optimum adsorption was obtained at pH 2 and adsorption data was better described by the pseudo-second-order kinetics and Langmuir adsorption isotherm. A maximum adsorption capacity of 263.2 mg g-1 was calculated. The thermodynamic parameters $\Delta G°$, $\Delta H°$ and $\Delta S°$ were also investigated at temperatures of 313, 303 and 293 K. Column studies were performed on the modified material and the data generated was applied to the Thomas model where high column adsorption capacities of 393.7, 580.9 and 603.6 mg g-1 at different concentrations were obtained.

Keywords: *Ionic liquid, 1-methyl 3-decahexyl imidazolium, montmorillonite, column studies, adsorption, Amaranth.*

4.2 INTRODUCTION

Montmorillonite has been extensively used for the adsorption of organic compounds.(Avisar et al., 2010; Meleshyn and Tunega, 2011; Wu et al., 2013) Recently, research has focused on the modification of montmorillonite using a variety of methods and modifiers. Montmorillonite has been modified using dimethyl dihydrogenated tallow ammonium, ammonium and phosphonium surfactants.(Ho et al., 2001; Singla et al., 2012) Other modifiers include polypropylene on bentonite,(Du et al., 2009) hexadecyltrimethylammonium (HDTMA) on montmorillonite, montmorillonite intercalated with cetyltrimethylammonium octadecylamine and cetylpyridinium(Boufatit et al., 2008; Pospışil et al., 2002; Pospíšil et al., 2001) among others.

These modifications have been based on the high cation exchange capacity (CEC) of montmorillonite, its swelling capacity and high surface area, all resulting in strong adsorption and adsorption capacities.(Zaghouane-Boudiaf and Boutahala, 2011; Huang et al., 2004) The aluminosilicate layer of montmorillonite has a ratio of 2:1 type structure, with an octahedral Al2–3(OH)6 layer.(Newman, 1987) The position of the aluminosilicate results in a weak interaction between adjacent lamellae (Si-O---O-Si). As a result, montmorillonite easily separates and coupled with its high cationic exchange capacity ensures favourable conditions for intercalation reactions. Si^{4+} substituted with Al^{3+} in the tetrahedral layer and Mg^{2+} substituted for Al^{3+} in the octahedral layer results in a net negative charge on the clay surfaces. The deficit in charge is balanced by the exchangeable Na^+ or Ca^{2+} cation in the interlayer.(Zaghouane-Boudiaf and Boutahala, 2011) If the inorganic cations of montmorillonite are replaced by large alkyl ammonium ions, the physical properties of the montmorillonite changes and the hydrophilic nature of montmorillonite is converted to a hydrophobic form (organo-montmorillonite). (Lee and Kim, 2002b) Organo-montmorillonite has been used for the adsorption of dye,(Lee et al., 2001; Vakili et al., 2014) phenolic compounds and other aromatic compounds(Upson and Burns, 2006) as well as pesticides (Hsu et al., 2000).

Ionic liquids (ILs) have recently been used for the modification of montmorillonite (Takahashi et al., 2013) and nanoparticles (Sajjadi et al., 2013). There is presently limited information on the adsorption of organics (including dye) using IL modified materials. To the best of our knowledge the only reported studies are for the adsorption of reactive red-120 (RR) and 4-(2-pyridylazo)

resorcinol (PAR) from aqueous solution by Fe_3O_4 magnetic nanoparticles using ionic liquid as a modifier which was recently studied by Absalan and co workers(Absalan et al., 2011) and who reported a significant increase in adsorption capacity. Also, adsorption of folic acid, riboflavin, and ascorbic acid from aqueous samples by Fe_3O^+ magnetic nanoparticles using ionic liquid as modifier was also investigated (Kamran et al., 2014) but no reports have been reported on IL modified montmorillonite. This lack of research on IL modified montmorrilonite for the adsorption of dyes has prompted our investigation into the adsorption behaviour of dyes on IL modified montmorillonite.

They (ILs) are low-melting-point salts and form liquids that consist only of cations and anions. Ionic liquids are often considered as green solvents capable of replacing traditional organic solvents (Welton, 1999), composing of an organic cation and an inorganic anion (Turner et al., 2003). The anion mainly controls their water miscibility (Huddleston et al., 2001) whereas the length of the alkyl chains of the cations influences all the other properties(Jess et al., 2005) such as the hydrophobicity of the material.

In this work, cationic IL (1-methyl, 3-decahexzyl imidazolium) was synthesised (the choice of 16 carbon atoms was guided by the work of Beall (Beall, 1985)) and used in modifying montmorillonite which was then used to adsorb anionic amaranth dye. Amaranth is a class of azo dye, which is toxic, and its removal from wastewaters is very important as its presence, even in very low concentration, affects aquatic life and invariably affects the food chain. To the best of our knowledge this is the first report of the use of ionic liquid modified montmorillonite for the adsorption of dye.

4.3 EXPERIMENTAL SECTION

4.3.1 Materials

Montmorillonite K 10 powder (CAS Number 1318-93-0) used in the present study was purchased from Sigma Aldrich. Its chemical formula is $Na_{2/3}Si_8(Al_{10/3}Mg_{2/3})O_{20}(OH)_4$. Methyl-imidazole, 1-bromodecahexane, montmorillonite, NaCl and amaranth (CAS Number 915-67-3) were purchased from Sigma Aldrich. Double distilled deionized water was used for all sample preparation.
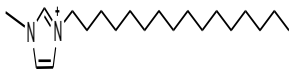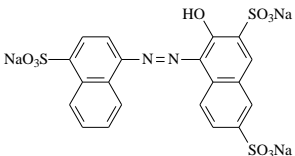
4.3.2 Apparatus

^{1}H and ^{13}C NMR spectra of the derivatives were recorded on an AVANCE DPX-400 (400 MHz) spectrophotometer (Bruker, U.S.A.) with tetramethylsilane (TMS) as the internal standard. High-resolution mass data were obtained using a Bruker micro TOF-Q II ESI instrument operating at ambient temperature. Thermal gravimetric analysis and differential thermal analysis (TGA-DTA/DSC) (SDT Q 600 V 20.9 Build 20 instrument) was used to measure changes in chemical and physical properties of the material. This was measured as a function of increasing temperature from ambient to 1000 °C (with a constant heating rate of 5 °C min^{-1}) under nitrogen atmosphere with a flow rate of 50 mL min^{-1}. FT-IR spectra of the IL - sodium montmorillonite (Na^{+}–Mt) and sodium montmorillonite modified with 1-methyl, 3-decahexyl imidazolium (Mt–IL) samples were recorded on a Perkin Elmer 100 series FT-IR spectrometer. BET Tri-star II 3020.VI.03 was used to determine the surface area, pore-size, pore volume and pore size distribution. The material was degassed using (Micromeritics vacprep 061, sample degas system) at 90 °C for 1 hr and was increased to 200 °C for 12 hr. The sample was then analysed by Tri-star II 3020.VI.03 under nitrogen atmosphere at 77 K. The surface morphology of the material was examined by scanning electron microscopy (SEM) using the Leo 435 VP model. Chemical composition analysis of montmorillonite was determined using on a Leo 1450 Scanning Electron Microscope equipped with energy dispersive X-ray analyser (EDX). The interlayer spacing of Na^{+}–Mt and Mt–IL was measured by X-ray powder diffraction (XRD, Shimadzu XRD-6000, Japan, Cu Kα radiation, 40 kV, 40 mA, Japan), and data were collected for 2θ ranging from 1.3° to 10° with the scan speed of 1° min[-1].

4.3.3 Preparation of Ionic Liquid (IL), 1-methyl, 3-decahexyl Imidazolium

1-methyl, 3-decahexyl imidazolium is a salt which consists of imidazolium (a five ring compound of two ammonium with one of them a quaternary ammonium) at the centre, a methyl group and decahexyl alkyl chain attached to the ammonium and the quaternary ammonium in the ring respectively. The method used by Dzyuba and Bartsch (Dzyuba and Bartsch, 2001) was modified for the synthesis of the salt. An oil bath with a stirred flask containing equimolar amounts of N-imidazole and the primary alkyl bromide (bromodecahexane) was heated at 140 °C for 10-15 min and thereafter cooled. The solution was heated again in the oil-bath at 140 °C for another 10-15 min, followed by drying under vacuum at 100-120 °C to give the desired product, a highly viscous golden liquid that solidified at room temperature.

Table 4.1 Properties of the surfactant and amaranth used in this study

Compound	Formula	Structure	Molecular Weight (M.W.) g mol^{-1}	Appearance	Melting point (°C)
1-methyl, 3-decahexyl imidazolium	$C_{20}H_{39}N_2^+$		307.311	Golden/solid at room temperature	62-64
Amaranth	$C_{20}H_{11}N_2Na_3O_{10}S_3$		604.473	Powder/Dark red	120

4.3.4 Preparation of Sodium-montmorillonite (Na$^+$–Mt) and Modification with IL

Montmorillonite was soaked in deionised water for 24 hr and thereafter centrifuged. The upper layer having very fine clay, was decanted and converted to sodium montmorillonite (Na$^+$-Mt) using the method employed by Zaghouane-Boudiaf and Boutahala (Zaghouane-Boudiaf and Boutahala, 2011). Briefly, 10 g of montmorillonite was mixed with 1 M NaCl solution and stirred for 24 hr. Thereafter, it was dialyzed in deionized water until it was free of chloride and dried at 80 °C. Na$^+$–Mt was further passed through a 53 µm sieve allowing for the fine Na$^+$-Mt particles to be collected. The cation exchange capacity (CEC) of Na$^+$–Mt and Mt-IL were determined using the Gillman and Sumpter method (Gillman and Sumpter, 1986), with a CEC value of 89 meq per 100 g.

The Na$^+$–Mt was then modified by adding IL in excess of the CEC of the clay to form Mt-IL. Newam (Newman, 1987) reported that clay can adsorb more than its CEC and in the work of Xu and Boyd (Xu and Boyd, 1995; Zhao et al., 1996), addition of an organic cation greater than the CEC of clay, led to the adsorption of the organic cation on the external surface of the material through cation exchange and hydrophobic bonding, which generated positive charges on the surface. The mass of IL required was calculated using the following equation (Soule and Burns, 2001):

$$mc = f * CEC * X * GMW ...4.1$$

Where *mc* is the mass of organic cation required to achieve the desired fraction of CEC (g), *f* is the fraction of cation-exchange capacity satisfied by the organic cation (no unit), CEC is the cation exchange capacity of the clay (mmol g^{-1} clay), X is the mass of clay (g) and GMW is the gram molecular weight of IL (g mol^{-1}).

The desired IL was slowly added to the desired mass of Na$^+$–Mt dispersed in methanol. The mixture was stirred overnight and the modified montmorillonite was washed several times with double distilled deionized water and thereafter dried in an oven at 100 °C overnight.

4.3.5 Batch Adsorption Studies

Adsorption experiments were performed in batch mode to investigate the effects of various process parameters such as pH, adsorbent and initial dye concentrations, contact time, and temperature on Na$^+$-Mt and Mt–IL. The effect of dose of the adsorbent was carried out with 0.005 g to 0.1 g in 30 mL of amaranth dye having a concentration of 50 mg L^{-1}; subsequent parameters (effect of concentration, pH, and temperature) were carried out using the same concentration and volume as in the case of dose. A blank was also determined under the same conditions but without the adsorbent. The concentration of the dye was always measured before and after the adsorption. All experiments were run for 24 hr, to allow sufficient time for the adsorption to reach equilibrium conditions and were carried out in duplicate.

Adsorption kinetics were determined by analysing the adsorptive uptake of amaranth dye from its aqueous solution of 20 mg L^{-1}, 50 mg L^{-1}, 100 mg L^{-1} and 200 mg L^{-1} concentrations at different times. The equilibrium data for developing the isotherms were obtained at different temperatures (20, 30, and 40 °C) by mixing 0.05 g of Mt–IL with amaranth for 36 hr. After equilibrium, the aqueous phase concentration of dye in the solution was determined by a double beam UV−Vis−NIR spectrophotometer (Shimadzu Model UV 3600, Japan) at λ_{max} 520 nm. The equilibrium adsorption capacity of Mt–IL and Na$^+$–IL were calculated from the following relationship:

$$q_e = \frac{C_o - C_e}{W} V ...4.2$$

Where q_e is the equilibrium adsorption capacity in (mg g^{-1}), C$_0$ and C$_e$ are the dye concentrations at initial and at equilibrium respectively, in mg L^{-1}, V is the volume of solution in (L), and W is the weight of adsorbent in (g).

Adsorption data were fitted to Freundlich (Freundlich, 1906), Langmuir (Langmuir, 1916), Temkin and Dubinin–Raduskevich (Dubinin and Radushkevich, 1947) isotherms. Linear equations of all the applied models are:

$$\text{Langmuir model: } \frac{C_e}{q_e} = \frac{C_e}{q_m} + \frac{1}{q_m b}...4.3$$

$$\text{Freundlich model: } \ln q_e = \ln K_f + \frac{1}{n} \ln C_e \ ...4.4$$

$$\text{Temkin model: } q_e = B \ln A + B \ln C_e...4.5$$

$$\text{Dubinin–Raduskevich model: } \ln q_e = \ln q_m - \beta \Sigma^2...4.6$$

$$\Sigma = RT \ln \left[1 + \frac{1}{C_e}\right]...4.7$$

$$E = \frac{1}{\sqrt{2\beta}}...4.8$$

Where C_e is the equilibrium dye concentration in the solution in mg L^{-1}, b is the Langmuir adsorption constant (L mg^{-1}), and q$_m$ is the theoretical maximum adsorption capacity (mg g^{-1}). K$_f$ (L mg^{-1}) and n are Freundlich isotherm constants indicating the capacity and intensity of the adsorption, respectively. A is the equilibrium binding constant (L mg^{-1}) and B is the heat of adsorption. β is the Dubinin–Raduskevich model constant (mol^2 kJ^{-2}) related to the mean free energy of adsorption per mole of the adsorbate and Σ is the polanyi potential. E is the mean free energy of adsorption (kJ mol^{-1}).

In order to determine the mechanism and potential rate-controlling steps involved in the process of adsorption, pseudo first order,(Lagergren, 1898) pseudo second order (Ho and McKay, 1999). The pseudo first order kinetic model equation is:

$$\ln (q_e - q_t) = \ln q_e - K_1 t...4.9$$

Where q_t is the amount of adsorption at time t in (mg g^{-1}), k_1 is the rate constant of the equation in (min^{-1}), and q_e is the amount of adsorption equilibrium in (mg g^{-1}). The adsorption rate constant (k_1) can be determined experimentally by plotting ln (q_e-q_t) *versus* t.

The pseudo second order kinetic model is expressed as:

$$\frac{t}{q_t} = \frac{1}{(k_2 q_e^2)} + \frac{t}{q_e}...4.10$$

Where k_2 is the equilibrium rate constant of pseudo second order adsorption in (g mg^{-1} min^{-1}). The values of k_2 and q_e can be determined from the slope and intercept of the plot t/q_t *versus* t, respectively.

The data was also fitted into the Weber–Morris model, to evaluate the possibility of intra-particle diffusion as the rate limiting step; it is given by (Weber and Morris, 1963):

$$q_t = k_{id} t^{1/2} + C...4.11$$

Where k_{id} (mg g^{-1} h$^{-1/2}$) is the intra-particle diffusion rate constant.

4.3.6 Fixed Bed Column Studies

Fixed bed column studies were conducted using glass columns of 1.5 cm internal diameter and 55 cm length. The column was packed with the modified montmorillonite between two supporting layers of glass wool to prevent the adsorbent floating from the outlet. The mass of the adsorbent and the flow rate (3.2 mL min^{-1}) were kept constant while the influent concentration was varied from 50 to 200 ppm. The data was fitted into the Thomas model (Thomas, 1944) in order to predict the adsorptive curve of breakthrough in a fixed-bed.

The Thomas expression is represented by equation 12:

$$\frac{C_t}{C_0} = \frac{1}{1+\exp[k_{Th}(q_o x - C_o V_{eff})/v}...4.12$$

91

Where k_{Th} is the Thomas rate constant (mL min^{-1} mg^{-1}), q_o is the equilibrium uptake of the the dye per g of the adsorbent (mg g^{-1}), x represents the mass of adsorbent in the column (g), V_{eff} is the effluent volume (mL), C_0 and C_t is the dye influent concentration and effluent concentration at time t (mg L^{-1}) respectively, and v is the flow rate (mL m^{-1}in). The value of C_t/C_0 is the ratio of effluent and influent of the dye concentrations. The value of time t (min) is t = V_{eff}/v. The kinetic coefficient k_{Th} and the adsorption capacity of the column q_o can be determined from a plot of C_t/C_0 against t at a given flow rate using non-linear regression from equation 13:

$$\ln\left(\frac{C_0}{C_t} - 1\right) = \frac{k_{Th}\, q_0 X}{v} - k_{Th} C_0 t \,...4.13$$

4.4 RESULTS AND DISCUSSION

4.4.1 Characterization of IL, Mt, Na$^+$–Mt and Mt–IL

^{1}H NMR, ^{13}C NMR and FT-IR analyses were carried out and thermal stabilities were confirmed by TGA-DTA/DSC (see supporting information (SI)). ^{1}H NMR of IL (400 MHz, CDCl$_3$): δ (ppm) 0.81 (t, 3H), 1.2 (m, 26H), 1.8 (q, 2H), 4.0 (s, 3H), 4.2 (t, 2H), 7.4 (d, 1H), 7.5 (d, 1H) and 10.2 (s, 1H). ^{13}C NMR of IL (400 MHz, CDCl$_3$) at δ (ppm): 14.1, 22.7, 26.3, 29.0, 29.3, 29.4, 29.5, 29.58, 29.6, 29.7, 30.3, 31.9, 36.7, 50.2, 121.7, 121.5, and 137.6). FT-IR of IL v = 3477 and 3430 (N–H stretch, 2˚ amines), 3145, 3083 and 3063 (C–H stretch, aromatics), 2950, 2915, 2850 (C–H stretch, alkanes), 2051, 1631, 1573 (C–C stretch (in–ring), aromatics), 1473, 1427 (C–H bend, alkanes), 1381, 1343, 1313 (C–H rocking, alkanes), 1175 (C–N stretch, aromatic amines), 1022, 862, 792, 739, 716, 662, 623, 512, 481, 434, 401 (C–H aromatics).

High-resolution mass spectroscopy was used to confirm the mass of the IL. The result of the HRMS is as follows: HRMS of [C$_{20}$H$_{13}$N$_2$]$^+$ (*m/z*): 307.3110; calculated mass is 307.3113 g mol^{-1} (see SI for the HRMS spectra). Thermogravimetric analysis (TGA) showed that the ionic liquid is thermally stable up to 350 °C (additional spectral data can be found in the supporting information). Other properties are shown in Table 4.1.

4.4.2 Chemical Composition of Montmorillonite

EDX analysis was used in determining the chemical composition of Na^+–Mt. Table 4.2 indicates that silica and alumina are the main components of the Na^+-Mt, with others such as sodium, potassium, iron, magnesium, and calcium in trace amounts. SiO_2 and Al_2O_3 will be the main adsorbing site (Özcan et al., 2004).

Table 4.2 showing the chemical composition of montmorillonite

Constituent	% weight
SiO_2	63.51
Al_2O_3	21.9
Na_2O	4.11
Fe_2O_3	3.1
CaO	3.22
K_2O	2.1
MgO	2.06

The XRD of Na^+–Mt was compared with IL intercalated montmorillonite (Mt–IL) as shown in Figs. 4.1a and 4.1b. IL intercalation of the Mt has decreased the intensity of the spectra compared to the unmodified and made the width of the peak at half-peak height broader, suggesting that IL intercalation caused extensive delamination (Li et al., 2010; Kulshrestha et al., 2004; Porubcan et al., 1978). A similar result has been reported by Lee and Kim.(Lee and Kim, 2002a) Also the peaks at 001, 002 and 020 reflect at 9.53 Å, 4.87 Å and 4.18 Å, respectively which are an integral part of montmorillonite, and the sharp reflection at the 2θ value of 27.15 (3.28 Å) corresponds to quartz in Na^+–Mt (Takahashi et al., 2013). When no water molecules are intercalated between the unit layers of montmorillonite the interlayer distance is at (001) and reflection around 9.53 Å (Grim, 1953).

When intercalation of IL in the interlayer of Na^+–Mt occurs, 001, 002 and 020 reflections shift to 11.65, 6.24, and 4.79 Å respectively. A similar trend had been reported by Singla and co-workers and Takahashi and co-workers (Takahashi et al., 2013; Singla et al., 2012). IL does not show any XRD peak due to its liquid nature. Furthermore, comparing Na^+–Mt with Mt–IL, the (001) d-spacing value increases from 9.53 to 11.65 Å and signifies the intercalation of IL in Mt–IL

(crystalline swelling). Fig 4.1c shows that the intensity of all the peaks in the Mt-IL spectrum after adsorption of amaranth dye has increased significantly compared to Mt-IL before adsorption. This suggests that the amaranth dye has been intercalated along with IL already within the Mt.
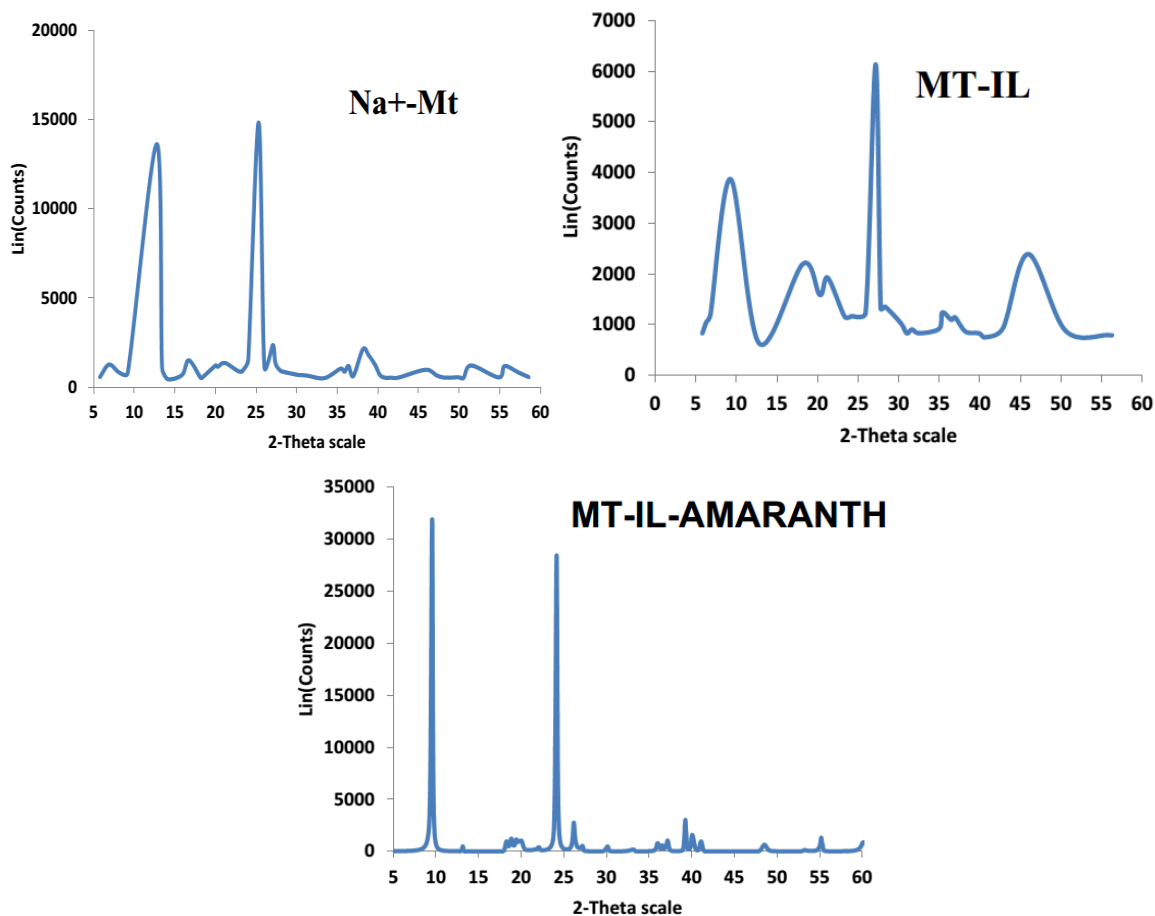
Fig. 4.1a, 4.1b and 4.1c showing the XRD of Na⁺-Mt, Mt-IL and Mt-IL after adsorption of amaranth

To ascertain that IL in excess of CEC of Na⁺–Mt is arranged in the silicate layer of Na⁺–Mt, the cation exchangeable capacity of Mt–IL was determined to be 112 meq per 100 g. Comparing the CEC with that of Na⁺–Mt (89 meq per100 g), it shows that all exchangeable cations present in the Na⁺–Mt had been exchanged in excess for IL, indicating 125% increase of the Na⁺–Mt CEC resulting in an aggregation on the surface of the clay and an overall positive surface.

94

Takahashi and co-workers have also reported the intercalation of ionic liquid in the interlayer of montmorillonite (Takahashi et al., 2013). To further ascertain that quaternary ammonium cations in 1-methyl, 3-decahexyl imidazolium were intercalated into the silicate lattice of Na^+–Mt, FT–IR of the pure montmorillonite, Na^+–Mt and Mt–IL spectra were recorded in the region 380–4000 cm^{-1} as shown in Fig. 4.2.

The presence of peaks in the region of 3392-3314 and 1639 cm^{-1}, represent the stretching and bending modes respectively of the –OH of water within the montmorillonite.(Boufatit et al., 2008) It is observed that the 3314 cm^{-1} band intensity on Mt–IL decreases when compared with Na^+–Mt which implies that water of hydration is lost as the cation (Na^+) is replaced by the cationic surfactant (alkyl chain). A similar result was also reported by Zaghouane-Boudiaf and Boutahala (Zaghouane-Boudiaf and Boutahala, 2011). The peaks at 2920 and 2851 cm^{-1} are assigned to symmetric and asymmetric stretching vibrations of the methylene groups in the ionic liquid while peaks 1573 and 1467 cm^{-1} are their bending vibrations respectively (Zhou et al., 2007), showing the intercalation of ionic liquid molecules between the silica layers. These peaks were not present in the unmodified montmorillonite.
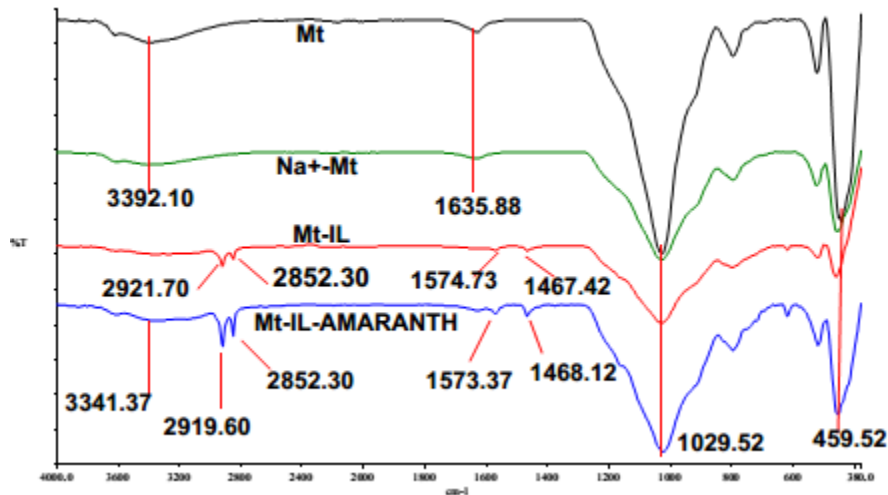
Fig. 4.2 FT-IR spectra of Mt, Na^+–Mt and Mt–IL

The peaks at 1029 and 459 cm^{-1} are the bands for Si-O-Si stretching and bending respectively (Adam et al., 2013; Endud and Wong, 2007; Kirschhock et al., 1999; Flanigen et al., 1974). There is little difference between the spectra for Mt-IL before after adsorption of amaranth dye (Mt-IL-amaranth). There was a slight shift in the peaks after adsorption of dye from 2921.70 and 2852.30 cm^{-1} to 2919.60 and 2851.87 cm^{-1} (symmetric and asymmetric stretching vibrations of the methylene groups), also from 1574.73 and 1467.42 cm^{-1} to 1573.37 and 1468.12 cm^{-1} (bending vibrations of the methylene groups) respectively. The presence of the OH peak is noticed after adsorption of dye signifying presence of water in the interlayer of Mt (3341.31 cm^{-1}).
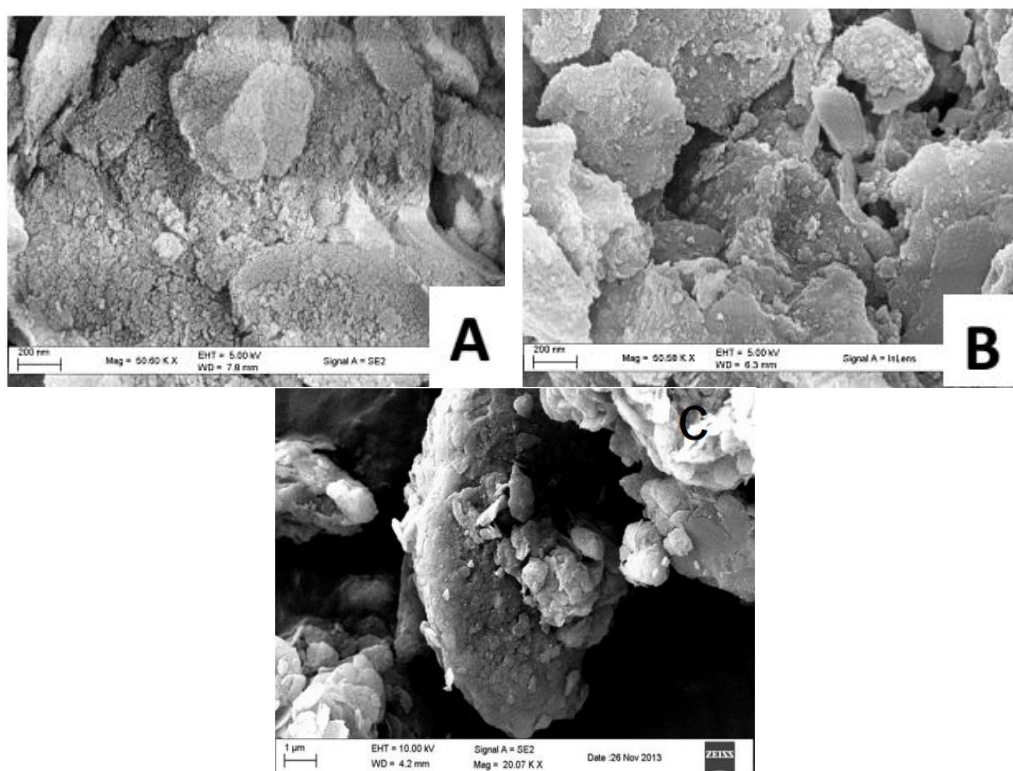
Fig. 4.3 SEM images of Na$^+$-Mt (a) and Mt-IL (b) before adsorption and (c) after adsorption

The surface morphologies of the Na$^+$–Mt and Mt–IL samples are analysed by SEM, with Mt–IL in Fig 4.3b showing more porosity and irregularity than Na$^+$–Mt in Fig. 4.3a. The modified

montmorillonite is slightly expanded, which indicates delamination of the layers of the montmorillonite due to the presence of cations of the salt (dos Santos et al., 2013). Fig. 4.3a (Na^+– Mt) also shows a clump like morphology with smooth surface as compared with Fig. 4.3b that shows agglomerated sheet like morphological characteristic with rough surface. Similar results have been reported by Anggraini and co-workers (Anggraini et al., 2014). Fig. 4.3c shows the morphology of the Mt–IL after adsorption and indicates that the adsorbed dye has blocked the pores of the material.

Fig. 4.4a shows the N_2 adsorption desorption isotherm of Na^+–Mt, where the material exhibited a type IV isotherm which is a characteristic of mesoporous material according to IUPAC classification (material having pores ranging from 1.5-100 nm) (Allen, 1997). The adsorbent also showed a H_3 hysterisis loop over the range of relative pressure P/P_0 0.40 - 1.00 which signifies that the material has pore blocking (forming slit shaped pores) with non-uniform pore size distribution and shape. The average pore diameter of the sample was within the mesoporous and macroporous range, with most of it being mesoporous. In Fig. 4.4b Na^+–Mt shows narrow pore size distribution with most pores centred at about 7.62 nm and a very broad range of pores from 7.62-249 nm.

The surface area of Na^+–Mt was 183.2 m^2 g^{-1} and with a pore volume of 0.52 cm^3 g^{-1}. There is a decrease in the surface area (175 m^2 g^{-1}) and pore volume (0.32 cm^3 g^{-1}) for Mt–IL, which is due to blocking of the pores by the ionic liquid cations. Also, Mt–IL in Figs. 4.5a and 4.5b also showed a type IV isotherm and H_3 hysterisis, but due to the modification by 1-methyl, 3-decahexyl imidazolium, the pore size has increased and is more macroporous than mesoporous.

The thermal study of the material shows loss of water observed in the Mt–IL TG-DTA spectra (see SI) which is due to the removal of the externally adsorbed and interlayer water at about 100 °C. The decomposition of the IL was observed in the range of 300 to 450 °C and an endothermic peak is observed around 700 °C which corresponds to the decomposition of the structural hydroxyl groups in the aluminosilicate (Bastow et al., 1991; Takahashi et al., 2013).
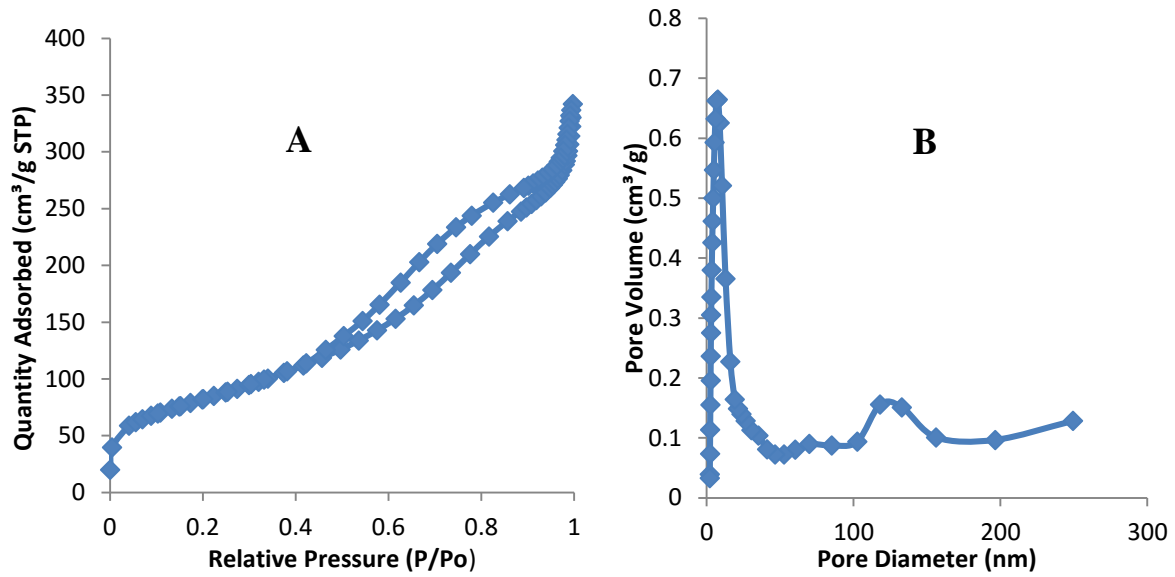
Fig. 4.4a and 4.4b N$_2$ adsorption desorption isotherm and pore size distribution of Na-Mt respectively.
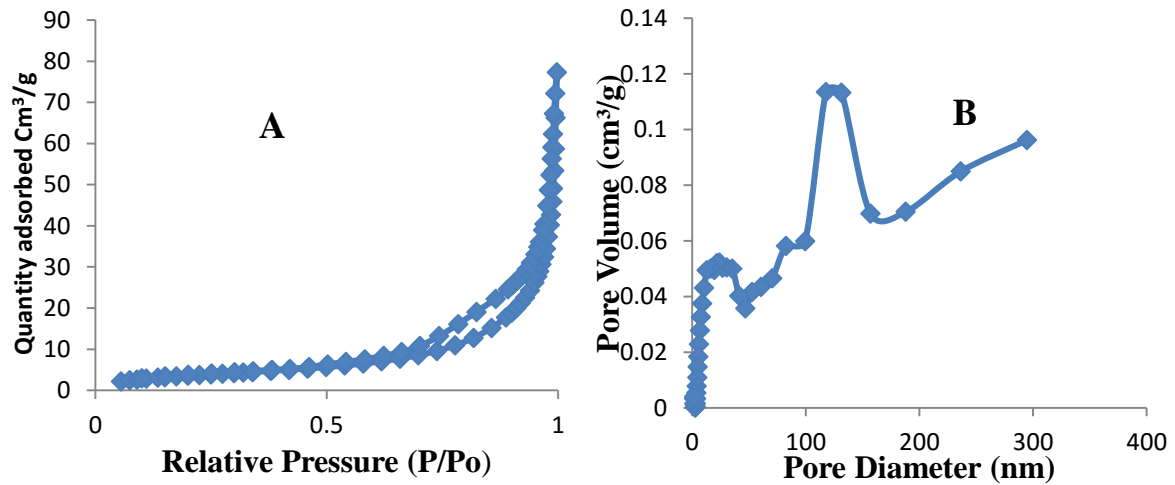
Fig. 4.5a and 4.5b N$_2$ adsorption desorption isotherm and pore size distribution of Mt-IL respectively

4.4.3 Batch Adsorption

The effect of amaranth on Na^+–Mt and Mt–IL doses from 0.005-0.1 g was carried out and showed an increase in adsorption of amaranth on Na^+–Mt and Mt–IL as their masses increased. This could be attributed to electrostatic attraction between the amaranth dye ion and the positively charged surface of the materials (Na^+–Mt and Mt–IL). Interaction between the rings on the amaranth dye molecule and the Mt–IL may also occur ($\pi - \pi$ interraction). Adsorption reached its maximum at about 0.01 g with 90% of the dye adsorbed (Fig. 4.6a). It was also observed that after adsorption reached equilibrium, the adsorbed dye showed a continuous decline as the amount of sorbent increased. Daneshvar and Ghosh (Daneshvar et al., 2012; Ghosh and Bhattacharyya, 2002), reported the same trend (Daneshvar et al., 2012) and suggested that it was as a result of increasing particle interaction and aggregation, leading to a reduction of total surface area. On the other hand, there is a gradual increase in the percentage removal of amaranth dye as the mass of Na^+–Mt increases which is due to the increase in surface area with a high dosage of the adsorbent. Na^+–Mt could adsorb about 30% at 0.1 g which could be attributed to fewer adsorption sites and lack of electrostatic interaction (Yoshida et al., 1993) between amaranth dye and Na^+–Mt. Since the optimized dose is 0.01 g for Mt–IL, all other optimization experiments were performed with 0.01 g of sorbent.

The effect of pH showed that maximum adsorption was at pH 2, and decreases gradually as the pH tends towards basic medium (Fig. 4.6b). Other researchers reported similar trends for adsorption of anionic dye (Özcan et al., 2004; Ahmad and Kumar, 2011). This can be explained by electrostatic attraction between the negatively charged adsorbate and positively charged adsorbent. At low pH levels a positively charged ion dominates the surface of the adsorbent because of the activities of the functional group on the adsorbent and the presence of IL in excess on the adsorbent. Amaranth is an anionic dye with predominantly negative charges at low pH. This negative charge on the dye at low pH results in a significantly high electrostatic attraction between the positive and negative charges on the adsorbent and the dye respectively (Ahmad and Kumar, 2011; Baskaralingam et al., 2006). Therefore, an increase in adsorption of the dye will occur at the Mt–IL surface. When pH is increased there will be more negative ions on the surface of the adsorbent, causing repulsion which will reduce adsorption. Also, at higher pH values excess of OH^- is present in the solution, which can lead to competition of adsorption sites with amaranth ions. Nevertheless, there is still significant amount of dye adsorbed onto Mt–IL at higher pH

values. This can be attributed to chemisorption (Özcan et al., 2004), i.e. chemical reaction between the adsorbent aromatic ring and the ring of the amaranth dye. All other experiments were carried out on Mt–IL only at pH of approximately 2. The adsorption capacity of Na^+–Mt (6 mg g^{-1}) is much lower than Mt–IL.
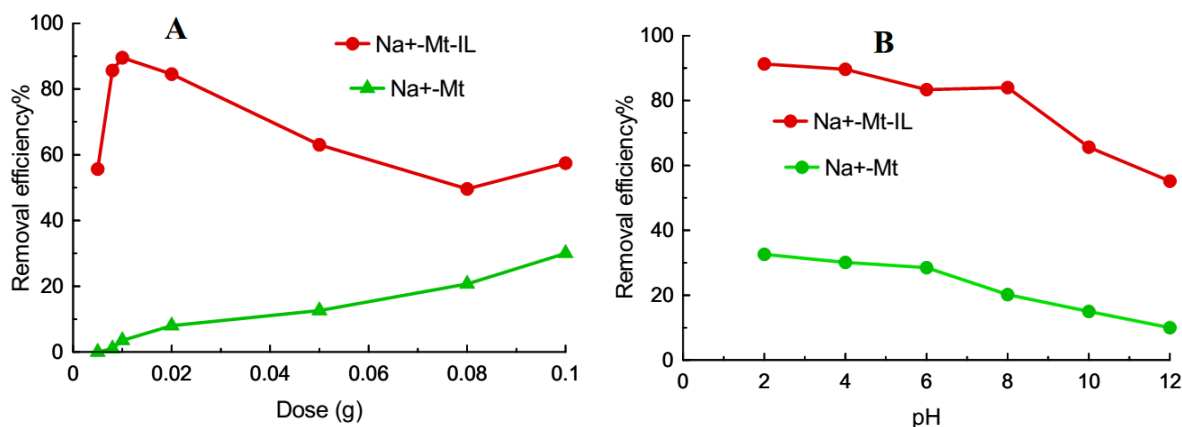
Fig. 4.6a and 4.6b showing the effect of dose of adsorbent and pH respectively

4.4.4 Adsorption Kinetics of Amaranth

The effect of contact time on the extent of amaranth adsorption of different concentrations in the plot of removal efficiency against time as shown in Fig. 4.7 indicated that the adsorption of amaranth on the adsorbent increased with time. Equilibrium time for 20 mg L^{-1}, 50 mg L^{-1}, 100 mg L^{-1} and 200 mg L^{-1} was about 120 min. Ahmad, also reported equilibrium times of 120 min for amaranth onto alumina reinforced polystyrene (Ahmad and Kumar, 2011).

It was also observed that the adsorption of amaranth is very rapid in the first 10 min at all concentrations but later decreased with time until equilibrium was reached. A large number of free adsorbent sites available for sorption are likely to be responsible for the high removal of the amaranth dye at the beginning of the experiment. The decrease in adsorption rate was as a result of a reduction in available sites and also because of repulsive forces among adsorbed dye molecules and unmodified adsorption sites present in the solution (Smaranda et al., 2009).

100
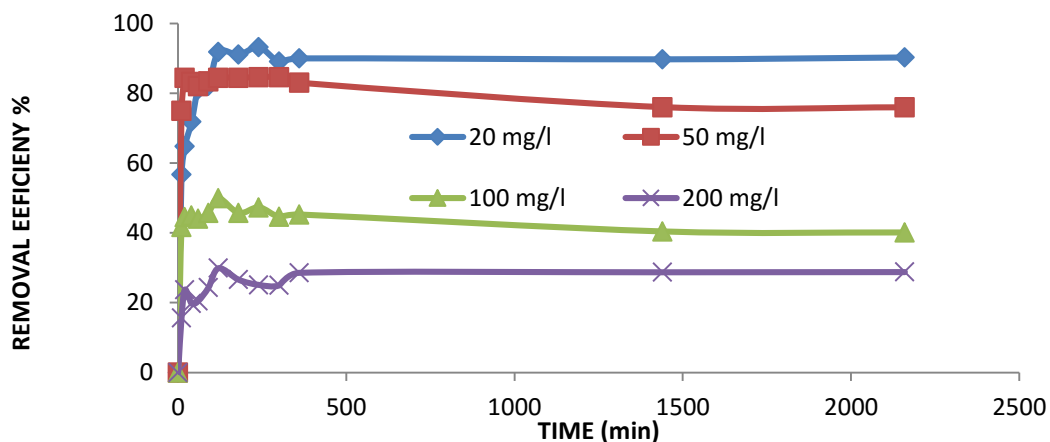
Fig. 4.7 Plot of removal efficiency % against time (min) for four different concentrations at pH 2

To have a better understanding of the adsorption kinetics, mechanism and the potential rate-controlling step involved in the process of adsorption, several kinetic models were used. These include Lagergan-first-order model, pseudo-second-order kinetic model and intra-particle diffusion. Table 4.3 showed that pseudo-second-order fitted best with $R^2 \geq 0.99$ for all the concentrations at different temperatures. From the result in the above models, amaranth adsorption on to Mt–IL was most probably chemisorption and took place through exchange of ions on the surface of the active sites which is in agreement with other studies (Ahmad and Kumar, 2011; Ho and McKay, 1998; Liao et al., 2013; Shen et al., 2009). Also, the adsorption capacity (q_e) calculated for all the concentrations were very close to q_e experimental as shown in Table 4.3. Similar results were reported by Ahmad and Zargar (Ahmad and Kumar, 2011; Zargar et al., 2009; Mittal and Gupta, 2005). According to Ho and co-workers and Liao and co-workers (Ho and McKay, 1999; Liao et al., 2013), three steps were involved in the pseudo second order kinetic model, which are: (i) the dye molecules diffuse from liquid phase to liquid–solid interface; (ii) the dye molecules move from liquid–solid interface to solid surface; and (iii) the dye molecules diffuse into the particle pores.

The data were further fitted into the intra-particle diffusion model to examine the relative contribution of surface and intra-particle diffusion to the kinetics process. The plot not passing through the origin indicated some degree of boundary layer control which further showed that the intra-particle diffusion was not the only rate controlling step, but other processes also controlled the rate of adsorption (Ahmad and Kumar, 2011; Liao et al., 2013; Crini et al., 2007), Surface diffusion mechanism is likely attributed to electrostatic attraction, since amaranth will be negatively charged at pH 2 and the surface of the material is positivity charged.

Table 4.4 showed that Langmuir was best fitted for the data with $R^2 > 0.99$ for all the temperatures. This further confirmed the previous statement that the adsorption process of the dye onto Mt–IL was chemisorbed onto its surface. The Langmuir isotherm fitted the experimental data for all the temperatures very well, which implied that the active sites on Mt–IL were homogeneously distributed, since the Langmuir equation assumed that the surface was homogeneous. Furthermore, the maximum sorption capacities (q_m) were 243.902, 238.095 and 263.158 mg g^{-1} at temperatures 313 K, 303 K and 313 K respectively, and it was concluded that Langmuir is the best fit isotherm. To the best of the authors' knowledge the adsorption capacity is high compared with other previous research carried out on amaranth which the authors attribute to the ionic liquid used in the modification of the montmorillonite. Also, from Dubinin-Raduskevich the mean sorption energy (E) derived from the D–R isotherm model can be used to distinguish chemical and physical adsorption. Table 4.4 showed E values of 10.00, 7.91 and 8.34 kJ mol^{-1}, which were in the range of 8–16 kJ mol^{-1} which suggested a dominating chemisorption (Helfferich, 1962) effect which is in agreement with other kinetics models. This is also evident in the XRD studies (Fig. 4.1c) where the intensity of the peaks increased which suggested a chemical reaction between IL on the Mt and the amaranth dye after adsorption.

Thermodynamic studies showed negative values of ΔG at temperatures 313, 303 and 293 K. The values of ΔH, ΔS and the R^2 are listed in the supplemental information. The positive value of ΔH indicated that the adsorption process was endothermic in nature and the positive value of ΔS may be due to the increase in the dye concentration at the solid phase (Gupta et al., 2006; Ahmad and Kumar, 2011; Liao et al., 2012; Bhatnagar and Jain, 2005; Lin and Juang, 2009). The negative values of ΔG showed that the process was thermodynamically feasible and spontaneous. This is

Table 4.3 Experimental values for q_e (mg L^{-1}) and parameters for pseudo-first-order, pseudo-second-order and intra-particle diffusion.

Concentrations (mg L^{-1})	Temp	q_e,exp (mg g^{-1})	Pseudo-first-order			Pseudo-second-order			Weber–Morris model		
			q_e, cal (mg g^{-1})	k_e (h^{-1})	R^2	q_e,cal (mg g^{-1})	k (g mg^{-1} h^{-1})	R^2	q_e (mg g^{-1})	k_{id} (mg g^{-1} h$^{-1/2}$)	R^2
200	313 k	239.360	6.869	0.002	0.697	222.222	0.000	0.987	142.790	4.525	0.519
100		199.787	0.714	0.002	0.817	181.818	0.004	0.998	174.480	0.652	0.170
50		168.853	2.115	0.004	0.157	178.571	0.003	0.999	159.710	0.566	0.278
20		73.493	3.492	0.004	0.671	74.074	0.000	0.999	47.640	1.611	0.747
200	303 k	224.853	4.119	-0.008	0.455	196.078	0.001	0.995	255.000	-2.720	0.217
100		192.853	3.650	0.098	0.817	227.273	0.000	0.996	165.590	2.026	0.468
50		165.440	4.268	0.004	0.768	166.667	0.001	0.999	126.030	2.454	0.721
20		60.267	3.160	0.004	0.824	60.606	0.002	0.998	41.449	1.164	0.739
200	293 k	246.613	5.933	-0.008	0.190	238.095	0.000	0.923	194.990	3.843	0.276
100		204.587	100.324	0.098	0.545	227.273	0.000	0.996	156.100	3.791	0.699
50		173.973	2.883	0.005	0.912	178.571	0.003	0.999	164.810	0.757	0.651
20		60.480	4.147	0.001	0.84	66.667	0.002	0.998	50.656	0.865	0.886

Table 4.4 The q_m and b values in Langmuir equation, the K_f and 1/n values in Freundlich equation, q_s and β values in Dubinin-Radushkevich, bT and AT values in Temkin models and their respective correlation coefficients values.

Temp	Langmuir model			Freundlich model			Dubinin–Radushkevich model				Temkin model		
	q_m	b	R^2	K_f	n (-)	R^2	q_m	β	E	R^2	bT	AT	R^2
	$(mg\ g^{-1})$	$(L\ mg^{-1})$		$(L\ mg^{-1})$	$(g\ L^{-1})$		$(mol\ g^{-1})$	$(mol^2\ kJ^{-2})$	$(kJ\ mol^{-1})$		$(g\ kJ\ mg^{-1}\ mol^{-1})$	(L/mg)	
313 k	243.902	0.0229	0.996	77.657	4.08	0.862	205.799	$5\ x10^{-9}$	10.000	0.939	75.53	8.044	0.935
303 k	238.095	0.099	0.995	54.435	3.25	0.654	250.711	$9\ x\ 10^{-9}$	8.452	0.797	41.165	0.836	0.851
293 k	263.158	0.091	0.992	59.973	3.305	0.598	250.711	$8\ x\ 10^{-9}$	7.906	0.831	56.875	2.302	0.861

similar to reports by other researchers (Liao et al., 2012; Ahmad and Kumar, 2011; Ghosh and Bhattacharyya, 2002).

Table 4.5 Comparison of adsorption capacities of MT-IL with other materials

pH	Adsorption capacity (mg g^{-1})	Material	Refercene
2	10.00	Alumina reinforced polystyrene	(R. Ahmad & Kumar, 2011)
2	14.90	Peanut hull	(Gong et al., 2005)
3-9	1.05	Iron oxide nanoparticles coated with cetyltrimethylammonium bromide	(Zargar et al., 2009)
2-11	18.80	Activated carbon and	(Jain & Sikarwar,
2	100.17	Activated de-oiled mustard	2011)
3	3.44	Pomegranate Peel	(Ali, Egzar, Kamal, abdulsaheb, & Mashkour, 2013)
6-12	65.04	tamarind pod shells	(Naidu, 2014)
9	95.12	Activated Carbon	(J.-J. Lee, 2011)
2	263.20	MT-IL	Present work
2	6.00	MT-IL	Present work

Table 4.5 indicate that the adsorption capacities obtained from this study were far higher having q_e value (263.20 mg g^{-1}) compared to that reported in previous literatures for the adsorption of amaranth dye from other adsorbents.

4.4.5 Column Studies

The effect of different concentrations from 50 to 200 mg L^{-1} of amaranth dye influent with a constant mass of Mt-IL and constant solution flow rate of 3.2 mL min^{-1} is shown in the breakthrough curve in Fig. 4.8. Fig. 4.8 showed increased breakthrough times with decreased influent concentrations of amaranth dye and steeper breakthrough curves at increased influent concentrations. The reason for this is because at higher influent concentrations, transportation of amaranth dye to the adsorbent is faster because of an increased diffusion coefficient or mass

transfer coefficient which is the driving force for the adsorption process.(Tan et al., 2008) As a result this leads to higher gradients of the breakthrough curves at increased concentrations. The larger the influent concentration, the steeper the slope of the breakthrough curve and the shorter the breakthrough time (Aksu and Gönen, 2004). These results also showed that a change in concentration of influent affects the saturation rate, and implies that the diffusion process is concentration dependent. Similar trends were obtained from other work (Han et al., 2007; Ahmad and Hameed, 2010; Lin et al., 2004).
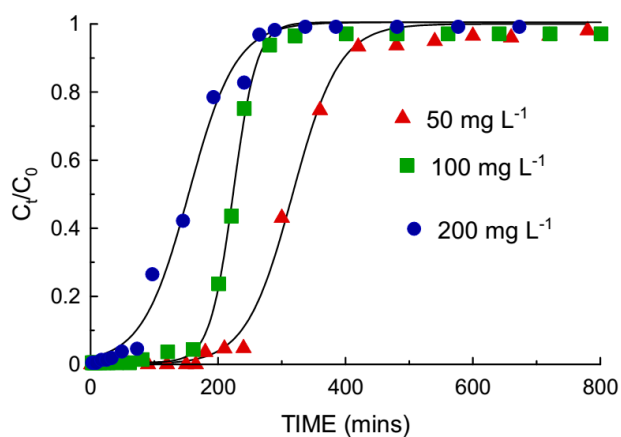
Fig. 4.8 The effect of influent concentration on dye

The column data were fitted into the Thomas model to determine the Thomas rate constant k_{Th}, and equilibrium uptake of amaranth dye per gram of the adsorbent (mg g^{-1}) q_o. Table 4.6 showed the parameters of the Thomas model, with R^2 values ranging from 0.941 to 0.998. This showed that the Thomas model is suitable for the adsorption of amaranth on Mt-IL. Also, from Table 4.6, as the influent concentration increased the value of column adsorption capacity q_o increased (393.63, 580.89 and 603.60 mg g^{-1} at 50, 100 and 200 mg L^{-1} respectively). The increased concentrations of solute in solution resulted in increased rates of transportation of solutes to the

adsorbent thus leading to increased adsorption capacities (Aksu and Gönen, 2004; Vijayaraghavan et al., 2004; Ahmad and Hameed, 2010). Thus column studies also confirmed the high adsorption capacity of IL modified montmorillonite for the adsorption of amaranth dye.

Table 4.6 Thomas model parameters at different concentrations using non-linear regression analysis

C_0 (mg L^{-1})	v (mL min^{-1})	K_{Th} (mL min^{-1} mg^{-1})	q_o (mg g^{-1})	R^2
50	3.2	1.4×10^{-4}	393.64	0.941
100	3.2	0.86×10^{-4}	580.89	0.998
200	3.2	0.95×10^{-4}	608.60	0.996

4.5 CONCLUSION

In this study, a novel, cationic ionic liquid was synthesized for the modification of sodium-montmorillonite. The modified material is hydrophobic with a large pore volume to trap pollutants and is a mixture of mesoporous and macroporous. Adsorption of Mt–IL studies showed that 1-methyl, 3-decahexyl imidazolium intercalated in the interlayer of montmorillonite is a possible good alternative for the removal of anionic amaranth dye from wastewater. The maximum removal percentage was > 90% at an optimum pH of 2. The adsorption behaviour was best described by the Langmuir isotherm with a high adsorption capacity of 263.2 mg g-1 and the kinetics by pseudo-second-order. Positive values of enthalpy change suggested the endothermic nature of the process, while the negative free energy proved its thermodynamic feasibility and spontaneity. Column experiments using the Thomas model also showed high adsorption capacities of 393.64, 580.89 and 603.60 mg g-1 at different concentrations. From the result in this research, ionic liquid modified montmorillonite is a good alternative for adsorption of dye from wastewater.

4.6 ACKNOWLEDGMENTS

4.7 REFERENCES

Absalan, G., Asadi, M., Kamran, S., Sheikhian, L. & Goltz, D. M. 2011. Removal of reactive red-120 and 4-(2-pyridylazo) resorcinol from aqueous samples by Fe3O4 magnetic nanoparticles using ionic liquid as modifier. *Journal of Hazardous Materials,* 192(2)**,** pp 476-484.

Adam, F., Appaturi, J. N., Khanam, Z., Thankappan, R. & Nawi, M. A. M. 2013. Utilization of tin and titanium incorporated rice husk silica nanocomposite as photocatalyst and adsorbent for the removal of methylene blue in aqueous medium. *Applied Surface Science,* 264(718-726.

Ahmad, A. & Hameed, B. 2010. Fixed-bed adsorption of reactive azo dye onto granular activated carbon prepared from waste. *Journal of Hazardous Materials,* 175(1)**,** pp 298-303.

Ahmad, R. & Kumar, R. 2011. Adsorption of amaranth dye onto alumina reinforced polystyrene. *Clean–Soil, Air, Water,* 39(1)**,** pp 74-82.

Aksu, Z. & Gönen, F. 2004. Biosorption of phenol by immobilized activated sludge in a continuous packed bed: prediction of breakthrough curves. *Process Biochemistry,* 39(5)**,** pp 599-613.

Allen, T. 1997. *Particle Size Measurement: Volume 2: Surface Area and Pore Size Determination*, 5th, London: Springer.

Anggraini, M., Kurniawan, A., Ong, L. K., Martin, M. A., Liu, J.-C., Soetaredjo, F. E., Indraswati, N. & Ismadji, S. 2014. Antibiotic detoxification from synthetic and real effluents using a novel MTAB surfactant-montmorillonite (organoclay) sorbent. *RSC Advances,* 4(31)**,** pp 16298-16311.

Avisar, D., Primor, O., Gozlan, I. & Mamane, H. 2010. Sorption of sulfonamides and tetracyclines to montmorillonite clay. *Water, Air, & Soil Pollution,* 209(1-4)**,** pp 439-450.

Baskaralingam, P., Pulikesi, M., Elango, D., Ramamurthi, V. & Sivanesan, S. 2006. Adsorption of acid dye onto organobentonite. *Journal of Hazardous Materials,* 128(2)**,** pp 138-144.

Bastow, T., Hardin, S. & Turney, T. 1991. The formation of β′-sialon from a montmorillonite-polyacrylonitrile composite by carbothermal reduction: an NMR, TGA, XRD and EM study. *Journal of Materials Science,* 26(6)**,** pp 1443-1453.

Beall, G. W. 1985. *Organoclay adsorption column followed by active carbon*.

Bhatnagar, A. & Jain, A. 2005. A comparative adsorption study with different industrial wastes as adsorbents for the removal of cationic dyes from water. *Journal of Colloid and Interface Science,* 281(1)**,** pp 49-55.

Boufatit, M., Ait-Amar, H. & Mc Whinnie, W. 2008. Development of an algerian material montmorillonite clay—Intercalation with selective long chain alkylammonium cations (Octadecytrimethylammonium, Cetylpyridium and Tetrabutylammonium) and with tellerium complexes. *Desalination,* 223(1)**,** pp 366-374.

Crini, G., Peindy, H. N., Gimbert, F. & Robert, C. 2007. Removal of CI Basic Green 4 (Malachite Green) from aqueous solutions by adsorption using cyclodextrin-based adsorbent: kinetic and equilibrium studies. *Separation and Purification Technology,* 53(1)**,** pp 97-110.

Daneshvar, E., Kousha, M., Sohrabi, M. S., Khataee, A. & Converti, A. 2012. Biosorption of three acid dyes by the brown macroalga Stoechospermum marginatum: Isotherm, kinetic and thermodynamic studies. *Chemical Engineering Journal,* 195–196(297-306.

dos Santos, O. A. A., Castellib, C. Z., Oliveirab, M. F., de Almeida Netob, A. F. & da Silvab, M. G. 2013. Adsorption of Synthetic Orange Dye Wastewater in Organoclay. *Chemical Engineering,* 32(307-312.

Du, B., Guo, Z., Song, P. a., Liu, H., Fang, Z. & Wu, Y. 2009. Flame retardant mechanism of organo-bentonite in polypropylene. *Applied Clay Science,* 45(3)**,** pp 178-184.

Dubinin, M. & Radushkevich, L. 1947. Equation of the characteristic curve of activated charcoal. *Chemisches Zentralblatt,* 1(1)**,** pp 875.

Dzyuba, S. V. & Bartsch, R. A. 2001. Efficient synthesis of 1-alkyl (aralkyl)-3-methyl (ethyl) imidazolium halides: precursors for room-temperature ionic liquids. *Journal of Heterocyclic Chemistry,* 38(1)**,** pp 265-268.

Endud, S. & Wong, K.-L. 2007. Mesoporous silica MCM-48 molecular sieve modified with $SnCl_2$ in alkaline medium for selective oxidation of alcohol. *Microporous and Mesoporous Materials,* 101(1)**,** pp 256-263.

Flanigen, E. M., Khatami, H. & Szymanski, H. A. 1974. Molecular Sieve Zeolites-I, Copyright, Advances in Chemistry Series, FOREWORD. *In:* Gould Robert, F. (ed.) *Molecular Sieve Zeolites-I.* Washington, DC: American Chemical Society.

Freundlich, H. 1906. Über die Adsorption in Lösungen. *Zeitschrift fur Physikalische Chemie,* 57(A)**,** pp 385-470.

Ghosh, D. & Bhattacharyya, K. G. 2002. Adsorption of methylene blue on kaolinite. *Applied Clay Science,* 20(6)**,** pp 295-300.

Gillman, G. & Sumpter, E. 1986. Modification to the compulsive exchange method for measuring exchange characteristics of soils. *Soil Research,* 24(1)**,** pp 61-66.

Grim, R. E. 1953. *Clay Mineralogy*, New York: McGraw-Hill.

Gupta, V., Mittal, A., Gajbe, V. & Mittal, J. 2006. Removal and recovery of the hazardous azo dye acid orange 7 through adsorption over waste materials: bottom ash and de-oiled soya. *Industrial & Engineering Chemistry Research,* 45(4)**,** pp 1446-1453.

Han, R., Wang, Y., Yu, W., Zou, W., Shi, J. & Liu, H. 2007. Biosorption of methylene blue from aqueous solution by rice husk in a fixed-bed column. *Journal of Hazardous Materials,* 141(3)**,** pp 713-718.

Helfferich, F. G. 1962. *Ion exchange*: Courier Dover Publications.

Ho, D. L., Briber, R. M. & Glinka, C. J. 2001. Characterization of organically modified clays using scattering and microscopy techniques. *Chemistry of Materials,* 13(5)**,** pp 1923-1931.

Ho, Y.-S. & McKay, G. 1998. Sorption of dye from aqueous solution by peat. *Chemical Engineering Journal,* 70(2)**,** pp 115-124.

Ho, Y.-S. & McKay, G. 1999. Pseudo-second order model for sorption processes. *Process Biochemistry,* 34(5)**,** pp 451-465.

Hsu, Y., Wang, M., Pai, C. & Wang, Y. 2000. Sorption of 2, 4-dichlorophenoxy propionic acid by organo-clay complexes. *Applied Clay Science,* 16(3)**,** pp 147-159.

Huang, F.-C., Lee, J.-F., Lee, C.-K. & Chao, H.-P. 2004. Effects of cation exchange on the pore and surface structure and adsorption characteristics of montmorillonite. *Colloids and Surfaces A: Physicochemical and Engineering Aspects,* 239(1)**,** pp 41-47.

Huddleston, J. G., Visser, A. E., Reichert, W. M., Willauer, H. D., Broker, G. A. & Rogers, R. D. 2001. Characterization and comparison of hydrophilic and hydrophobic room temperature ionic liquids incorporating the imidazolium cation. *Green Chemistry,* 3(4)**,** pp 156-164.

Jess, A., Große Böwing, A. & Wasserscheid, P. 2005. Kinetik und reaktionstechnik der synthese ionischer flüssigkeiten. *Chemie Ingenieur Technik,* 77(9)**,** pp 1430-1439.

Kamran, S., Asadi, M. & Absalan, G. 2014. Adsorption of folic acid, riboflavin, and ascorbic acid from aqueous samples by Fe3O4 magnetic nanoparticles using ionic liquid as modifier. *Analytical Methods,* 6(3)**,** pp 798-806.

Kirschhock, C. E. A., Ravishankar, R., Verspeurt, F., Grobet, P. J., Jacobs, P. A. & Martens, J. A. 1999. Identification of Precursor Species in the Formation of MFI Zeolite in the TPAOH−TEOS−H2O System. *The Journal of Physical Chemistry B,* 103(24)**,** pp 4965-4971.

Kulshrestha, P., Giese, R. F. & Aga, D. S. 2004. Investigating the Molecular Interactions of Oxytetracycline in Clay and Organic Matter: Insights on Factors Affecting Its Mobility in Soil. *Environmental Science & Technology,* 38(15)**,** pp 4097-4105.

Lagergren, S. 1898. About the theory of so-called adsorption of soluble substances. *Kungliga Svenska Vetenskapsakademiens Handlingar,* 24(4)**,** pp 1-39.

Langmuir, I. 1916. The Constitutionand Fundamental Properties of Solid and Liquids. Part I. Solids. *Journal of the American Chemical Society,* 38(11)**,** pp 2221-2295.

Lee, S. H., Song, D. I. & Jeon, Y. W. 2001. An Investigation of the Adsorption of Organic Dyes onto Organo-Montmorillonite. *Environmental Technology,* 22(3)**,** pp 247-254.

Lee, S. Y. & Kim, S. J. 2002a. Delamination behavior of silicate layers by adsorption of cationic surfactants. *Journal of Colloid and Interface Science,* 248(2)**,** pp 231-238.

Lee, S. Y. & Kim, S. J. 2002b. Expansion of smectite by hexadecyltrimethylammonium. *Clays and Clay Minerals,* 50(4)**,** pp 435-445.

Li, Z., Chang, P.-H., Jean, J.-S., Jiang, W.-T. & Wang, C.-J. 2010. Interaction between tetracycline and smectite in aqueous solution. *Journal of Colloid and Interface Science,* 341(2)**,** pp 311-319.

Liao, P., Malik Ismael, Z., Zhang, W., Yuan, S., Tong, M., Wang, K. & Bao, J. 2012. Adsorption of dyes from aqueous solutions by microwave modified bamboo charcoal. *Chemical Engineering Journal,* 195(339-346.

Liao, P., Zhan, Z., Dai, J., Wu, X., Zhang, W., Wang, K. & Yuan, S. 2013. Adsorption of tetracycline and chloramphenicol in aqueous solutions by bamboo charcoal: A batch and fixed-bed column study. *Chemical Engineering Journal,* 228(496–505.

Lin, S.-H. & Juang, R.-S. 2009. Adsorption of phenol and its derivatives from water using synthetic resins and low-cost natural adsorbents: A review. *Journal of Environmental Management,* 90(3)**,** pp 1336-1349.

Lin, S.-H., Juang, R.-S. & Wang, Y.-H. 2004. Adsorption of acid dye from water onto pristine and acid-activated clays in fixed beds. *Journal of Hazardous Materials,* 113(1)**,** pp 195-200.

Meleshyn, A. & Tunega, D. 2011. Adsorption of phenanthrene on Na-montmorillonite: A model study. *Geoderma,* 169(0)**,** pp 41-46.

Mittal, A. & Gupta, V. K. 2005. Use of waste materials—bottom ash and de-oiled soya, as potential adsorbents for the removal of amaranth from aqueous solutions. *Journal of Hazardous Materials,* 117(2)**,** pp 171-178.

Newman, A. C. 1987. *Chemistry of Clays and Clay Minerals*: Longman scientific and technical.

Özcan, A. S., Erdem, B. & Özcan, A. 2004. Adsorption of Acid Blue 193 from aqueous solutions onto Na–bentonite and DTMA–bentonite. *Journal of Colloid and Interface Science,* 280(1)**,** pp 44-54.

Porubcan, L. S., Serna, C. J., White, J. L. & Hem, S. L. 1978. Mechanism of adsorption of clindamycin and tetracycline by montmorillonite. *Journal of Pharmaceutical Sciences,* 67(8)**,** pp 1081-1087.

Pospíšil, M., Čapková, P., Měřínská, D., Maláč, Z. & Šimoník, J. 2001. Structure analysis of montmorillonite intercalated with cetylpyridinium and cetyltrimethylammonium: molecular simulations and XRD analysis. *Journal of Colloid and Interface Science,* 236(1)**,** pp 127-131.

Pospıšil, M., Čapková, P., Weiss, Z., Maláč, Z. & Šimonık, J. 2002. Intercalation of octadecylamine into montmorillonite: molecular simulations and XRD analysis. *Journal of Colloid and Interface Science,* 245(1)**,** pp 126-132.

Sajjadi, H., Modaressi, A., Magri, P., Domańska, U., Sindt, M., Mieloszynski, J.-L., Mutelet, F. & Rogalski, M. 2013. Aggregation of nanoparticles in aqueous solutions of ionic liquids. *Journal of Molecular Liquids,* 186(1-6.

Shen, X.-E., Shan, X.-Q., Dong, D.-M., Hua, X.-Y. & Owens, G. 2009. Kinetics and thermodynamics of sorption of nitroaromatic compounds to as-grown and oxidized multiwalled carbon nanotubes. *Journal of Colloid and Interface Science,* 330(1)**,** pp 1-8.

Singla, P., Mehta, R. & Upadhyay, S. N. 2012. Clay modification by the use of organic cations. *Green and Sustainable Chemistry,* 2(21-25.

Smaranda, C., Bulgariu, D. & Gavrilescu, M. 2009. An investigation of the sorption of Acid Orange 7 from aqueous solution onto soil. *Environmental Engineering and Management Journal,* 8(6)**,** pp 1391-1402.

Soule, N. M. & Burns, S. E. 2001. Effects of organic cation structure on behavior of organobentonites. *Journal of Geotechnical and Geoenvironmental Engineering,* 127(4)**,** pp 363-370.

Takahashi, C., Shirai, T., Hayashi, Y. & Fuji, M. 2013. Study of intercalation compounds using ionic liquids into montmorillonite and their thermal stability. *Solid State Ionics,* 241(53-61.

Tan, I. A. W., Ahmad, A. L. & Hameed, B. H. 2008. Adsorption of basic dye using activated carbon prepared from oil palm shell: batch and fixed bed studies. *Desalination,* 225(1–3)**,** pp 13-28.

Thomas, H. C. 1944. Heterogeneous Ion Exchange in a Flowing System. *Journal of the American Chemical Society,* 66(10)**,** pp 1664-1666.

Turner, E. A., Pye, C. C. & Singer, R. D. 2003. Use of ab initio calculations toward the rational design of room temperature ionic liquids. *The Journal of Physical Chemistry A,* 107(13)**,** pp 2277-2288.

Upson, R. & Burns, S. 2006. Sorption of nitroaromatic compounds to synthesized organoclays. *Journal of Colloid and Interface Science,* 297(1)**,** pp 70-76.

Vakili, M., Rafatullah, M., Salamatinia, B., Abdullah, A. Z., Ibrahim, M. H., Tan, K. B., Gholami, Z. & Amouzgar, P. 2014. Application of chitosan and its derivatives as adsorbents for dye removal from water and wastewater: A review. *Carbohydrate Polymers,* 113(115-130.

Vijayaraghavan, K., Jegan, J., Palanivelu, K. & Velan, M. 2004. Removal of nickel (II) ions from aqueous solution using crab shell particles in a packed bed up-flow column. *Journal of Hazardous Materials,* 113(1)**,** pp 223-230.

Weber, W. J. & Morris, J. C. 1963. Kinetics of adsorption on carbon from solution. *Journal of the Sanitary Engineering Division. ASCE,,* 89(31.

Welton, T. 1999. Room-temperature ionic liquids. Solvents for synthesis and catalysis. *Chemical Reviews,* 99(2071-2084.

Wu, Q., Li, Z. & Hong, H. 2013. Adsorption of the quinolone antibiotic nalidixic acid onto montmorillonite and kaolinite. *Applied Clay Science,* 74(66-73.

Xu, S. & Boyd, S. A. 1995. Cationic surfactant sorption to a vermiculitic subsoil via hydrophobic bonding. *Environmental Science & Technology,* 29(2)**,** pp 312-320.

Yoshida, H., Okamoto, A. & Kataoka, T. 1993. Adsorption of acid dye on cross-linked chitosan fibers: Equilibria. *Chemical Engineering Science,* 48(12)**,** pp 2267-2272.

Zaghouane-Boudiaf, H. & Boutahala, M. 2011. Preparation and characterization of organo-montmorillonites. Application in adsorption of the 2, 4, 5-trichlorophenol from aqueous solution. *Advanced Powder Technology,* 22(6)**,** pp 735-740.

Zargar, B., Parham, H. & Hatamie, A. 2009. Fast removal and recovery of amaranth by modified iron oxide magnetic nanoparticles. *Chemosphere,* 76(4)**,** pp 554-557.

Zhao, H., Jaynes, W. F. & Vance, G. F. 1996. Sorption of the ionizable organic compound, dicamba (3, 6-dichloro-2-methoxy benzoic acid), by organo-clays. *Chemosphere,* 33(10)**,** pp 2089-2100.

Zhou, Q., Frost, R. L., He, H., Xi, Y. & Liu, H. 2007. Adsorbed para-nitrophenol on HDTMAB organoclay—A TEM and infrared spectroscopic study. *Journal of Colloid and Interface Science,* 307(2)**,** pp 357-363.

CHAPTER 5: KINETIC AND ISOTHERM STUDIES OF PHENANTHRENE AND ACID RED ON KAOLIN MODIFIED WITH 1-HEXYL, 3-DECAHEXYL IMIDAZOLIUM IONIC LIQUID

Isiaka A. Lawal[a] and Brenda Moodley[a]*

[a]School of Chemistry and Physics, College of Agriculture, Engineering and Science, University of KwaZulu-Natal, P/Bag X45001, Westville Campus, Durban, 4000, South Africa

*corresponding author email: moodleyb3@ukzn.ac.za

Tel: +27 31 2602796; Fax: +27 31 2603091

First author: lawalishaq000123@yahoo.com

5.1 ABSTRACT

Batch and column adsorption studies were carried out to determine the efficiency of kaolin modified with a novel long chain ionic liquid (IL) 1-hexyl, 3-decahexyl imidazolium. Synthesis of 1-hexyl, 3-decahexyl imidazolium was carried out and subsequently characterised by nuclear magnetic resonance (^{1}H and ^{13}C NMR) and fourier transform infrared (FT-IR) spectroscopy. The chemical composition of kaolin (K) was determined using energy dispersive x-ray analyzer (EDX). Kaolin was modified with IL to form hydrophobic kaolin (K-IL) by adding IL in excess of the cation exchange capacity (CEC) of K. This (K-IL) was then characterised using FT-IR, x-ray diffraction (XRD), Brunauer−Emmett−Teller (BET), thermal gravimetric analysis and differential thermal (TGA/DCS) analysis, and scanning electron microscopy (SEM). The CEC of K-IL (21 meq per 100 g) and K (18 meq per 100 g) were also determined. K-IL was subsequently used in column and batch adsorption studies for both polyaromatic hydrocarbon (phenanthrene) and dye (acid red). These studies revealed that K-IL was an efficient material for the removal of both phenanthrene and acid red dye. For column studies, the adsorption capacity, depth of exchange zone, time required for exchange zone to move its own height and adsorption rates were investigated using Adams-Bohart, Yoon-Nelson model flow and Thomas sorption model. The

effect of flow rate and influent concentration on breakthrough curves were also investigated. The column adsorption capacity at the same flow rate and different concentrations for phenanthrene were 222.9, 611.8 and 1093.5 mg g^{-1}, while that of acid red dye were 877.0, 1337.4 and 1350.7 mg g^{-1}. Thomas and Yoon–Nelson models best explained the column studies. Data from both batch studies fitted well to pseudo-second order for the rate determining step. The Langmuir isotherm had the best fit with an adsorption capacity of 842.7 mg g^{-1} for dye and the Freundlich isotherm best described phenanthrene with an adsorption capacity of 188.9 mg g^{-1}.

Keywords: Ionic liquid, 1-hexyl 3-decahexyl imidazolium, kaolin, column studies, adsorption, polycyclic aromatic hydrocarbon, phenanthrene, acid red.

5.2 INTRODUCTION

Water pollution with organic compounds such as polycyclic aromatic hydrocarbons (PAHs) and dyes are a worldwide concern. PAHs are considered possible human carcinogens by the US EPA (Van Metre et al., 2006). Much attention has been drawn to their distribution in the environment and potential risks to human health (Registry, 1995). Phenanthrene (PHN), which is a PAH is an abundant component of crude oil and can enter natural water through oil spillage or leakage, industrial effluents, urban run-off, and municipal effluents (Manoli and Samara, 1999). Dyes get into wastewater from various industries such as dyestuff, textile, leather, paper and plastics. Dyes are difficult to remove, they resist aerobic breakdown, and are stable with oxidizing agents. Moreover, wastes generated from dyes are not just considered toxic, but they are also potentially carcinogenic (Crini and Badot, 2008). Therefore, removal of these organic pollutants from effluents becomes environmentally important.

A number of methods have been used for the removal of PAHs and dyes from wastewater including chlorination, oxidation, and ultrasonic irradiation. Photo degradation, coagulation, precipitation, biodegradation, membrane separation and adsorption have also been utilized (Crini and Badot, 2008; Peternel et al., 2007). Adsorption is commonly applied in the removal of organic compounds

and dyes from wastewater due to its high removal efficiency (Eckenfelder, 2000). Activated carbon is the most commonly used adsorbent, but it does have limitations in application which includes its inefficiency in removing oil, grease, natural organic matter, and other large organic molecules (Alther, 2002). Organoclays are however capable of removing oil and grease at 5–7 times the rate of activated carbon or at 50% of its dry weight (Alther, 1995). The affinity of clay for hydrophobic organic compounds is generally considered less significant due to its hydrophilic surface (Hassett and Banwart, 1989). However, clays can be activated for hydrophobic sorption *via* simple ion exchange reactions using organic cations (Boyd et al., 1988; El-Nahhal et al., 1998) thus converting it to organoclay.

The adsorption of organic molecules (ionic and non-ionic) on organoclays has been extensively studied (Theng, 1974; Boyd et al., 1988). Also, previous studies showed that organoclays are good adsorbents for the removal of organic pollutants (Smith et al., 1990; Zhu et al., 1997; Dentel et al., 1998; Upson and Burns, 2006; Sheng and Boyd, 2000). The adsorption mechanism and capacity depend on the molecular structure, amount of exchanged organic cations or ammonium cation, chemical properties of the organic compounds, and the CEC of the clay mineral (Smith et al., 1990; Sheng Guangyao and Stephen, 1997; Zhu et al., 1997; Bartelt-Hunt et al., 2003; Upson and Burns, 2006; Gullick and Weber, 2001). Long hydrocarbon chains that are greater than 12 carbon atoms have proven to be very good modifiers of clay for the purpose of adsorbing ionic and non-ionic compounds (Gullick and Weber, 2001; Lee et al., 1989b; Nir et al., 2007).

The alkyl chains create an organic partition medium that can adsorb organic pollutants through hydrophobic interaction (Rodriguez-Cruz et al., 2008). In the work of Upson and co-workers as well as other researchers, hexadecyltrimethylammonium was used for the adsorption of organic pollutants (Redding et al., 2002; Bartelt-Hunt et al., 2003; Upson and Burns, 2006). A similar result was reported for the adsorption of xylene onto smectite modified with tetramethylammonium (Lee et al., 1989a). Huang and co-workers reported that kaolin and montmorillonite modified with aromatic organic constituents have higher adsorption capacities for naphthalene and phenanthrene than those modified with aliphatic organic compounds (Huang et al., 2005). Organo-montmorillonite has also been used for the adsorption of dye (Lee et al., 2001; Özcan et al., 2004).

Ionic liquids have also been used to modify adsorbents for the adsorption of organic pollutants. Recently, Lawal and Moodley (Lawal and Moodley, 2015) adsorbed amaranth dye using montmorillonite modified with 1-methyl, 3-decahexyl imidazolium. Absalan and co-workers reported the adsorption of reactive red-120 and 4-(2-pyridylazo) resorcinol from aqueous solution by ionic liquid modified Fe_3O_4 magnetic nanoparticles (Absalan et al., 2011). Also, the adsorption of folic acid, riboflavin, and ascorbic acid has been reported using ionic liquid modified Fe_3O^+ magnetic nanoparticles (Kamran et al., 2014). There is presently limited information on the adsorption of organics using IL modified materials and to the best of our knowledge there are no reports on IL modified kaolin for the adsorption of either polycyclic aromatic hydrocarbons (phenanthrene) or dye (acid red). This lack of research on IL modified kaolin for the adsorption of phenanthrene or acid red dyes has therefore prompted our investigation into the adsorption behaviour of these two organic pollutants on IL modified kaolin.

In this work, cationic IL (1-hexyl, 3-decahexzyl imidazolium) was synthesised and used in modifying kaolin. The modified kaolin was then used to adsorb phenanthrene and acid red dye (ARD) using column and batch studies.

5.3 EXPERIMENTAL SECTION

5.3.1 Materials
Kaolin (CAS Number 1318-747) used in the study with chemical formula of $Al_2O_7SiO_2.2H_2O$ DMSO (CAS Number 67-68-5) were purchased from Sigma Aldrich. 1-bromodecahexane (CAS Number 1318-93-0), imidazole (CAS Number 288-32-4), 1-bromohexane (CAS Number 111-25-1), benzyl bromide (CAS Number 602-057-002), acid red dye and phenanthrene were purchased from Merck. Double distilled water was used for all sample preparation.

5.3.2 Apparatus
1-hexyl, 3-decahexyl imidazolium (IL) is a salt consisting of imidazolium (a five membered ring compound with two nitrogen atoms with one of them a quaternary ammonium) at the center with a hexyl group and decahexyl alkyl (16 carbon) chain attached to the ammonium and the quaternary

ammonium in the ring respectively. The preparation was in two stages, formation of the 1-hexyl imidazole and formation of the salt.

The formation of the 1-hexyl imidazole was achieved by modification of the method used by Starikova and co-workers (Starikova et al., 2003). Briefly, KOH (0.84 g, 0.015 mmol) was added to the solution of imidazole (0.01 mol) in DMSO (30 mL) and stirred at room temperature for 2 h. Freshly distilled alkyl halide (0.01 mol) was added drop wise to the mixture under vigorous stirring and thereafter cooled in a water bath. After 5 h the mixture was diluted with distilled water and extracted with dichloromethane (10 x 10 mL), the organic layers were washed with distilled water to pH 7, and dried over $MgSO_4$. After removal of chloroform the residue was distilled under vacuum. Column chromatography was used for product purification. Before formation of the salt, the product was characterised by ^{1}H and ^{13}C NMR to ascertain its purity. (Spectral data can be found in Appendix C 2 and C 2.0).

Formation of the salt was achieved using the Dzyuba and Bartsch method (Dzyuba and Bartsch, 2001). An oil bath with a stirred flask containing equimolar amounts of 1-hexyl imidazole and the primary alkyl bromide (bromodecahexane) was heated at 140 °C for 10-15 min and thereafter cooled. The solution was heated again in the oil-bath at 140 °C for another 10-15 min, followed by drying under vacuum at 100-120 °C to give the desired product of a highly viscous golden coloured liquid that solidified at room temperature.
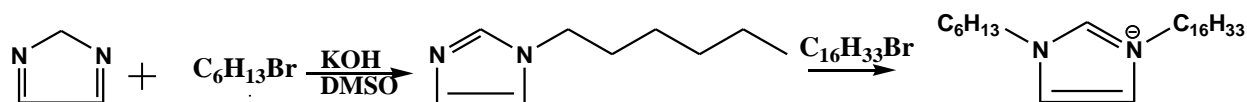
Scheme 1. Synthesis of 1- hexyl, 3-decahexyl imidazolium

5.3.3 Preparation of Modified Kaolin

Kaolin (K) was soaked in deionized water overnight and thereafter centrifuged. The fine upper clay layer was decanted, dried and thereafter passed through a 53 μm sieve. The cations exchangeable capacity, CEC, was determined using the Gillman and Sumpter method (Gillman and Sumpter, 1986) resulting in a CEC of 18 meq per 100 g. K was modified by adding IL in

excess of its CEC to make the surface of the material positively charged (Newman, 1987). K and 1-hexyl, 3-decahexyl imidazolium IL were thoroughly mixed with methanol, stirring for about 1 h and then oven dried overnight at 80 °C. Newman (Newman, 1987) reported that clay can adsorb more than its CEC and in the work of Xu and Boyd (Xu and Boyd, 1995; Zhao et al., 1996), addition of the organic cation greater than the CEC of the clay leads to the adsorption of the organic cation on the external surface of the material, through cation exchange and hydrophobic bonding, which generates positive charges on the surface. The mass of IL required was calculated using the following equation (Soule and Burns, 2001):

$$Mc = f * CEC * X * GMW...5.1$$

Mc is the mass of organic cation required to achieve the desired fraction of CEC (g), f is the fraction of cation-exchange capacity satisfied by the organic cation (no unit), CEC is the cation exchange capacity of the clay (mmol per g clay), X is the mass of clay (g) and GMW is the gram molecular weight of IL (g mol^{-1})

5.3.4 Column Studies

Column studies were conducted using glass columns of 1.5 cm internal diameter and 55 cm length. The columns were packed with a known quantity of the modified kaolin between two supporting layers of glass wool to prevent the adsorbent floating from the outlet. The mass of the adsorbent was kept constant all through the experiment. The flow rate was varied from 2 mL min^{-1} to 8.4 mL min^{-1} and influent concentration varied from 50 to 200 mg L^{-1} for both PHN and ARD. Aliquots were removed at different intervals, from the phenanthrene and dye column for quantification.

5.3.5 Analysis of Column Data

The shape and time for breakthrough curve are very important characteristics for determining the operation and the dynamic response of adsorption in a column. The loading behavior of solute, to be removed from solution, in a column is shown by its breakthrough curves and is expressed in terms of adsorbed solute concentration (Cad), influent concentration of solute (Co), effluent concentration of solute (Ct) or normalized concentration defined as the ratio of effluent of solute

concentration to influent solute concentration (Ct/Co) as a function of time or volume of effluent for a given bed height (Guo and Lua, 2003).

Effluent volume (V_{eff}) can be calculated as:

$$V_{eff} = Qt_{total}...5.2$$

Where t_{total} and Q are the total flow time (min) and volumetric flow rate (mL min^{-1}) respectively. The plot of the area under the breakthrough curve (A) obtained by integrating the adsorbed concentration (Cad in mg L^{-1}) *versus* t (min), and can be used to find the total adsorbed quantity of solute (maximum column capacity). Total adsorbed quantity of solute q_{total} (mg) in the column for a given influent concentration and flow rate is calculated as (Aksu and Gönen, 2004):

$$q_{total} = \frac{Q}{1000} \int_{t=0}^{t=t_{total}} Cad \ dt...5.3$$

Equilibrium uptake q_{eq} (mg g^{-1}) or maximum capacity of the column is defined as the total amount of pollutant adsorbed (q_{total}) per gram of adsorbent w (g), at the end of total flow time (Aksu and Gönen, 2004):

$$q_{eq} = \frac{q_{total}}{W}...5.4$$

5.3.6 Column Models

5.3.6.1 Thomas model
The data obtained were fitted into the Thomas model (Thomas, 1944) in order to predict the adsorptive curve of breakthrough of the effluent and the determination of the maximum adsorption capacity of the adsorbent in the column.

The Thomas expression is represented by equation 5.5.

$$\frac{Ct}{C_0} = \frac{1}{1+\exp[k_{Th}(q_0x - C_0V_{eff})/v}...5.5$$

Where k_{Th} is the Thomas rate constant (mL min^{-1} mg^{-1}), q_o is the equilibrium uptake of PHN and ARD per g of the adsorbent (mg g^{-1}), x represents the mass of adsorbent in the column (g), V_{eff} is the effluent volume (mL), C_0 and C_t is the solute influent concentration and effluent concentration at time t (mg L^{-1}) respectively, and v is the flow rate (mL min^{-1}). The value of C_t/C_0 is the ratio of effluent and influent of the dye concentrations. The value of time t (min) is $t = V_{eff}/v$. The kinetic coefficient k_{Th} and the adsorption capacity of the column q_o can be determined from a plot of C_t/C_0 against t at a given flow rate using non-linear regression from equation 6.

$$\ln\left(\frac{C_0}{C_t} - 1\right) = \frac{k_{Th}\, q_0 X}{v} - k_{Th} C_0 t ...5.6$$

5.3.6.2 Adams–Bohart model

The data were also fitted into the Adams-Bohart model (Bohart and Adams, 1920). This model assumes that the concentration of the adsorbing species and residual capacity of the adsorbent are both proportional to the adsorption rate. The Adams–Bohart model is used for the description of the initial part of the breakthrough curve.

$$\frac{C_t}{C_0} = \exp\left(k_{AB}C_0 t - k_{AB}N_0 \frac{Z}{F}\right)...5.7$$

$$\ln\frac{C_t}{C_0} = k_{AB}C_0 t - k_{AB}N_0 \frac{Z}{F}...5.8$$

Where C_0 and C_t are the initial concentration and concentration at a given time (mg L^{-1}), F is the velocity (mL min^{-1}), K_{AB} is the kinetic constant (mL min^{-1} mg^{-1}), N_o (mg L^{-1}) is the maximum adsorption capacity and Z is the bed height of the column. From the linearized equation, values describing the characteristic operational parameters of the column can be determined from a plot of ln C_t/C_0 against t at a given bed height and flow rate.

5.3.6.3 Yoon–Nelson model

The Yoon–Nelson is based on the assumption that the rate of decrease in the probability of adsorption for each adsorbate molecule is proportional to the probability of adsorbate adsorption and the probability of adsorbate breakthrough on the adsorbent (Yoon and Nelson, 1984). The Yoon–Nelson equation is expressed as in equation (9) and as the linearized form in equation (10).

$$\frac{C}{C_{o-C}} = exp\,(k_{YN}t - \tau k_{YN}) \,...5.9$$

$$\ln\frac{C}{(C_{o}-C)} = k_{YN}t - \tau k_{YN}...5.10$$

Where k_{YN} is the rate constant (min^{-1}); τ is the time required for 50% adsorbate breakthrough in min and t is the breakthrough sampling time also in min. The calculation of theoretical breakthrough curves for a single-component system requires the determination of the parameters k_{YN} and τ for the adsorbate of interest. The parameters in the equation can be determined from available experimental data by plotting ln (C/Co−C) *versus* sampling time (t). If the theoretical model accurately characterizes the experimental data, this plot will result in a straight line with slope of k_{YN} and intercept τ k_{YN}

5.3.7 Kinetics and Equilibrium Studies

Adsorption kinetics were determined by analyzing the adsorptive uptake of PHN and ARD from its aqueous solutions ranging from 25 mg L^{-1} to 500 mg L^{-1} at different times with no pH adjustment for PHN and at pH 2 for ARD. The equilibrium data for developing the isotherms were obtained by mixing 0.1 g and 0.08 g of K-IL with PHN and ARD respectively for 36 h. After equilibrium, the aqueous phase concentration of PHN was determined by an Agilent high-pressure liquid chromatography (HPLC) system equipped with a UV detector. The mobile phase used was acetonitrile/water in a ratio of 80:20 in isocratic mode. A C_{18} column was used with an I.D. of 4.6 mm and a length of 150 mm. The flow rate was 1 mL min^{-1} and the detection wavelength was 254 nm. ARD was determined by a double beam UV−Vis−NIR spectrophotometer (Shimadzu Model UV 3600, Japan) at λ_{max} 532. The equilibrium adsorption capacity of K-IL was calculated from the following relationship:

$$q_e = \frac{C_o - C_e}{W} V \quad ...5.11$$

Where q_e is the equilibrium adsorption capacity in (mg g^{-1}), C_0 and C_e are the dye concentrations at initial and at equilibrium respectively (in mg L^{-1}), V is the volume of solution in (L), and W is the weight of adsorbent in (g).

Adsorption data from both PHN and ARD were fitted to the Freundlich (Freundlich, 1906), Langmuir (Langmuir, 1916), Temkin and Dubinin–Raduskevich (Dubinin and Radushkevich, 1947) isotherms. Linear equations of all the applied models are:

$$\text{Langmuir model: } \frac{C_e}{q_e} = \frac{C_e}{q_m} + \frac{1}{q_m b} ...5.12$$

$$\text{Freundlich model: } \ln q_e = \ln K_f + \frac{1}{n} \ln C_e ...5.13$$

$$\text{Temkin model: } q_e = B \ln A + B \ln C_e ...5.14$$

$$\text{Dubinin–Raduskevich model: } \ln q_e = \ln q_m - \beta \Sigma^2 ...5.15$$

$$\Sigma = RT \ln \left[1 + \frac{1}{C_e} \right] ...5.16$$

$$E = \frac{1}{\sqrt{2\beta}} ...5.17$$

Where C_e is the equilibrium dye concentration in the solution in mg L^{-1}, b is the Langmuir adsorption constant (L mg^{-1}), and q_m is the theoretical maximum adsorption capacity (mg g^{-1}). K_f (L mg^{-1}) and n are Freundlich isotherm constants indicating the capacity and intensity of the adsorption, respectively. A is the equilibrium binding constant (L mg^{-1}) and B is the heat of adsorption. β is the Dubinin–Raduskevich model constant (mol^2 kJ^{-2}) related to the mean free energy of adsorption per mole of the adsorbate and Σ is the polanyi potential. E is the mean free energy of adsorption (kJ mol^{-1}).

In order to determine the mechanism and potential rate-controlling steps involved in the process of adsorption, both data were also fitted into pseudo first order (Lagergren, 1898), pseudo second

order (Ho and McKay, 1999), and intra-particle diffusion models. The pseudo first order kinetic model equation is:

$$\ln(q_e - q_t) = \ln q_e - k_1 t \ldots 5.18$$

Where q_t is the amount of adsorption at time t in (mg g^{-1}), k_1 is the rate constant of the equation in (L min^{-1}), and q_e is the amount of adsorption equilibrium in (mg g^{-1}). The adsorption rate constant (k_1) can be determined experimentally by plotting ln (q_e-q_t) *versus* t.

The pseudo second order kinetic model is expressed as:

$$\frac{t}{q_t} = \frac{1}{k_2 q_e^2} + \frac{t}{q_e} \ldots 5.19$$

Where k_2 is the equilibrium rate constant of pseudo second order adsorption in (g mg^{-1} min^{-1}). The values of k_2 and q_e can be determined from the slope and intercept of the plot t/q_t *versus* t, respectively.

The data were further fitted into the Weber–Morris model, to evaluate the possibility of intra-particle diffusion as the rate limiting step; it is given by equation 20 (Weber and Morris, 1963):

$$q_t = k_{id} t^{1/2} \ldots 5.20$$

Where k_{id} (mg g^{-1} h$^{-1/2}$), is the intra-particle diffusion rate constant.
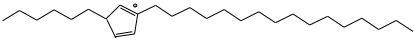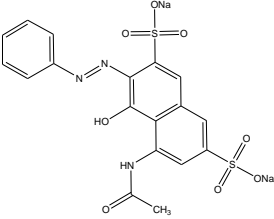
5.4 RESULTS AND DISCUSSION

5.4.1 Characterization of 1-hexyl, 3-decahexyl Imidazolium Ionic Liquid

Characterization was done using ^{1}H NMR and ^{13}C NMR.

^{1}H NMR (400 MHz, CDCl$_3$): δ (ppm) 0.85 (t, 6H), 1.2 (m, 32H) 1.88 (q, 4H), 4.33 (t, 4H), 7.3 (d 2H), 10.6 (s, 1H). ^{13}C NMR (400 MHz, CDCl$_3$): δ (ppm) 13.90, 14.10, 22.37, 22.68, 25.88, 26.26, 28.17, 28.76, 29.00, 29.34, 29.43, 29.53, 29.64, 29.68, 30.24, 30.30, 31.06, 31.91, 32.84, 34.06, 50.19, 50.21, 121.59, 121.57, 137.61. FT-IR v = 3406 (N–H stretch, 2° amines), 3125, 3087 and 3061 (C–H stretch, aromatics), 2981, 2945, 2916, 2849 (C–H stretch, alkanes), 1667, 1605, 1561, (C–C stretch (in–ring), aromatics), 1495, 1471, 1464 (C–H bend, alkanes), 1367, 1336, 1327 (C–H rocking, alkanes), 1207, 1197, 1146, 1088, 1030, 1001 (C–N stretch, aromatic amines), 835, 815, 778, 734, 710, 678, 616, 568, 474, 401 (C–H aromatics). Further information is shown in Table 5.1 and additional spectral data can be found (Appendix C 2.2, C 2.3 and D 1.0).

Table 5.1 Properties of the surfactant and pollutants used in this study

Compound	Formula	Structure	Molecular Weight (M.W.) g mol^{-1}
1-hexyl, 3-decahexyl imidazolium ionic liquid	C$_{25}$H$_{52}$N$_2$$^+$		380.69
Phenanthrene	C$_{14}$H$_{10}$		178.23
Acid red dye 1	C$_{18}$H$_{13}$N$_3$Na$_2$O$_8$S$_2$		509.42

5.4.2 Characterization of K and K-IL

EDX analysis was used to determine the chemical composition of kaolin. Table 5.2, indicates that silica and alumina are the main components of kaolin, with impurities such as sodium, potassium, iron, magnesium, calcium, and titanium oxides in trace amounts. SiO_2 and Al_2O_3 will therefore be the main adsorbing sites (Özcan et al., 2004).

Table 5.2 Chemical composition of kaolin

Composition	% weight
SiO_2	52.7
Al_2O_3	38.6
K_2O	1.9
TiO_2	1.3
CaO	1.1
Fe_2O_3	0.9
MgO	0.8
Na_2O	0.6
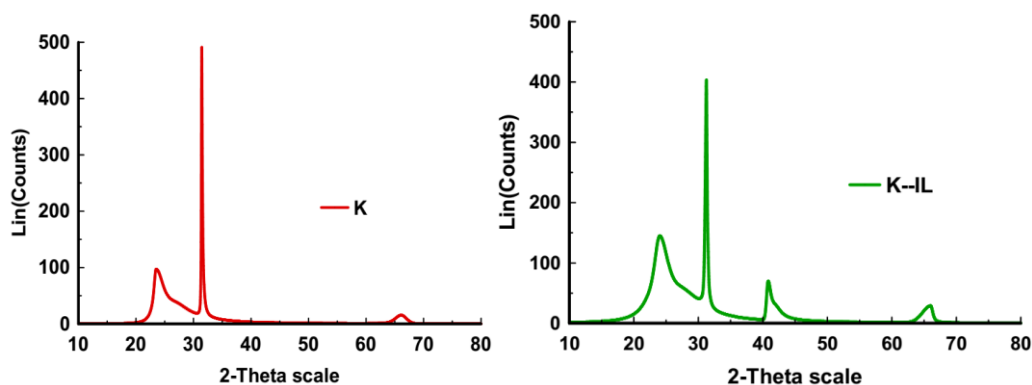
Fig. 5.1 XRD spectra of (a) K and (b) K–IL

The XRD of K was compared with IL intercalated kaolin (K–IL) as shown in Figs. 5.1a and 1b. IL intercalation of the kaolin decreased the intensity of the spectra compared to the unmodified

130

kaolin and made the width of the peak at half-peak height broader. A similar trend was observed in the modification of montmorillonite with ionic liquid (Lawal and Moodley, 2015) and similar results have been reported with other surfactants (Lee and Kim, 2002; Yahaya et al., 2009; Domka et al., 2008).

The CEC of modified kaolin (K-IL) was determined to be 21 meq per 100 g, which implies that IL is in excess of CEC of K in the interlayer silicate layer of K-IL when compared with the CEC of K (18 meq per 100 g) which further proved that K had been modified by IL.
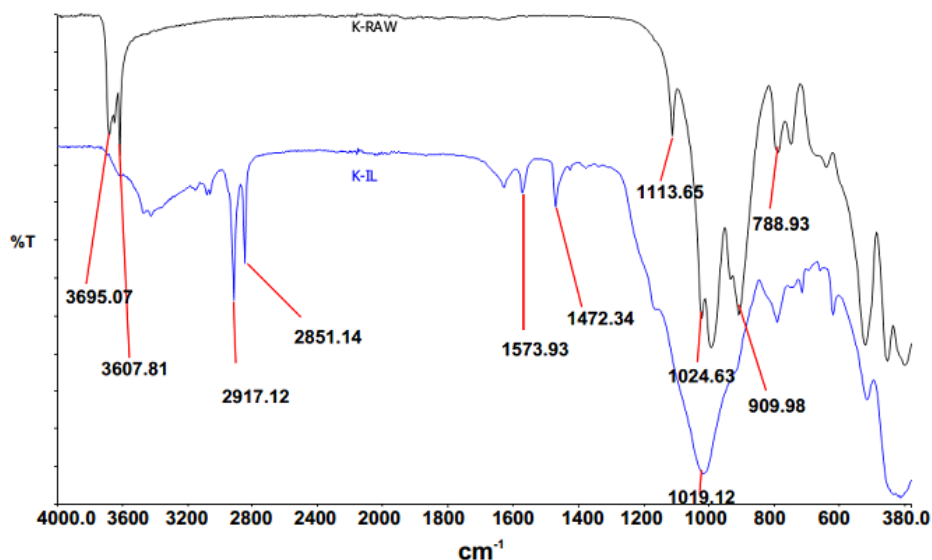
Fig. 5.2 FT-IR spectra of K and K-IL

FT-IR of K and K-IL was recorded in the region of 380-4000 cm^{-1} as shown in Fig 5.2. These spectra further showed that IL actually intercalated into the silicate lattice of K-IL. The presence of peaks in the region of 3695-3607 cm^{-1} represent the OH stretching of inner-surface hydroxyl groups within the clay (Boufatit et al., 2008). There was a significant reduction of these peaks when IL was added, indicating that the water of hydration is lost as the OH is replaced by cationic surfactant (alkyl chain). The same trend was reported when ionic liquid was modified with montmorillonite (Lawal and Moodley, 2015). The peaks at 2917 and 2851 cm^{-1} represent the

symmetric and asymmetric stretching vibrations of the methylene groups in the ionic liquid while peaks 1573 and 1472 cm^{-1} are their bending vibrations respectively (Zhou et al., 2007). The peak at 1113 cm^{-1} is assigned to Si–O stretching (longitudinal mode), while that at 1024–1019 cm^{-1} is the in-plane Si–O stretching. The peak at 909 cm^{-1} is the OH deformation of the inner-surface hydroxyl group, while 788 cm^{-1} is assigned to Si–O.

The surface morphologies of the K and K-IL samples were analyzed using SEM. Different morphologies were observed for both materials and a higher porosity was noticed for K (Fig 5.3a). K-IL showed delamination of the layers of the clay mineral due to the presence of cations of the salt (dos Santos et al., 2013). K and K-IL indicated dominant layers of groups of hexagonal sheets which is characteristic of kaolin (Murray, 2000). Also, a smoother surface morphology for K-IL can be observed compared with K. Similar results have been reported by Sunardi and co-workers (Sunardi et al., 2011).
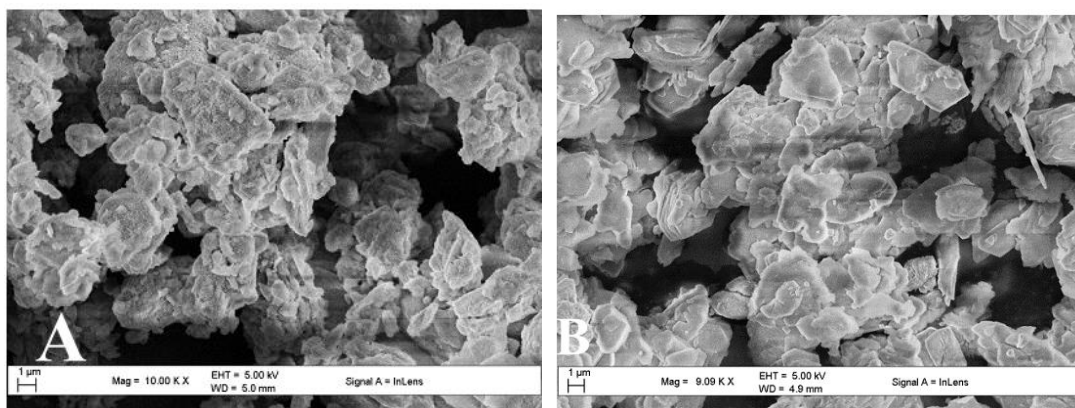
Fig. 5.3a and 5.3b SEM images (mag 10 000x) of (a) K and (b) K-IL

The surface area was determined using Brunauer−Emmett−Teller (BET). K has a surface area of 12.63 m^2 g^{-1} and a pore volume of 0.21 cm^3 g^{-1} and K-IL has a surface area of 10.52 m^2 g^{-1} and pore volume of 0.19 cm^3 g^{-1}. The decrease in the surface area and pore volume of K-IL further confirmed modification of the adsorbent (blocking of the pores by the ionic liquid cation).
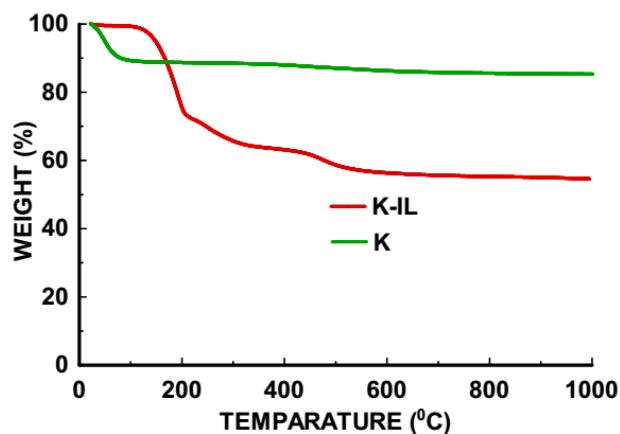
Fig. 5.4 TGA spectra of K and K-IL

The thermal study (TGA) of the material showed loss of water from K (Fig 5.4) at about 100 °C which is due to the removal of the externally absorbed and interlayer water, leaving behind the kaolin, which gives rise to a near straight line. The TGA for K-IL showed no decomposition below 150 °C. This indicated that the alkyl chain in the IL has exchanged all the water of hydration in the interlayer of the K. The decomposition of K-IL was observed in the range of 180 to 550 °C which is due to the decomposition of the alkyl chain on IL. Similar results have been reported by other researchers (Bastow et al., 1991; Takahashi et al., 2013; Lawal and Moodley, 2015). The TGA results further confirmed that kaolin had been modified with IL.

5.4.3 Column Studies

5.4.3.1 Effect of initial concentration

The effect of different concentrations (50 to 200 mg L^{-1}) of phenanthrene and acid red influent with the same mass of K-IL (0.5 g) and solution flow rate of 5 mL min^{-1} is shown in the breakthrough curves in Fig. 5.5a and 5b. As shown in these figures, the breakthrough time increases with a decrease in the influent concentration for both PHN and ADR. Sharper breakthrough curves were also observed at increased influent concentration. At higher influent concentrations, transport of the two solutes to the adsorbent are faster, leading to higher gradients

due to increased diffusion coefficients or mass transfer coefficients which are the driving force for the adsorption process (Tan et al., 2008). The larger the influent concentration, the steeper the slope of breakthrough curve and the smaller the breakthrough time (Aksu and Gönen, 2004).

Fig. 5.5a and 5.5b Breakthrough curves of the (a) effect of initial concentration of phenanthrene and (b) acid red dye adsorption onto modified Kaolin

These results also show that changes in concentrations of the influent affects the saturation rate and breakthrough time, or in other words, the diffusion process is concentration dependent. Similar trends were obtained from other studies (Han et al., 2007; Ahmad and Hameed, 2010; Lin et al., 2004). Also the adsorption capacity increases with increasing influent concentrations due to the fact that high concentration provides a higher driving force for the adsorption process, as shown in Table 5.3.

5.4.3.2 Effect of the solution flow rate

The effect of the flow rate on the adsorption of phenanthrene and dye on modified kaolin was investigated by varying the flow rate (2, 5 and 8.4 mL min^{-1}) with a K-IL mass (0.5 g) and the influent concentrations (100 mg L^{-1}) for both PHN and ARD (Fig. 5.6a and 5.6b). Faster breakthrough was observed as the flow rate increased. This was because at a slow flow rate the influent had more contact time with the adsorbent material in the column, which in turn led to higher removal of PHN and ARD in the column. This resulted in slope variation of the

134

breakthrough curve and adsorption capacity as shown Fig. 5.6 and Table 5.3. Mass transfer explains why at higher flow rate, adsorption of PHN and ARD onto K-IL is increased leading to quick saturation (Ko et al., 2000). As shown in Table 5.3, the faster the flow rate, the lower the adsorption capacity. This is due to insufficient contact time of the solute (PHN and ARD) with the material in the column, and therefore the adsorbate leaves the column before equilibrium occurs. These results were in agreement with other studies carried out on adsorption of metal ions on bone char and *Pinus sylvestris* sawdust (Ko et al., 2000; Taty-Costodes et al., 2005).
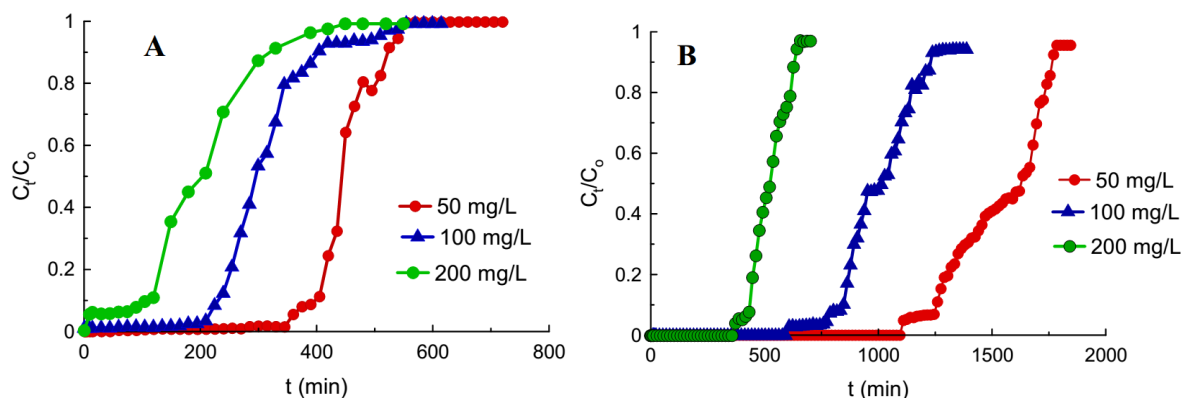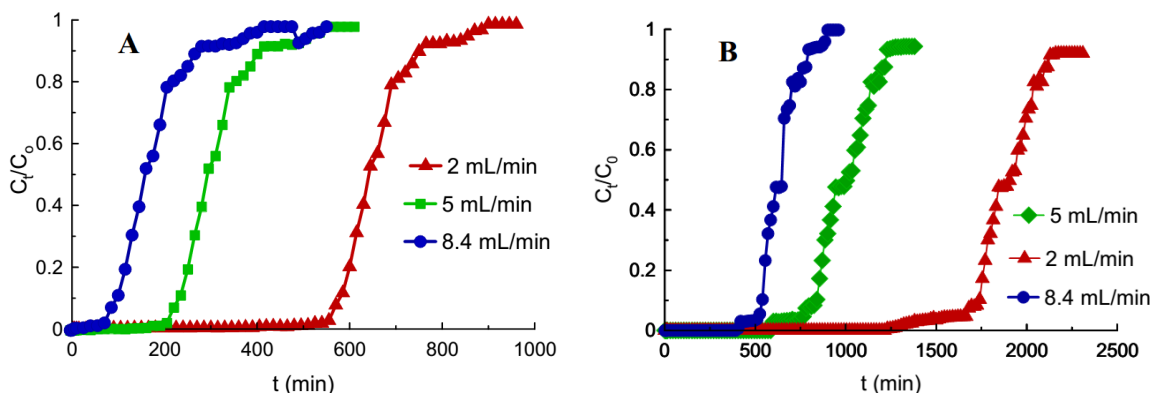

Fig. 5.6a and 5.6b Breakthrough curves of the effect of flow rate of (a) phenanthrene and (b) acid red dye adsorption onto modified kaolin

5.4.4 Column Models

5.4.4.1 Thomas model

The column data were fitted into the Thomas model to determine the Thomas rate constant k_{Th} and equilibrium uptake (q_o) of PHN and ARD per g of the adsorbent (mg g^{-1}). Table 5.3 shows the parameters of the Thomas model, with R^2 values ranging from 0.894 to 0.966 for PHN, and 0.928 to 0.979 for ARD. Also, from Table 5.3, as the influent concentration increased the value of q_o increased, while the values of k_{Th} decreased. This can be attributed to the driving force for adsorption which is the concentration difference between the solutes on the adsorbent and the solutes in the solution (Aksu and Gönen, 2004; Vijayaraghavan et al., 2004; Ahmad and Hameed, 2010). Furthermore, as the flow rate increased, the value of q_o decreased and the values of k_{Th}

Table 5.3 Column q$_e$, Thomas, Adams-Bohart, and Yoon-Nelson model parameters using linear regression analysis for PAH adsorption with varying concentrations and flow rates

	C$_0$ (mg L^{-1})	V (mL min^{-1})	Column q$_e$ (mg g^{-1})	Thomas model K$_{Th}$ (mL min^{-1} mg^{-1})	q$_0$ (mg g^{-1})	R^2	Adams-Bohart model K$_{AB}$ (mL min^{-1} mg^{-1})	N$_o$ (mg L^{-1})	R^2	Yoon-Nelson model K$_{YN}$ (L min^{-1})	τ (min)	R^2
	50	5.0	222.92	0.000452	205.4	0.900	0.00022	242.77	0.900	0.0115	711.60	0.900
	100	2.0	927.35	0.000134	562.4	0.894	0.00009	338.55	0.888	0.0132	668.58	0.887
PHN	100	5.0	611.78	0.000185	334.7	0.964	0.00011	426.50	0.904	0.0185	334.74	0.964
	100	8.4	382.62	0.000195	231.0	0.964	0.00014	155.17	0.677	0.0174	225.80	0.871
	200	5.0	1093.49	0.000088	419.8	0.966	0.00004	1157.03	0.749	0.0176	209.88	0.966
	50	5.0	877.00	0.000452	766.3	0.928	0.000082	444.98	0.919	0.0077	1532.59	0.927
	100	2.0	1601.10	0.000184	1083.3	0.959	0.00005	703.69	0.935	0.0077	1908.83	0.964
ARD	100	5.0	1337.43	0.000217	1019.7	0.976	0.000104	613.84	0.872	0.0097	1019.67	0.976
	100	8.4	918.35	0.000277	763.5	0.965	0.000112	429.96	0.657	0.0184	644.84	0.959
	200	5.0	1350.74	0.000432	1263.5	0.979	0.000182	939.81	0.919	0.0216	526.99	0.978

increased. Therefore, the column performed better at higher concentrations and slower flow rates of PHN and ARD.

5.4.4.2 Adam's–Bohart model

The values of N_0, k_{AB} and R^2 were calculated from the Adam's-Bohart model for PHN and ARD and are presented in Table 5.3. This model was applied to experimental data for both PHN and ARD to describe the initial part of the breakthrough curve. The adsorption capacity of the adsorbent N_0 for both solutes increased, as the influent concentration increased. Also, as the concentrations and flow rate of both solutes increased k_{AB} increased, but the adsorption capacity of the adsorbent N_0 decreased for the two solutes. This signified that the overall system kinetics was dominated by external mass transfer in the initial part of adsorption in the column (Aksu and Gönen, 2004). This also, indicated that the Adams–Bohart model is valid for the relative concentration region up to 50%. Similar results have been reported by Han and co-workers (Han et al., 2009).

5.4.4.3 The Yoon–Nelson model

The values of K_{YN}, τ and R^2 for PHN and ARD are listed in Table 5.3. It was observed that the rate constant k_{YN} and time required for 50% adsorbate breakthrough, τ, increased and decreased respectively as both flow rate and influent concentrations of both PHN and ARD increased. Table 5.3 shows that the correlation coefficient value (R^2) for both PHN and ARD are best fitted to the Thomas and Yoon–Nelson models with a least R^2 value of 0.887. Therefore, both Thomas and Yoon–Nelson models can be used to describe the behavior of the adsorption on to K-IL in a column. The value of R^2 in the Adam's–Bohart model is slightly lower than Thomas and Yoon–Nelson models under the same experimental conditions. The Adam's–Bohart model is best fitted to the relative concentration up to 0.5 (Ct/Co) and only used for describing the initial part of the breakthrough curve. Studies conducted by other researchers showed similar results (Han et al., 2008; Han et al., 2009; Ahmad and Hameed, 2010).

5.4.4.4 Adsorption kinetics and equilibrium of phenanthrene and acid red dye

The effect of contact time on the extent of PHN and ARD removal at different concentrations is shown in Fig. 5.7a and 7b, where the removal efficiency is plotted against time. Fig. 5.7a and 5.7b indicates that the adsorption of PHN and ARD on the adsorbent increased with time and reached equilibrium in less than 2 min. For acid red dye, equilibrium is reached in less than 5 min as shown in Fig. 5.7b. It is further noticed that at higher concentrations of 500 ppm, 300 ppm and 200 ppm, the % removal efficiency were 67%, 86% and 100% respectively. This trend was expected because at higher concentrations, the adsorption sites are blocked by the pollutant therefore leading to lower removal %.
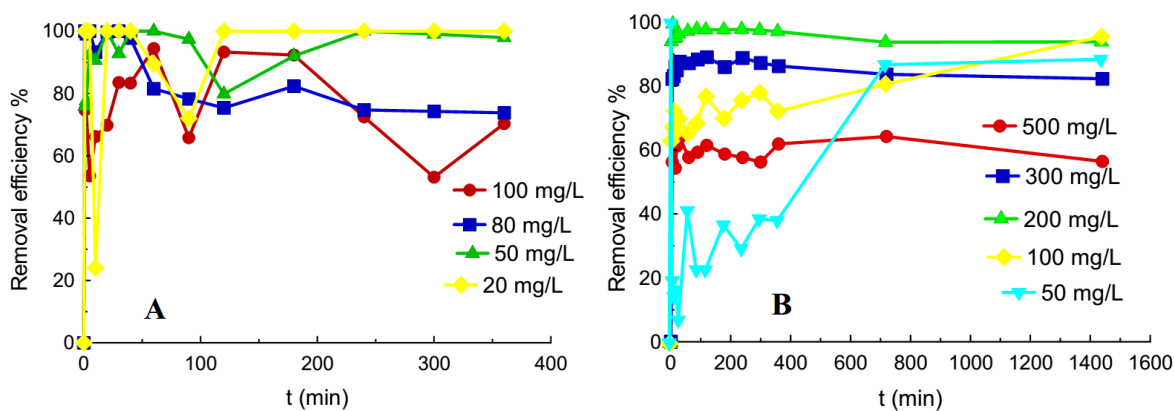
Fig. 5.7a and 5.7b Removal efficiency % of (a) PHN and (b) ARD

The reasonably high adsorptive capacity of PHN and ARD on K-IL indicates that both molecules could penetrate through the three-dimensional channels of the K-IL complex or be adsorbed onto the surface *via* physical forces (El-Nahhal and Safi, 2004). Phenyl rings on both systems PHN and ARD can also interact with the IL on the surface of the K-IL. The possible electronic π–π interaction between the pollutants and K-IL may significantly lead to higher removal % as well (El-Nahhal and Safi, 2004). Similar outcomes have been reported by several researchers (Diagboya et al., 2014; Xu et al., 2012; Changchaivong and Khaodhiar, 2009; Olu-Owolabi et al., 2014). In the case of acid red, it was observed that the removal efficiency decreased at lower concentrations of the dye. At 100 mg g^{-1} the removal % was 67 %, while for 50 mg g^{-1} the removal

efficiency reduced from 100 % after 5 - 14 min to 40 %. This reduction in % removal at lower concentration can be attributed to increasing particle interaction and aggregation of the adsorbent, leading to a reduction of total surface area of the adsorbent (Daneshvar et al., 2012). Furthermore, at low adsorbate concentration, the excess cationic charge on the adsorbent repels each other and may diminish the hydrophobic character of the interlayer spacing of the clay, thereby leading to a reduction in the adsorption of acid red dye (Bonczek et al., 2002).

In order to ascertain the kinetic mechanism(s) and potential rate-controlling step involved in the sorption of PHN and ARD onto K-IL, data from the effect of time experiments were fitted into the Lagergren-first-order model, pseudo-second-order kinetic model and intra-particle diffusion kinetic model. The pseudo-second order kinetics fitted the data better than the pseudo-first order kinetics as shown in Table 5.4. The experimentally determined adsorption capacities (qe_{exp}) and the calculated adsorption capacities (qe_{cal}) for pseudo – second order is closer than that of pseudo-first order and with R^2 values very close to unity. Acid red dye adsorption onto K-IL is most probably chemisorption and took place through exchange of ions on the surface of the active sites which is in agreement with other researchers (Ahmad and Kumar, 2011; Ho and McKay, 1998; Liao et al., 2013; Shen et al., 2009). The Weber and Morris (1963) intra–particle diffusion kinetics model was used to determine whether the rate limiting step is film diffusion or intra-particle diffusion. The Weber Morris model suggests that if the sorption mechanism is not only through intra-particle diffusion, the plot of qt *versus* t½ will be linear, but if intra-particle diffusion is the sole rate-limiting step the plot will pass through the origin.

Since the plot does not pass through the origin, it indicates some degree of boundary layer control. Therefore, intra-particle diffusion is not the only rate controlling step, but other processes are also controlling the rate of adsorption for both phenanthrene and acid red dye (Ahmad and Kumar, 2011; Liao et al., 2013; Crini et al., 2007). Adsorption experiments for acid red dye took place at pH 2, since preliminary experiments showed that it adsorbed best at lower pH. At pH 2, surface diffusion mechanism is likely attributed to electrostatic attraction, since acid red dye will be negatively charged and the surface of the material is positively charged. On the other hand, non-adjusted pH was used in the adsorption experiment of phenanthrene because previous studies have shown that pH values of the solution do not significantly affect the adsorption process of PAHs (Zeledón-Toruño et al., 2007) phenanthrene inclusive.

Table 5.4 Experimental values for q_e (mg L^{-1}) and parameters for pseudo-first-order, pseudo-second-order and intra-particle diffusion.

	Concentrations		Pseudo-first-order			Pseudo-second-order			Weber–Morris model		
	(mg L^{-1})	q_e,exp (mg g^{-1})	q_e, cal (mg g^{-1})	K_e x10^{-3} (h^{-1})	R^2	q_e,cal (mg g^{-1})	K x 10^4 (g mg^{-1} h^{-1})	R^2	q_e (mg g^{-1})	k_{id} (mg g^{-1} h$^{-1/2}$)	R^2
PHN	100	167.034	6.869	2.000	0.697	222.222	-1 x 10^4	0.987	149.67	0.012	7 x 10^{-6}
	80	131.738	0.714	2.000	0.817	181.818	38 x 10^4	0.998	163.43	-2.723	0.799
	50	90.597	2.115	4.000	0.157	178.571	-25 x 10^4	0.999	86.71	0.692	0.230
	25	44.713	3.492	4.000	0.671	74.074	-17 x 10^4	0.999	42.59	0.396	0.052
	500	842.703	40.516	-1.000	0.056	714.286	2.613	0.997	753.00	-0.489	0.011
	300	667.883	2.645	-0.500	0.105	625.000	2.813	0.999	649.35	-0.038	0.049
ARD	200	491.746	1.417	-0.600	0.135	475.191	6.041	0.999	488.67	0.297	0.114
	100	240.072	5.804	0.900	0.244	232.558	1.422	0.989	159.84	1.859	0.819
	50	88.7559	1.5728	1.000	0.314	95.238	0.479	0.788	24.22	1.409	0.175

Table 5.5 The q_m and b values for the Langmuir equation, the K_f and n values for the Freundlich equation, q_s and β values in the Dubinin-Radushkevich, bT and AT values in the Temkin model and their respective correlation coefficient values

		Langmuir model		Freundlich model			Dubinin–Radushkevich model				Temkin model		
	q_m	b	R^2	K_f	n	R^2	q_m	B	E	R^2	bT	AT	R^2
	(mg g^{-1})	(L mg^{-1})		(L mg^{-1})	(g L^{-1})		(mol g^{-1})	(mol^2 kJ^{-2})	(kJ mol^{-1})		(g kJ mg^{-1} mol^{-1})	(L mg^{-1})	
PHN	263.158	0.088	0.910	27.762	1.59	0.925	1.643	2×10^{-8}	5.000	0.947	42.45	1.142	0.948
ARD	909.091	0.057	0.954	141.925	2.74	0.468	1.545	9×10^{-9}	8.453	0.455	16.29	1.705	0.716

This is due to the inertness and chemical stability of PAHs which is as a result of their bond linkages. Therefore, pH has a lesser effect on heavier PAHs containing more carbon double bonds. In addition, phenanthrene does not have ionizable groups that can be influenced by the pH (Raber et al., 1998; Zeledón-Toruño et al., 2007; De Paolis and Kukkonen, 1997). Hydrophobic interaction is probably the major interaction between phenanthrene and K-IL, that is, the interaction between the phenanthrene ring and that of ionic liquid intercalated between the interlayer spaces of kaolin (through π–π interactions) (El-Nahhal and Safi, 2004; Huang et al., 2005). Huang and co-workers and Smith and co-workers had hypothesized similar observations (Smith and Jaffe, 1991; Huang et al., 2005; Smith and Galan, 1995).

Langmuir, Freundlich, Dubinin–Raduskevich and Temkin models were used to ascertain which adsorption isotherm best described the sorption. Values of the isotherm parameters for the models are presented in Table 5.5. The R^2 values indicated that the Langmuir isotherm with an adsorption capacity of 909.00 mg g^{-1} best described acid red dye adsorption on K-IL. This further confirmed the previous statement that the adsorption process of the acid red dye onto K-IL is chemisorbed onto its surface. Meanwhile, adsorption of phenanthrene can be best described by Freundlich and Langmuir with R^2 values of 0.925 and 0.91 respectively but Freundlich is the best fit. This confirms the earlier statement that intra-particle diffusion is not the only rate-controlling step, but other processes are responsible for controlling the rate of adsorption of phenanthrene. The small "n" values for the Freundlich equation (Table 5.5), indicates the non-linearity of the isotherms, meaning sorption of phenanthrene is predominantly on heterogeneous adsorption sites (Olu-Owolabi et al., 2014; Weber Jr et al., 1992) which is in agreement with Zhang et al., (Zhang et al., 2011). Langmuir and Freundlich adsorption capacities (q_e) of phenanthrene onto K-IL (Table 5.5) are higher than unmodified kaolin as reported by Zhang and co-workers who reported a q_e value less than 6 mg g^{-1} (Zhang et al., 2011). Hundal and co-workers reported q_e values of < 60 to < 15 μg g^{-1} on different types of modified smectites (Hundal et al., 2001), and a q_e value of 12 mg kg^{-1} was reported by Huang and co-workers (Huang et al., 2005).

Also, from the Dubinin-Raduskevich model the mean sorption energy (E) can be used to distinguish chemical and physical adsorption. Table 5.5 shows that the E value for phenanthrene is 5 kJ mol^{-1}, meaning adsorption is mostly physisorption, i.e. adsorption onto the pores of the

material. The E value for acid red dye is 8.5 kJ mol^{-1}, which is within the range of 8–16 kJ mol^{-1} for chemisorption (Helfferich, 1962) which is in agreement with other kinetics models.

5.5 CONCLUSION

This is the first report of the synthesis of 1-hexyl, 3-decahexyl imidazolium ionic liquid and its use in the modification of kaolin. The ionic liquid and the modified kaolin were characterised and adsorption studies using both column and batch processes for the removal of both phenanthrene and acid red dye were carried out. The column adsorption system was found to perform better at higher influent concentrations and a lower influent flow rate. Column adsorption capacity at the same flow rate and different concentrations of phenanthrene was 222.0, 611.7 and 1093.4 mg g^{-1}, and 877.0, 1337.4 and 1350.7 mg g^{-1} for acid red dye. The column models show that the data were best fitted into the Thomas and Yoon–Nelson models with R^2 values close to unity for both solutes. The kinetics of the two were well described by pseudo-second-order adsorption, but the Langmuir isotherm best described acid red dye with an adsorption capacity of 909 mg g^{-1} and the reaction is likely to be chemisorption based on the D-R value of 8.5 kJ mol^{-1}. Meanwhile, Freundlich and Langmuir models described phenanthrene adsorption with an adsorption capacity of 263 mg g^{-1} with π–π interactions as the means of sorption. Therefore, 1-hexyl, 3-decahexyl imidazolium can potentially be used as a modifier of adsorbents for the removal of phenanthrene and acid red dye from wastewater.

5.6 ACKNOWLEDGEMENTS

5.7 REFERENCES

Absalan, G., Asadi, M., Kamran, S., Sheikhian, L. & Goltz, D. M. 2011. Removal of reactive red-120 and 4-(2-pyridylazo) resorcinol from aqueous samples by Fe3O4 magnetic nanoparticles using ionic liquid as modifier. *Journal of Hazardous Materials,* 192(2)**,** pp 476-484.

Ahmad, A. & Hameed, B. 2010. Fixed-bed adsorption of reactive azo dye onto granular activated carbon prepared from waste. *Journal of Hazardous Materials,* 175(1)**,** pp 298-303.

Ahmad, R. & Kumar, R. 2011. Adsorption of amaranth dye onto alumina reinforced polystyrene. *Clean–Soil, Air, Water,* 39(1)**,** pp 74-82.

Aksu, Z. & Gönen, F. 2004. Biosorption of phenol by immobilized activated sludge in a continuous packed bed: prediction of breakthrough curves. *Process Biochemistry,* 39(5)**,** pp 599-613.

Alther, G. 2002. Using organoclays to enhance carbon filtration. *Waste Management,* 22(5)**,** pp 507-513.

Alther, G. R. 1995. Organically modified clay removes oil from water. *Waste Management,* 15(8)**,** pp 623-628.

Bartelt-Hunt, S. L., Burns, S. E. & Smith, J. A. 2003. Nonionic organic solute sorption onto two organobentonites as a function of organic-carbon content. *Journal of Colloid and Interface Science,* 266(2)**,** pp 251-258.

Bastow, T., Hardin, S. & Turney, T. 1991. The formation of β′-sialon from a montmorillonite-polyacrylonitrile composite by carbothermal reduction: an NMR, TGA, XRD and EM study. *Journal of Materials Science,* 26(6)**,** pp 1443-1453.

Bohart, G. & Adams, E. 1920. Some aspects of the behavior of charcoal with respect to chlorine. 1. *Journal of the American Chemical Society,* 42(3)**,** pp 523-544.

Bonczek, J. L., Harris, W. & Nkedi-Kizza, P. 2002. Monolayer to bilayer transitional arrangements of hexadecyltrimethylammonium cations on Na-montmorillonite. *Clays and Clay Minerals,* 50(1)**,** pp 11-17.

Boufatit, M., Ait-Amar, H. & Mc Whinnie, W. 2008. Development of an algerian material montmorillonite clay—Intercalation with selective long chain alkylammonium cations (Octadecytrimethylammonium, Cetylpyridium and Tetrabutylammonium) and with tellerium complexes. *Desalination,* 223(1)**,** pp 366-374.

Boyd, S. A., Mortland, M. M. & Chiou, C. T. 1988. Sorption characteristics of organic compounds on hexadecyltrimethylammonium-smectite. *Soil Science Society of America Journal,* 52(3)**,** pp 652-657.

Changchaivong, S. & Khaodhiar, S. 2009. Adsorption of naphthalene and phenanthrene on dodecylpyridinium-modified bentonite. *Applied Clay Science,* 43(3)**,** pp 317-321.

Crini, G. & Badot, P.-M. 2008. Application of chitosan, a natural aminopolysaccharide, for dye removal from aqueous solutions by adsorption processes using batch studies: A review of recent literature. *Progress in Polymer Science,* 33(4)**,** pp 399-447.

Crini, G., Peindy, H. N., Gimbert, F. & Robert, C. 2007. Removal of CI Basic Green 4 (Malachite Green) from aqueous solutions by adsorption using cyclodextrin-based adsorbent: kinetic and equilibrium studies. *Separation and Purification Technology,* 53(1)**,** pp 97-110.

Daneshvar, E., Kousha, M., Sohrabi, M. S., Khataee, A. & Converti, A. 2012. Biosorption of three acid dyes by the brown macroalga Stoechospermum marginatum: Isotherm, kinetic and thermodynamic studies. *Chemical Engineering Journal,* 195–196(297-306.

De Paolis, F. & Kukkonen, J. 1997. Binding of organic pollutants to humic and fulvic acids: influence of pH and the structure of humic material. *Chemosphere,* 34(8)**,** pp 1693-1704.

Dentel, S. K., Jamrah, A. I. & Sparks, D. L. 1998. Sorption and cosorption of 1, 2, 4-trichlorobenzene and tannic acid by organo-clays. *Water Research,* 32(12)**,** pp 3689-3697.

Diagboya, P. N., Olu-Owolabi, B. I., Zhou, D. & Han, B.-H. 2014. Graphene oxide–tripolyphosphate hybrid used as a potent sorbent for cationic dyes. *Carbon,* 79(1)**,** pp 174-182.

Domka, L., Malicka, A. & Stachowiak, N. 2008. Production and structural investigation of polyethylene composites with modified kaolin. *Acta Physica Polonica-Series A General Physics,* 114(2)**,** pp 413.

dos Santos, O. A. A., Castellib, C. Z., Oliveirab, M. F., de Almeida Netob, A. F. & da Silvab, M. G. 2013. Adsorption of Synthetic Orange Dye Wastewater in Organoclay. *Chemical Engineering,* 32(307-312.

Dubinin, M. & Radushkevich, L. 1947. Equation of the characteristic curve of activated charcoal. *Chemisches Zentralblatt,* 1(1)**,** pp 875.

Dzyuba, S. V. & Bartsch, R. A. 2001. Efficient synthesis of 1-alkyl (aralkyl)-3-methyl (ethyl) imidazolium halides: precursors for room-temperature ionic liquids. *Journal of Heterocyclic Chemistry,* 38(1)**,** pp 265-268.

Eckenfelder, W. W. 2000. *Industrial Water Pollution Control*, third ed., New York: McGraw-Hill.

El-Nahhal, Y., Nir, S., Polubesova, T., Margulies, L. & Rubin, B. 1998. Leaching, phytotoxicity, and weed control of new formulations of alachlor. *Journal of Agricultural and Food Chemistry,* 46(8)**,** pp 3305-3313.

El-Nahhal, Y. Z. & Safi, J. M. 2004. Adsorption of phenanthrene on organoclays from distilled and saline water. *Journal of Colloid and Interface Science,* 269(2)**,** pp 265-273.

Freundlich, H. 1906. Über die Adsorption in Lösungen. *Zeitschrift fur Physikalische Chemie,* 57(A)**,** pp 385-470.

Gillman, G. & Sumpter, E. 1986. Modification to the compulsive exchange method for measuring exchange characteristics of soils. *Soil Research,* 24(1)**,** pp 61-66.

Gullick, R. W. & Weber, W. J. 2001. Evaluation of shale and organoclays as sorbent additives for low-permeability soil containment barriers. *Environmental science & technology,* 35(7)**,** pp 1523-1530.

Guo, J. & Lua, A. C. 2003. Textural and chemical properties of adsorbent prepared from palm shell by phosphoric acid activation. *Materials Chemistry and Physics,* 80(1)**,** pp 114-119.

Han, R., Ding, D., Xu, Y., Zou, W., Wang, Y., Li, Y. & Zou, L. 2008. Use of rice husk for the adsorption of congo red from aqueous solution in column mode. *Bioresource Technology,* 99(8)**,** pp 2938-2946.

Han, R., Wang, Y., Yu, W., Zou, W., Shi, J. & Liu, H. 2007. Biosorption of methylene blue from aqueous solution by rice husk in a fixed-bed column. *Journal of Hazardous Materials,* 141(3)**,** pp 713-718.

Han, R., Wang, Y., Zhao, X., Wang, Y., Xie, F., Cheng, J. & Tang, M. 2009. Adsorption of methylene blue by phoenix tree leaf powder in a fixed-bed column: experiments and prediction of breakthrough curves. *Desalination,* 245(1)**,** pp 284-297.

Helfferich, F. G. 1962. *Ion exchange*: Courier Dover Publications.

Ho, Y.-S. & McKay, G. 1998. Sorption of dye from aqueous solution by peat. *Chemical Engineering Journal,* 70(2)**,** pp 115-124.

Ho, Y.-S. & McKay, G. 1999. Pseudo-second order model for sorption processes. *Process Biochemistry,* 34(5)**,** pp 451-465.

Huang, H.-C., Lee, J.-F., Chao, H.-P., Yeh, P.-W., Yang, Y.-F. & Liao, W.-L. 2005. The influences of solid-phase organic constituents on the partition of aliphatic and aromatic organic contaminants. *Journal of Colloid and Interface Science,* 286(1)**,** pp 127-133.

Hundal, L. S., Thompson, M. L., Laird, D. A. & Carmo, A. M. 2001. Sorption of phenanthrene by reference smectites. *Environmental Science & Technology,* 35(17)**,** pp 3456-3461.

J.J. Hassett & L.W. Banwart 1989. Front Matter. *In:* Sawhney, B. L. & Brown, K. (eds.) *Reactions and Movement of Organic Chemicals in Soils.* Soil Science Society of America and American Society of Agronomy.

Kamran, S., Asadi, M. & Absalan, G. 2014. Adsorption of folic acid, riboflavin, and ascorbic acid from aqueous samples by Fe3O4 magnetic nanoparticles using ionic liquid as modifier. *Analytical Methods,* 6(3)**,** pp 798-806.

Ko, D. C., Porter, J. F. & McKay, G. 2000. Optimised correlations for the fixed-bed adsorption of metal ions on bone char. *Chemical Engineering Science,* 55(23)**,** pp 5819-5829.

Lagergren, S. 1898. About the theory of so-called adsorption of soluble substances. *Kungliga Svenska Vetenskapsakademiens Handlingar,* 24(4)**,** pp 1-39.

Langmuir, I. 1916. The constitution and fundamental properties of solids and liquids. *Journal of the American Chemical Society,* 38(11)**,** pp 2221-2295.

Lawal, I. A. & Moodley, B. 2015. Synthesis, characterisation and application of imidazolium based ionic liquid modified montmorillonite sorbents for the removal of amaranth dye. *RSC Advances*.

Lee, J.-F., Mortland, M. M., Boyd, S. A. & Chiou, C. T. 1989a. Shape-selective adsorption of aromatic molecules from water by tetramethylammonium–smectite. *Journal of the Chemical Society, Faraday Transactions 1: Physical Chemistry in Condensed Phases,* 85(9)**,** pp 2953-2962.

Lee, J. F., Crum, J. R. & Boyd, S. A. 1989b. Enhanced retention of organic contaminants by soils exchanged with organic cations. *Environmental science & technology,* 23(11)**,** pp 1365-1372.

Lee, S. H., Song, D. I. & Jeon, Y. W. 2001. An Investigation of the Adsorption of Organic Dyes onto Organo-Montmorillonite. *Environmental Technology,* 22(3)**,** pp 247-254.

Lee, S. Y. & Kim, S. J. 2002. Delamination behavior of silicate layers by adsorption of cationic surfactants. *Journal of Colloid and Interface Science,* 248(2)**,** pp 231-238.

Liao, P., Zhan, Z., Dai, J., Wu, X., Zhang, W., Wang, K. & Yuan, S. 2013. Adsorption of tetracycline and chloramphenicol in aqueous solutions by bamboo charcoal: A batch and fixed-bed column study. *Chemical Engineering Journal,* 228(1)**,** pp 496–505.

Lin, S.-H., Juang, R.-S. & Wang, Y.-H. 2004. Adsorption of acid dye from water onto pristine and acid-activated clays in fixed beds. *Journal of Hazardous Materials,* 113(1)**,** pp 195-200.

Manoli, E. & Samara, C. 1999. Polycyclic aromatic hydrocarbons in natural waters: sources, occurrence and analysis. *TrAC Trends in Analytical Chemistry,* 18(6)**,** pp 417-428.

Murray, H. H. 2000. Traditional and new applications for kaolin, smectite, and palygorskite: a general overview. *Applied Clay Science,* 17(5–6)**,** pp 207-221.

Newman, A. C. 1987. *Chemistry of Clays and Clay Minerals*, USA: Wiley-Interscience.

Nir, S., Rubin, B., Mishael, Y. G., Zadaka, D., Polubesova, T., Wakshal, E. & Rabinovitz, O. 2007. *REMOVAL OF ORGANIC POLLUTANTS FROM CONTAMINATED WATER.*

149

Olu-Owolabi, B. I., Diagboya, P. N. & Adebowale, K. O. 2014. Evaluation of pyrene sorption–desorption on tropical soils. *Journal of Environmental Management,* 137(1)**,** pp 1-9.

Özcan, A. S., Erdem, B. & Özcan, A. 2004. Adsorption of acid blue 193 from aqueous solutions onto Na–bentonite and DTMA–bentonite. *Journal of Colloid and Interface Science,* 280(1)**,** pp 44-54.

Peternel, I. T., Koprivanac, N., Božić, A. M. L. & Kušić, H. M. 2007. Comparative study of UV/TiO2, UV/ZnO and photo-Fenton processes for the organic reactive dye degradation in aqueous solution. *Journal of Hazardous Materials,* 148(1–2)**,** pp 477-484.

Raber, B., Kögel-Knabner, I., Stein, C. & Klem, D. 1998. Partitioning of polycyclic aromatic hydrocarbons to dissolved organic matter from different soils. *Chemosphere,* 36(1)**,** pp 79-97.

Redding, A., Burns, S., Upson, R. & Anderson, E. 2002. Organoclay sorption of benzene as a function of total organic carbon content. *Journal of Colloid and Interface Science,* 250(1)**,** pp 261-264.

Registry, A. f. T. S. a. D., 1995. Toxicological profile for Polycyclic Aromatic Hydrocarbons (PAHs), Registry, A. f. T. S. a. D.

Rodriguez-Cruz, M., Andrades, M. & Sanchez-Martin, M. 2008. Significance of the long-chain organic cation structure in the sorption of the penconazole and metalaxyl fungicides by organo clays. *Journal of Hazardous Materials,* 160(1)**,** pp 200-207.

Shen, X.-E., Shan, X.-Q., Dong, D.-M., Hua, X.-Y. & Owens, G. 2009. Kinetics and thermodynamics of sorption of nitroaromatic compounds to as-grown and oxidized multiwalled carbon nanotubes. *Journal of Colloid and Interface Science,* 330(1)**,** pp 1-8.

Sheng, G. & Boyd, S. A. 2000. Polarity effect on dichlorobenzene sorption by hexadecyltrimethylammonium-exchanged clays. *Clays and Clay Minerals,* 48(1)**,** pp 43-50.

Sheng Guangyao, S. X. & Stephen, B. A. 1997. Surface heterogeneity of trimethylphenylammoniumsmectite as revealed by adsorption of aromatic hydrocarbons from water. *Clays and Clay Minerals,* 45 (4)**,** pp 659- 669.

Smith, J. A. & Galan, A. 1995. Sorption of nonionic organic contaminants to single and dual organic cation bentonites from water. *Environmental Science & Technology,* 29(3)**,** pp 685-692.

Smith, J. A. & Jaffe, P. R. 1991. Comparison of tetrachloromethane sorption to an alkylammonium-clay and an alkyldiammonium-clay. *Environmental Science & Technology,* 25(12)**,** pp 2054-2058.

Smith, J. A., Jaffe, P. R. & Chiou, C. T. 1990. Effect of ten quaternary ammonium cations on tetrachloromethane sorption to clay from water. *Environmental Science & Technology,* 24(8)**,** pp 1167-1172.

Soule, N. M. & Burns, S. E. 2001. Effects of organic cation structure on behavior of organobentonites. *Journal of Geotechnical and Geoenvironmental Engineering,* 127(4)**,** pp 363-370.

Starikova, O., Dolgushin, G., Larina, L., Komarova, T. & Lopyrev, V. 2003. Synthesis of new stable carbenes from the corresponding 1, 3-dialkylimidazolium and benzimidazolium salts. *Arkivoc,* 13(2)**,** pp 119-124.

Sunardi, S., Irawati, U., Arryanto, Y. & Sutarno, S. 2011. Modified kaolin with cationic surfactant for gibberellic acid carrier materials. *Indonesian Journal of Chemistry,* 11(1)**,** pp 96-102.

Takahashi, C., Shirai, T., Hayashi, Y. & Fuji, M. 2013. Study of intercalation compounds using ionic liquids into montmorillonite and their thermal stability. *Solid State Ionics,* 241(3)**,** pp 53-61.

Tan, I. A. W., Ahmad, A. L. & Hameed, B. H. 2008. Adsorption of basic dye using activated carbon prepared from oil palm shell: batch and fixed bed studies. *Desalination,* 225(1–3)**,** pp 13-28.

Taty-Costodes, V. C., Fauduet, H., Porte, C. & Ho, Y.-S. 2005. Removal of lead (II) ions from synthetic and real effluents using immobilized Pinus sylvestris sawdust: Adsorption on a fixed-bed column. *Journal of Hazardous Materials,* 123(1–3)**,** pp 135-144.

Theng, B. K. 1974. *The chemistry of clay-organic reactions*, London: Adam Hilger Ltd., Rank Precision Industries.

Thomas, H. C. 1944. Heterogeneous Ion Exchange in a Flowing System. *Journal of the American Chemical Society,* 66(10)**,** pp 1664-1666.

Upson, R. & Burns, S. 2006. Sorption of nitroaromatic compounds to synthesized organoclays. *Journal of Colloid and Interface Science,* 297(1)**,** pp 70-76.

Vijayaraghavan, K., Jegan, J., Palanivelu, K. & Velan, M. 2004. Removal of nickel (II) ions from aqueous solution using crab shell particles in a packed bed up-flow column. *Journal of Hazardous Materials,* 113(1)**,** pp 223-230.

Weber Jr, W. J., McGinley, P. M. & Katz, L. E. 1992. A distributed reactivity model for sorption by soils and sediments. 1. Conceptual basis and equilibrium assessments. *Environmental Science & Technology,* 26(10)**,** pp 1955-1962.

Weber, W. J. & Morris, J. C. 1963. Kinetics of adsorption on carbon from solution. *Journal of the Sanitary Engineering Division. ASCE,,* 89(1)**,** pp 31.

Xu, J., Wang, L. & Zhu, Y. 2012. Decontamination of bisphenol A from aqueous solution by graphene adsorption. *Langmuir,* 28(22)**,** pp 8418-8425.

Xu, S. & Boyd, S. A. 1995. Cationic surfactant sorption to a vermiculitic subsoil via hydrophobic bonding. *Environmental Science & Technology,* 29(2)**,** pp 312-320.

Yahaya, L., Adebowale, K. & Menon, A. 2009. Mechanical properties of organomodified kaolin/natural rubber vulcanizates. *Applied Clay Science,* 46(3)**,** pp 283-288.

Yoon, Y. H. & Nelson, J. H. 1984. Application of gas adsorption kinetics I. A theoretical model for respirator cartridge service life. *The American Industrial Hygiene Association Journal,* 45(8)**,** pp 509-516.

Zeledón-Toruño, Z. C., Lao-Luque, C., de las Heras, F. X. C. & Sole-Sardans, M. 2007. Removal of PAHs from water using an immature coal (leonardite). *Chemosphere,* 67(3)**,** pp 505-512.

Zhang, L., Luo, L. & Zhang, S. 2011. Adsorption of phenanthrene and 1,3-dinitrobenzene on cation-modified clay minerals. *Colloids and Surfaces A: Physicochemical and Engineering Aspects,* 377(1–3)**,** pp 278-283.

Zhao, H., Jaynes, W. F. & Vance, G. F. 1996. Sorption of the ionizable organic compound, dicamba (3, 6-dichloro-2-methoxy benzoic acid), by organo-clays. *Chemosphere,* 33(10)**,** pp 2089-2100.

Zhou, Q., Frost, R. L., He, H., Xi, Y. & Liu, H. 2007. Adsorbed para-nitrophenol on HDTMAB organoclay—A TEM and infrared spectroscopic study. *Journal of Colloid and Interface Science,* 307(2)**,** pp 357-363.

Zhu, L., Li, Y. & Zhang, J. 1997. Sorption of organobentonites to some organic pollutants in water. *Environmental Science & Technology,* 31(5)**,** pp 1407-1410.

CHAPTER 6: KINETICS, ISOTHERM AND SORPTION STUDIES OF EMERGING CONTAMINANT (PHARMACEUTICALS) ON IONIC LIQUID MODIFIED MONTMORILLONITE

Isiaka A. Lawal[a] and Brenda Moodley[a]*

[a]School of Chemistry and Physics, College of Agriculture, Engineering and Science, University of KwaZulu-Natal, P/Bag X45001, Westville Campus, Durban, 4000, South Africa

*corresponding author email: moodleyb3@ukzn.ac.za

Tel: +27 31 2602796; Fax: +27 31 2603091

First author: lawalishaq000123@yahoo.com

6.1 ABSTRACT

This study evaluates the adsorption of four pharmaceuticals, tetracycline (TC), sulfamethoxazole (SMZ), nalidixic acid (NAD) and chloramphenicol (CHL) on ionic liquid modified montmorillonite (Mt–IL). Previously modified montmorillonite with ionic liquid (1-methyl, 3-decahexyl imidazolium) was used in batch adsorption experiments to examine the effects of pH and contact time and the data were fitted into kinetics and isotherm models. All the pharmaceuticals investigated adsorbed maximally between pH range 3 and 10. The maximum adsorption capacities (q_e) of TC, SMZ, NAD and CHL were 765.7, 504.1, 150.4 and 30.9 mg g^{-1} respectively onto Mt–IL. These were considerably higher than the q_e of unmodified montmorillonite clay and of other materials reported in literature. The equilibrium experimental data were best fitted into the Freundlich model. The pseudo-second-order kinetic model was the best fit for all the pharmaceuticals adsorbed onto Mt–IL.

Keywords: Ionic liquid, 1-methyl 3-decahexyl imidazolium, montmorillonite, pharmaceuticals, adsorption

6.2 INTRODUCTION

Pharmaceuticals are extensively used world-wide in human therapy and in the animal farming industry. They are used in livestock rearing as veterinary drugs, in medical service deliveries and human healthcare globally. They have attracted increasing concern in recent years, because they have proven to be a class of potent emerging pollutants in the environment (Ji et al., 2010b). The occurrences of these pharmaceuticals in the environment have started to raise serious concerns for both the scientific community and the general public due to their undesirable effects even at trace concentrations (Fent et al., 2006). Pharmaceuticals are generally used to treat diseases in animals and are incorporated into animal feeds to promote growth efficiency (Sarmah et al., 2006). However poor absorption of these drugs in the digestive tracts of animals results in it often being excreted in feces or urine as a mixture of the parent compound and its metabolites (Kulshrestha et al., 2004; Ji et al., 2009; Ji et al., 2010a; Li et al., 2011). Together with this and the application of feces to agricultural land as fertilizer, it has been reported that residues of these antibiotics from agricultural runoff and municipal wastewater treatment plants have been detected in water systems and the environment at large (Sun et al., 2010). The global use of antibiotics has become a serious concern because of its various potential adverse effects when present in the environment. Antibiotics are regarded as ''pseudopersistent'' contaminants due to their continuous introduction into the ecosystem (Çalışkan and Göktürk, 2010). Acute and chronic toxicity, impact on aquatic photosynthetic organisms, disruption of indigenous microbial populations, and dissemination into antibiotic-resistant genes in microorganisms amongst others have been reported (Li et al., 2011; Sun et al., 2010). Therefore removal of these pharmaceuticals is important and necessary in the study of water remediation.

In this study adsorption of tetracycline (TC), sulfamethoxazole (SMZ), nalidixic acid (NAD) and chloramphenicol (CHL) were investigated. Tetracycline is among the commonly used antibiotics and has been shown to disrupt microbial soil respiration (Boleas et al., 2005), Fe(III) reduction (Thiele-Bruhn and Beck, 2005), nitrification (Halling-Sørensen, 2001), and phosphatase activities (Boleas et al., 2005). TC has different charges on different sites depending on the solution pH. At pH below 3.3, TC exists in a cationic form of $+\,0\,0$ due to protonation of the dimethylammonium group. It is predominantly a zwitterion $+-0$ between pH 3.3 and 7.7 due to the loss of the proton

from the phenolic diketone moiety. But at pH above 7.7, it is present as a monovalent anion, $+ -$ $-$, or a divalent anion, $0- -$, resulting from the loss of protons from the tricarbonyl system and phenolic diketone moiety. Its pKa_1, pKa_2 and pKa_3 values in aqueous solutions are 3.3, 7.7 and 9.7 respectively (Kulshrestha et al., 2004).

Sulfamethoxazole (SMZ) is a sulfonamide bacteriostatic antibiotic commonly used to treat urinary tract infections. Sulfamethoxazole (SMZ) may exist as a cation, anion and/or neutral molecule depending on the pH of the solution because of its two pKa values. It has a pK_{a1} value of 1.7 and pK_{a2} value of 5.6 (Lucida et al., 2000). SMZ is among the most frequently detected antibiotics in streams and groundwater (Barnes et al., 2004; Kolpin et al., 2002). SMZ is characterized as a low reactive antibiotic (Holten Lützhøft et al., 2000). Park and Choi (Park and Choi, 2008) reported that SMZ could cause acute toxicity as well as chronic toxic effects with low milligrams per liter level exposure and mutagenic effects of SMZ has also been reported (Isidori et al., 2005).

Nalidixic acid (NAD) and chloramphenicol (CHL) are also widely used in human and veterinary medicine. Researchers (Lin et al., 2008; Tamtam et al., 2011; Watkinson et al., 2009) have reported the presence of NAD in hospital effluents, wastewater treatment plant effluents, and environmental waters and soils. NAD concentrations of 0.04, 0.45 and 0.75 µg L^{-1} were detected in hospital effluents, municipal sewage treatment plant effluents, and environmental waters, respectively (Watkinson et al., 2009). A separate study reported that the NAD concentrations in the effluents of hospital and sewage treatment plants were up to 0.178 and 0.186 µg L^{-1}, respectively (Lin et al., 2008). NAD was detected with a concentration up to 22 µg kg^{-1} in eight of nine samples collected from soils 4 years after cessation of 100 years irrigation with urban wastewater from the Paris agglomeration (Tamtam et al., 2011).

Various concentrations of CHL have also been reported in wastewater from different countries. Singh and coworker (Singh et al., 2012) reported concentrations of CHL as high as 9.74 µg L^{-1} in surface and wastewater in India. Some negative effects in humans, such as bone marrow depression (aplastic anemia) have been linked to CHL in some individuals (Woodward and Watson, 2004). This has led to its proscription in animal food production in many countries (Regulation, 1994).
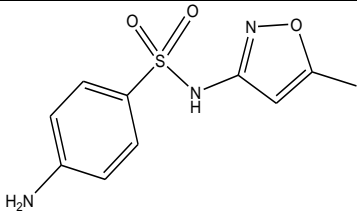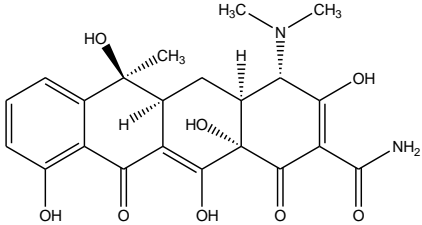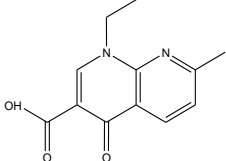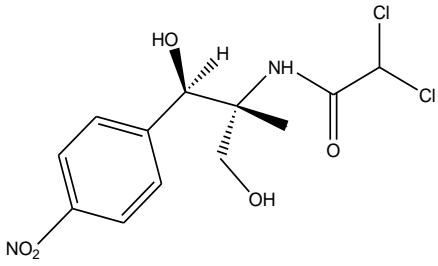
Since there is no total removal of pharmaceuticals by conventional water and wastewater treatment technologies (Gao et al., 2012; Nam et al., 2014; Ternes et al., 2002; Rudder et al., 2004), improved technologies for effective removal of residual pharmaceuticals needs to be developed. Scientists have investigated the adsorption and removal of pharmaceutical antibiotics using several adsorbents, amongst them: smectite (Li et al., 2010a), montmorillonite (Liu et al., 2011; Wu et al., 2013; Gao and Pedersen, 2005; Avisar et al., 2010; Wang et al., 2008; Chang et al., 2009b; Zhao et al., 2012; Figueroa et al., 2003; Liu et al., 2012; Wang et al., 2010; Parolo et al., 2008), kaolin (Liu et al., 2011; Wu et al., 2013; Li et al., 2010b; Figueroa et al., 2003; Bansal, 2013; Wang et al., 2010), goethite (Zhao et al., 2011), rectorite (Chang et al., 2009a), illite (Chang et al., 2012; Bansal, 2013), palygorskite (Chang et al., 2009c), chitosan particles (Caroni et al., 2012), aluminum oxide (Lorphensri et al., 2006; Chen and Huang, 2010), bamboo charcoal (Liao et al., 2013), coal (Sun et al., 2010), activated carbon (Çalışkan and Göktürk, 2010), polymers (Robberson et al., 2006), mesoporous silica SBA-15 (Kim et al., 2014), quartz sand (Chen et al., 2011), graphene oxide (Gao et al., 2012) and multiwalled/single-walled carbon nanotubes (Zhang et al., 2011a; Zhang et al., 2010; Ji et al., 2010a; Ji et al., 2009).

Among all of these adsorbents, montmorillonite has drawn attention as a suitable material for environmental remediation. The hydrophilic properties of montmorillonite surface have been changed to hydrophobic through modification by surfactants to form organo-montmorillonite (Liu et al., 2012; Sheng et al., 1998) for the purpose of adsorbing organic pollutants (Parolo et al., 2008; Smith et al., 1990; Zhu et al., 1997). Ionic liquids have attracted an increasing amount of interest, owing to their low volatility, non-flammability, high chemical and thermal stabilities, high ionic conductivity, and broad electrochemical windows (Zhang et al., 2006). Due to these properties they are considered as a substitute for the modern surfactants and researchers have started using ILs for modification of materials for the purpose of adsorption. Kamran and co-workers modified Fe_3O_4 magnetic nanoparticles with 1-octyl-3-methylimidazolium bromide ([C_8MIM]-Fe_3O_4) and used it for the removal of reactive red 141 (RR141) and reactive yellow 81 (RY81) dyes from aqueous solutions (Kamran et al., 2014). Absalan and coworkers modified Fe_3O_4 magnetic nanoparticles using ionic liquid for the adsorption of reactive red 120 and 4-(2-pyridylazo) resorcinol from aqueous solution (Absalan et al., 2011). Recently Lawal and Moodley modified

montmorillonite with 1-methyl, 3-decahexyl imidazolium ionic liquid (Mt-IL) for the adsorption of amaranth dye (Lawal and Moodley, 2015).

This study is aimed at studying the kinetic and equilibrium adsorption of pharmaceuticals (TC, SMZ, NAD and CHL) from aqueous solution on organo-montmorillonite (ionic liquid modified montmorillonite).

Table 6.1 Properties of the pharmaceuticals and surfactant used in this study

Compound	Formula	Structure	Molecular Weight (M.W.) g mol^{-1}
Sulfamethoxazole	$C_{10}H_{11}N_3O_3S$		253.279
Tetracycline	$C_{22}H_{24}N_2O_8$		444.435
Nalidixic acid	$C_{12}H_{12}N_2O_3$		232.235
Chloramphenicol	$C_{11}H_{12}Cl_2N_2O_5$		323.132
1-methyl, 3-decahexyl imidazolium	$C_{20}H_{39}N_2^+$		307.54

6.3 EXPERIMENTAL SECTION

6.3.1 Materials

Montmorillonite powder (CAS Number: 1318-93-0), methyl-imidazole, 1-bromodecahexane, sulfamethoxazole (CAS Number: 723-46-6), tetracycline (CAS Number: 60-54-8), nalidixic acid (CAS Number 389-08-2) and chloramphenicol (CAS Number: 56-75-7) were all purchased from Sigma Aldrich. Double distilled water was used for all sample preparation.

6.3.2 Preparation of Ionic Liquid (IL), 1-methyl, 3-decahexyl Imidazolium, Sodium-montmorillonite (Na$^+$–Mt) and its Modification with IL

Preparation of IL (1-methyl, 3-decahexyl imidazolium), Na$^+$–Mt and Mt–IL has been reported in chapter 4.

6.3.3 Adsorption Experiments

Adsorption experiments were performed in batch mode to investigate the effects of pH, and contact time of pharmaceutical concentrations on Mt–IL. The effect of pH and contact time was carried out using 50 mL of a 100 mg L^{-1} pharmaceutical solution mixed with 0.1 g of Mt–IL in a stoppered glass conical flask and placed on a shaker. A blank was also determined under the same conditions but without the adsorbent. The concentrations of the pharmaceuticals were always measured before and after the adsorption. All experiments were carried out in duplicate and run for 24 h to allow sufficient time for the adsorption to reach equilibrium conditions.

Adsorption kinetics was determined by analyzing the adsorptive uptake of pharmaceuticals (10 to 200 mg L^{-1} concentrations) from its aqueous solution containing 0.2 g of Mt–IL. The mixture was placed on a shaker for 24 hr and aliquots of the solution were analysed at regular time intervals. Equilibrium data for developing the isotherms were obtained at 25 °C and the aqueous phase concentration of SMZ and CHL in the solution was determined using high performance liquid chromatography (Agilent HPLC (1200 SL) equipped with a UV detector using Agilent C18,4.6 x 150 mm, 5 μm column). The elution solvent system for SMZ was 0.05 M phosphoric acid: acetonitrile (83% : 17%) and a wavelength of 265 nm was used. While the elution solvent system for CHL was acetonitrile: H$_2$O (40% : 60%) and a wavelength of 230 nm was used. The aqueous

phase concentration of TC and NAD were determined using a double beam UV−Vis−NIR spectrophotometer (Shimadzu Model UV 3600, Japan) at λ_{max} 360 and 260 respectively. The equilibrium adsorption capacity of Mt–IL was calculated from the following relationship:

$$q_e = \frac{C_o - C_e}{W} V ...6.1$$

Where q_e is the equilibrium adsorption capacity in (mg g^{-1}), C_0 and C_e are the dye concentrations at initial and at equilibrium respectively, in mg L^{-1}, V is the volume of solution in (L), and W is the weight of adsorbent in (g).

Adsorption data were fitted to Freundlich (Freundlich, 1906), Langmuir (Langmuir, 1916), Temkin and Dubinin–Raduskevich (Dubinin and Radushkevich, 1947) isotherms. The linear equations of all the applied models are:

$$\text{Langmuir model: } \frac{C_e}{q_e} = \frac{C_e}{q_m} + \frac{1}{q_m b} ...6.2$$

$$\text{Freundlich model: } \ln q_e = \ln K_f + \frac{1}{n} \ln C_e ...6.3$$

$$\text{Temkin model: } q_e = B \ln A + B \ln C_e ...6.4$$

$$\text{Dubinin–Raduskevich model: } \ln q_e = \ln q_m - \beta \sum{}^2 ...6.5$$

$$\sum = RT \ln \left[1 + \frac{1}{C_e} \right] ...6.6$$

$$E = \frac{1}{\sqrt{2\beta}} ...6.7$$

Where C_e is the equilibrium dye concentration in the solution in mg L^{-1}, b is the Langmuir adsorption constant (L mg^{-1}), and q_m is the theoretical maximum adsorption capacity (mg g^{-1}). K_f (L mg^{-1}) and n are Freundlich isotherm constants indicating the capacity and intensity of the adsorption, respectively. A is the equilibrium binding constant (L mg^{-1}) and B is the heat of adsorption. β is the Dubinin–Raduskevich model constant (mol^2 kJ^{-2}) related to the mean free energy of adsorption per mole of the adsorbate and $\sum$ is the polanyi potential. E is the mean free energy of adsorption (kJ mol^{-1}).

In order to determine the mechanism and potential rate-controlling steps involved in the process of adsorption, pseudo first order (Lagergren, 1898), pseudo second order (Ho and McKay, 1999), and intra-particle diffusion models were used. The pseudo first order kinetic model equation is:

$$\ln (q_e-q_t) = \ln q_e - k_1 t ...6.8$$

Where q_t is the amount of adsorption at time t in (mg g^{-1}), k_1 is the rate constant of the equation in (L min^{-1}), and q_e is the amount of adsorption at equilibrium in (mg g^{-1}). The adsorption rate constant (k_1) can be determined experimentally by plotting ln (q_e-q_t) *versus* t.

The pseudo second order kinetic model is expressed as:

$$\frac{t}{q_t} = \frac{1}{(k_2 q_e^2)} + \frac{t}{q_e} ...6.9$$

Where k_2 is the equilibrium rate constant of pseudo second order adsorption in (g mg^{-1} min^{-1}). The values of k_2 and q_e can be determined from the slope and intercept of the plot t/q_t *versus* t, respectively.

The data was also fitted into the Weber–Morris model, to evaluate the possibility of intra-particle diffusion as the rate limiting step; it is given by (Weber and Morris, 1963):

$$q_t = k_{id} t^{1/2} ...6.10$$

Where k_{id} (mg g^{-1} h$^{-1/2}$) is the intra-particle diffusion rate constant.

6.4 RESULTS AND DISCUSSION

Preliminary experiments on Mt–IL (modified montmorillonite) and Na$^+$-Mt (unmodified montmorillonite) showed that the adsorption capacities of the pharmaceuticals discussed in this work on Na$^+$-Mt (TC, SMZ, CHL, and NAD were 152.2, 87.4, 2.3 and 9.0 mg g^{-1} respectively)

were far lower than Mt–IL as shown in Table 6.4. Therefore, all further experiments were performed using Mt–IL.

6.4.1 Effect of pH

The results in Fig 6.1a show that the reaction between the selected pharmaceuticals and the adsorbent strongly depends on pH. In the work of Vasudevan and co-workers, pH of the solution was an important parameter controlling the adsorption capacity of ionic organics onto an adsorbent (Vasudevan et al., 2009). He further stated that pH not only affects surface charge of the adsorbents, but also affects ionization of the pharmaceuticals. The effect of pH on adsorption efficiency of TC, SMZ, NAD and CHL from pH 2-10 is shown in Fig 6.1a. For SMZ, the isoelectric point (pI) of SMZ is around 4.5 (Avisar et al., 2010), meaning that at this pH, the molecule has no net electrical charge. Below its pI, a SMZ molecule has a net positive charge, and above it has a negative charge (100 % at pH 9.5) (Lucida et al., 2000). Mt–IL has surfaces that are positively charged, and therefore, it was expected that adsorption will increase at higher pH due to electrostatic interaction between the adsorbent and the adsorbate. However, Fig 6.1a shows SMZ has significantly high adsorption at pH 3 suggesting that electrostatic interaction was not the only mechanism with which SMZ is adsorbed onto Mt–IL, but other hydrophobic interactions (organic pollutant and organo-montmorillonite) between SMZ and Mt–IL as well as pore trapping were also involved in adsorption (Zhang et al., 2011a; Zhang et al., 2010). Similar effects of pH were suggested by other researchers as well (Chen et al., 2011; Gao and Pedersen, 2005; Kim et al., 2014; Lu et al., 2014). It is evident that the amount of SMZ adsorbed onto Mt–IL depends on the solution pH. Maximum adsorption efficiency was reached at pH 4 and as the pH decreased (pH < 4) it is clear that electrostatic interaction was dominant. At these low pH values the SMZ molecule, with a pKa$_1$ of 1.7, mainly exists in the cationic form (Lu et al., 2014), therefore, experiencing electrostatic repulsion between SMZ$^+$ and the cationic surface of Mt–IL and a decrease in adsorption capacity.
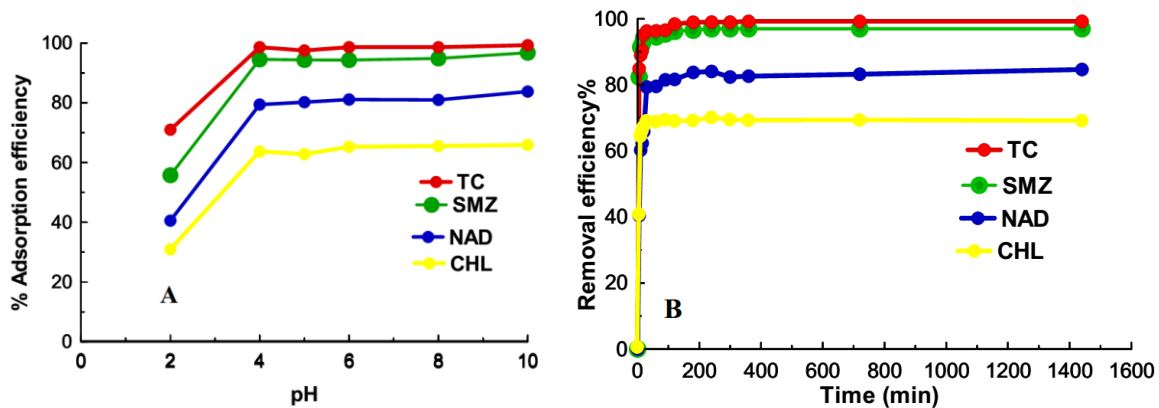
162

Fig. 6.1a and b effect of pH and contact time respectively

Fig 6.1a showed that an increase in pH of TC led to an increase in the adsorption capacity of Mt–IL. The observed pH dependence of TC can be simplified by estimating the charge on TC and Mt–IL. At pH values > 4, TC exists as neutral molecules or zwitterions ($H_2L^{+/-}$ at $pK_{a1} <$ pH $< pK_{a2} = 7.78$) to negatively charged ions (HL^- at pH $> pK_{a2} = 7.78$) (Chen and Huang, 2010). Thus adsorption is favoured at pH range 4 and above based on electrostatic interaction and hydrophobic interaction between TC and the surface of Mt–IL, as well as pore trapping. At a lower pH (< 4) electrostatic repulsion between the positively charged solution of TC and positively charged Mt–IL surface results in the reduced adsorption capacity of Mt–IL. Similar results have been reported by other researchers (Figueroa et al., 2003; Kulshrestha et al., 2004; Chang et al., 2009b). The significant adsorption capacity of TC at low pH values signifies that electrostatic interaction is not the only and main mechanism of adsorption but hydrophobicity also plays an important role. Studies by Lui and co-workers showed similar results, suggesting that hydrophobicity induced by the surfactants plays a larger role in adsorption of TC on organo-montmorillonite than electrostatic interaction (Liu et al., 2012). As seen in SMZ, there is no further significant effect of pH on TC from pH range 4-10.

NAD follows the same trend as SMZ and TC, where at low pH (3-5) NAD is predominately positively charged. Since the surface of Mt–IL is positively charged a reduction is expected in the adsorption of NAD in this pH range which is not the case. Wu and co-workers (Wu et al., 2013)

163

reported that NAD is predominately hydrophobic at low pH. Therefore, the increase in adsorption capacity at low pH may be attributed to hydrophobic interaction between NAD and Mt–IL. As solution pH increases to values higher than its pK_a (5.95), NAD becomes negatively charged and less hydrophobic. The high adsorption capacity at this pH is now mainly electrostatic attraction between NAD^- and the positively charged surface of Mt–IL.

The same explanation also applies to CHL, at pH values higher than the pK_a of CHL; it exists as anions while Mt–IL surface is positive. Electrostatic attraction between Mt–IL and CHL leads to the high adsorption in that range and hydrophobic interaction is suggested to be responsible for adsorption at pH values below the pK_a of CHL.

6.4.2 Effect of Contact Time

The effect of contact time was also investigated, as shown in Fig 6.1b. Maximum adsorption occurred in the first 30 min for all pharmaceuticals and the rate of adsorption slowed down significantly thereafter even though adsorption still continued. Fig 6.1b showed that adsorption increased with time for all analytes, and over 80 % of SMZ was removed in less than 5 min and reached above 90 % before 10 min. After 10 min the rate of adsorption still continued but was slower, though any increase in adsorption capacity from this time to about 24 h was minimal. This was faster than what has been previously reported (Lu et al., 2014; Akhtar et al., 2011).

For TC, adsorption of more than 85 % took place in the first 5 min and over 95 % before 20 min. A similar trend was reported by Chen and Huang (Chen and Huang, 2010). Approximately 60 % of NAD was adsorbed before 10 min and over 80 % was adsorbed before 30 min. The same was observed for CHL, where 60 % was adsorbed in less than 10 min and over 68 % before 30 min.

6.4.3 Adsorption Isotherms

Adsorption isotherms were also investigated. Freundlich, Langmuir, Temkin and D-R isotherm models were used to interpret the equilibrium data in order to further ascertain the adsorption behavior of SMZ, TC, NAD and CHL onto Mt–IL. The n values for all adsorption systems studied were less than unity, reflecting the high adsorption nonlinearity. In other words, adsorption of these pharmaceuticals was favored over the entire concentration range used in this study. From Table 6.2, adsorption nonlinearity for Mt–IL was in the order TC > SMZ > NAD > CHL, as indicated by their n values (Liao et al., 2013). The adsorption data best fitted to Freundlich on the basis of the correlation coefficient values (R^2) (Table 6.2), for all the pharmaceuticals considered which suggests heterogeneous adsorption (more than one mechanism of adsorption). The fit further confirmed that hydrophobic interaction between the aromatic rings of the pharmaceuticals and the adsorbent was not the only probable means of adsorption, with electrostatic interactions between the anions and the cations in the solution and the surfaces of Mt–IL, and molecular sieving of the pharmaceuticals (trapping of pharmaceuticals by the pores of Mt–IL) also played a role (Diagboya et al., 2014). However, researchers (Hari et al., 2005; Lorphensri et al., 2006; Robberson et al., 2006) have reported that hydrophobic and electrostatic interaction were the main mechanisms for pharmaceutical adsorption. Langmuir could also fit for adsorption of the pharmaceuticals as indicated by R^2 values > 0.9 shown in Table 6.2. The mean free energy of adsorption (E value) calculated from the D-R isotherm showed values < 8 kJ mol^{-1} for all the pharmaceuticals. Therefore, the adsorption of all the pharmaceuticals studied on Mt–IL was physical in nature.

Table 6.2 Results for q_m and b values in the Langmuir equation, K_f and n values in the Freundlich equation, q_m and β values in Dubinin-Radushkevich, bT and AT values in Temkin models and their respective correlation coefficient values

Pharmacuetical	Langmuir model			Freundlich model			Dubinin–Radushkevich model				Temkin model		
	q_m (mg g^{-1})	b (L mg^{-1})	R^2	K_f (L mg^{-1})	n (g L^{-1})	R^2	q_m (mol g^{-1})	β (mol^2 kJ^{-2})	E (kJ mol^{-1})	R^2	bT (g kJ mg^{-1} mol^{-1})	AT (L mg^{-1})	R^2
SMZ	520.457	0.088	0.982	9.748	0.520	0.991	0.846	2 x10^{-8}	5.00	0.998	82.01	1.143	0.990
TC	770.624	0.024	0.918	0.196	0.410	0.992	0.370	3 x 10^{-8}	4.08	0.992	94.79	0.168	0.970
NAD	152.360	0.036	0.964	5.681	0.720	0.988	0.215	2 x 10^{-8}	5.00	0.945	49.35	0.214	0.923
CHL	33.578	0.091	0.951	0.897	1.840	0.998	0.092	3 x 10^{-8}	4.12	0.987	37.95	0.587	0.967

Table 6.3 Experimental values for q_e (mg g^{-1}) and parameters for pseudo-first-order, pseudo-second-order and intra-particle diffusion

	Concentrations (mg L^{-1})	q_e,exp (mg g^{-1})	Pseudo-first-order			Pseudo-second-order			Weber–Morris model		
			q_e, cal (mg g^{-1})	k_e (h^{-1})	R^2	q_e,cal (mg g^{-1})	K (x 10) (g mg^{-1} h^{-1})	R^2	q_e (mg g^{-1})	k_{id} (mg g^{-1} h$^{-1/2}$)	R^2
SMZ	200	504.123	3.262	8 x10^{-5}	0.019	493.458	0.004	0.999	95.194	-0.003	0.004
	100	263.367	2.357	2 x10^{-5}	0.002	256.497	0.003	0.999	55.184	0.001	0.001
	50	128.976	1.541	-2x10^{-4}	0.318	130.395	0.004	0.998	27.812	0.001	0.393
	20	51.330	1.154	3x10^{-5}	0.055	51.709	0.053	0.999	12.07	-0.002	0.048
	10	26.667	0.959	-8x10^{-6}	0.005	32.747	0.090	0.999	6.052	-0.001	0.067
TC	100	765.728	0.995	-9x10^{-4}	0.368	743.478	0.025	0.995	33.207	0.123	0.307
	50	526.259	0.678	-7x10^{-3}	0.678	518.215	0.054	0.996	19.806	0.069	0.317
	25	287.878	0.110	7x10^{-4}	0.005	293.452	0.106	0.951	9.209	0.002	0.004
	15	178.069	0.044	-2x10^{-4}	0.053	182.144	0.121	0.998	3.802	0.015	0.580
	10	135.162	0.009	4x10^{-4}	0.005	121.897	0.527	0.947	1.988	-0.002	0.027
NAD	100	150.350	12.541	2x10^{-2}	0.502	154.231	0.005	0.945	46.325	0.004	0.530
	50	71.521	8.321	5x10^{-3}	0.632	70.587	0.023	0.996	28.567	0.005	0.231
	25	39.213	4.213	-9x10^{-2}	0.032	32.057	0.002	0.952	13.998	0.001	0.504
	15	29.321	2.361	-2x10^{-1}	0.751	24.365	0.254	0.999	7.214	-0.002	0.582
	10	15.120	1.897	1x10^{-4}	0.254	13.987	0.213	0.997	2.365	0.001	0.035
CHL	100	30.987	5.368	-2x10^{-5}	0.219	33.240	0.005	0.996	23.258	-0.128	0.050
	50	18.697	3.365	-5x10^{-5}	0.032	20.348	0.023	0.993	15.368	0.006	0.023
	25	10.258	2.158	-1x10^{-2}	0.418	12.365	0.002	0.981	9.874	-0.092	0.054
	15	5.214	1.945	-2x10^{-3}	0.155	5.321	0.254	0.989	4.956	0.001	0.182
	10	1.560	1.035	1x10^{-4}	0.205	1.254	0.213	0.954	2.321	-0.012	0.025

6.4.4 Adsorption Kinetics

Pseudo-first-order, second-order and intraparticle diffusion models were used to study the adsorption kinetics of the pharmaceuticals. Adsorption kinetics describes the solute uptake rate and this rate controls the residence time of the adsorbate uptake at the solid-solution interface. Adsorption rate constants for the pharmaceuticals were calculated by using kinetic models which were used to describe the mechanism of the adsorption. Correlation coefficient values (R^2) indicated that the adsorption process was best described by the pseudo second-order model with correlation coefficients > 0.995 for all the solutes and the predicted values very close to experimental q_e for all pharmaceuticals studied (Table 6.3). The plot of intraparticle diffusion showed that it did not pass through the origin which indicated that the rate controlling step was not the only process, and that other processes were involved. A comparison of the adsorption capacities of SMZ, TC, NAD, and CHL on MT–IL with other adsorbent materials (Table 6.4) showed that MT–IL is a good adsorber of pharmaceuticals from aqueous solutions.

Table 6.4 Comparison of Mt–IL with other adsorbent materials

Compound	Material	Adsorption Capacities (mg g^{-1})	References
	kaolinite	4.3	(Li et al., 2010b)
	Na–kaolinite	14.0	(Figueroa et al., 2003)
	Na–montmorillonite	54.0	(Figueroa et al., 2003)
	palygorskite	99.0	(Chang et al., 2009c)
	montmorillonite	4.3	(Parolo et al., 2008)
	rectorite	140.0	(Chang et al., 2009a)
	different smectites	355.0-460.0	(Li et al., 2010a)
	natural montmorillonite	450.0	(Liu et al., 2011)
	graphene oxide	313.5	(Gao et al., 2012)
	single-walled carbon nanotubes (SWNTs)	340.0	(Ji et al., 2009)
tetracycline	multiwalled carbon nanotubes (MWNTs)	100.0	(Ji et al., 2009)
	montmorillonite	84.0	(Wang et al., 2008)
	Fe$_3$O$_4$–rGO composites	95.0	(Zhang et al., 2011b)
	montmorillonite	250.0	(Zhao et al., 2012)
	illite	25.0	(Chang et al., 2012)
	Ca–montmorillonite	124.0	(Sithole and Guy, 1987)
	goethite	24.0	(Zhao et al., 2011)
	bamboo charcoal	22.7	(Liao et al., 2013)
	Na–montmorillonite	369.0	(Liu et al., 2012)
	organo montmorillonites	480.0-960.0	(Liu et al., 2012)
	Na$^+$-Mt	152.2	Present study
	Mt–IL	770.0	Present study
Sulfamethoxazole	activated carbon	185.2	(Çalışkan and Göktürk, 2010)
	CTMAB– montmorillonite	235.3	(Lu et al., 2014)
	HDAPS – montmorillonites	155.3	(Lu et al., 2014)
	BHDAP –montmorillonite	242.7	(Lu et al., 2014)
	Na$^+$-Mt	87.4	Present study
	Mt–IL	520.0	Present study
chloramphenicol	bamboo charcoal	8.1.0	(Liao et al., 2013)
	Na$^+$-Mt	2.3	Present study
	Mt–IL	33.0	Present study
nalidixic acid	montmorillonite	24.0	(Wu et al., 2013)
	Na$^+$-Mt	9.0	Present study
	Mt–IL	152.0	Present study

6.5 CONCLUSION

The present study showed that ionic liquid modified montmorillonite, Mt–IL, (an organo-montmorillonite) is an effective adsorber of pharmaceuticals (TC, SMZ, NAD and CHL) from aqueous solutions and has the potential for remediating water polluted with these pharmaceuticals. All the pharmaceuticals studied showed high adsorption capacities at pH values above 3. Maximum removal of pharmaceuticals occurred within the first 30 min, and the kinetic studies showed the adsorption processes followed a pseudo second-order model. The Freundlich isotherm model was the best fit for all the pharmaceuticals but the Langmuir isotherm model can also be used to explain them. The maximum adsorption capacity is relatively high compared to the unmodified montmorillonite as well as previously reported adsorption capacities. The adsorption of the selected pharmaceuticals onto Mt–IL is in the order: TC > SMZ > NAD > CHL. This study showed that ionic liquids can replace the traditional surfactants used for modification of materials for the purpose of adsorption of pharmaceuticals.

6.6 ACKNOWLEDGEMENTS

6.7 REFERENCES

Absalan, G., Asadi, M., Kamran, S., Sheikhian, L. & Goltz, D. M. 2011. Removal of reactive red-120 and 4-(2-pyridylazo) resorcinol from aqueous samples by Fe_3O_4 magnetic nanoparticles using ionic liquid as modifier. *Journal of Hazardous Materials,* 192(2), pp 476-484.

Akhtar, J., Amin, N. S. & Aris, A. 2011. Combined adsorption and catalytic ozonation for removal of sulfamethoxazole using Fe203/Ce02 loaded activated carbon. *Chemical Engineering Journal,* 170(1), pp 136-144.

Avisar, D., Primor, O., Gozlan, I. & Mamane, H. 2010. Sorption of sulfonamides and tetracyclines to montmorillonite clay. *Water, Air, & Soil Pollution,* 209(1-4), pp 439-450.

Bansal, O. 2013. Sorption of tetracycline, oxytetracycline, and chlortetracycline in illite and kaolinite suspensions. *ISRN Environmental Chemistry,* 2013(1), pp 1-8.

Barnes, K. K., Christenson, S. C., Kolpin, D. W., Focazio, M. J., Furlong, E. T., Zaugg, S. D., Meyer, M. T. & Barber, L. B. 2004. Pharmaceuticals and other organic waste water contaminants within a leachate plume downgradient of a municipal landfill. *Groundwater Monitoring & Remediation,* 24(2), pp 119-126.

Boleas, S., Alonso, C., Pro, J., Fernández, C., Carbonell, G. & Tarazona, J. V. 2005. Toxicity of the antimicrobial oxytetracycline to soil organisms in a multi-species-soil system (MS·3) and influence of manure co-addition. *Journal of Hazardous Materials,* 122(3), pp 233-241.

Çalışkan, E. & Göktürk, S. 2010. Adsorption characteristics of sulfamethoxazole and metronidazole on activated carbon. *Separation Science and Technology,* 45(2), pp 244-255.

Caroni, A. L. P. F., de Lima, C. R. M., Pereira, M. R. & Fonseca, J. L. C. 2012. Tetracycline adsorption on chitosan: A mechanistic description based on mass uptake and zeta potential measurements. *Colloids and Surfaces B: Biointerfaces,* 100(1), pp 222-228.

Chang, P.-H., Jean, J.-S., Jiang, W.-T. & Li, Z. 2009a. Mechanism of tetracycline sorption on rectorite. *Colloids and Surfaces A: Physicochemical and Engineering Aspects,* 339(1), pp 94-99.

Chang, P.-H., Li, Z., Jean, J.-S., Jiang, W.-T., Wang, C.-J. & Lin, K.-H. 2012. Adsorption of tetracycline on 2:1 layered non-swelling clay mineral illite. *Applied Clay Science,* 67–68(1), pp 158-163.

Chang, P.-H., Li, Z., Jiang, W.-T. & Jean, J.-S. 2009b. Adsorption and intercalation of tetracycline by swelling clay minerals. *Applied Clay Science,* 46(1), pp 27-36.

Chang, P.-H., Li, Z., Yu, T.-L., Munkhbayer, S., Kuo, T.-H., Hung, Y.-C., Jean, J.-S. & Lin, K.-H. 2009c. Sorptive removal of tetracycline from water by palygorskite. *Journal of Hazardous Materials,* 165(1), pp 148-155.

Chen, H., Gao, B., Li, H. & Ma, L. Q. 2011. Effects of pH and ionic strength on sulfamethoxazole and ciprofloxacin transport in saturated porous media. *Journal of Contaminant Hydrology,* 126(1), pp 29-36.

Chen, W.-R. & Huang, C.-H. 2010. Adsorption and transformation of tetracycline antibiotics with aluminum oxide. *Chemosphere,* 79(8), pp 779-785.

Diagboya, P. N., Olu-Owolabi, B. I., Zhou, D. & Han, B.-H. 2014. Graphene oxide–tripolyphosphate hybrid used as a potent sorbent for cationic dyes. *Carbon,* 79(1), pp 174-182.

Dubinin, M. & Radushkevich, L. 1947. Equation of the characteristic curve of activated charcoal. *Chemisches Zentralblatt,* 1(1), pp 875.

Fent, K., Weston, A. A. & Caminada, D. 2006. Ecotoxicology of human pharmaceuticals. *Aquatic Toxicology,* 76(2), pp 122-159.

Figueroa, R. A., Leonard, A. & MacKay, A. A. 2003. Modeling tetracycline antibiotic sorption to clays. *Environmental Science & Technology,* 38(2), pp 476-483.

Freundlich, H. 1906. Über die Adsorption in Lösungen. *Zeitschrift fur Physikalische Chemie,* 57(A), pp 385-470.

Gao, J. & Pedersen, J. A. 2005. Adsorption of sulfonamide antimicrobial agents to clay minerals. *Environmental Science & Technology,* 39(24), pp 9509-9516.

Gao, Y., Li, Y., Zhang, L., Huang, H., Hu, J., Shah, S. M. & Su, X. 2012. Adsorption and removal of tetracycline antibiotics from aqueous solution by graphene oxide. *Journal of Colloid and Interface Science,* 368(1), pp 540-546.

Halling-Sørensen, B. 2001. Inhibition of aerobic growth and nitrification of bacteria in sewage sludge by antibacterial agents. *Archives of Environmental Contamination and Toxicology,* 40(4), pp 451-460.

Hari, A. C., Paruchuri, R. A., Sabatini, D. A. & Kibbey, T. C. 2005. Effects of pH and cationic and nonionic surfactants on the adsorption of pharmaceuticals to a natural aquifer material. *Environmental Science & Technology,* 39(8), pp 2592-2598.

Ho, Y.-S. & McKay, G. 1999. Pseudo-second order model for sorption processes. *Process Biochemistry,* 34(5), pp 451-465.

Holten Lützhøft, H.-C., Vaes, W. H., Freidig, A. P., Halling-Sørensen, B. & Hermens, J. L. 2000. Influence of pH and other modifying factors on the distribution behavior of 4-quinolones to solid phases and humic acids studied by "negligible-depletion" SPME-HPLC. *Environmental Science & Technology,* 34(23), pp 4989-4994.

Isidori, M., Lavorgna, M., Nardelli, A., Pascarella, L. & Parrella, A. 2005. Toxic and genotoxic evaluation of six antibiotics on non-target organisms. *Science of the Total Environment,* 346(1), pp 87-98.

Ji, L., Chen, W., Bi, J., Zheng, S., Xu, Z., Zhu, D. & Alvarez, P. J. 2010a. Adsorption of tetracycline on single-walled and multi-walled carbon nanotubes as affected by aqueous solution chemistry. *Environmental Toxicology and Chemistry,* 29(12), pp 2713-2719.

Ji, L., Chen, W., Duan, L. & Zhu, D. 2009. Mechanisms for strong adsorption of tetracycline to carbon nanotubes: A comparative study using activated carbon and graphite as adsorbents. *Environmental Science & Technology,* 43(7), pp 2322-2327.

Ji, L., Liu, F., Xu, Z., Zheng, S. & Zhu, D. 2010b. Adsorption of pharmaceutical antibiotics on template-synthesized ordered micro-and mesoporous carbons. *Environmental Science & Technology,* 44(8), pp 3116-3122.

Kamran, S., Hossein Tavallali & Azad, A. 2014. Fast removal of reactive red 141 and reactive yellow 81 from aqueous solution by Fe_3O_4 magnetic nanoparticles modified with ionic liquid 1-octyl-3-methylimidazolium bromide. *Iranian Journal of Analytical chemistry,* 1(1), pp 78-86.

Kim, Y., Bae, J., Park, J., Suh, J., Lee, S., Park, H. & Choi, H. 2014. Removal of 12 selected pharmaceuticals by granular mesoporous silica SBA-15 in aqueous phase. *Chemical Engineering Journal,* 256(1), pp 475-485.

Kolpin, D. W., Furlong, E. T., Meyer, M. T., Thurman, E. M., Zaugg, S. D., Barber, L. B. & Buxton, H. T. 2002. Pharmaceuticals, hormones, and other organic wastewater contaminants in US streams, 1999-2000: A national reconnaissance. *Environmental Science & Technology,* 36(6), pp 1202-1211.

Kulshrestha, P., Giese, R. F. & Aga, D. S. 2004. Investigating the molecular interactions of oxytetracycline in clay and organic matter: Insights on factors affecting its mobility in soil. *Environmental Science & Technology,* 38(15), pp 4097-4105.

Lagergren, S. 1898. About the theory of so-called adsorption of soluble substances. *Kungliga Svenska Vetenskapsakademiens Handlingar,* 24(4), pp 1-39.

Langmuir, I. 1916. The constitutionand fundamental properties of solid and liquids. Part I. Solids. *Journal of the American Chemical Society,* 38(11), pp 2221-2295.

Lawal, I. A. & Moodley, B. 2015. Synthesis, characterisation and application of imidazolium based ionic liquid modified montmorillonite sorbents for the removal of amaranth dye. *RSC Advances,* 5(76), pp 61913-61924.

Li, R., Yuan, Q., Zhang, Y., Ling, J. & Han, T. 2011. Hydrophilic interaction chromatographic determination of oxytetracycline in the environmental water using silica column. *Journal of Liquid Chromatography & Related Technologies,* 34(7), pp 511-520.

Li, Z., Chang, P.-H., Jean, J.-S., Jiang, W.-T. & Wang, C.-J. 2010a. Interaction between tetracycline and smectite in aqueous solution. *Journal of Colloid and Interface Science,* 341(2), pp 311-319.

Li, Z., Schulz, L., Ackley, C. & Fenske, N. 2010b. Adsorption of tetracycline on kaolinite with pH-dependent surface charges. *Journal of Colloid and Interface Science,* 351(1), pp 254-260.

Liao, P., Zhan, Z., Dai, J., Wu, X., Zhang, W., Wang, K. & Yuan, S. 2013. Adsorption of tetracycline and chloramphenicol in aqueous solutions by bamboo charcoal: A batch and fixed-bed column study. *Chemical Engineering Journal,* 228(1), pp 496–505.

Lin, A. Y.-C., Yu, T.-H. & Lin, C.-F. 2008. Pharmaceutical contamination in residential, industrial, and agricultural waste streams: Risk to aqueous environments in Taiwan. *Chemosphere,* 74(1), pp 131-141.

Liu, N., Wang, M.-x., Liu, M.-m., Liu, F., Weng, L., Koopal, L. K. & Tan, W.-f. 2012. Sorption of tetracycline on organo-montmorillonites. *Journal of Hazardous Materials,* 225–226(1), pp 28-35.

Liu, Y., Lu, X., Wu, F. & Deng, N. 2011. Adsorption and photooxidation of pharmaceuticals and personal care products on clay minerals. *Reaction Kinetics, Mechanisms and Catalysis,* 104(1), pp 61-73.

Lorphensri, O., Intravijit, J., Sabatini, D. A., Kibbey, T. C. G., Osathaphan, K. & Saiwan, C. 2006. Sorption of acetaminophen, 17α-ethynyl estradiol, nalidixic acid, and norfloxacin to silica, alumina, and a hydrophobic medium. *Water Research,* 40(7), pp 1481-1491.

Lu, L., Gao, M., Gu, Z., Yang, S. & Liu, Y. 2014. A comparative study and evaluation of sulfamethoxazole adsorption onto organo-montmorillonites. *Journal of Environmental Sciences,* 26(12), pp 2535-2545.

Lucida, H., Parkin, J. & Sunderland, V. 2000. Kinetic study of the reaction of sulfamethoxazole and glucose under acidic conditions: I. Effect of pH and temperature. *International Journal of Pharmaceutics,* 202(1), pp 47-62.

Nam, S.-W., Choi, D.-J., Kim, S.-K., Her, N. & Zoh, K.-D. 2014. Adsorption characteristics of selected hydrophilic and hydrophobic micropollutants in water using activated carbon. *Journal of Hazardous Materials,* 270(1), pp 144-152.

Park, S. & Choi, K. 2008. Hazard assessment of commonly used agricultural antibiotics on aquatic ecosystems. *Ecotoxicology,* 17(6), pp 526-538.

Parolo, M. E., Savini, M. C., Vallés, J. M., Baschini, M. T. & Avena, M. J. 2008. Tetracycline adsorption on montmorillonite: pH and ionic strength effects. *Applied Clay Science,* 40(1–4), pp 179-186.

Regulation, C., 1994. No. 2377/90 Laying down a community procedure for the establishment of maximum residue limits of veterinary medicinal products in foodstuffs of animal origin, amending regulation No. 1430/94 of 22 June 1994, Off, Regulation, C.

Robberson, K. A., Waghe, A. B., Sabatini, D. A. & Butler, E. C. 2006. Adsorption of the quinolone antibiotic nalidixic acid onto anion-exchange and neutral polymers. *Chemosphere,* 63(6), pp 934-941.

Rudder, J. d., Wiele, T., Dhooge, W., Comhaire, F. & Verstraete, W. 2004. Advanced water treatment with manganese oxide for the removal of 17α-ethynylestradiol (EE2). *Water Research,* 38(1), pp 184-192.

Sarmah, A. K., Meyer, M. T. & Boxall, A. 2006. A global perspective on the use, sales, exposure pathways, occurrence, fate and effects of veterinary antibiotics (VAs) in the environment. *Chemosphere,* 65(5), pp 725-759.

Sheng, G., Wang, X., Wu, S. & Boyd, S. A. 1998. Enhanced sorption of organic contaminants by smectitic soils modified with a cationic surfactant. *Journal of Environmental Quality,* 27(4), pp 806-814.

Singh, K., Singh, A., Gupta, S. & Rai, P. 2012. Modeling and optimization of reductive degradation of chloramphenicol in aqueous solution by zero-valent bimetallic nanoparticles. *Environmental Science and Pollution Research,* 19(6), pp 2063-2078.

Sithole, B. & Guy, R. 1987. Models for tetracycline in aquatic environments. *Water, Air, and Soil Pollution,* 32(3-4), pp 303-314.

Smith, J. A., Jaffe, P. R. & Chiou, C. T. 1990. Effect of ten quaternary ammonium cations on tetrachloromethane sorption to clay from water. *Environmental Science & Technology,* 24(8), pp 1167-1172.

Sun, H., Shi, X., Mao, J. & Zhu, D. 2010. Tetracycline sorption to coal and soil humic acids: An examination of humic structural heterogeneity. *Environmental Toxicology and Chemistry,* 29(9), pp 1934-1942.

Tamtam, F., Van Oort, F., Le Bot, B., Dinh, T., Mompelat, S., Chevreuil, M., Lamy, I. & Thiry, M. 2011. Assessing the fate of antibiotic contaminants in metal contaminated soils four years after cessation of long-term waste water irrigation. *Science of the Total Environment,* 409(3), pp 540-547.

Ternes, T. A., Meisenheimer, M., McDowell, D., Sacher, F., Brauch, H.-J., Haist-Gulde, B., Preuss, G., Wilme, U. & Zulei-Seibert, N. 2002. Removal of pharmaceuticals during drinking water treatment. *Environmental Science & Technology,* 36(17), pp 3855-3863.

Thiele-Bruhn, S. & Beck, I.-C. 2005. Effects of sulfonamide and tetracycline antibiotics on soil microbial activity and microbial biomass. *Chemosphere,* 59(4), pp 457-465.

Vasudevan, D., Bruland, G. L., Torrance, B. S., Upchurch, V. G. & MacKay, A. A. 2009. pH-dependent ciprofloxacin sorption to soils: Interaction mechanisms and soil factors influencing sorption. *Geoderma,* 151(3), pp 68-76.

Wang, J., Hu, J. & Zhang, S. 2010. Studies on the sorption of tetracycline onto clays and marine sediment from seawater. *Journal of Colloid and Interface Science,* 349(2), pp 578-582.

Wang, Y.-J., Jia, D.-A., Sun, R.-J., Zhu, H.-W. & Zhou, D.-M. 2008. Adsorption and cosorption of tetracycline and copper(II) on montmorillonite as affected by solution pH. *Environmental Science & Technology,* 42(9), pp 3254-3259.

Watkinson, A., Murby, E., Kolpin, D. & Costanzo, S. 2009. The occurrence of antibiotics in an urban watershed: from wastewater to drinking water. *Science of the Total Environment,* 407(8), pp 2711-2723.

Weber, W. J. & Morris, J. C. 1963. Kinetics of adsorption on carbon from solution. *Journal of the Sanitary Engineering Division. ASCE,,* 89(1), pp 31.

Woodward, K. & Watson, D. 2004. Pesticide, veterinary and other residues in food. *Woodward Publisher Limited, Cambridge.*

Wu, Q., Li, Z. & Hong, H. 2013. Adsorption of the quinolone antibiotic nalidixic acid onto montmorillonite and kaolinite. *Applied Clay Science,* 74(1), pp 66-73.

Zhang, D., Pan, B., Wu, M., Wang, B., Zhang, H., Peng, H., Wu, D. & Ning, P. 2011a. Adsorption of sulfamethoxazole on functionalized carbon nanotubes as affected by cations and anions. *Environmental Pollution,* 159(10), pp 2616-2621.

Zhang, D., Pan, B., Zhang, H., Ning, P. & Xing, B. 2010. Contribution of different sulfamethoxazole species to their overall adsorption on functionalized carbon nanotubes. *Environmental Science & Technology,* 44(10), pp 3806-3811.

Zhang, Y., Chen, B., Zhang, L., Huang, J., Chen, F., Yang, Z., Yao, J. & Zhang, Z. 2011b. Controlled assembly of Fe_3O_4 magnetic nanoparticles on graphene oxide. *Nanoscale,* 3(4), pp 1446-1450.

Zhang, Y., Shen, Y., Yuan, J., Han, D., Wang, Z., Zhang, Q. & Niu, L. 2006. Design and synthesis of multifunctional material based on an ionic-liquid backbone. *Angewandte Chemie International Edition,* 45(35), pp 5867 –5870.

Zhao, Y., Geng, J., Wang, X., Gu, X. & Gao, S. 2011. Adsorption of tetracycline onto goethite in the presence of metal cations and humic substances. *Journal of Colloid and Interface Science,* 361(1), pp 247-251.

Zhao, Y., Gu, X., Gao, S., Geng, J. & Wang, X. 2012. Adsorption of tetracycline (TC) onto montmorillonite: Cations and humic acid effects. *Geoderma,* 183–184(1), pp 12-18.

Zhu, L., Li, Y. & Zhang, J. 1997. Sorption of organobentonites to some organic pollutants in water. *Environmental Science & Technology,* 31(5), pp 1407-1410.

CHAPTER 7: SORPTION OF CONGO RED AND REACTIVE BLUE ON PEANUT SHELL AND ACTIVATED CARBON DERIVED FROM PEANUT MODIFIED BY IONIC LIQUID

Isiaka A. Lawal[a], Darren Chetty[a] and Brenda Moodley[a]*

[a]School of Chemistry and Physics, College of Agriculture, Engineering and Science, University of KwaZulu-Natal, P/Bag X45001, Westville Campus, Durban, 4000, South Africa

*corresponding author email: moodleyb3@ukzn.ac.za

Tel: +27 31 2602796; Fax: +27 31 2603091

First author: lawalishaq000123@yahoo.com

7.1 ABSTRACT

Sorption studies of congo red (CR) and reactive blue 4 (RB) dyes from aqueous solution onto four peanut shell derived sorbent materials were examined. Raw powdered peanut shell (NS) was produced by treating with sodium hydroxide, and activated carbon (AC) was produced from NS by calcination in an inert atmosphere. 1-methyl-3-decahexyl imidazolium ionic liquid (IL) was used to modify NS and AC to produce ionic liquid NS (ILNS) and ionic liquid AC (ILAC) respectively. These four materials were characterised by fourier transform infrared (FTIR), Brunauer−Emmett−Teller (BET), x-ray diffraction (XRD), thermal gravimetric analysis (TGA) and scanning electron microscopy (SEM). These materials were thereafter used for the sorption of CR and RB; the effects of sorbent dosage, initial solution pH and electrolyte concentration were evaluated. NS, ILNS, AC and ILAC were found to have BET surface areas of 3.3, 3.3, 981.0 and 976.0 $m^2 g^{-1}$ respectively. NS and AC had adsorption capacities of 3.6 and 29.3 mg g^{-1} for CR and 4.8 and 65.6 mg g^{-1} for RB respectively. Corresponding valves for ILNS and ILAC were 136.4 and 150.0 mg g^{-1} for CR and 290.0 and 364.4 mg g^{-1} for RB respectively. Adsorption was pH dependant, with pH 1 – 6 identified for optimum adsorption of CR and RB onto ILAC, while, CR and RB adsorption onto ILNS was favourable at pH 7 – 9. Increasing electrolyte concentration decreased adsorption. The adsorption followed pseudo second order kinetics and the rate of

adsorption increased with a decreasing sorbate concentration. The adsorption of CR and RB onto ILAC followed the Freundlich isotherm, while ILNS was described by Freundlich and Langmuir. Mean free adsorption energies calculated from the Dubinin – Radushkevich isotherm plot were less than 8 kJ mol^{-1} for both dyes for both ILAC and ILNS indicating that physisorption predominated over chemisorption. Modification with ionic liquid resulted an increase in adsorption capacity.

7.2 INTRODUCTION

Approximately several hundred thousand tonnes of nearly ten thousand different dyes are produced annually for use in various industries ranging from textiles and tanning to paper and pulp. Of these, between 35 and 70 thousand tonnes of this dye ends up in industrial effluent which in most cases is simply dumped into natural water ways (Dawood and Sen, 2012). The extremely adverse effects these dyes have on aquatic flora and fauna are exacerbated by the compounds recalcitrance in nature. Not only do the dyes discolour the water but they also consume dissolved oxygen quite readily (i.e. they have high chemical and biological oxygen demands) (Dawood and Sen, 2012).

Industrial dyes can be categorised into two factions depending on the net charge the active component of the dye has when placed in water. The dyes in each faction can be further categorised depending on the functional groups present on the active component. Anionic or acidic dyes carry a net negative charge whereas cationic or basic dyes carry a net positive charge (Dawood and Sen, 2012). This study focuses primarily on the adsorption of the anionic dyes congo red (CR) and reactive blue (RB) (Fig. 7.1). These dyes are highly water soluble and are used in the colouring of natural materials such as cotton and wool as well as synthetic materials such as polyamide and acrylic fibres. The functional groups present on the active component of these dye molecules form covalent bonds with the atoms of the adsorbent material (Yagub et al., 2014). CR is regarded as a an azo-type anionic dye due to the nitrogen-nitrogen multibonds and RB is classified as an

anthraquinone-type anionic dye due to the incorporation of polysubstituted anthraquinone rings into its structure (Yagub et al., 2014).

Both CR and RB are known to have a negative impact on the environment. Benzidine, one of the products resulting from the degradation of CR is a known carcinogen. Extended exposure to RB has been noted to cause renal complications in addition to central nervous and reproductive system disorders (Dawood and Sen, 2012; Yagub et al., 2014).
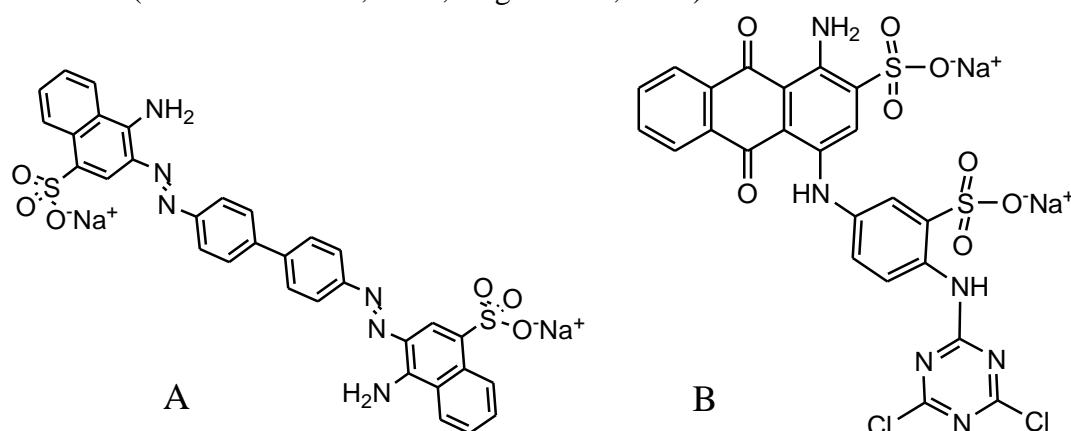

Fig. 7.1a Congo red (CR) and 7.1b Reactive blue (RB)

The present methods of wastewater remediation include chemical techniques such as oxidation and photochemical degradation. These methods however have questionable environmental friendliness as the former makes use of hydrogen peroxide and the latter forms toxic and sometimes carcinogenic by-products (Yagub et al., 2014; Salleh et al., 2011). Also, physical remediation methods including membrane filtration and ion exchange have their own practical problems. The use of membrane filters results in the formation of concentrated sludge which must then be disposed in a proper manner as well as the general high cost of ion exchange columns makes it an expensive method for use (Salleh et al., 2011). The most efficient and environmentally friendly method of effluent remediation with regard to dye removal is adsorption onto activated carbon. Activated carbon in turn is extremely expensive. There is therefore a need for inexpensive yet efficient and competitive adsorbent materials to be developed.

Biosorbents, which include bark and wood chips, chitosan, peat, sugarcane bagasse, straw and rice husks, activated bamboo and many more, are some of the recent low-cost materials used for the removal of pollutants from water bodies because they are cheap, easy to use and readily available

compared to other techniques such as ion exchange, reverse osmosis, electrochemical treatment, evaporation recovery, solvent extraction, and adsorption (Olu-Owolabi et al., 2012). Low adsorption capacity has been the bane of biosorption, particularly its industrial use in cleaning up toxic pollutants from wastewater (Deng and Ting, 2005). This has led to the modification of biosorbents to enhance its adsorption capacity. Treatments range from acid or alkaline treatment (Montazer-Rahmati et al., 2011; Li et al., 2010), acetone and ethanol treatments (Feng et al., 2011) as well as formaldehyde treatment (Feng et al., 2011; Montazer-Rahmati et al., 2011).

Research into the modification of agricultural waste materials for the adsorption of a variety of chemical species has been widely explored in the past decade. Recent trends in the modification of biosorbents with surfactants, for the adsorption of organics has increased (Brandão et al., 2010). It has been confirmed that surfactant-modified solid surfaces improve the removal of some organic contaminants from aqueous solutions (Adak et al., 2006). Studies have shown that modified biosorbents have superior adsorptive capabilities compared to their native counterparts. Akar and Divriklioglu investigated the overall, batch and continuous mode adsorption of surfactant modified biomass (CTAB-modified fungal biomass) as well as unmodified dried fungal biomass. Their results showed that surfactant modified biomass was much better than the unmodified dried biomass for the removal of reactive blue dye (Akar and Divriklioglu, 2010). Also, the biosorption of methylene blue onto dried *Rhizopus arrhizus*, a filamentous fungus, was investigated in the absence and in the presence of increasing concentrations of surfactant (sodium dodecylsulfate (SDS)) (Aksu et al., 2010). The results clearly showed a maximum adsorption capacity of 370.3 mg g^{-1} was achieved for the dried biomass in the absence of the surfactant and with just addition of 1 mM (288.4 mg L^{-1}) of SDS, the adsorption capacity increased 4.5-fold to 1666.6 mg g^{-1}.

Activated carbon from biomass is another way of improving the adsorption capacity of biomass. Foo and coworkers reported superior adsorptive capabilities of activated carbon compared to its natively prepared counterparts (native biosorbents prepared from pineapple, guava peels and Parkia bean pods) (Foo et al., 2012). The native materials displayed adsorption capacities ranging between 18 and 39 mg g^{-1} which were much lower in comparison to the adsorption capacities determined from activated carbon derived from them.

Activated carbon has also been prepared from peanut shell (Girgis et al., 2002), which contains high concentrations of carbon-rich cellulose and hemicellulose. Cellulose structures consist of a monomeric unit of a β-D-glucopyranose linked through a 1,4-glucosidic linkage. It is renewable, cheap and low in density, exhibits better processing flexibility, and is a biodegradable material. Cellulose is a highly functionalized, rigid linear chain homopolymer, characterized by its hydrophilicity, chirality, biodegradability and broad chemical modifying capacity (Gupta et al., 2013). Several research studies report that peanut shell can be converted into activated carbon and used to adsorb various metal ions and organic compounds (Wilson et al., 2006; Periasamy and Namasivayam, 1994; Periasamy and Namasivayam, 1995).

Recently to further improve the adsorption capacity of activated carbon, surfactants have been used to modify them as well. Since activated carbon is not efficient in removing oil, grease, natural organic matter, and other large organic molecules (Alther, 2002), therefore modification of this activated carbon is essential to make it more suitable for the adsorption of organic pollutants. Choi and co-workers reported that reactive black 5 was adsorbed from aqueous solution using activated carbon modified with cetylpyridinium chloride, and their results showed that modification of AC using surfactants enhanced the sorption capacity of reactive black 5 (Choi et al., 2008). Cota-Espericueta also modified AC with hexadecyltrimethylammonium bromide and dodecyltrimethylammonium bromide for the adsorption of 2,4-dinitrophenol and 2,4-dinitrotoluene (Cota-Espericueta, 2003).

Ionic liquids as surfactants have recently attracted an increasing amount of interest, owing to their low volatility, non-flammability, high chemical and thermal stabilities, high ionic conductivity and broad electrochemical windows (Zhang et al., 2006). They are essentially the liquid form of a salt, comprising of mainly ions and temporary ion pairs (Zheng et al., 2014; Singh et al., 2014). Recently they have been used as surfactants for the modification of materials for adsorption. Montmorillonite modified by ionic liquid (1-methyl-3-decahexyl imidazolium) was used in the adsorption of amaranth dye (Lawal and Moodley, 2015). Kamran and co-workers modified Fe_3O_4 magnetic nanoparticles modified with 1-octyl-3-methylimidazolium bromide and used it for the removal of reactive red 141 and reactive yellow 81 from aqueous solutions (Kamran et al., 2014b). Adsorption of reactive red-120 and 4-(2-pyridylazo) resorcinol from aqueous solution by Fe_3O_4 magnetic nanoparticles using ionic liquid as modifier was studied (Absalan et al., 2011). Also,

adsorption of folic acid, riboflavin, and ascorbic acid from aqueous samples by Fe_3O^+ magnetic nanoparticles using ionic liquid as a modifier has also been reported (Kamran et al., 2014a). To the best of our knowledge, no research has been reported on the modification of biosorbents and activated carbon from biosorbents with ionic liquids and this is the first report on sorption studies of dye onto 1-methyl-3-decahexyl imidazolium modified biosorbent and activated carbon.

The aim of this study was to investigate and evaluate the adsorption behaviour and compare the adsorption capacities of sorbent materials derived from peanut shells (sp *Arachis hypogaea*) (native (NS), activated carbon (AC) derived from NS and their modification with ionic liquid to produce ILNS and ILAC respectively). The ionic liquid that was used was 1-methyl-3-decahexyl imidazolium which contains a sixteen carbon backbone (Fig. 7.2). The quaternary nitrogen in the imidazolium ring makes the ionic liquid cationic in nature.
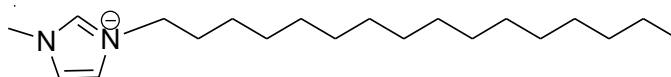
Fig. 7.2 Structure of 1-methyl-3-decahexyl imidazolium salt

7.3 EXPERIMENTAL

7.3.1 Materials

The raw peanuts (sp *Arachis hypogaea*) was sourced in Durban, and the ionic liquid, 1-methyl-3-decahexyl imidazolium was synthesised in the laboratory. All other chemicals used were of analytical grade and sourced from Sigma Aldrich (99.999% purity).

7.3.2 Adsorbent Preparation

7.3.2.1 Synthesis and characterisation of 1-methyl-3-decahexyl imidazolium

The synthesis and characterisation of ionic liquid (1-methyl-3-decahexyl imidazolium) used in this research has been reported in chapter 4. Briefly, an oil bath with a stirred flask containing equimolar amounts of N-imidazole and the primary alkyl bromide (bromodecahexane) was heated at 140 °C for 10-15 min and thereafter cooled. The solution was heated again in the oil-bath at 140 °C for another 10-15 min, followed by drying under vacuum at 100-120 °C to give the desired product of a highly viscous golden liquid that solidified at room temperature.

7.3.2.2 Preparation of nut shell (NS)

The peanut was removed from the shell and the shell was washed successively with tap water and double distilled deionized water to remove any unwanted particles and membranes. Thereafter, the shell was dried in an oven at 85 °C until dry, ground in an Angstrom TE250 ring and puck pulveriser and sieved through a 120 micron sieve. A mass of 50 g powdered peanut shell was mixed with 100 mL of 1 M sodium hydroxide and then stirred for approximately three hours at room temperature. Thereafter, it was filtered off and washed repeatedly with double distilled deionised water until a neutral pH was achieved. The material was then dried in an oven at 85 °C until dry and was labelled NS and stored in a desiccator until further use.

7.3.2.3 Preparation of activated carbon from NS

NS was calcined in a furnace under constant nitrogen flow, at a heating rate of 10 °C min^{-1} until a temperature of 500 °C was reached. The temperature was then maintained for a further two hours. After two hours the calcined material was activated by increasing the temperature to 800 °C (under nitrogen) for a further one and a half hours. The activated carbon obtained from calcination was stored in a desiccator and labelled AC**.**

7.3.2.4 Modification of NS and AC

The modification of NS and AC by ionic liquid was done by adding ionic liquid in excess of its critical micelle concentration (CMC) (0.01×10^{-3} mol dm^{-3}) as determined by Mandavi (Mandavi et al., 2008). A mass (in grams) of NS or AC powder was added to an already dissolved and known

amount of ionic liquid in methanol. The mixture was stirred at room temperature for 24 hours, and thereafter, dried in an oven at 80 °C overnight. The resulting modified material was cooled down, washed several times with double distilled deionized water and dried in an oven (80 °C). The resulting materials were labelled ILNS and ILAC respectively and stored in a desiccator until further use.

7.3.3 Characterisation of NS, ILNS, AC and ILAC

Each of the four prepared materials (NS, ILNS, AC and ILAC) were characterised by FTIR using the KBr disc preparation method, and scanning electron microscopy (SEM) using the Leo 435 VP model. Thermal gravimetric analysis and differential thermal analysis (TGA-DTA/DSC) (SDT Q 600 V 20.9 Build 20 instrument) was used to measure changes in chemical and physical properties of the material. It was measured as a function of increasing temperature from ambient to 1000 °C (with a constant heating rate of 5 °C min^{-1}) under nitrogen atmosphere with a flow rate of 50 mL min^{-1}. The materials were analysed using x-ray diffraction (XRD) (Bruker D8, Cu Kα radiation, 45 kV, 40 mA), and data were collected for 2θ ranging from 10° to 90° with a scan speed of 1 ° min^{-1}. BET (Tri-star II 3020.VI.03) was used to determine the surface area, pore-size, pore volume and pore size distribution. The materials were first degassed (Micromeritics vacprep 061, sample degas system) at 90 °C for 1 hr and was increased to 200 °C for 12 hr. The sample was then analysed under a nitrogen atmosphere at 77 K.

7.3.4 Adsorption Experiments

7.3.4.1 Batch equilibrium experiments

Stock solutions (1000 mg L^{-1}) of congo red dye and reactive blue dye solution were prepared in double distilled deionised water. Batch experiments included the investigation of the effects of sorbent dosage, initial solution pH and electrolyte concentration for both CR and RB. In the determination of the effect of dose, varying masses of each of the four materials (NS, ILNS, AC and ILAC) ranging from 0.01 - 0.15 g were added to 30 mL of 100 mg L^{-1} of each dye in series. The effect of pH and electrolyte concentration was carried out at the same adsorbate concentration (100 mg L^{-1}) and constant mass of the materials but varying pH and electrolyte concentrations respectively. The concentration of the supernatant was analysed using a double beam

UV−Vis−NIR spectrophotometer (Shimadzu Model UV 3600, Japan) at λ_{max} 498 nm for CR and 594 nm for RB.

7.3.4.2 Kinetic and isotherm experiments

A constant mass of each material was added to separate conical flasks containing 150 mL of dye in the concentration range of 20 – 200 mg L^{-1}. The capped flasks were then wrapped in foil and placed on an orbital shaker set at 220 rpm. Aliquots of the solution from each flask were removed at regular time intervals over a period of 24 hours, filtered under vacuum and the filtrates collected for analysis by UV spectrophotometry.

The adsorption capacities q_e (mg g^{-1}) of the materials were calculated using the following equation.

$$q_e = \frac{(C_0 - C_e)}{W} V ... 7.1$$

Where C_o and C_e are the dye concentrations at initial and at equilibrium respectively, in mg L^{-1}, V is the volume of solution in (L), and W is the weight of adsorbent in (g).

The data obtained were fitted into kinetic models, pseudo-first-order (Lagergren, 1898), pseudo-second-order (Ho and McKay, 1999) and intra-particle diffusion model, to determine the kinetic and mechanistic details of adsorption respectively.

The equation describing the pseudo-first-order kinetic model is:

$$In(q_e - q_t) = lnq_e - k_1 t ... 7.2$$

Where q_t is the amount of adsorption at time t in mg g^{-1}, k_1 is the rate constant of the equation in min^{-1}, and q_e is the amount of adsorption equilibrium in mg g^{-1}. The adsorption rate constant (k_1) can be determined experimentally by plotting ln (q_e-q_t) *versus* t.

The pseudo second order kinetic model is expressed as:

$$\frac{t}{q_t} = \frac{1}{k_2 q_e^2} + \frac{1}{q_e} t ...7.3$$

Where k_2 is the equilibrium rate constant of pseudo second order adsorption in g mg^{-1} min^{-1}. The values of k_2 and q_e can be determined from the slope and intercept of the plot of t/q_t *versus* t, respectively.

The data was also fitted into the Weber–Morris model, to evaluate the possibility of intra-particle diffusion as the rate limiting step. It is given by (Weber and Morris, 1963):

$$q_t = k_{id} t^{1/2} ...7.4$$

Where k_{id} (mg g^{-1}h$^{-1/2}$) is the intra-particle diffusion rate constant.

Isotherm models were also employed to interpret the data, and the adsorption data were fitted to Freundlich (Freundlich, 1906), Langmuir (Langmuir, 1916), Temkin and Dubinin–Raduskevich (Dubinin and Radushkevich, 1947) isotherms. Linear equations of all the applied models are:

$$\text{Langmuir model:} \frac{C_e}{q_e} = \frac{C_e}{q_m} + \frac{1}{q_m b} ...7.5$$

The value of b serves as a more meaningful function in the calculation of the dimensionless Langmuir separation factor (R_L) according to equation (6) (Yagub et al., 2014).

$$R_L = \frac{1}{1 + (1 + K_L C_i)} ...7.6$$

R_L values greater than one indicate unfavourable adsorption conditions whereas R_L values between one and zero indicate favourable adsorption. A R_L value equal to one or equal to zero indicates linear or irreversible adsorption respectively (Yagub et al., 2014).

$$\text{Freundlich model: } \ln q_e = \ln K_f + \frac{1}{n} \ln C_e ...7.7$$

$$\text{Temkin model: } q_e = B \ln A + B \ln C_e ...7.8$$

189

$$\text{Dubinin–Raduskevich model: } \ln q_e = \ln q_m - \beta \Sigma^2 \dots 7.9$$

$$\Sigma = RT \, \ln\left[1 + \frac{1}{C_e}\right] \dots 7.10$$

$$E = \frac{1}{\sqrt{2\beta}} \dots 7.11$$

Where C_e is the equilibrium dye concentration in the solution in mg L^{-1}, b is the Langmuir adsorption constant (L mg^{-1}), and q_m is the theoretical maximum adsorption capacity (mg g^{-1}). K_f (L mg^{-1}) and n are Freundlich isotherm constants indicating the capacity and intensity of the adsorption, respectively. A is the equilibrium binding constant (L mg^{-1}) and B is the heat of adsorption. β is the Dubinin–Raduskevich model constant (mol^2 kJ^{-2}) related to the mean free energy of adsorption per mole of the adsorbate and Σ is the polanyi potential. E is the mean free energy of adsorption (kJ mol^{-1}).

7.4 RESULTS AND DISCUSSION

7.4.1 Characterisation

Peanut shells are primarily comprised of lignin and cellulose (Annadurai et al., 2002). Lignin's large framework of linked 6-membered aromatic carbon rings contains a number of functional groups including hydroxyl, carbonyl and carboxyl moieties. Ether linkages and hydroxyl groups are also present in the structure of cellulose (Annadurai et al., 2002; Girgis et al., 2002). To establish that 1-methyl, 3-decahexyl imidazolium (IL) had modified the materials, the FT-IR spectra of NS and AC before and after modification were obtained. The spectra were recorded in the region 380–4000 cm^{-1} as shown in Fig. 7.3. The peaks at 2928 and 2851 cm^{-1} were assigned to symmetric and asymmetric stretching vibrations of the methylene groups (Zhou et al., 2007). When comparing the FTIR spectra of NS and ILNS as well as AC and ILAC, the enhancement of the peaks at this characteristic wavelength can be clearly seen for the modified material thus confirming the modification of NS and AC with ionic liquid. The presence of peaks in the region of 3331-3305 represents the –OH of water within the materials.
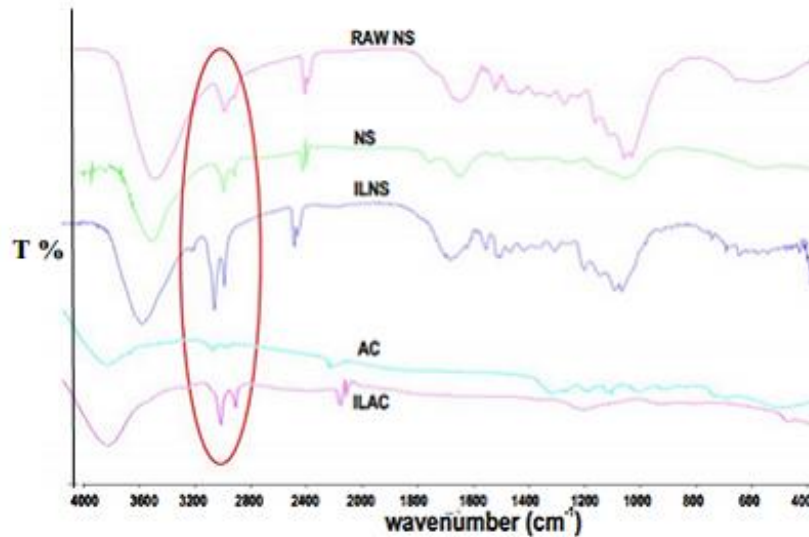
Fig. 7.3 FT-IR spectra of raw peanut shell, NS, ILNS, AC and ILAC

The surface morphologies of the materials were analysed using SEM. The treatment of raw peanut shell (NS) with sodium hydroxide served a dual function. Firstly, sodium hydroxide removed a significant amount of the natural oils and waxy compounds present on peanut shells (Liu et al., 2010; Slimani et al., 2014). The natural oils and waxes present in native peanut shells are responsible for maintaining the smooth outer surface (Fig. 7.4a). Secondly, sodium hydroxide increased the surface porosity of the nutshell powder due to the concentration of sodium hydroxide used (1 M) and was caustic enough to degrade the lignin present, thus generating ridges, valleys and pores (Fig. 7.4b) necessary for adsorption. Modification of NS and AC with IL resulted in a decrease in surface area and pore volume due to the occupation of adsorption sites by the IL and is known as "pore filling" (Singh et al., 2014) which is observed in Figs. 7.4c and 7.4E.

191
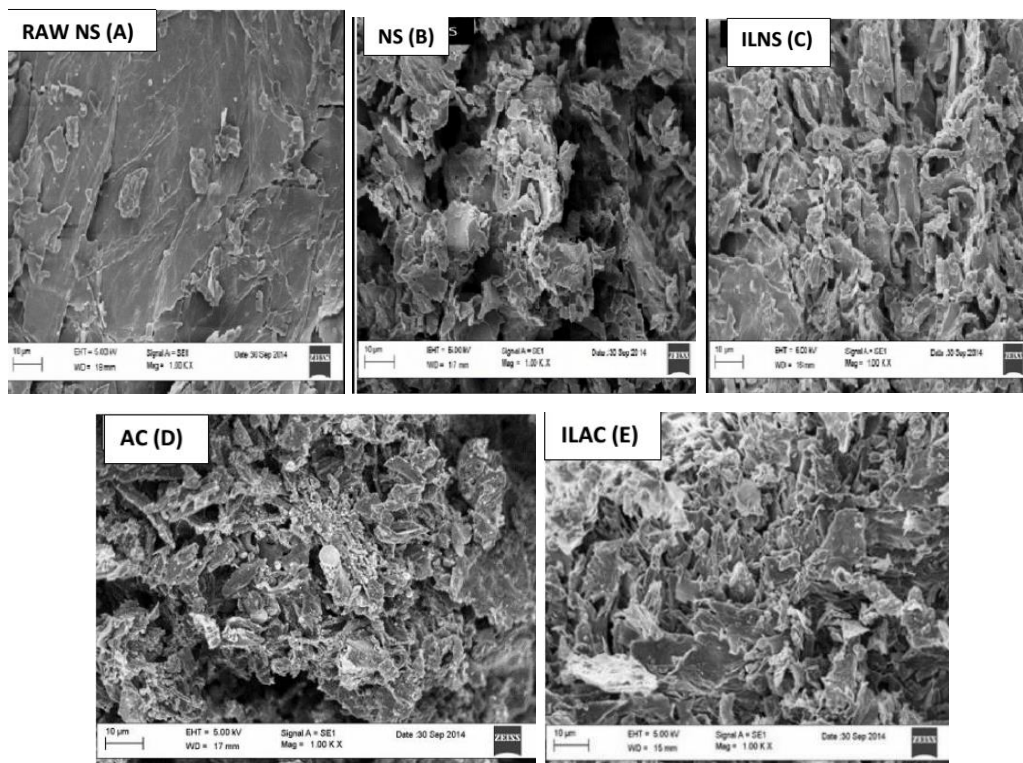
Fig. 7.4 SEM micrographs (1000 x) of raw NS (a), NS (b), ILNS (c), AC (d) and ILAC (e)

The ionic liquid used is similar in structure to ethylenediamine, in that the imidazolium ring also contains a nitrogen atom (with a lone pair of electrons) that can form covalent bonds to the sorbent's surface atoms (Liu et al., 2010). The positively charged quaternary nitrogen present on the imidazolium ring may also be electrostatically attracted to electron rich atoms (such as oxygen) on the sorbent surface, thus physically bonding the ionic liquid to the surface (Singh et al., 2014).

X-ray diffractograms obtained for AC and ILAC (Fig. 7.5) further confirmed that the activated carbon was modified. Essentially the amorphous form of carbon and the diffractogram for AC is characterised by broad peaks, indicative of a non-crystalline structure. The diffractogram for ILAC however exhibits sharper peaks at the same 2Θ values as AC. The sharpness of the peaks is as a result of the ionic liquid which has a more crystalline structure than that of AC. Similar changes in diffraction pattern were also seen for NS and ILNS.
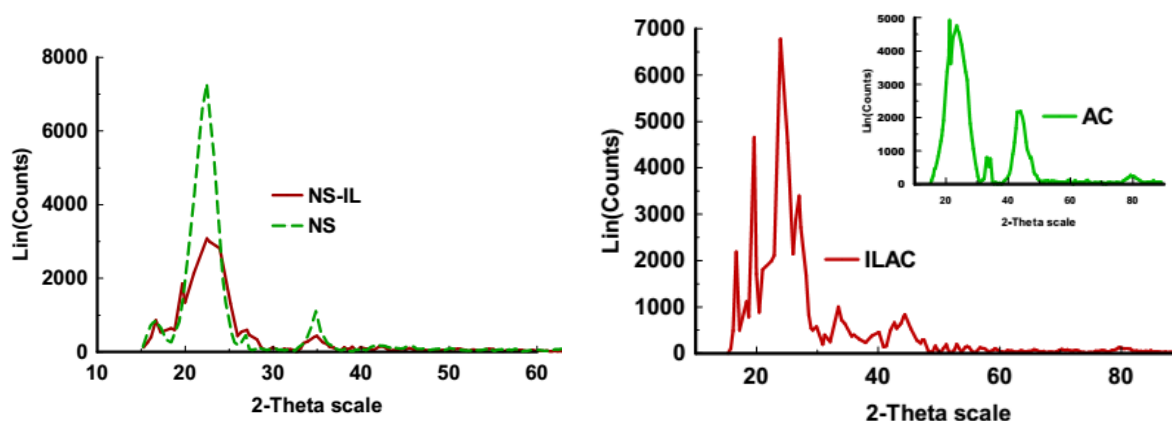
Fig. 7.5 X-ray diffractograms of AC, ILAC, NS and ILNS

It is important to understand the temperature maxima at which this material remains stable, as certain industrial effluent streams are purged at high temperatures. Thermogravimetric analysis (TGA) (Fig 7.6) of the ionic liquid modified materials revealed that up until approximately 200 °C the material remained stable, thereafter the ionic liquid began to degrade and decompose. AC (Fig 7.6a) remained relatively stable throughout the entire heating program and experienced little or no significant mass losses. Assuming that AC can act as a standard against which ILAC can be compared, the significant mass loss experienced by ILAC at approximately 200 °C is most likely to be as a result of the loss of the ionic liquid. ILNS (Fig 7.6b) experienced a significantly greater decrease in mass at approximately 200 °C as a result of the loss of the organic material together with the ionic liquid as compared to NS which experienced a slightly lower mass loss due to the loss of the organic matter alone (Wu et al., 2013).
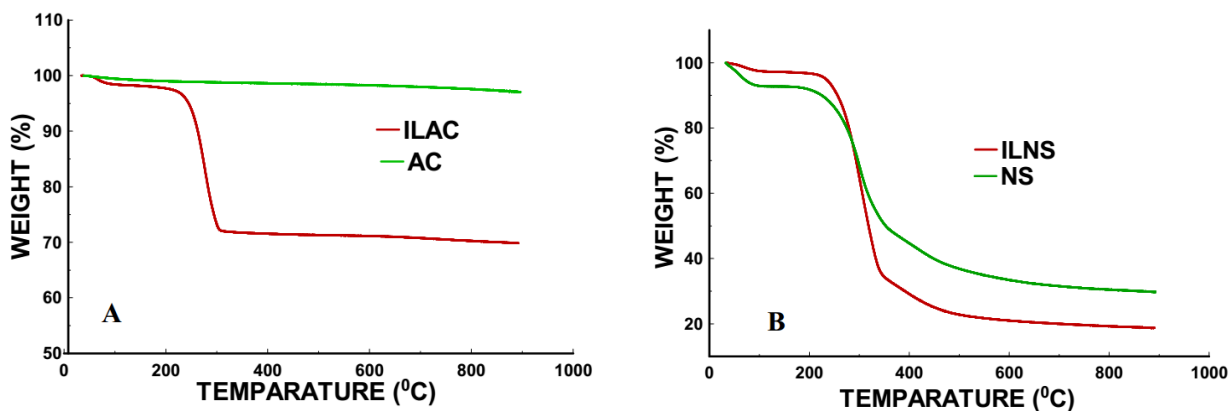
Fig. 7.6 TGA profile of (a) ILAC and AC and (b) ILNS and NS

Surface area and pore volume of the materials were also investigated using BET. NS has a surface area of 3.32 m^2 g^{-1} and pore volume of 0.35 cm^3 g^{-1}, but after modification it reduced to 3.29 m^2 g^{-1} and 0.26 cm^3 g^{-1} respectively. Likewise AC has a surface area of 981 m^2 g^{-1} and pore volume of 0.61 cm^3 g^{-1} and was reduced to 976 m^2 g^{-1} and 0.55 cm^3 g^{-1} respectively. The reduction in surface area and pore volume is as a result of the modification with IL which has filled up the surface and the pores of the materials.

7.4.2 Adsorption Experiments

7.4.2.1 Batch adsorption

Effect of sorbent dosage

The effect of dose of NS, ILNS, AC and ILAC on CR and RB were investigated as shown in Fig 7.7. As the sorbent mass increased, the percentage of dye that was adsorbed also increased. This can be attributed to an increased number of adsorption sites available for the dye molecules to attach onto. However, after a dosage of approximately 0.35 g (for NS) the graph reaches a plateau, above which an increase in sorbent dosage minimally affects the percentage of dye removed. For AC, a maximum adsorption dose of 0.1 g is observed and thereafter a drastic decrease in the percentage of adsorption is seen.
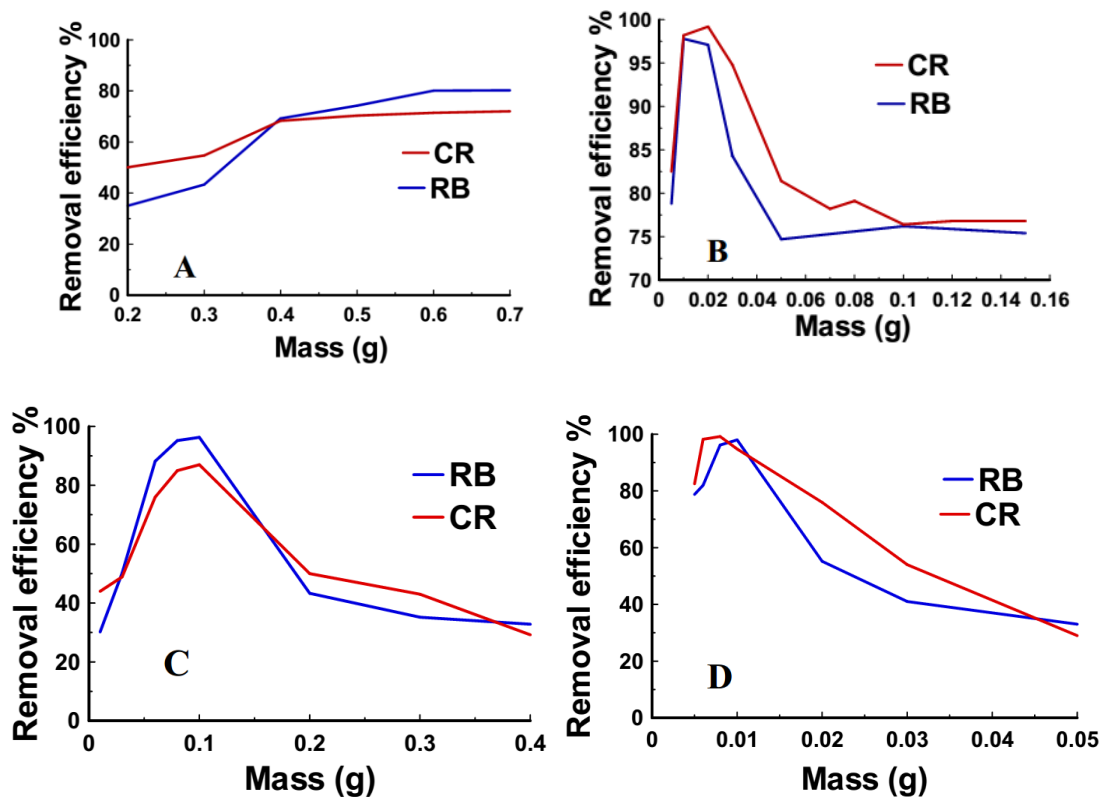
Fig. 7.7 Effect of sorbent dosage on (a) NS and (b) ILNS on the adsorption of CR and RB, (c) AC and (d) ILAC on CR and RB.

The percentage of dye adsorbed reaches its maximum of above 97% at relatively lower sorbent dosages (0.01 g) for ILNS and ILAC. Thereafter increases in sorbent dosage result in a rapid decrease in adsorption ability. This trend was exhibited by both ILNS, AC and ILAC and is most likely due to agglomeration of the adsorbent particles that form large "clumps" and an increase in the inter-particle interactions (Daneshvar et al., 2012). The ionic liquid is hydrophobic and at higher dosages the affinity between the particles treated with the ionic liquid increases resulting in them sticking together (leading to a reduction of total surface area of the materials). The larger clumps have fewer adsorption sites that are able to interact with the dye molecules in the aqueous solution as compared to well dispersed particles of the adsorbent. The formation of a hydrophobic barrier around the large clumps also drastically inhibits the diffusion of sorbate molecules from the bulk solution to the pores of the sorbent.

195

Table 7.1 Maximum adsorption capacities (mg g^{-1}) of NS, ILNS, AC and ILAC

Adsorbents	Adsorption Capacities (mg g^{-1})	
	Congo Red	Reactive Blue
NS	3.55	4.80
ILNS	136.41	290.00
AC	29.27	65.58
ILAC	150.00	364.14

Similar results were reported by other researchers (Daneshvar et al., 2012; Lawal and Moodley, 2015) for the adsorption of dyes onto macroalga and ionic liquid modified montmorillonite.

Table 7.1 summarises the maximum adsorption capacities for each material. The ionic liquid modified materials exhibited far greater adsorption as compared to their unmodified counterparts. These findings clearly show the advantage of modifying sorbent materials with ionic liquids for the adsorption of large molecules. The sorbents derived from activated carbon (i.e. AC and ILAC) had greater capacities as compared to the biosorbents (NS and ILNS). This was due to activated carbon having a greater specific surface area and greater degree of porosity as compared to the native biosorbent material. Table 7.2 summarises the adsorption capacities of a few other sorbent materials from similar dye studies.

Table 7.2 Adsorption capacities of other biosorbents

Material	Dye	q_e (mg g^{-1})	Reference
Tree fern[a]	Basic Red 13	408	(Bhattacharyya and Sharma, 2005)
Coffee residue[a]	Basic Blue 3G	179	(Kyzas et al., 2012)
Banana peel	Methylene Blue	20.8	(Annadurai et al., 2002)
Coconut waste[a]	Methylene Blue	70.92	(Hameed et al., 2008)
Garlic peel	Methylene Blue	82.64	(Hameed and Ahmad, 2009)
Grapefruit peel[a]	Crystal Violet	254.16	(Saeed et al., 2010)

[a] Chemically treated but unmodified

The ionic liquid modified biosorbents (ILNS and ILAC) displayed comparatively high adsorption capacities when juxtaposed against the results obtained from other published works of the same nature. Since ILNS and ILAC displayed the highest adsorption capacities, the subsequent studies on the effect of pH and electrolyte concentration as well as the kinetic experiments were only conducted on them.

Effect of pH

Industrial effluent is often disposed of at varying pH values (Yagub et al., 2014; Salleh et al., 2011; Fu and Viraraghavan, 2002). It is therefore important to evaluate the effect of varying pH on the adsorption efficiency of the material. Studies have shown that pH has the greatest effect on adsorption due to changes in sorbent surface charge and variation in the degree of ionisation of the sorbate molecule that occurs at either high or low pH values (Yagub et al., 2014; Fu and Viraraghavan, 2002). The effect of pH variation is also dependant on the nature of the analyte. The active component of anionic dyes such as RB and CR carry a net negative charge in solution. Fig. 7.8a illustrates the effect of varying pH on the adsorption capability of ILNS. The adsorption of CR onto ILNS appeared to be minimally affected by variations in pH whereas the adsorption of RB followed a normal shaped curve as a function of pH. Namsivayam and Kavitha also found that the adsorption capacity of CR onto coir pith biosorbent varied minimally between the pH extremes (Namasivayam and Kavitha, 2002). The vastly different adsorption characteristics of CR and RB onto ILNS could be attributed to their varying degree of ionisation in solution (RB and CR have pKa's of -1.44 and 4.1 respectively (Salleh et al., 2011).

Congo red is far less ionised in solution than reactive blue and therefore CR molecules are much less charged (i.e. they are more non-polar in nature as compared to RB molecules). For this reason, the attractive force existing between the ionic liquid molecules on the surface of the sorbent and the aqueous CR molecules is far greater than the electrostatic forces of repulsion that exist at high pH due to the accumulation of negative charges on the sorbent surface (Salleh et al., 2011). In comparison, the adsorption of RB molecules is mostly influenced by the attraction generated by the ionic liquid, and therefore changes in pH affect its adsorption (Namasivayam and Kavitha, 2002).

197

RB is more readily ionised and is more polar in nature. For this reason, RB molecules are more sensitive to electrostatic forces as compared to CR (Abdelwahab and Amin, 2013). Additionally, the adsorption of RB appears to be heavily influenced by the effect of increasing the ionic strength of the sorbate solution (Fig. 7.8). Essentially, the adsorption of RB occurs most optimally at approximately neutral pH because at either higher or lower pH values, the bulk solution possesses a higher ionic concentration. Interfering ions may have outcompeted the RB molecules for adsorption sites resulting in the observed trend in adsorption. Abdelwahab and Amin discovered similar trends in the adsorption of phenol from aqueous solution onto *Luffa cylindrica* biosorbent and in the adsorption of divalent mercury onto thiol functionalised magnetic particles respectively (Abdelwahab and Amin, 2013).

The adsorption of the two dyes onto ILAC (Fig. 7.7b) followed a more routine trend that has been widely described by various authors (Yagub et al., 2014; Salleh et al., 2011). The adsorption of the dyes can be assumed to take place initially as a result of electrostatic attraction between the sorbent surface and sorbate molecules. Towards the lower end of the pH scale, the sorbent surface can be assumed to take on a largely positive charge as a result of excess hydronium ions affixing themselves to the sorbent surface and protonating the hydroxyl, carboxyl and amine functional groups present (Yagub et al., 2014; Salleh et al., 2011). There is therefore a greater electrostatic attraction between the sorbent surface and the anionic sorbate molecules which subsequently resulted in adsorption efficiencies close to 100% between pH values of 1 and 6 (for both RB and CR). As the pH of the solution was increased to more basic, the sorbent surface assumed a largely negative charge (Dawood and Sen, 2012).
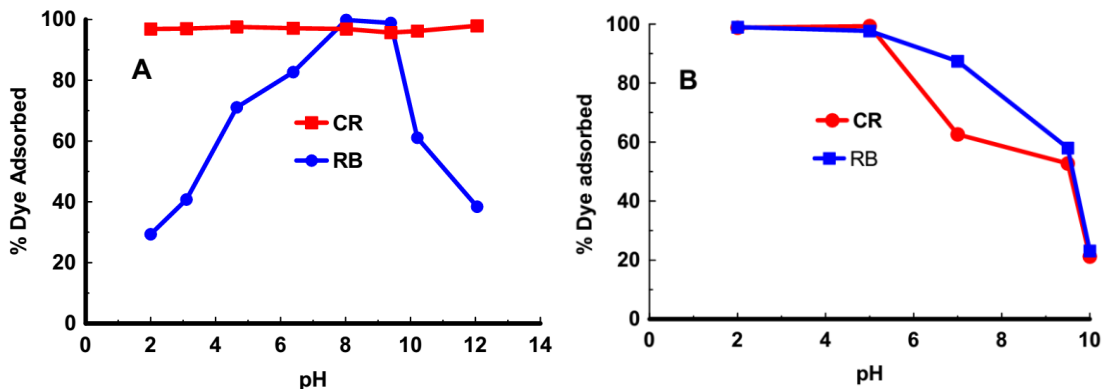
Fig 7.8 Effect of initial solution pH on the adsorption of RB and CR onto (a) ILNS and (b) ILAC

This resulted in electrostatic repulsion between the similarly charged sorbent surface and the negatively charged dye molecules. The influence of the ionic liquid was relatively weaker than the strong electrostatic repulsive forces, resulting in a decrease in adsorption from 100% (pH 2 – 6) to approximately 20% (for both dyes) at a pH of 10.

Effect of electrolyte concentration

It is necessary to evaluate the effect of increasing the electrolyte concentration of the initial sorbate solution on the adsorption of CR and RB as industrial (dye-containing) wastewaters often possess high concentrations of various ions (Netpradit et al., 2004; Qu et al., 2008; Alver and Metin, 2012). It is believed that high ionic concentrations negatively affect adsorption as cations and anions serve to occupy adsorption sites. Fig. 7.9 illustrates the trend observed for both ILNS and ILAC. The decrease in adsorption that occurs at high sodium chloride concentrations maybe attributed to the competition between the chloride ions (Cl$^-$) and negative charges of the anionic dyes for the positively charged sites of the materials (Lu et al., 2014).
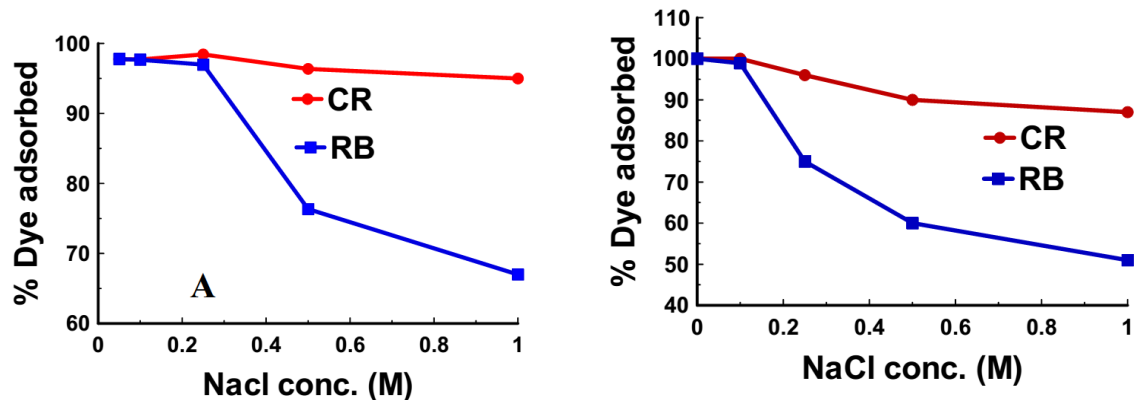
Fig. 7.9 Effect of electrolyte concentration on adsorption of CR and RB onto (a) ILNS and (b) ILAC

Also, since chloride ions are far more mobile in solution than the large CR and RB molecules, chloride ions travel much faster to the sorbent surface (Yagub et al., 2014). This accumulation of chloride ions on the surface of the sorbent results in the surface adopting a negative charge. The negatively charged surface then repels the anionic dye molecules instead of attracting them and thus a decrease in adsorption efficiency is observed. CR behaved in a similar manner to that of the pH experiments. Changes in electrolyte concentration altered the adsorption capacity minimally, however closer inspection of the data revealed that adsorption did in fact decrease (albeit slightly) upon increasing the ionic concentration of the solution. RB proved much more sensitive to increases in ionic concentration as illustrated by the drastic decrease in adsorption efficiency as a function of increasing electrolyte molarity. This is in keeping with RB's sensitivity to changes in pH and operating optimally at approximately neutral pH (Fig. 7.8a).

7.4.2.2 Kinetic experiments

In addition to evaluating the batch adsorption characteristics of the biosorbent material, the kinetic rate of adsorption of the dye molecules were also investigated. Details of the adsorption mechanism were also elucidated from analysing the changes in sorbate concentration as a function of time.

Effect of initial sorbate concentration and contact time

The adsorption capacity increased as a function of increasing dye concentration and contact time as showed in Fig 7.10. This was due to the increased contact time of interactions between dye molecules and the sorbent surface which further increased at higher concentrations thus facilitating adsorption. Additionally, at higher concentrations, the sorbent was able to adsorb more dye before equilibrium was reached and the rates of adsorption and desorption equalised. Adsorption increased rapidly for a short period of time until maximum adsorption capacity was reached.
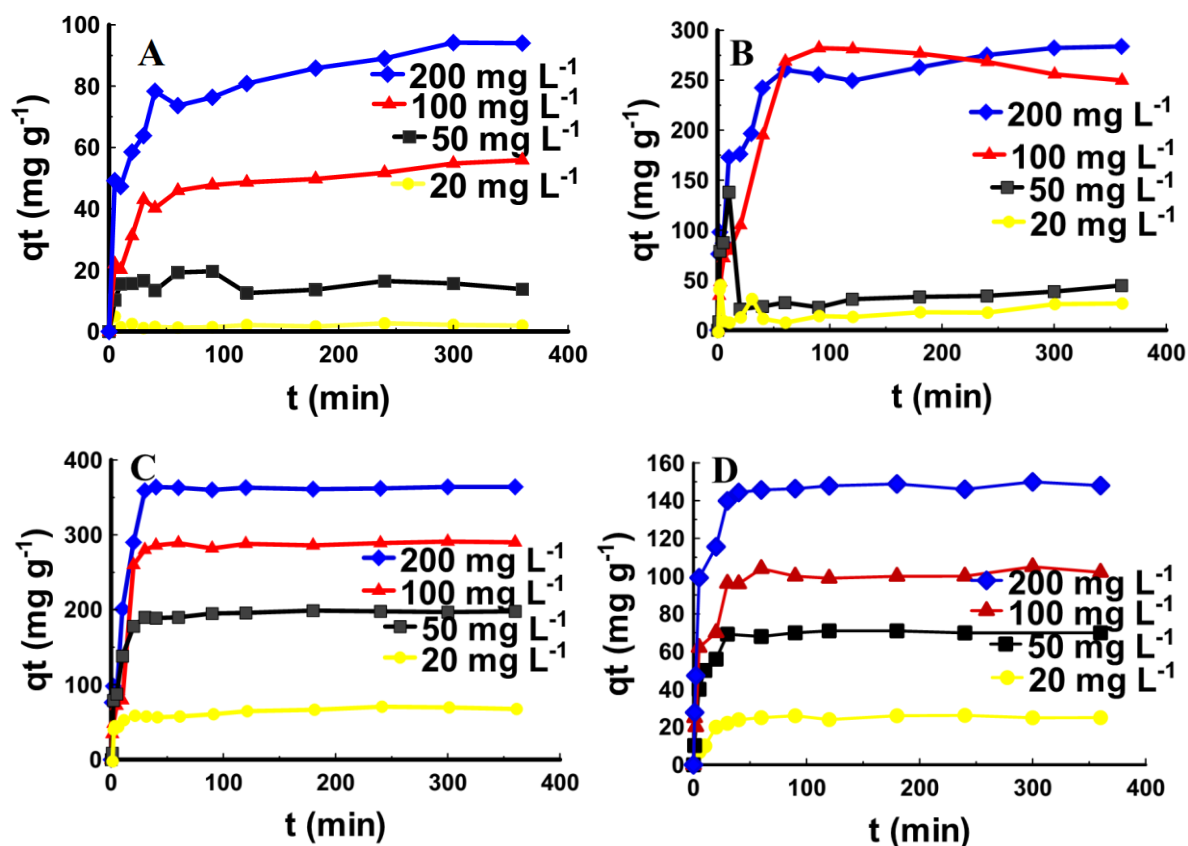
Fig. 7.10 The adsorption capacity (q_t (mg g^{-1}) as a function of time (min) for the adsorption of CR onto ILNS (a), RB onto ILNS (b), RB onto ILAC (c) and CR onto ILAC (d)

Thereafter the curve plateaued and any further increase in exposure time played no significant role in adsorption. The same trends were observed for ILNS and ILAC on both RB and CR as showed in Figs 7.10a to d.

Kinetic modelling

The data obtained were fitted into Lagergren pseudo-first (Appendix F 1.0) and pseudo-second-order models. The data followed the pseudo-second-order model with greater linear correlation than the pseudo-first-order model (for both dyes, onto both ILNS and ILAC).

At lower concentrations the rate of adsorption (k) of CR was faster than at higher concentrations. However, the adsorption capacity (q_e cal) was drastically decreased at lower sorbate concentrations (Table 7.3). According to literature, the adsorption capacity and rate of adsorption are inversely proportional to one another (Yagub et al., 2014; Salleh et al., 2011; Bhattacharyya and Sharma, 2005).

At lower concentrations (20 and 50 mg L^{-1}) equilibrium adsorption capacity was reached within 10 minutes. Whereas at higher concentrations (100 and 200 mg L^{-1}) equilibrium adsorption capacity was reached within 40 minutes. At lower concentrations there were more adsorption sites for the fewer dye molecules thus dye molecules very quickly adsorb onto the material and reached equilibrium. Compared to higher concentrations, there were more dye molecules for the same number of adsorption sites and thus a longer time is required for equilibrium to be reached (Bhattacharyya and Sharma, 2005).

The adsorption capacities calculated from the pseudo-second-order models were very close to the experimental adsorption capacities, and the R^2 values were close to unity. Therefore pseudo-second-order model is said to be the best model for adsorption of both dyes onto both ILNS and ILAC.

Table 7.3 Pseudo-second-order parameters for the adsorption of CR and RB onto ILNS and ILAC

Dyes	Conc.			ILNS Pseudo-second-order				ILAC Pseudo-second-order		
	$(mg\ L^{-1})$	q_e, exp $(mg\ g^{-1})$	q_e, cal $(mg\ g^{-1})$	$k \times 10^{-3}$ $(g\ mg^{-1}\ min^{-1})$	R^2	q_e, exp $(mg\ g^{-1})$	q_e,cal $(mg\ g^{-1})$	$k \times 10^{-3}$ $(g\ mg^{-1}\ min^{-1})$	R^2
Congo Red	200	136.41	181.82	0.44	0.996	150.00	147.69	0.38	0.996
	100		90.09	3.78	0.993		98.58	5.24	0.976
	50		25.66	10.61	0.988		48.74	8.36	0.985
	20		5.85	27.17	0.989		10.00	21.14	0.997
Reactive Blue	200	290.00	285.71	0.37	0.998	364.51	312.50	0.32	0.989
	100		170.27	3.66	0.979		280.47	5.16	0.987
	50		33.55	4.02	0.986		36.25	11.10	0.991
	20		19.35	8.70	0.976		11.48	20.12	0.996

The intra-particle diffusion (IPD) model gives insight into the mechanism of adsorption. The mathematical model, proposed by Weber and Morris (Table 7.3 and Fig. 7.11), describes a linear relationship between the adsorption capacity of a given material and the square root of time. The plot of ILAC on both CR and RB does not pass through the origin (Appendix F 1.1 and F 1.2). This signifies some degree of boundary layer control which showed that the intra-particle diffusion was not the only rate controlling step, but other processes also controlled the rate of adsorption (Liao et al., 2013; Crini et al., 2007).

However, the IPD model of CR and RB onto ILNS at room temperature did not remain linear (as showed in Fig. 7.11a and b) over the entire time range. Instead each of the graphs generated for each concentration could be separated into two linear regions (suggesting a multi-stage adsorption process). Similar results were also obtained by Dawood and Sen (Dawood and Sen, 2012) for the adsorption of CR onto treated pinecone powder. These results are in agreement with the results obtained from the isotherm studies.
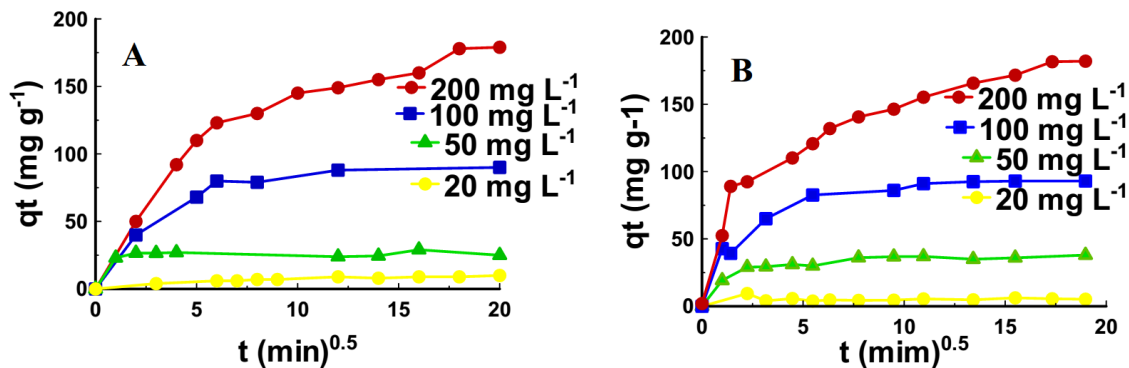
Fig. 7.11 Intra-particle diffusion model for the adsorption of (a) CR and (b) RB onto ILNS at 25 °C

The adsorption initially increased rapidly as a function of time and was most likely as a result of physical interactions (electrostatic and Van der Waals forces of attraction) between the sorbent surface and the sorbate molecules. This rapid diffusion of sorbate to the sorbent surface is regarded as bulk diffusion and is extremely fast. Once at the sorbent surface, the sorbate molecules diffused into the pores of the material. This phenomenon, known as intra-particle diffusion, was characterised by the plateauing of the graphs as time proceeded. Intra-particle diffusion was far slower than bulk diffusion as it is associated with chemical interactions between the adsorbed molecules and the inner surfaces of the sorbent. Bulk diffusion and intra-particle diffusion are associated with the Freundlich and Langmuir isotherms respectively (Dawood and Sen, 2012). The trends observed in Fig. 7.11 compliment the results of the isotherm experiment, which described both chemical and physical adsorption taking place at the same time. Since the IPD curves are continuous, it can be inferred that both modes of mass transport take place simultaneously (Dawood and Sen, 2012). The same trend was observed for RB on ILNS, as shown in Fig. 7.11b.

7.4.2.3 Adsorption isotherms

The data were further fitted into Langmuir, Freundlich and D-R models. The constants corresponding to each of the three isotherms modelled in this experiment are listed in Table 7.4. The adsorption of both dyes onto ILAC followed the Freundlich isotherm with the highest linear correlation, indicating that the adsorption was physical in nature and that a multilayer of dye molecules adsorbed onto the sorbent surface. The values of n for CR and RB adsorbed onto ILAC

204

were 1.21 and 1.58 respectively, indicating that adsorption was favourable. The mean free energies of adsorption calculated from the D – R model were less than 8 (0.048 and 0.060 kJ mol^{-1} for CR and RB respectively) further substantiating that the dyes physisorbed onto ILAC.

Table 7.4 Isotherm parameters for the adsorption of CR and RB onto ILNS and ILAC at 25 ℃

Dyes	Adsorbents	Langmuir model				Freundlich model			Dubinin–Radushkevich model	
		q_m	b	R_L	R^2	K_f	n	R^2	E	R^2
		(mg g^{-1})	(L mg^{-1})			(L mg^{-1})	(g L^{-1})		(kJ mol^{-1})	
CR	ILNS	833.00	0.022	0.490	0.996	1054	1.86	0.983	0.041	0.977
	ILAC	-	-	-	0.012	0.028	1.21	0.998	0.048	0.996
RB	ILNS	53.89	00.018	0.135	0.968	34.90	1.30	0.995	0.012	0.927
	ILAC	-	-	-	0.009	0.012	1.58	0.984	0.060	0.994

Unlike with ILAC where one isotherm clearly predominated over the other; the adsorption of both dyes onto ILNS appeared to follow both the Langmuir and Freundlich isotherms with reasonably good correlation. This trend is not uncommon in native biosorbents and was described by Daneshvar and co-workers in the adsorption of acidic dyes onto *Stoechospermum Marginatum* macroalga (Daneshvar et al., 2012). During the initial stages of adsorption the Freundlich isotherm predominates, and as the dye molecules enter the pores of the sorbent and begin interacting with the internal surfaces, the Langmuir isotherm becomes more prominent. In order to determine the most prominent mode of adsorption, the data was modelled according to the D – R isotherm. The E_D values for CR and RB were both below eight (0.041 and 0.012 kJ mol^{-1} respectively) indicating that physical adsorption is the most notable mode of adsorption. It is thought that the heterogeneous adsorption of the dye molecules is the primary mode of adsorption with chemisorption only taking place after the formation of multiple layers of the adsorbed sorbate (Daneshvar et al., 2012).

The values of n and R_L both indicated that the adsorption of CR and RB onto ILNS was favourable with regard to both physical and chemical adsorption however the Freundlich model is the most applicable isotherm.

7.5 CONCLUSION

Modified peanut shell derived biosorbent (NS) and activated carbon modified with 1-methyl-3-decahexyl imidazolium increased the adsorption capacity of NS and AC from 4.8 to 290 mg g^{-1} and 65.58 to 364.14 mg g^{-1} respectively. This was achieved in spite of a reduction in the surface area (981 to 976 m^2 g^{-1}) and pore volume (0.61 to 0.55 cm^3 g^{-1}) of the activated carbon, suggesting that physical adsorption was not the only and main mechanism of adsorption. ILAC exhibited the highest adsorption capacities (150 and 364.14 mg g^{-1}) for both CR and RB respectively. The adsorption was dependant on pH. The optimum pH range for adsorption of both dyes onto ILAC was 1 – 6. The adsorption of RB onto ILNS was optimum between pH 7 and 9 and adsorption of CR onto ILNS was not affected by changes in pH. Adsorption was also negatively affected by increasing electrolyte concentrations.

The adsorption of RB and CR onto both ILNS and ILAC followed second order kinetics. The rate of adsorption was found to decrease with increasing initial sorbate concentration however the adsorption capacity of the two materials increased with increasing initial dye concentration. The adsorption of both dyes onto ILAC followed the Freundlich isotherm (R^2 values of 0.998 and 0.993 for CR and RB respectively). Physical adsorption was confirmed by the Dubinin – Radushkevich model which yielded mean free adsorption energies (E) of 0.048 and 0.060 kJ mol^{-1} for CR and RB respectively.

The adsorption of both dyes onto ILNS followed both the Langmuir and Freundlich isotherms with good linear correlation. It was determined from the intra-particle diffusion model that two modes of mass transfer (bulk and intra-particle diffusion) co-existed during the adsorption process. Mean free adsorption energy values calculated from the D – R isotherm revealed that physisorption is one of the adsorption mechanisms of both dyes onto ILNS with values of 0.041 and 0.012 kJ mol^{-1} for CR and RB respectively.

7.6 ACKNOWLEDGEMENTS

7.7 REFERENCES

Abdelwahab, O. & Amin, N. K. 2013. Adsorption of phenol from aqueous solutions by Luffa cylindrica fibers: Kinetics, isotherm and thermodynamic studies. *The Egyptian Journal of Aquatic Research,* 39(4)**,** pp 215-223.

Absalan, G., Asadi, M., Kamran, S., Sheikhian, L. & Goltz, D. M. 2011. Removal of reactive red-120 and 4-(2-pyridylazo) resorcinol from aqueous samples by Fe3O4 magnetic nanoparticles using ionic liquid as modifier. *Journal of Hazardous Materials,* 192(2)**,** pp 476-484.

Adak, A., Bandyopadhyay, M. & Pal, A. 2006. Fixed bed column study for the removal of crystal violet (CI Basic Violet 3) dye from aquatic environment by surfactant-modified alumina. *Dyes and Pigments,* 69(3)**,** pp 245-251.

Akar, T. & Divriklioglu, M. 2010. Biosorption applications of modified fungal biomass for decolorization of Reactive Red 2 contaminated solutions: Batch and dynamic flow mode studies. *Bioresource Technology,* 101(19)**,** pp 7271-7277.

Aksu, Z., Ertuğrul, S. & Dönmez, G. 2010. Methylene Blue biosorption by Rhizopus arrhizus: Effect of SDS (sodium dodecylsulfate) surfactant on biosorption properties. *Chemical Engineering Journal,* 158(3)**,** pp 474-481.

Alther, G. 2002. Using organoclays to enhance carbon filtration. *Waste Management,* 22(5)**,** pp 507-513.

Alver, E. & Metin, A. Ü. 2012. Anionic dye removal from aqueous solutions using modified zeolite: Adsorption kinetics and isotherm studies. *Chemical Engineering Journal,* 200–202(1)**,** pp 59-67.

Annadurai, G., Juang, R.-S. & Lee, D.-J. 2002. Use of cellulose-based wastes for adsorption of dyes from aqueous solutions. *Journal of Hazardous Materials,* 92(3)**,** pp 263-274.

Bhattacharyya, K. G. & Sharma, A. 2005. Kinetics and thermodynamics of Methylene Blue adsorption on Neem (Azadirachta indica) leaf powder. *Dyes and Pigments,* 65(1)**,** pp 51-59.

Brandão, P. C., Souza, T. C., Ferreira, C. A., Hori, C. E. & Romanielo, L. L. 2010. Removal of petroleum hydrocarbons from aqueous solution using sugarcane bagasse as adsorbent. *Journal of Hazardous Materials,* 175(1–3)**,** pp 1106-1112.

Choi, H.-D., Shin, M.-C., Kim, D.-H., Jeon, C.-S. & Baek, K. 2008. Removal characteristics of reactive black 5 using surfactant-modified activated carbon. *Desalination,* 223(1–3)**,** pp 290-298.

Cota-Espericueta, A. D. 2003. *Removal of 2, 4-dinitrophenol and 2, 4-dinitrotoluene from Water Using Surfactant Modified Activated Carbon.* New Mexico State University.

Crini, G., Peindy, H. N., Gimbert, F. & Robert, C. 2007. Removal of CI Basic Green 4 (Malachite Green) from aqueous solutions by adsorption using cyclodextrin-based adsorbent: kinetic and equilibrium studies. *Separation and Purification Technology,* 53(1)**,** pp 97-110.

Daneshvar, E., Kousha, M., Sohrabi, M. S., Khataee, A. & Converti, A. 2012. Biosorption of three acid dyes by the brown macroalga Stoechospermum marginatum: Isotherm, kinetic and thermodynamic studies. *Chemical Engineering Journal,* 195(1)**,** pp 297-306.

Dawood, S. & Sen, T. K. 2012. Removal of anionic dye Congo red from aqueous solution by raw pine and acid-treated pine cone powder as adsorbent: Equilibrium, thermodynamic, kinetics, mechanism and process design. *Water Research,* 46(6)**,** pp 1933-1946.

Deng, S. & Ting, Y.-P. 2005. Characterization of PEI-modified biomass and biosorption of Cu(II), Pb(II) and Ni(II). *Water Research,* 39(10)**,** pp 2167-2177.

Dubinin, M. & Radushkevich, L. 1947. Equation of the characteristic curve of activated charcoal. *Chemisches Zentralblatt,* 1(1)**,** pp 875.

Feng, N., Guo, X., Liang, S., Zhu, Y. & Liu, J. 2011. Biosorption of heavy metals from aqueous solutions by chemically modified orange peel. *Journal of Hazardous Materials,* 185(1)**,** pp 49-54.

Foo, L. P. Y., Tee, C. Z., Raimy, N. R., Hassell, D. G. & Lee, L. Y. 2012. Potential Malaysia agricultural waste materials for the biosorption of cadmium(II) from aqueous solution. *Clean Technologies and Environmental Policy,* 14(2)**,** pp 273-280.

Freundlich, H. 1906. Über die Adsorption in Lösungen. *Zeitschrift fur Physikalische Chemie,* 57(A)**,** pp 385-470.

Fu, Y. & Viraraghavan, T. 2002. Removal of Congo Red from an aqueous solution by fungus Aspergillus niger. *Advances in Environmental Research,* 7(1)**,** pp 239-247.

Girgis, B. S., Yunis, S. S. & Soliman, A. M. 2002. Characteristics of activated carbon from peanut hulls in relation to conditions of preparation. *Materials Letters,* 57(1)**,** pp 164-172.

Gupta, V. K., Agarwal, S., Singh, P. & Pathania, D. 2013. Acrylic acid grafted cellulosic Luffa cylindrical fiber for the removal of dye and metal ions. *Carbohydrate Polymers,* 98(1)**,** pp 1214-1221.

Hameed, B. H. & Ahmad, A. A. 2009. Batch adsorption of methylene blue from aqueous solution by garlic peel, an agricultural waste biomass. *Journal of Hazardous Materials,* 164(2–3)**,** pp 870-875.

Hameed, B. H., Mahmoud, D. K. & Ahmad, A. L. 2008. Equilibrium modeling and kinetic studies on the adsorption of basic dye by a low-cost adsorbent: Coconut (Cocos nucifera) bunch waste. *Journal of Hazardous Materials,* 158(1)**,** pp 65-72.

Ho, Y.-S. & McKay, G. 1999. Pseudo-second order model for sorption processes. *Process Biochemistry,* 34(5)**,** pp 451-465.

Kamran, S., Asadi, M. & Absalan, G. 2014a. Adsorption of folic acid, riboflavin, and ascorbic acid from aqueous samples by Fe3O4 magnetic nanoparticles using ionic liquid as modifier. *Analytical Methods,* 6(3)**,** pp 798-806.

Kamran, S., Hossein Tavallali & Azad, A. 2014b. Fast Removal of Reactive Red 141 and Reactive Yellow 81 From Aqueous Solution by Fe3O4 Magnetic Nanoparticles Modified With Ionic Liquid 1-Octyl-3-methylimidazolium Bromide. *Iranian Journal of Analytical Chemistry,* 1(1)**,** pp 78-86.

Kyzas, G. Z., Lazaridis, N. K. & Mitropoulos, A. C. 2012. Removal of dyes from aqueous solutions with untreated coffee residues as potential low-cost adsorbents: Equilibrium, reuse and thermodynamic approach. *Chemical Engineering Journal,* 189–190(1)**,** pp 148-159.

Lagergren, S. 1898. About the theory of so-called adsorption of soluble substances. *Kungliga Svenska Vetenskapsakademiens Handlingar,* 24(4)**,** pp 1-39.

Langmuir, I. 1916. The Constitutionand Fundamental Properties of Solid and Liquids. Part I. Solids. *Journal of the American Chemical Society,* 38(11)**,** pp 2221-2295.

Lawal, I. A. & Moodley, B. 2015. Synthesis, characterisation and application of imidazolium based ionic liquid modified montmorillonite sorbents for the removal of amaranth dye. *RSC Advances,* 5(76)**,** pp 61913-61924.

Li, Y., Chen, B. & Zhu, L. 2010. Enhanced sorption of polycyclic aromatic hydrocarbons from aqueous solution by modified pine bark. *Bioresource Technology,* 101(19)**,** pp 7307-7313.

Liao, P., Zhan, Z., Dai, J., Wu, X., Zhang, W., Wang, K. & Yuan, S. 2013. Adsorption of tetracycline and chloramphenicol in aqueous solutions by bamboo charcoal: A batch and fixed-bed column study. *Chemical Engineering Journal,* 228(1)**,** pp 496–505.

Liu, Y., Sun, X. & Li, B. 2010. Adsorption of Hg^{2+} and Cd^{2+} by ethylenediamine modified peanut shells. *Carbohydrate Polymers,* 81(2)**,** pp 335-339.

Lu, L., Gao, M., Gu, Z., Yang, S. & Liu, Y. 2014. A comparative study and evaluation of sulfamethoxazole adsorption onto organo-montmorillonites. *Journal of Environmental Sciences,* 26(12)**,** pp 2535-2545.

Mandavi, R., Sar, S. K. & Rathore, N. 2008. Critical micelle concentration of surfactant, mixed–surfactant and polymer by different method at room temperature and its importance. *Oriental Journal of Chemistry,* 24(2)**,** pp 559-564.

Montazer-Rahmati, M. M., Rabbani, P., Abdolali, A. & Keshtkar, A. R. 2011. Kinetics and equilibrium studies on biosorption of cadmium, lead, and nickel ions from aqueous solutions by intact and chemically modified brown algae. *Journal of Hazardous Materials,* 185(1)**,** pp 401-407.

Namasivayam, C. & Kavitha, D. 2002. Removal of Congo Red from water by adsorption onto activated carbon prepared from coir pith, an agricultural solid waste. *Dyes and Pigments,* 54(1)**,** pp 47-58.

Netpradit, S., Thiravetyan, P. & Towprayoon, S. 2004. Adsorption of three azo reactive dyes by metal hydroxide sludge: effect of temperature, pH, and electrolytes. *Journal of Colloid and Interface Science,* 270(2)**,** pp 255-261.

Olu-Owolabi, B. I., Diagboya, P. N. & Ebaddan, W. C. 2012. Mechanism of Pb^{2+} removal from aqueous solution using a nonliving moss biomass. *Chemical Engineering Journal,* 195–196(1)**,** pp 270-275.

Periasamy, K. & Namasivayam, C. 1994. Process Development for Removal and Recovery of Cadmium from Wastewater by a Low-Cost Adsorbent: Adsorption Rates and Equilibrium Studies. *Industrial & Engineering Chemistry Research,* 33(2)**,** pp 317-320.

Periasamy, K. & Namasivayam, C. 1995. Adsorption of Pb(II) by Peanut Hull Carbon from Aqueous Solution. *Separation Science and Technology,* 30(10)**,** pp 2223-2237.

Qu, B., Zhou, J., Xiang, X., Zheng, C., Zhao, H. & Zhou, X. 2008. Adsorption behavior of Azo Dye C. I. Acid Red 14 in aqueous solution on surface soils. *Journal of Environmental Sciences,* 20(6)**,** pp 704-709.

Saeed, A., Sharif, M. & Iqbal, M. 2010. Application potential of grapefruit peel as dye sorbent: Kinetics, equilibrium and mechanism of crystal violet adsorption. *Journal of Hazardous Materials,* 179(1–3)**,** pp 564-572.

Salleh, M. A. M., Mahmoud, D. K., Karim, W. A. W. A. & Idris, A. 2011. Cationic and anionic dye adsorption by agricultural solid wastes: A comprehensive review. *Desalination,* 280(1–3)**,** pp 1-13.

Singh, M. P., Singh, R. K. & Chandra, S. 2014. Ionic liquids confined in porous matrices: Physicochemical properties and applications. *Progress in Materials Science,* 64(1)**,** pp 73-120.

Slimani, R., El Ouahabi, I., Abidi, F., El Haddad, M., Regti, A., Laamari, M. R., Antri, S. E. & Lazar, S. 2014. Calcined eggshells as a new biosorbent to remove basic dye from aqueous solutions: Thermodynamics, kinetics, isotherms and error analysis. *Journal of the Taiwan Institute of Chemical Engineers,* 45(4)**,** pp 1578-1587.

Weber, W. J. & Morris, J. C. 1963. Kinetics of adsorption on carbon from solution. *Journal of the Sanitary Engineering Division. ASCE,,* 89(1)**,** pp 31.

Wilson, K., Yang, H., Seo, C. W. & Marshall, W. E. 2006. Select metal adsorption by activated carbon made from peanut shells. *Bioresource Technology,* 97(18)**,** pp 2266-2270.

Wu, M., Guo, Q. & Fu, G. 2013. Preparation and characteristics of medicinal activated carbon powders by CO2 activation of peanut shells. *Powder Technology,* 247(0)**,** pp 188-196.

Yagub, M. T., Sen, T. K., Afroze, S. & Ang, H. M. 2014. Dye and its removal from aqueous solution by adsorption: A review. *Advances in Colloid and Interface Science,* 209(1)**,** pp 172-184.

Zhang, Y., Shen, Y., Yuan, J., Han, D., Wang, Z., Zhang, Q. & Niu, L. 2006. Design and Synthesis of Multifunctional Materi Based on an Ionic-Liquid Backbone. *Angewandte Chemie International Edition,* 45(35)**,** pp 5867 –5870.

Zheng, D., Dong, L., Huang, W., Wu, X. & Nie, N. 2014. A review of imidazolium ionic liquids research and development towards working pair of absorption cycle. *Renewable and Sustainable Energy Reviews,* 37(1)**,** pp 47-68.

Zhou, Q., Frost, R. L., He, H., Xi, Y. & Liu, H. 2007. Adsorbed para-nitrophenol on HDTMAB organoclay—A TEM and infrared spectroscopic study. *Journal of Colloid and Interface Science,* 307(2)**,** pp 357-363.

CHAPTER 8: SORPTION OF PERSONAL CARE PRODUCTS FROM AQUEOUS MEDIUM ON RAW *KIGELIA PINNATA* AND *KIGELIA PINNATA* MODIFIED WITH IONIC LIQUID

Isiaka A. Lawal[a] and Brenda Moodley[a]*

[a]School of Chemistry and Physics, College of Agriculture, Engineering and Science, University of KwaZulu-Natal, P/Bag X45001, Westville Campus, Durban, 4000, South Africa

*corresponding author email: moodleyb3@ukzn.ac.za

Tel: +27 31 2602796; Fax: +27 31 2603091

First author: lawalishaq000123@yahoo.com

8.1 ABSTRACT

The sorption of pharmaceuticals on biomass and biomass modified with an ionic liquid (IL) was investigated. *Kigelia pinnata* (KP) was modified with an ionic liquid to form the modified biomass (KP-IL). Elemental analysis quantified the amount of carbon, hydrogen, nitrogen and sulfur in the biomass. Modified *kigelia pinnata* (KP–IL) and KP were characterised using fourier transform infrared (FT-IR) spectroscopy, scanning electron microscopy (SEM), x-ray diffraction (XRD) and Brunauer−Emmett−Teller (BET), and thereafter they were used in the sorption study of pharmaceuticals. The pharmaceuticals investigated were ibuprofen (IBU), ketoprofen (KET), ampicillin (AMP) and diclofenac (DCL). The effects of sorbent dosage, pharmaceutical concentration, solution pH and contact time were investigated in order to determine optimal experimental conditions. Optimum adsorption was achieved at pH 2.5 for AMP and pH 5 for IBU, KET and DCL. Sorption data for all the pharmaceuticals were best described by the pseudo-second-order kinetics and the Langmuir adsorption isotherm. Maximum sorption capacities of 251.2, 197.1, 276.8 and 73 mg g^{-1} were obtained for KET, DCL, IBU and AMP respectively, which were higher than for unmodified KP and that previously reported in literature.

8.2 INTRODUCTION

Pharmaceuticals and personal care products are used on a daily basis and total overall use has been on an upward trend. Some of these pharmaceutical compounds used by humans and animals (both prescription and non-prescription) have been identified as evolving or emerging pollutants due to their undesirable effects even at low concentrations (Fent et al., 2006). Despite low environmental concentrations of pharmaceuticals, continuous introduction of these compounds into the environment may lead to long-term hazards to all living beings. Therefore, it is important to evaluate the risks, monitor, as well as remove these emerging pollutants from the environment. Although evidence of severe toxicity of these contaminants has not been fully documented, the continuous introduction of these drugs in the water cycle can lead to bioaccumulation over time which could have protracted effects (Fent et al., 2006; Boyd and Furlong, 2002). Studies have shown that these contaminants are capable of causing physiological responses in animals and humans. Pharmaceuticals in the environment have been linked to acute and chronic toxicity impacts on aquatic photosynthetic organisms, disruption of indigenous microbial populations, and dissemination into antibiotic-resistant genes in microorganisms (Li et al., 2011; Sun et al., 2010). Pharmaceuticals are expected to be stable against biodegradation and retain their chemical structure over long periods of time necessary to perform their targeted or intended therapeutic action, but this characteristic makes them equally persistent in the environment (Chatzitakis et al., 2008; Méndez-Arriaga et al., 2008).

Currently, there is a lack of regular monitoring of pharmaceuticals due to them still emerging as pollutants as well as a non-legislation of limits of concentrations of these compounds in the environment. The current global shortage of water has also resulted in much research being conducted on recycling of water. The presence of pharmaceuticals, in water that needs to be recycled, may lead to challenges, where increasing concentrations in recycled potable water may lead to increased chronic exposure (Stackelberg et al., 2004). Also, the existing methods of removing pollutants from wastewater treatment plants have proven to be ineffective in the removal of pharmaceuticals (Tambosi et al., 2010; Ternes, 1998; Stumpf et al., 1999). This has necessitated

216

the development of alternate methods for the removal of pharmaceuticals from water bodies. Researchers have developed and reported different methods for the removal of these pollutants, amongst them are coagulation/flocculation (Snyder et al., 2008), conventional activated sludge, membrane bioreactors (Dordio et al., 2009; Mestre et al., 2009; Snyder et al., 2007) and reverse osmosis (Quintanilla, 2010; Kim et al., 2007). Other methods also used include ozonation and advanced oxidation processes (AOPs) (Klavarioti et al., 2009; Chatzitakis et al., 2008; Méndez-Arriaga et al., 2008), nanofiltration (NF) (Quintanilla, 2010; Kim et al., 2007), disinfection (Rodriguez-Fuentes et al., 2005), natural polishing treatment by constructed wetlands and adsorption onto activated carbon (Mestre et al., 2009; Kim et al., 2007; Almendra, 2011).

These treatments have already been successfully applied for the removal of pharmaceuticals, but due to high costs associated with them, they have not been implemented (Dordio et al., 2009). Adsorption onto activated carbon (AC) is another potential method for removing pharmaceuticals from aqueous solutions (Mestre et al., 2007; Mestre et al., 2009), but it is equally expensive. Therefore, it is important to develop a less expensive means of removing pharmaceuticals from water bodies.

Biomasses are currently used for biosorption of both organic and inorganic pollutants, because of their potential reduced cost as well as their effectiveness (Daneshvar et al., 2012; Vijayaraghavan and Yun, 2008). Bacteria, fungi, algae, and byproducts of food and beverages, are all examples of biomass that may be viable alternatives for the development of inexpensive adsorption processes (Reddad et al., 2002; Yun et al., 2001). However, low sorption capacity has been the limitation of native biomass due their poor mechanical strength (Pagnanelli et al., 2000; Skowronski et al., 2001).

To improve the sorption capacity of these biomasses, researchers have modified their surfaces with surfactants. Surfactants, also known to activate surfaces, are not naturally occurring but are manufactured by chemical reactions (Aksu et al., 2010). Surfactants have both hydrophilic and hydrophobic parts all in one molecule and may be classified into four groups depending on the charge of the hydrophilic part: non-ionic (0), anionic (−), cationic (+) and zwitterionic (±) (Aksu et al., 2010).

Researchers have reported an increase in sorption capacity after modification of biomass with different types of surfactants for the adsorption of both organic and inorganic pollutants. Akar and Divriklioglu reported an increase in sorption capacity after modification of *Agaricus bisporus* with cetyl trimethyl ammonium bromide (CTAB) (Akar and Divriklioglu, 2010). In addition, many researchers have reported various biomass modifications by different surfactants, both for the adsorption of organic and inorganic pollutants (Bingol et al., 2009; Loukidou et al., 2003; Xi and Chen, 2014; Montazer-Rahmati et al., 2011; Li et al., 2010; Feng et al., 2011; Brandão et al., 2010; Ansari et al., 2012; Zhou et al., 2011; Ibrahim et al., 2010; Ibrahim et al., 2012; Zhou et al., 2012b; Zhou et al., 2012a; Akar et al., 2015; Aksu et al., 2010; Deng and Ting, 2005).

Ionic liquid has recently been considered as an alternative surfactant for modification of materials for the purpose of adsorption of pollutants from aqueous solutions (Kamran et al., 2014b; Absalan et al., 2011; Kamran et al., 2014a; Lawal and Moodley, 2015).

Biosorption of metals, dyes and some poly aromatic hydrocarbons have been extensively reported, however studies on biosorption of pharmaceuticals have been limited in literature. To the best of the authors' knowledge, no work has been reported on the adsorption of pharmaceuticals on biomass modified with IL and specifically the modification of *kigelia pinnata*. Therefore, the aim of this work was to study the kinetics and equilibrium adsorption of four different pharmaceuticals, ketoprofen (KET), diclofenac (DCL), ibuprofen (IBU) and ampicillin (AMP) on an ionic liquid modified biomass (KP-IL). These four pharmaceuticals (KET, IBU, AMP, and DCL) are commonly used analgesics, antipyretics and antibiotics and previous studies have reported their presence in wastewater effluents and surface waters (Andreozzi et al., 2005; Wang et al., 2010; Grundwasser et al., 1998; Tixier et al., 2003; Kolpin et al., 2002). *Kigelia pinnata* has been used for various purposes, including production of ornamental and roadside planting. It also has traditional use in the healing of various diseases such as fungal infections, boils, syphilis and leprosy (Thomas and Puthur, 2004). The biomass of *kigelia pinnata* is left as a waste after the extraction of the active and useful ingredient which was the reason it was selected for this research.

8.3 EXPERIMENTAL TECHNIQUES

8.3.1 Materials

Ketoprofen (CAS no 22071-15-4), diclofenac sodium salt (CAS number 15307-79-6), ibuprofen (CAS number 15687-27-1) and ampicillin (CAS number 69-53-4) were purchased from Aldrich. 1-methyl, 3-decahexyl imidazolium was synthesized in our laboratory and the synthesis and characterization has been reported in chapter 4. Double distilled deionized water was used throughout the study.
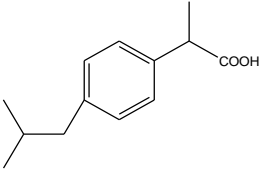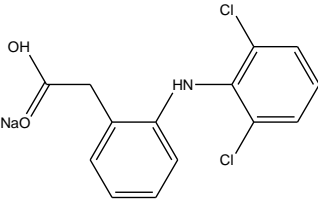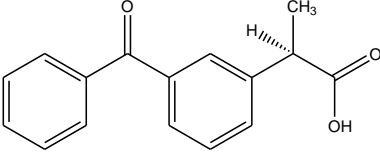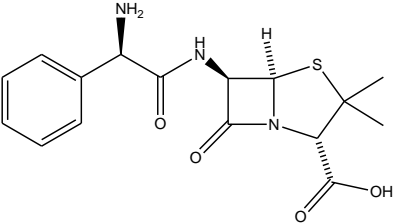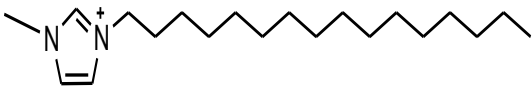
8.3.2 Preparation of Plant Samples

Mature sausage fruit (*kigelia pinnata*), KP, collected from a number of sausage trees in the Durban, KwaZulu-Natal area, were washed with distilled water to remove impurities and thereafter dried in the oven at 70 °C till dry. The dried KP was ground, sieved through a 53 μm seive and labeled KP. Modification with ionic liquid (IL) was achieved by the following procedure (Ibrahim et al., 2010). Briefly, KP (5 g) was soaked in 200 mL of 1-methyl, 3-decahexyl imidazolium (0.25 mmol L^{-1}) in methanol solution. The suspension was placed on an orbital shaker for 24 h at room temperature (25 °C). The modified KP was separated from the aqueous solution by vacuum filtration, and thereafter washed several times with distilled water to remove any IL retained on the surface. It was oven dried at 70 °C overnight and labelled as KP-IL.

8.3.3 Characterization of KP and KP-IL

Thermal gravimetric analysis and differential thermal analysis (TGA-DTA/DSC) (SDT Q 600 V 20.9 Build 20 instrument) was used to measure changes in chemical and physical properties of the material. This was measured as a function of increasing temperature, from ambient to 1000 °C (with a constant heating rate of 5 °C min^{-1}) under nitrogen atmosphere with a flow rate of 50 mL min^{-1}. BET Tri-star II 3020.VI.03 was used to determine the surface area, pore-size, pore volume and pore size distribution. The material was degassed (Micromeritics vacprep 061, sample degas system) at 90 °C for 1 h and then increased to 200 °C for 12 h. The sample was then analyzed by Tri-star II 3020.VI.03 under a nitrogen atmosphere at 77 K. The surface morphology of the material was examined by scanning electron microscopy (SEM) using the Leo 435 VP model.

Table 8.1 Propperties of pharmaceuticals and surfactant used in the study

Compound	Formula	Structure	Molecular Weight (M.W.) g mol⁻¹
Ibuprofen	$C_{13}H_{18}O_2$		206.28
Diclofenac sodium salt	$C_{14}H_{11}Cl_2NNaO_2$		318.13
Ketoprofen	$C_{16}H_{14}O_3$		254.28
Ampicillin	$C_{16}H_{19}N_3O_4S$		349.40
1- methyl, 3-decahexyl imidazolium	$C_{20}H_{39}N_2{}^+$		307.54

The pore size distribution was obtained using the Barrett-Joyner-Halenda (BJH) method. Microstructure and surface morphology of KP and KP-IL samples were characterized by a JEOL 6400 field emission scanning electron microscope (SEM) with an accelerating voltage of 15.0 kV at various magnifications. The samples were coated in a JEOL JFC-1300 Auto Fine Coater fitted with a Pt target before the analysis. Fourier transform infrared (FT-IR) spectra of KP and KP-IL were obtained on a PerkinElmer Spectrum 100 spectrophotometer using an attenuated total reflectance (ATR) technique. The spectrum was scanned at 650–4000 cm⁻¹. The Carlo Erba 1100

CHNS elemental analyzer was used to quantify the amount of C, H, N O and S present in the plant sample.

8.3.4 Sorption Isotherms and Kinetic Studies

Known amounts of each biosorbent were placed in a series of 500 mL Erlenmeyer flasks filled with 200 mL of the pharmaceutical solution. The pharmaceutical concentrations were in the range of 10 to 200 mg L^{-1}. All experiments were carried out at 25 °C. The solutions were placed on a shaker for 24 h to allow for equilibrium to be reached. For kinetics studies, samples were taken at pre-determined time intervals from the solutions. The biosorbent was separated from the samples by centrifugation and the supernatant was then analyzed for residual concentration of pharmaceuticals. The initial and the equilibrium concentrations of the four pharmaceuticals were analyzed using an Agilent HPLC (1200 SL) equipped with a UV detector. The method parameters for analysis of the four pharmaceuticals are shown in Table 8.2. In addition, sorption experiments were carried out to determine the effect of pH (in the pH range of 2-11) and contact time. Each experiment was carried out in duplicate and the average results are presented in this work.

The equilibrium adsorption capacities of KP and KP-IL were calculated from the following relationship:

$$q_e = \frac{C_o - C_e}{W}V...8.1$$

Where q$_e$ is the equilibrium adsorption capacity in (mg g^{-1}), C$_o$ and C$_e$ are the dye concentrations at initial and at equilibrium respectively, in mg L^{-1}, V is the volume of solution in (L), and W is the weight of adsorbent in (g).

Adsorption data were fitted to Freundlich (Freundlich, 1906), Langmuir (Langmuir, 1916), Temkin and Dubinin–Raduskevich (Dubinin and Radushkevich, 1947) isotherms. Linear equations of all the applied models are:

$$\text{Langmuir model: } \frac{C_e}{q_e} = \frac{C_e}{q_m} + \frac{1}{q_m b}...8.2$$

$$\text{Freundlich model: } \ln q_e = \ln K_f + \frac{1}{n} \ln C_e...8.3$$

221

$$\text{Temkin model: } q_e = B \text{In} A + B \text{In} C_e...8.4$$

$$\text{Dubinin–Raduskevich model: } \text{In} q_e = \text{In} q_m - \beta \Sigma^2 ...8.5$$

$$\Sigma = RT \, In \left[1 + \frac{1}{C_e}\right]...8.6$$

$$E = \frac{1}{\sqrt{2\beta}}...8.7$$

Table 8.2 HPLC-UV method parameters for IBU, KET, DCL and AMP

Parameters	Ibuprofen	Ketoprofen	Diclofenac	Ampicillin
Column type		Agilent C18,4.6 x 150 mm, 5 µm		
Injection volume (µL)	10.00	10.00	10.00	10.00
Elution solvent system (Volume in %)	Methanol: acetonitrile:water (85:15:5)	Aq. acetic:acetonitrile (57:43)	Acetonitrile:water (40:60)	
Wavelength (nm)	230	260	277	230
Flow rate (mL min^{-1})	1.00	1.00	1.00	1.00
Retention time (min)	4.50	8.36	3.10	3.04

Where C_e is the equilibrium dye concentration in the solution in mg L^{-1}, b is the Langmuir adsorption constant (L mg^{-1}), and q_m is the theoretical maximum adsorption capacity (mg g^{-1}). K_f (L mg^{-1}) and n are Freundlich isotherm constants indicating the capacity and intensity of the adsorption, respectively. A is the equilibrium binding constant (L mg^{-1}) and B is the heat of adsorption. β is the Dubinin–Raduskevich model constant (mol^2 kJ^{-2}) related to the mean free energy of adsorption per mole of the adsorbate and Σ is the polanyi potential. E is the mean free energy of adsorption (kJ mol^{-1}).

In order to determine the mechanism and potential rate-controlling steps involved in the process of adsorption, pseudo first order (Lagergren, 1898), pseudo second order (Ho and McKay, 1999), and intra-particle diffusion models were used. The pseudo first order kinetic model equation is:

$$\text{In } (q_e\text{-}q_t) = \ln q_e - k_1 t ...8.8$$

Where q_t is the amount of adsorption at time t in (mg g^{-1}), k_1 is the rate constant of the equation in (min^{-1}), and q_e is the amount of adsorption equilibrium in (mg g^{-1}). The adsorption rate constant (k_1) can be determined experimentally by plotting ln (q_e-q_t) *versus* t.

The pseudo second order kinetic model is expressed as:

$$\frac{t}{q_t} = \frac{1}{k_2 q_e^2} + \frac{t}{q_e} ...8.9$$

Where k_2 is the equilibrium rate constant of pseudo second order adsorption in (g mg^{-1} min^{-1}). The values of k_2 and q_e can be determined from the slope and intercept of the plot t/q_t *versus* t, respectively.

The data was also fitted into the Weber–Morris model, to evaluate the possibility of intra-particle diffusion as the rate limiting step; it is given by (Weber and Morris, 1963):

$$q_t = k_{id} t^{1/2} ...8.10$$

Where k_{id} (mg g^{-1} h$^{-1/2}$) is the intra-particle diffusion rate constant.

8.4 RESULTS AND DISCUSSION

8.4.1 Characterization of KP and KP-IL

The ionic liquid (1-methyl, 3-decahexyl imidazolium) used in this study was synthesized and its characterization has been reported in chapter 4. Elemental analysis of KP showed that carbon was the major element (40.3 %) followed by oxygen (33.7 %), hydrogen (5.8 %) and nitrogen (0.9 %).

FT-IR analyses were carried out on KP and KP-IL and the presence of peaks (Fig. 8.1) in the region of 3349 cm^{-1} were assigned to –OH and -NH groups. The band at 1630 cm^{-1} represents the bending modes of the –OH of water within the raw plant. Intense peaks at 2915 and 2850 cm^{-1} on KP-IL were assigned to symmetric and asymmetric stretching vibrations of the methylene groups in the ionic liquid showing the modification of the biomass with ionic liquid molecules. These peaks were not as pronounced in the unmodified plant material.
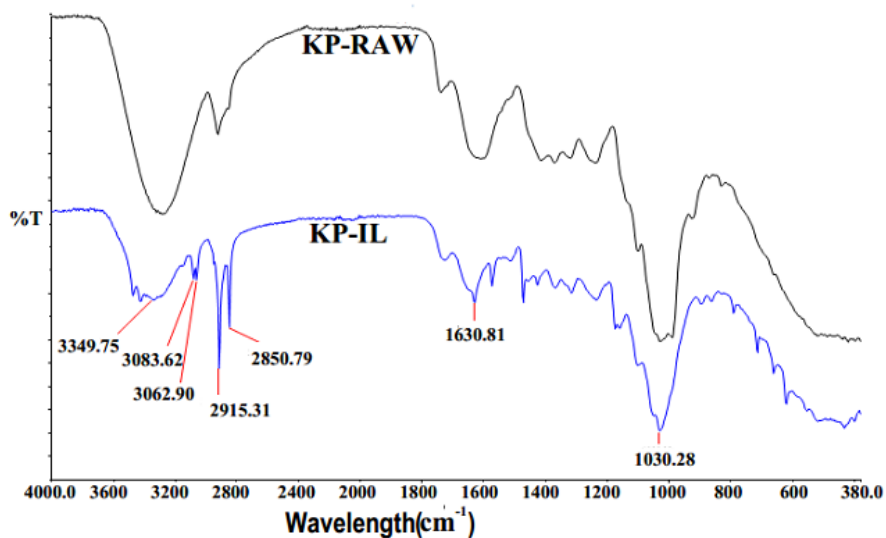
Fig. 8.1 FTIR spectra of KP and KP-IL

The surface morphologies of KP-IL and KP were determined using SEM. KP showed a smooth surface due to the presence of natural oils and waxy compounds (Liu et al., 2010; Slimani et al., 2014). KP-IL (Fig. 8.2b) showed increased surface porosity, ridges and valleys compared to KP (Fig. 8.2a) which are necessary for adsorption.
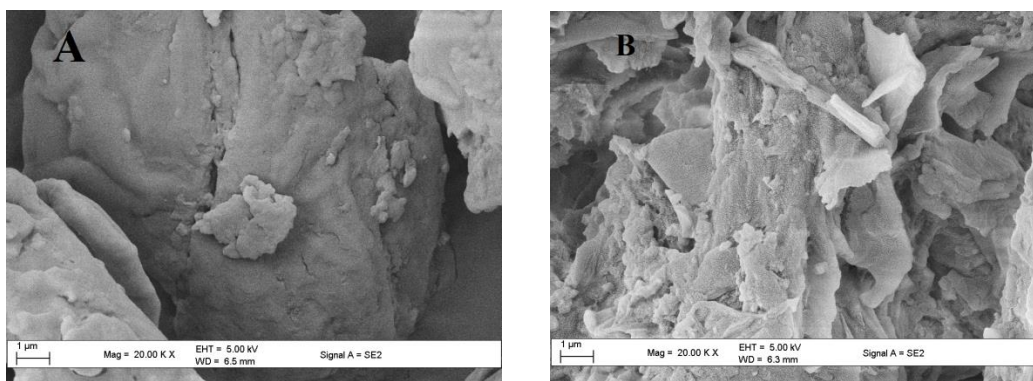
Fig. 8.2 SEM imgae of (a) KP and (b) KP-IL

The thermal behavior of KP-IL and KP were investigated by TG analysis (Fig. 8.3). The loss of mass on both KP-IL and KP at ~100 °C was due to the removal of moisture from the biomass.
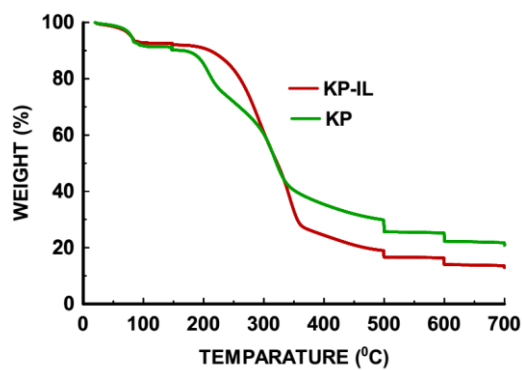
Fig. 8.3 TGA spectral of KP and KP-IL

In addition, at temperatures ranging between 120 and 380 °C mass loss at this stage was attributed to loss in organic matter. Comparing KP-IL and KP, it was observed that the degradation pattern was different and the mass loss was greater in KP-IL due to the loading of more carbon from IL onto KP. Comparing the TGA curve of KP-IL and KP it is clear that the former is more thermally stable than the latter.

225
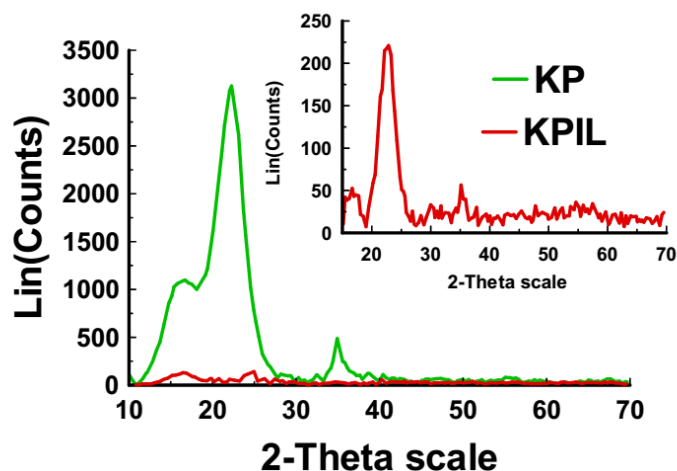
Fig. 8.4 XRD spectra of KP and KP-IL

The amorphous form of KP (Fig. 8.4) is characterised by broad peaks, suggesting a non-crystalline structure. The diffractogram for KP-IL (Fig. 8.4) exhibits sharper peaks and a reduction in intensity at the same 2Θ values as KP. The sharpness of the peaks and reduction in the intensity are due to the loading of carbon (from the ionic liquid), leading to a more crystalline structure compared to KP. Also, the surface area and pore volume of KP and KP-IL were investigated using BET. KP has a surface area of 15.21 m^2 g^{-1} and pore volume of 0.45 cm^3 g^{-1}, but after modification the surface area and pore volume of KP-IL is reduced to 8.29 m^2 g^{-1} and 0.38 cm^3 g^{-1} respectively. This signified blockage of the pores by IL, which led to the reduction in the surface area of KP-IL. This further confirmed that KP had been modified.

8.4.2 Equilibrium

A preliminary test was carried out on KP and KP-IL, KP showed that the highest biosorption capacity (q_e) was around 20 mg g^{-1}. KET had the highest sorption capacity of 21.45 mg g^{-1} followed by DCL, IBU and AMP with q_e values of 12 mg g^{-1}, 7 mg g^{-1} and 5.51 mg g^{-1} respectively. On the other hand, KP-IL showed a significant improvement in q_e, ranging from 75 to 289 mg g^{-1}. Therefore, all other experiments were performed only on KP-IL.

Freundlich and Langmuir (Table 8.3) were used to explain the mode of adsorption. The results in Table 8.3 showed that Freundlich was the best fit with R^2 values closest to unity for all the pharmaceuticals. Thus, the adsorption process on to KP-IL most likely occurred in more than one layer. All the values of n were less than 1.0, expect for DCL. The n values less than unity, reflects nonlinearity at high adsorption. Therefore, adsorption of these pharmaceuticals was favored over the entire concentration range used in this study. For n values greater than 1, it implies that adsorption of DCL onto KP-IL was favorable (Qiu et al., 2009; Antunes et al., 2012).

In addition, the K_F value signifies the adsorption capacity of the adsorbent for a given pharmaceutical, which reflects the affinity of the pharmaceutical towards the adsorbent. As indicated from the K_F values in Table 8.3, the adsorption of pharmaceuticals on KP-IL is in the order of ibuprofen > ketoprofen > diclofenac > ampicillin. A similar trend was also observed by Bui and Choi for the adsorption of pharmaceuticals on mesoporous silica SBA-15 (Bui and Choi, 2009). Bui and Choi further explained that for acidic pharmaceuticals, this affinity order fitted well with their pKa values, in this case ibuprofen (pKa= 4.91) > ketoprofen (pKa= 4.45) > diclofenac (pKa= 4.15) > ampicillin (pKa = 2.5) which is in agreement with this study as well (Bui and Choi, 2009). A K_F value of 80.6 L g^{-1} for DCL indicated that 1 g of KP-IL could treat almost 80 L of DCL effluent. This is significantly higher than what was reported using grape bagasse biomass as an adsorbent for DCL. Antunes and co-workers reported a K_F value of 1.7 L g^{-1} for DCL adsorbed onto grape bagasse (Antunes et al., 2012). In addition, the adsorption of DCL on mesoporous silica SBA-15 was reported to have a K_F value of 0.7 L g^{-1} (Bui and Choi, 2009). Furthermore, in this study, the K_F values for IBU, KET and AMP are 125.7, 100.2 and 20.8 L g^{-1} respectively, which are higher than that reported by other researchers (Mestre et al., 2007; Bui and Choi, 2009; Dubey et al., 2010; Essandoh et al., 2015; Mestre et al., 2009; Gao and Deshusses, 2011; Kim et al., 2014).

The Freundlich isotherm best fitted the data, which suggested that the adsorption of these pharmaceuticals on to KP-IL was heterogeneous and adsorption took place *via* many processes. Researchers (Hari et al., 2005; Lorphensri et al., 2006; Robberson et al., 2006) have reported that hydrophobic and electrostatic interaction were the main mechanism for adsorption of pharmaceuticals.

Table 8.3 The q_m and b values in the Langmuir equation, the K_f and n values in the Freundlich equation, q_m and β values in Dubinin-Radushkevich, bT and AT values in the Temkin model and their respective correlation coefficient values.

	Langmuir model			Freundlich model			Dubinin–Radushkevich model				Temkin model		
	q_m	b	R^2	K_f	n	R^2	q_m	β	E	R^2	bT	AT	R^2
	$(mg\ g^{-1})$	$(L\ mg^{-1})$		$(L\ g^{-1})$	$(g\ L^{-1})$		$(mol\ g^{-1})$	$(mol^2\ kJ^{-2})$	$(kJ\ mol^{-1})$		$(g\ kJ\ mg^{-1}\ mol^{-1})$	$(L\ mg^{-1})$	
Ketoprofen	251.81	0.006	0.973	100.230	0.20	0.992	0.94	3×10^{-8}	7.32	0.998	87.58	0.299	0.790
Dichlofenac	197.16	0.366	0.984	80.557	1.23	0.992	0.72	2×10^{-8}	5.00	0.972	65.58	3.673	0.804
Ibuprofen	276.78	0.013	0.964	125.681	0.12	0.985	1.10	2×10^{-8}	5.30	0.945	49.35	0.214	0.923
Ampicillin	73.57	0.001	0.951	20.897	0.84	0.998	0.35	3×10^{-8}	4.12	0.987	37.95	0.587	0.867

Table 8.4 Experimental values for q_e (mg g^{-1}) and parameters for pseudo-first-order, pseudo-second-order and intra-particle diffusion.

	Concentrations (mg L^{-1})	q_e,exp (mg g^{-1})	Pseudo-first-order			Pseudo-second-order			Weber–Morris model		
			q_e, cal (mg g^{-1})	k_e (-) (min^{-1})	R^2	q_e,cal (mg g^{-1})	k (10) (g mg^{-1} h^{-1})	R^2	q_e (mg g^{-1})	k_{id} (mg g^{-1} h$^{-1/2}$)	R^2
Ketoprofen	200	262.25	2.27	0.0043	0.198	249.50	0.049	0.999	239.16	1.262	0.957
	100	126.36	1.49	0.0047	0.228	128.81	17.201	0.998	126.68	0.278	0.912
	50	56.59	1.17	0.0043	0.346	50.52	0.076	0.999	64.56	0.182	0.942
	20	30.90	0.99	0.0064	0.519	25.57	0.687	0.998	40.86	0.084	0.948
	10	18.58	0.86	0.0042	0.476	15.30	0.356	0.997	20.86	0.047	0.995
Diclofenac	200	189.35	73.74	0.024	0.845	190.65	0.008	0.994	-	-	-
	100	119.43	32.11	0.011	0.528	99.82	0.024	0.996	-	-	-
	50	59.74	22.04	0.016	0.546	60.03	0.035	0.994	-	-	-
	20	37.85	11.42	0.017	0.795	34.00	0.084	0.995	-	-	-
	10	13.89	5.96	0.017	0.769	15.97	0.200	0.996	-	-	-
Ibuprofen	200	289.23	82.54	0.022	0.342	284.23	0.005	0.995	-	-	-
	100	151.53	48.32	0.005	0.732	149.87	0.073	0.996	-	-	-
	50	92.23	24.21	0.034	0.832	94.07	0.002	0.982	-	-	-
	20	50.34	12.36	0.005	0.651	53.36	0.234	0.999	-	-	-
	10	28.12	9.00	0.023	0.546	25.98	0.223	0.997	-	-	-
Ampicillin	200	75.98	7.36	0.002	0.519	71.24	0.005	0.996	23.25	0.117	0.184
	100	40.69	3.36	0.001	0.432	38.34	0.023	0.993	15.36	0.182	0.505
	50	20.23	1.15	0.005	0.318	20.54	0.002	0.981	9.87	0.084	0.487
	20	12.23	0.94	0.002	0.255	10.32	0.254	0.989	4.95	0.047	0.195
	10	5.56	0.03	0.003	0.243	5.25	0.213	0.954	2.32	-0.031	0.268

Contact time

The effect of contact time on pharmaceuticals at different concentrations are shown in Figs. 8.5A, B, C and D where the removal efficiencies are plotted against time. Figs. 8.5a - d indicate that the adsorption of pharmaceuticals on KP-IL increased with time and equilibrium was reached in less than 25 min, except for AMP, which reached equilibrium in 30 min.
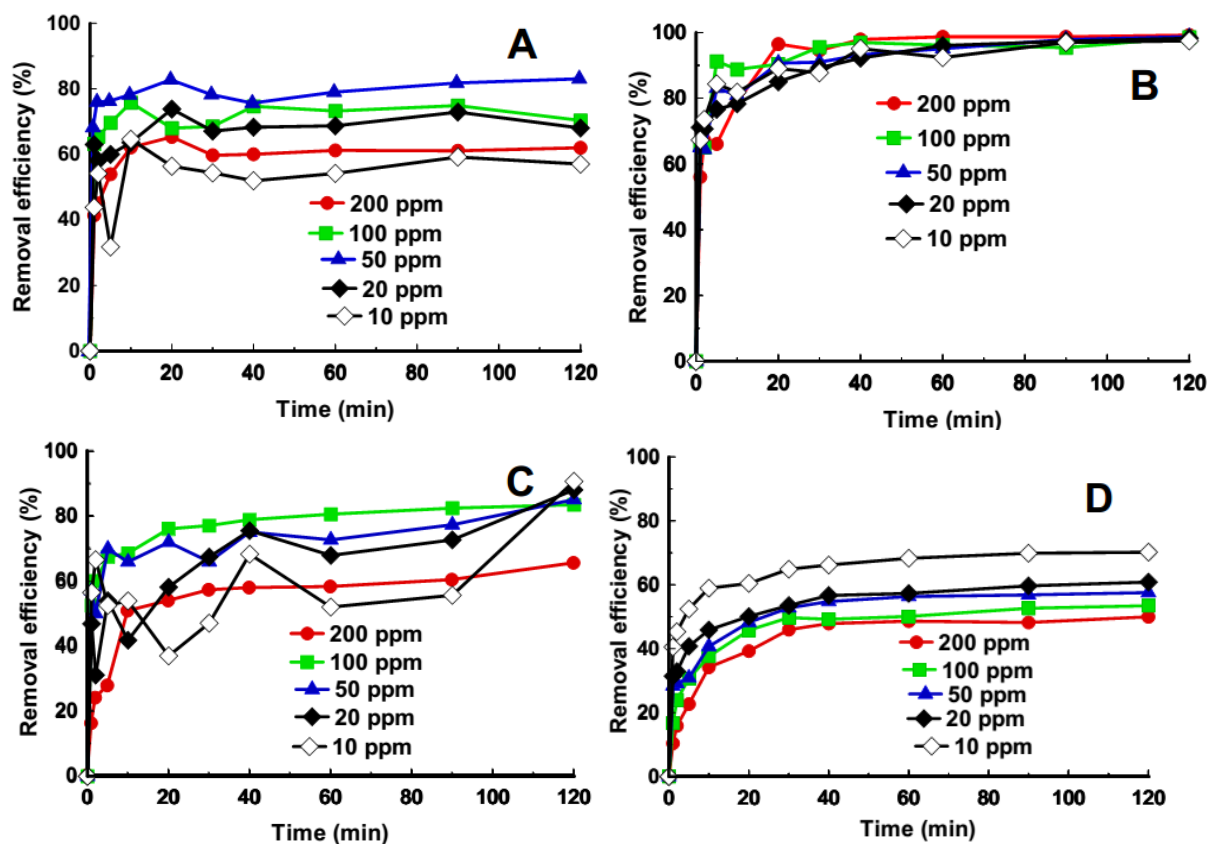
Fig. 8.5 Effect of contact time on (a) KET, (b) DCL, (c) IBU and (d) AMP

This indicated that sorption of these pharmaceuticals on KP-IL was much faster than that previously reported. Antunes and co-workers reported an equilibrium time of 24 h (Antunes et al., 2012), Ruiz and co-workers, and Snyder and co-workers reported an equilibrium time of 48 h

(Ruiz et al., 2010; Snyder et al., 2008). It was further observed that for AMP, removal efficiency % increased as the concentration decreased. This was because a larger number of sorption sites were available when the concentration of the analyte was low which led to a higher removal percentage. KET and IBU behaved differently from AMP on KP-IL, where low removal efficiencies occurred at low concentrations (10 and 20 ppm). This could be attributed to increasing particle interaction and aggregation of the adsorbent as the concentrations of the KET and IBU decreased which caused a reduction in the total surface area of the adsorbent (Daneshvar et al., 2012; Ghosh and Bhattacharyya, 2002). High sorption capacities of these pharmaceuticals on KP-IL indicated that their molecules could penetrate through the channels of the KP-IL complex or adsorb onto the surface *via* physical forces (El-Nahhal and Safi, 2004). The phenyl rings of the pharmaceuticals and the imidazole ring on the sorbent (KP-IL) may also interact *via* the electronic π–π interactions between both molecules which may lead to higher removal % (El-Nahhal and Safi, 2004). Similar outcomes have been reported by other researchers (Diagboya et al., 2014; Xu et al., 2012; Changchaivong and Khaodhiar, 2009; Olu-Owolabi et al., 2014).

8.4.3 Kinetics of Adsorption Process

To determine the kinetic process for the adsorption of pharmaceuticals on KP-IL, the data were fitted into pseudo-first-order, pseudo-second-order and intraparticle diffusion kinetic models. As shown in Table 8.4, the data fitted well to the pseudo-second-order model, with R^2 values close to unity and q_e cal close to q_e exp. This kinetic model suggests that physicochemical interaction is the rate-controlling step, which was also reported by Antunes and co-workers (Antunes et al., 2012). From the intraparticle diffusion model in Table 8.4, the value of the intercept correlates to the thickness of the boundary layer (the larger the intercept, the greater will be the boundary layer effect) (Kannan and Sundaram, 2001). The reason for this is that as the concentration of pharmaceuticals increases in the solution, the resistance to mass transfer from the adsorbent surroundings also increases (Ruiz et al., 2010; Antunes et al., 2012). As shown in Fig. 8.6a (IBU) and b (DCL), the entire plot is not a straight line passing through the origin.
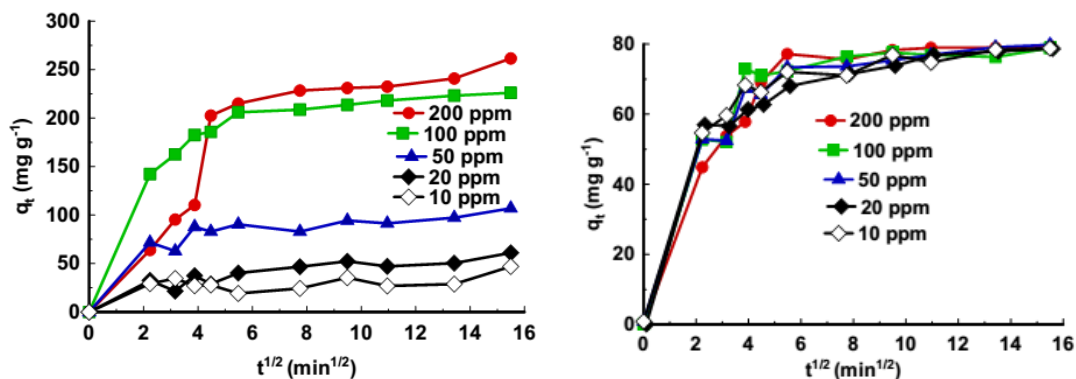
Fig. 8.6 Intraparticle diffusion plots for (a) IBU and (b) DCL

Bajpai and Bhowmik suggested that the deviation from straight lines from the origin may be due to the difference between the rates of mass transfer in the initial and final steps of adsorption (Bajpai and Bhowmik, 2010). This deviation also suggested that pore diffusion was not the sole rate-controlling step. In addition, the adsorption of the pharmaceuticals are of two phases, the first phase indicated bulk diffusion, while the second part signified intraparticle diffusion. In addition, the plots of KET and AMP do not pass through the origin (Appendix F 2.0 and F 2.1). This indicated some degree of boundary layer control and showed that processes other than intra-particle diffusion also contributed to adsorption rate (Liao et al., 2013; Crini et al., 2007).

Effect of pH

The effect of pH on removal efficiencies of pharmaceuticals on KP-IL is presented in Fig. 8.7. The adsorption of IBU, KET, DCL and AMP on KP-IL is attributed to both non-electrostatic and electrostatic interaction evidenced from Fig. 8.7. Non-electrostatic interaction plays an important and dominant role in the adsorption of pharmaceuticals at pH values below their pKa. At pH values above 2.5 for AMP, and above pH 5 for IBU, KET, and DCL the net charge on the molecule will be negative. This leads to electrostatic attraction between KP-IL and the pharmaceuticals. Meanwhile, at pH values below their pKa values, the net charge on the molecule is positive

232

resulting in electrostatic repulsion between the positively charged molecule and the positive adsorbent and any minimal adsorption observed is due to interactions other than electrostatic.
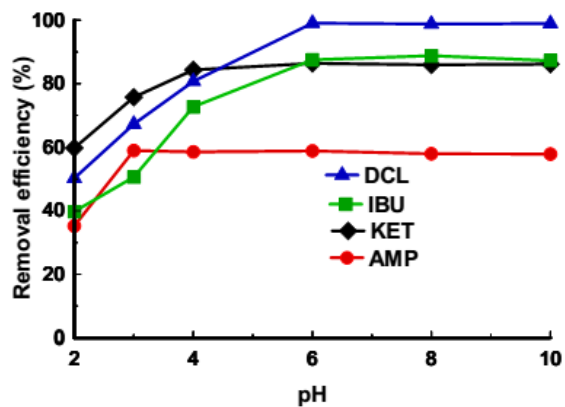
Fig. 8.7 Effect of pH on KET, DCL, IBU and AMP removal efficiency

This accounts for the reduction in adsorption observed at pH values below pKa values. The same trend has been noted by Bui and Choi (2009) and Mestre et al. (2007). Table 8.5 shows the q_e of IBU, KET, DCL and AMP on different types of adsorbent materials and its comparison with KP–IL. All the pharmaceuticals studied in this work showed higher adsorption onto KP-IL compared to previous reports in literature except for IBU, which showed better adsorption on carbon based materials than onto KP-IL.

Table 8.5 Comparison of adsorption capacities of KP-IL with other materials

Compound	q_e (mg g^{-1})	Adsorbent Materials	References
Ibuprofen	10.74	Pine wood biochar	(Essandoh et al., 2015)
	15.01	Mesoporous silican SBA-15	(Kim et al., 2014)
	416.7	Activated carbon	(Mestre et al., 2007)
	145.2	Carbon from cork	(Mestre et al., 2009)
	378.1	Carbon from municipal waste (plastic)	(Mestre et al., 2009)
	291.9	Commercial activated carbons	(Mestre et al., 2009)
	149.1	Commercial activated carbons	(Mestre et al., 2009)
	491.9	Surface-modified activated carbon cloths	(Guedidi et al., 2014)
	138.1	Commercial granular AC	(Guedidi et al., 2013)
	16.73	AC from artemisia vulgaris	(Dubey et al., 2010)
	64.5	Commercial activated charcoal	(Khalaf et al., 2013)
	0.41	Mesoporous silica SBA-15	(Bui and Choi, 2009)
	9.09	AC from olive waste cake	(Baccar et al., 2012)
	7.00	KP	Present work
	276.8	KP-IL	Present work
Ketoprofen	18.21	AC from olive waste cake	(Baccar et al., 2012)
	10.12 ug g^{-1}	Mesoporous silica SBA-15	(Kim et al., 2014)
	0.28	Mesoporous silica SBA-15	(Bui and Choi, 2009)
	120	Powdered activated carbon	(Gao and Deshusses, 2011)
	21.45	KP	Present work
	251.2	KP-IL	Present work
Diclofenac	56.17	AC from olive waste cake	(Baccar et al., 2012)
	0.34	Mesoporous silica SBA-15	(Bui and Choi, 2009)
	42.918	Polyaniline	(Bajpai and Bhowmik, 2010)
	329.0	Activated Carbon	(Sotelo et al., 2012)
	29.9	Carbon nanofibers	(Sotelo et al., 2012)
	41.4	Carbon nanotubes	(Sotelo et al., 2012)
	31.93 ug g^{-1}	Hexagonal mesoporous silicate HMS	(Suriyanon et al., 2013)
	35.59 ug g^{-1}	Mercapto-HMS	(Suriyanon et al., 2013)
	5.89 ug g^{-1}	Amino-HMS	(Suriyanon et al., 2013)
	34.18 ug g^{-1}	SBA-15	(Suriyanon et al., 2013)
	32.64 ug g^{-1}	MCM-41	(Suriyanon et al., 2013)
	40.55 ug g^{-1}	Powdered activated carbon	(Suriyanon et al., 2013)
	23.77	Isabel grape bagasse	(Antunes et al., 2012)
	324.8	Molecularly imprinted polymer	(Dai et al., 2011)
	12	KP	Present work
	197.1	KP-IL	Present work
Ampicillin	0.1441 mmol g^{-1}	Natural bentonite	(Rahardjo et al., 2011)
	0.2477 mmol g^{-1}	Organobentonite	(Rahardjo et al., 2011)
	5.51	KP	Present work
	73.00	KP-IL	Present work

8.5 CONCLUSION

This study showed that *kigelia pinnata* was successfully modified with ionic liquid 1-methyl, 3-decahexyl imidazolium to form KP-IL and was effectively applied as an adsorbent for removal of IBU, KET, DCL and AMP from aqueous medium. All the pharmaceuticals studied showed high adsorption capacities at pH above 5, except AMP that showed a high adsorptive capacity from pH 3 and above. Approximately 80 % of q_e was reached within 25 mins for each of the selected pharmaceuticals expect for AMP, which reached 80 % equilibrium in approximately 30 min. The kinetics study showed that the adsorption processes followed a pseudo second-order model. The Freundlich isotherm model fitted best for all the pharmaceuticals but the Langmuir isotherm model could also be used to explain them. The maximum adsorption capacity was relatively high compared to that reported previously in literature, which showed a vast improvement in adsorption. Adsorption of pharmaceuticals on KP-IL was in the order: ibuprofen > ketoprofen > diclofenac > ampicillin. This work has further shown that ionic liquids can replace the traditional surfactants used for modification of materials for the purpose of adsorption.

8.6 ACKNOWLEDGEMENTS

8.7 REFERENCES

Absalan, G., Asadi, M., Kamran, S., Sheikhian, L. & Goltz, D. M. 2011. Removal of reactive red-120 and 4-(2-pyridylazo) resorcinol from aqueous samples by Fe3O4 magnetic nanoparticles using ionic liquid as modifier. *Journal of Hazardous Materials,* 192(2)**,** pp 476-484.

Akar, S. T., Yilmazer, D., Celik, S., Balk, Y. Y. & Akar, T. 2015. Effective biodecolorization potential of surface modified lignocellulosic industrial waste biomass. *Chemical Engineering Journal,* 259(1)**,** pp 286-292.

Akar, T. & Divriklioglu, M. 2010. Biosorption applications of modified fungal biomass for decolorization of Reactive Red 2 contaminated solutions: Batch and dynamic flow mode studies. *Bioresource Technology,* 101(19)**,** pp 7271-7277.

Aksu, Z., Ertuğrul, S. & Dönmez, G. 2010. Methylene Blue biosorption by Rhizopus arrhizus: Effect of SDS (sodium dodecylsulfate) surfactant on biosorption properties. *Chemical Engineering Journal,* 158(3)**,** pp 474-481.

Almendra, A. R. P. 2011. *The effect of water inorganic matrix in ibuprofen adsorption onto activated carbon for water and wastewater treatment.* Master 's Degree, Universidade Nova de Lisboa.

Andreozzi, R., Canterino, M., Marotta, R. & Paxeus, N. 2005. Antibiotic removal from wastewaters: the ozonation of amoxicillin. *Journal of Hazardous Materials,* 122(3)**,** pp 243-250.

Ansari, R., Seyghali, B., Mohammad-khah, A. & Zanjanchi, M. A. 2012. Application of Nano Surfactant Modified Biosorbent as an Efficient Adsorbent for Dye Removal. *Separation Science and Technology,* 47(12)**,** pp 1802-1812.

Antunes, M., Esteves, V. I., Guégan, R., Crespo, J. S., Fernandes, A. N. & Giovanela, M. 2012. Removal of diclofenac sodium from aqueous solution by Isabel grape bagasse. *Chemical Engineering Journal,* 192(1)**,** pp 114-121.

Baccar, R., Sarrà, M., Bouzid, J., Feki, M. & Blánquez, P. 2012. Removal of pharmaceutical compounds by activated carbon prepared from agricultural by-product. *Chemical Engineering Journal,* 211–212(1)**,** pp 310-317.

Bajpai, S. & Bhowmik, M. 2010. Adsorption of diclofenac sodium from aqueous solution using polyaniline as a potential sorbent. I. Kinetic studies. *Journal of Applied Polymer Science,* 117(6)**,** pp 3615-3622.

Bingol, A., Aslan, A. & Cakici, A. 2009. Biosorption of chromate anions from aqueous solution by a cationic surfactant-modified lichen (Cladonia rangiformis (L.)). *Journal of Hazardous Materials,* 161(2)**,** pp 747-752.

Boyd, R. A. & Furlong, E. T. 2002. Human-health pharmaceutical compounds in Lake Mead, Nevada and Arizona, and Las Vegas Wash, Nevada, October 2000-August 2001,

Brandão, P. C., Souza, T. C., Ferreira, C. A., Hori, C. E. & Romanielo, L. L. 2010. Removal of petroleum hydrocarbons from aqueous solution using sugarcane bagasse as adsorbent. *Journal of Hazardous Materials,* 175(1–3)**,** pp 1106-1112.

Bui, T. X. & Choi, H. 2009. Adsorptive removal of selected pharmaceuticals by mesoporous silica SBA-15. *Journal of Hazardous Materials,* 168(2)**,** pp 602-608.

Changchaivong, S. & Khaodhiar, S. 2009. Adsorption of naphthalene and phenanthrene on dodecylpyridinium-modified bentonite. *Applied Clay Science,* 43(3)**,** pp 317-321.

Chatzitakis, A., Berberidou, C., Paspaltsis, I., Kyriakou, G., Sklaviadis, T. & Poulios, I. 2008. Photocatalytic degradation and drug activity reduction of chloramphenicol. *Water Research,* 42(1)**,** pp 386-394.

Crini, G., Peindy, H. N., Gimbert, F. & Robert, C. 2007. Removal of CI Basic Green 4 (Malachite Green) from aqueous solutions by adsorption using cyclodextrin-based adsorbent: kinetic and equilibrium studies. *Separation and Purification Technology,* 53(1)**,** pp 97-110.

Dai, C.-m., Geissen, S.-U., Zhang, Y.-l., Zhang, Y.-j. & Zhou, X.-f. 2011. Selective removal of diclofenac from contaminated water using molecularly imprinted polymer microspheres. *Environmental Pollution,* 159(6)**,** pp 1660-1666.

Daneshvar, E., Kousha, M., Sohrabi, M. S., Khataee, A. & Converti, A. 2012. Biosorption of three acid dyes by the brown macroalga Stoechospermum marginatum: Isotherm, kinetic and thermodynamic studies. *Chemical Engineering Journal,* 195–196(297-306.

Deng, S. & Ting, Y.-P. 2005. Characterization of PEI-modified biomass and biosorption of Cu(II), Pb(II) and Ni(II). *Water Research,* 39(10)**,** pp 2167-2177.

Diagboya, P. N., Olu-Owolabi, B. I., Zhou, D. & Han, B.-H. 2014. Graphene oxide–tripolyphosphate hybrid used as a potent sorbent for cationic dyes. *Carbon,* 79(1)**,** pp 174-182.

Dordio, A. V., Duarte, C., Barreiros, M., Carvalho, A. P., Pinto, A. & da Costa, C. T. 2009. Toxicity and removal efficiency of pharmaceutical metabolite clofibric acid by Typha spp.–Potential use for phytoremediation? *Bioresource Technology,* 100(3)**,** pp 1156-1161.

Dubey, S. P., Dwivedi, A. D., Sillanpää, M. & Gopal, K. 2010. Artemisia vulgaris-derived mesoporous honeycomb-shaped activated carbon for ibuprofen adsorption. *Chemical Engineering Journal,* 165(2)**,** pp 537-544.

Dubinin, M. & Radushkevich, L. 1947. Equation of the characteristic curve of activated charcoal. *Chemisches Zentralblatt,* 1(1)**,** pp 875.

El-Nahhal, Y. Z. & Safi, J. M. 2004. Adsorption of phenanthrene on organoclays from distilled and saline water. *Journal of Colloid and Interface Science,* 269(2)**,** pp 265-273.

Essandoh, M., Kunwar, B., Pittman, C. U., Mohan, D. & Mlsna, T. 2015. Sorptive removal of salicylic acid and ibuprofen from aqueous solutions using pine wood fast pyrolysis biochar. *Chemical Engineering Journal,* 265(1)**,** pp 219-227.

Feng, N., Guo, X., Liang, S., Zhu, Y. & Liu, J. 2011. Biosorption of heavy metals from aqueous solutions by chemically modified orange peel. *Journal of Hazardous Materials,* 185(1)**,** pp 49-54.

Fent, K., Weston, A. A. & Caminada, D. 2006. Ecotoxicology of human pharmaceuticals. *Aquatic Toxicology,* 76(2)**,** pp 122-159.

Freundlich, H. 1906. Über die Adsorption in Lösungen. *Zeitschrift fur Physikalische Chemie,* 57(A)**,** pp 385-470.

Gao, Y. & Deshusses, M. A. 2011. Adsorption of clofibric acid and ketoprofen onto powdered activated carbon: effect of natural organic matter. *Environmental Technology,* 32(15)**,** pp 1719-1727.

Ghosh, D. & Bhattacharyya, K. G. 2002. Adsorption of methylene blue on kaolinite. *Applied Clay Science,* 20(6)**,** pp 295-300.

Grundwasser, K. i. B. O.-u., Heberer, T., Schmidt-Bäumler, K. & Stan, H. 1998. Occurrence and distribution of organic contaminants in the aquatic system in Berlin. Part I: Drug residues and other polar contaminants in Berlin surface and groundwater. *Acta hydrochimica et hydrobiologica,* 26(5)**,** pp 272-278.

Guedidi, H., Reinert, L., Lévêque, J.-M., Soneda, Y., Bellakhal, N. & Duclaux, L. 2013. The effects of the surface oxidation of activated carbon, the solution pH and the temperature on adsorption of ibuprofen. *Carbon,* 54(1)**,** pp 432-443.

Guedidi, H., Reinert, L., Soneda, Y., Bellakhal, N. & Duclaux, L. 2014. Adsorption of ibuprofen from aqueous solution on chemically surface-modified activated carbon cloths. *Arabian Journal of Chemistry,* 20(1)**,** pp 503-520.

Hari, A. C., Paruchuri, R. A., Sabatini, D. A. & Kibbey, T. C. 2005. Effects of pH and cationic and nonionic surfactants on the adsorption of pharmaceuticals to a natural aquifer material. *Environmental Science & Technology,* 39(8)**,** pp 2592-2598.

Ho, Y.-S. & McKay, G. 1999. Pseudo-second order model for sorption processes. *Process Biochemistry,* 34(5)**,** pp 451-465.

Ibrahim, S., Ang, H.-M. & Wang, S. 2012. Adsorptive separation of emulsified oil in wastewater using biosorbents. *Asia-Pacific Journal of Chemical Engineering,* 7(2)**,** pp S216-S221.

Ibrahim, S., Wang, S. & Ang, H. M. 2010. Removal of emulsified oil from oily wastewater using agricultural waste barley straw. *Biochemical Engineering Journal,* 49(1)**,** pp 78-83.

Kamran, S., Asadi, M. & Absalan, G. 2014a. Adsorption of folic acid, riboflavin, and ascorbic acid from aqueous samples by Fe3O4 magnetic nanoparticles using ionic liquid as modifier. *Analytical Methods,* 6(3)**,** pp 798-806.

Kamran, S., Hossein Tavallali & Azad, A. 2014b. Fast Removal of Reactive Red 141 and Reactive Yellow 81 From Aqueous Solution by Fe3O4 Magnetic Nanoparticles Modified With Ionic Liquid 1-Octyl-3-methylimidazolium Bromide. *Iranian Journal of Analytical Chemistry,* 1(1)**,** pp 78-86.

Kannan, N. & Sundaram, M. M. 2001. Kinetics and mechanism of removal of methylene blue by adsorption on various carbons—a comparative study. *Dyes and Pigments,* 51(1)**,** pp 25-40.

Khalaf, S., Al-Rimawi, F., Khamis, M., Zimmerman, D., Shuali, U., Nir, S., Scrano, L., Bufo, S. A. & Karaman, R. 2013. Efficiency of advanced wastewater treatment plant system and laboratory-scale micelle-clay filtration for the removal of ibuprofen residues. *Journal of Environmental Science and Health, Part B,* 48(9)**,** pp 814-821.

Kim, S. D., Cho, J., Kim, I. S., Vanderford, B. J. & Snyder, S. A. 2007. Occurrence and removal of pharmaceuticals and endocrine disruptors in South Korean surface, drinking, and waste waters. *Water Research,* 41(5)**,** pp 1013-1021.

Kim, Y., Bae, J., Park, J., Suh, J., Lee, S., Park, H. & Choi, H. 2014. Removal of 12 selected pharmaceuticals by granular mesoporous silica SBA-15 in aqueous phase. *Chemical Engineering Journal,* 256(1)**,** pp 475-485.

Klavarioti, M., Mantzavinos, D. & Kassinos, D. 2009. Removal of residual pharmaceuticals from aqueous systems by advanced oxidation processes. *Environment International,* 35(2)**,** pp 402-417.

Kolpin, D. W., Furlong, E. T., Meyer, M. T., Thurman, E. M., Zaugg, S. D., Barber, L. B. & Buxton, H. T. 2002. Pharmaceuticals, hormones, and other organic wastewater contaminants in US streams, 1999-2000: A national reconnaissance. *Environmental Science & Technology,* 36(6)**,** pp 1202-1211.

Lagergren, S. 1898. About the theory of so-called adsorption of soluble substances. *Kungliga Svenska Vetenskapsakademiens Handlingar,* 24(4)**,** pp 1-39.

Langmuir, I. 1916. The Constitutionand Fundamental Properties of Solid and Liquids. Part I. Solids. *Journal of the American Chemical Society,* 38(11)**,** pp 2221-2295.

Lawal, I. A. & Moodley, B. 2015. Synthesis, characterisation and application of imidazolium based ionic liquid modified montmorillonite sorbents for the removal of amaranth dye. *RSC Advances,* 5(76)**,** pp 61913-61924.

Li, R., Yuan, Q., Zhang, Y., Ling, J. & Han, T. 2011. Hydrophilic interaction chromatographic determination of oxytetracycline in the environmental water using silica colum. *Journal of Liquid Chromatography & Related Technologies,* 34(7)**,** pp 511-520.

Li, Y., Chen, B. & Zhu, L. 2010. Enhanced sorption of polycyclic aromatic hydrocarbons from aqueous solution by modified pine bark. *Bioresource Technology,* 101(19)**,** pp 7307-7313.

Liao, P., Zhan, Z., Dai, J., Wu, X., Zhang, W., Wang, K. & Yuan, S. 2013. Adsorption of tetracycline and chloramphenicol in aqueous solutions by bamboo charcoal: A batch and fixed-bed column study. *Chemical Engineering Journal,* 228(1)**,** pp 496–505.

Liu, Y., Sun, X. & Li, B. 2010. Adsorption of Hg^{2+} and Cd^{2+} by ethylenediamine modified peanut shells. *Carbohydrate Polymers,* 81(2)**,** pp 335-339.

Lorphensri, O., Intravijit, J., Sabatini, D. A., Kibbey, T. C. G., Osathaphan, K. & Saiwan, C. 2006. Sorption of acetaminophen, 17α-ethynyl estradiol, nalidixic acid, and norfloxacin to silica, alumina, and a hydrophobic medium. *Water Research,* 40(7)**,** pp 1481-1491.

Loukidou, M. X., Matis, K. A., Zouboulis, A. I. & Liakopoulou-Kyriakidou, M. 2003. Removal of As (V) from wastewaters by chemically modified fungal biomass. *Water Research,* 37(18)**,** pp 4544-4552.

Méndez-Arriaga, F., Esplugas, S. & Giménez, J. 2008. Photocatalytic degradation of non-steroidal anti-inflammatory drugs with TiO 2 and simulated solar irradiation. *Water Research,* 42(3)**,** pp 585-594.

Mestre, A., Pires, J., Nogueira, J. & Carvalho, A. 2007. Activated carbons for the adsorption of ibuprofen. *Carbon,* 45(10)**,** pp 1979-1988.

Mestre, A. S., Pires, J., Nogueira, J. M., Parra, J. B., Carvalho, A. P. & Ania, C. O. 2009. Waste-derived activated carbons for removal of ibuprofen from solution: role of surface chemistry and pore structure. *Bioresource Technology,* 100(5)**,** pp 1720-1726.

Montazer-Rahmati, M. M., Rabbani, P., Abdolali, A. & Keshtkar, A. R. 2011. Kinetics and equilibrium studies on biosorption of cadmium, lead, and nickel ions from aqueous solutions by intact and chemically modified brown algae. *Journal of Hazardous Materials,* 185(1)**,** pp 401-407.

Olu-Owolabi, B. I., Diagboya, P. N. & Adebowale, K. O. 2014. Evaluation of pyrene sorption–desorption on tropical soils. *Journal of Environmental Management,* 137(1)**,** pp 1-9.

Pagnanelli, F., Petrangeli Papini, M., Toro, L., Trifoni, M. & Veglio, F. 2000. Biosorption of metal ions on Arthrobacter sp.: biomass characterization and biosorption modeling. *Environmental Science & Technology,* 34(13)**,** pp 2773-2778.

Qiu, H., Lv, L., Pan, B.-c., Zhang, Q.-j., Zhang, W.-m. & Zhang, Q.-x. 2009. Critical review in adsorption kinetic models. *Journal of Zhejiang University Science A,* 10(5)**,** pp 716-724.

Quintanilla, V. A. Y. 2010. *Rejection of Emerging Organic Contaminants by Nanofiltration and Reverse Osmosis Membranes: Effects of Fouling, Modelling and Water Reuse*: CRC Press.

Rahardjo, A. K., Susanto, M. J. J., Kurniawan, A., Indraswati, N. & Ismadji, S. 2011. Modified Ponorogo bentonite for the removal of ampicillin from wastewater. *Journal of Hazardous Materials,* 190(1)**,** pp 1001-1008.

Reddad, Z., Gerente, C., Andres, Y. & Le Cloirec, P. 2002. Adsorption of several metal ions onto a low-cost biosorbent: kinetic and equilibrium studies. *Environmental Science & Technology,* 36(9)**,** pp 2067-2073.

Robberson, K. A., Waghe, A. B., Sabatini, D. A. & Butler, E. C. 2006. Adsorption of the quinolone antibiotic nalidixic acid onto anion-exchange and neutral polymers. *Chemosphere,* 63(6)**,** pp 934-941.

Rodriguez-Fuentes, R., Hilts, B. A. & Dvorak, B. I. 2005. Disinfection by-product precursor adsorption as function of GAC properties: Case study. *Journal of Environmental Engineering,* 131(10)**,** pp 1462-1465.

Ruiz, B., Cabrita, I., Mestre, A., Parra, J., Pires, J., Carvalho, A. & Ania, C. 2010. Surface heterogeneity effects of activated carbons on the kinetics of paracetamol removal from aqueous solution. *Applied Surface Science,* 256(17)**,** pp 5171-5175.

Skowronski, T., Pirszel, J. & Pawlik-Skowronska, B. 2001. Heavy metal removal by the waste biomass of Penicillium chrysogenum. *Water Quality Research Journal of Canada,* 36(4)**,** pp 793-803.

Slimani, R., El Ouahabi, I., Abidi, F., El Haddad, M., Regti, A., Laamari, M. R., Antri, S. E. & Lazar, S. 2014. Calcined eggshells as a new biosorbent to remove basic dye from aqueous solutions: Thermodynamics, kinetics, isotherms and error analysis. *Journal of the Taiwan Institute of Chemical Engineers,* 45(4)**,** pp 1578-1587.

Snyder, S., Lei, H., Wert, E., Westerhoff, P. & Yoon, Y. 2008. *Removal of EDCs and Pharmaceuticals in Drinking Water*: Water Environment Research Foundation.

Snyder, S. A., Adham, S., Redding, A. M., Cannon, F. S., DeCarolis, J., Oppenheimer, J., Wert, E. C. & Yoon, Y. 2007. Role of membranes and activated carbon in the removal of endocrine disruptors and pharmaceuticals. *Desalination,* 202(1)**,** pp 156-181.

Sotelo, J. L., Rodríguez, A. R., Mateos, M. M., Hernández, S. D., Torrellas, S. A. & Rodríguez, J. G. 2012. Adsorption of pharmaceutical compounds and an endocrine disruptor from aqueous solutions by carbon materials. *Journal of Environmental Science and Health, Part B,* 47(7)**,** pp 640-652.

Stackelberg, P. E., Furlong, E. T., Meyer, M. T., Zaugg, S. D., Henderson, A. K. & Reissman, D. B. 2004. Persistence of pharmaceutical compounds and other organic wastewater contaminants in a conventional drinking-water-treatment plant. *Science of The Total Environment,* 329(1)**,** pp 99-113.

Stumpf, M., Ternes, T. A., Wilken, R.-D., Silvana Vianna, R. & Baumann, W. 1999. Polar drug residues in sewage and natural waters in the state of Rio de Janeiro, Brazil. *Science of The Total Environment,* 225(1–2)**,** pp 135-141.

Sun, H., Shi, X., Mao, J. & Zhu, D. 2010. Tetracycline sorption to coal and soil humic acids: An examination of humic structural heterogeneity. *Environmental Toxicology and Chemistry,* 29(9)**,** pp 1934-1942.

Suriyanon, N., Punyapalakul, P. & Ngamcharussrivichai, C. 2013. Mechanistic study of diclofenac and carbamazepine adsorption on functionalized silica-based porous materials. *Chemical Engineering Journal,* 214(1)**,** pp 208-218.

Tambosi, J. L., Yamanaka, L. Y., José, H. J., Moreira, R. d. F. P. M. & Schröder, H. F. 2010. Recent research data on the removal of pharmaceuticals from sewage treatment plants (STP). *Química Nova,* 33(2)**,** pp 411-420.

Ternes, T. A. 1998. Occurrence of drugs in German sewage treatment plants and rivers1. *Water Research,* 32(11)**,** pp 3245-3260.

Thomas, T. D. & Puthur, J. T. 2004. Thidiazuron induced high frequency shoot organogenesis in callus from Kigelia pinnata L. *Botanical Bulletin of Academia Sinica,* 45(307-313.

Tixier, C., Singer, H. P., Oellers, S. & Müller, S. R. 2003. Occurrence and fate of carbamazepine, clofibric acid, diclofenac, ibuprofen, ketoprofen, and naproxen in surface waters. *Environmental Science & Technology,* 37(6)**,** pp 1061-1068.

Vijayaraghavan, K. & Yun, Y.-S. 2008. Bacterial biosorbents and biosorption. *Biotechnology Advances,* 26(3)**,** pp 266-291.

Wang, J., Hu, J. & Zhang, S. 2010. Studies on the sorption of tetracycline onto clays and marine sediment from seawater. *Journal of Colloid and Interface Science,* 349(2)**,** pp 578-582.

Weber, W. J. & Morris, J. C. 1963. Kinetics of adsorption on carbon from solution. *Journal of the Sanitary Engineering Division. ASCE,,* 89(1)**,** pp 31.

Xi, Z. & Chen, B. 2014. Removal of polycyclic aromatic hydrocarbons from aqueous solution by raw and modified plant residue materials as biosorbents. *Journal of Environmental Sciences,* 26(4)**,** pp 737-748.

Xu, J., Wang, L. & Zhu, Y. 2012. Decontamination of bisphenol A from aqueous solution by graphene adsorption. *Langmuir,* 28(22)**,** pp 8418-8425.

Yun, Y.-S., Park, D., Park, J. M. & Volesky, B. 2001. Biosorption of trivalent chromium on the brown seaweed biomass. *Environmental Science & Technology,* 35(21)**,** pp 4353-4358.

Zhou, Y., Chen, L., Lu, P., Tang, X. & Lu, J. 2011. Removal of bisphenol A from aqueous solution using modified fibric peat as a novel biosorbent. *Separation and Purification Technology,* 81(2)**,** pp 184-190.

Zhou, Y., Chen, L., Wang, X., Xu, Y. & Lu, J. 2012a. Adsorption of phenanthrene by quaternary ammonium surfactant modified peat and the mechanism involved. *Water Science & Technology,* 66(4)**,** pp 810-815.

Zhou, Y., Lu, P. & Lu, J. 2012b. Application of natural biosorbent and modified peat for bisphenol a removal from aqueous solutions. *Carbohydrate Polymers,* 88(2)**,** pp 502-508.

CHAPTER 9: CONCLUSIONS AND RECOMMENDATIONS

9.1 CONCLUSION

Recently ionic liquid have been proposed as a suitable replacement for these known surfactants. Ionic liquid was used to modify different materials for adsorption of organic pollutants (amaranth, Congo red, reactive blue, acid red, ibuprofen, ketoprofen, ampicillin, diclofenac tetracycline, sulfamethoxazole, nalidixic acid and chloramphenicol and phenanthrene).

In this study, two new cationic ionic liquids (1-hexyl, 3-decahexyl imidazolium and 1-methyl, 3-decahexyl imidazolium) were synthesized and characterized. Thereafter they were used in the modification of clays (montmorillonite and kaolin), biomasses (peanut shell and *kigelia pinnata*) and activated carbon from peanut shell which were also characterized. Optimized adsoption studies of organic pollutants were carried out using the modified materials. Montmorillonite was modified with 1-methyl, 3-decahexyl imidazolium and used in the adsorption of amaranth dye. Montmorillonite modified 1-methyl, 3-decahexyl imidazolium (Mt–IL) showed a very good adsorptive capacity with batch q_e of 263.2 mg g^{-1} and column of adsorption capacities of 393.64, 580.89 and 603.60 mg g^{-1} at different concentrations. Adsorption data was better described by the pseudo-second-order kinetics and Langmuir adsorption isotherm. Furthermore, Mt–IL was used for the adsorption of pharmaceuticals (tetracycline (TC), sulfamethoxazole (SMZ), nalidixic acid (NAD) and chloramphenicol (CHL)). Freundlich and pseudo-second-order kinetics model were best in describing the adsorption mechanism. The maximum adsorption capacities (q_e) of TC, SMZ, NAD and CHL were 765.7, 504.1, 150.4 and 30.9 mg g^{-1} respectively. These were considerably higher than the q_e of unmodified montmorillonite clay and of other materials reported in literature.

1-hexyl, 3-decahexyl imidazolium was used to modify kaolin and thereafter used in batch and column adsorption studies of acid red dye and phenanthrene. The column adsorption capacity at the same flow rate and different concentration for phenanthrene is 222, 611 and 1093 mg g^{-1}, and

877, 1337 and 1350 mg g^{-1} for acid red dye. Acid red dye had an adsorption capacity of 909 mg g^{-1} and phenanthrene had an adsorption capacity of 263 mg g^{-1}. Data from both batch studies fitted well to pseudo-second order and Langmuir isotherm models.

1-methyl, 3-decahexyl imidazolium was also used to modify *kigelia pinnata*. The maximum sorption capacity of 251.2, 197.1, 276.8 and 73 mg g^{-1} was achieved for KET, DCL, IBU and AMP respectively, which is higher than unmodified KP and that reported for some other surfactant modifications of biomasses in the literature. Pseudo-second-order kinetics and the Langmuir adsorption isotherm best described the adsorption mechanism. Also, 1-methyl, 3-decahexyl imidazolium was used in modifying peanut shell (ILNS) and activated carbon from peanut shell (ILAC) and thereafter used in the adsorption of Congo red and reactive blue dyes. ILNS and ILAC had adsorption capacities of 136.4 and 150.0 mg g^{-1} for CR and 290.0 and 364.4 mg g^{-1} for RB respectively. Their adsorption kinetics followed pseudo second order, the adsorption of CR and RB onto ILAC followed the Freundlich isotherm, while ILNS was described by Freundlich and Langmuir.

This study has showed that ionic liquids can be used as surfactants for improving the adsorption capacity of clay and biomass in the adsorption of various organic pollutants from aqueous medium.

9.2 RECOMMENDATIONS

❖ This study was carried out using simulated organic pollutants in the laboratory, real industrial effluent should be used to estimate the efficiency for industrial application.

❖ Studies on the recovery of the materials should be done in terms of process and percentage purification of compounds.

❖ Considering the complex mixtures of organic pollutants present in wastewater, rivers and streams, it is recommended that the adsorption study using these materials should be done in treating simulated wastewater containing more than one organic pollutant.

❖ The continuous experiment in this study was done with a column in the laboratory; the materials should be tested in a real continuous wastewater treatment plant.

APPENDIX A: CALIBRATION CURVES

Appendix A 1: Calibration graphs for dyes
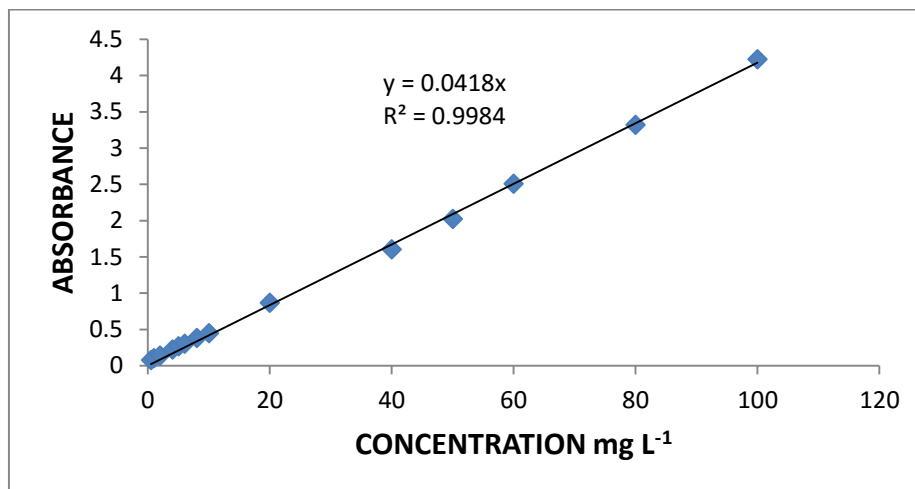
Appendix A 1.1- Calibration curve for acid red dye
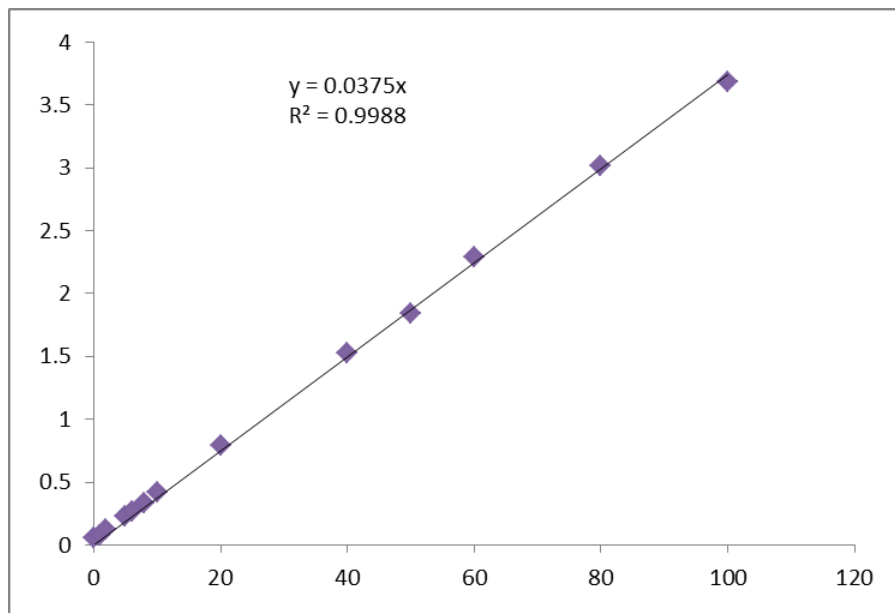
Appendix A 1.2- Calibration curve for amaranth
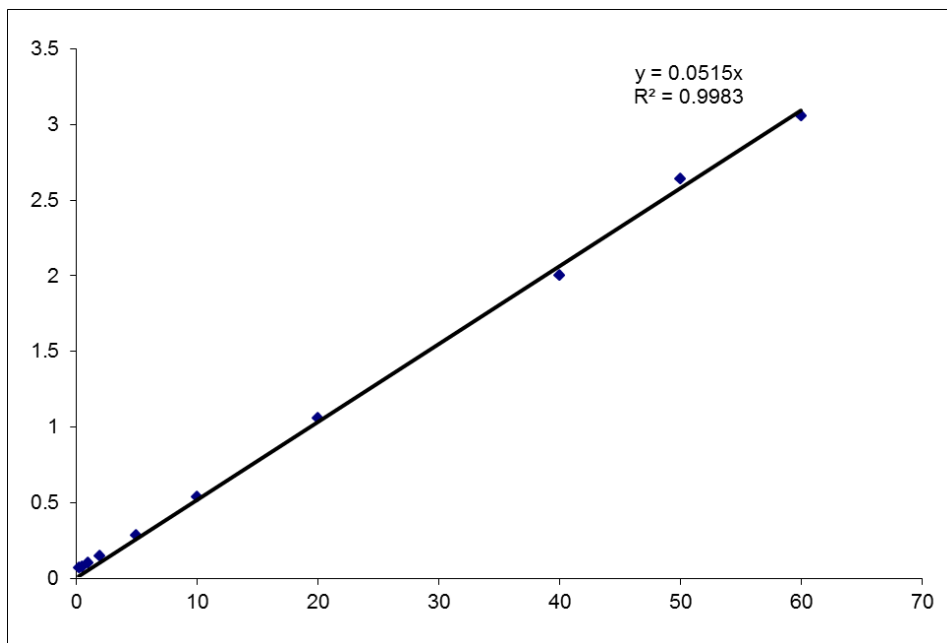
Appendix A 1.3- Calibration curve for Congo red
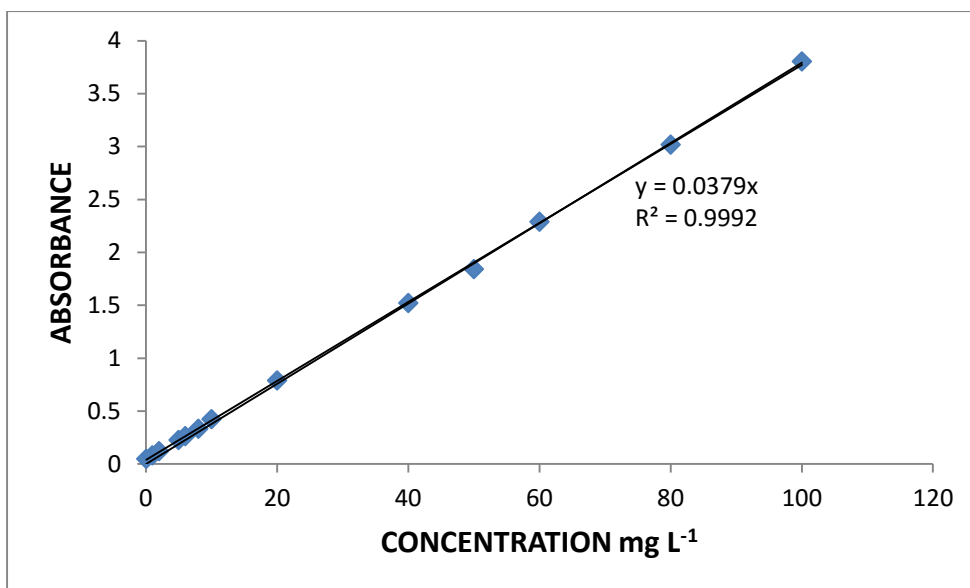
Appendix A 1.4- Calibration curve for reactive blue dye

Appendix A 2

Calibration graphs for pharmaceuticals
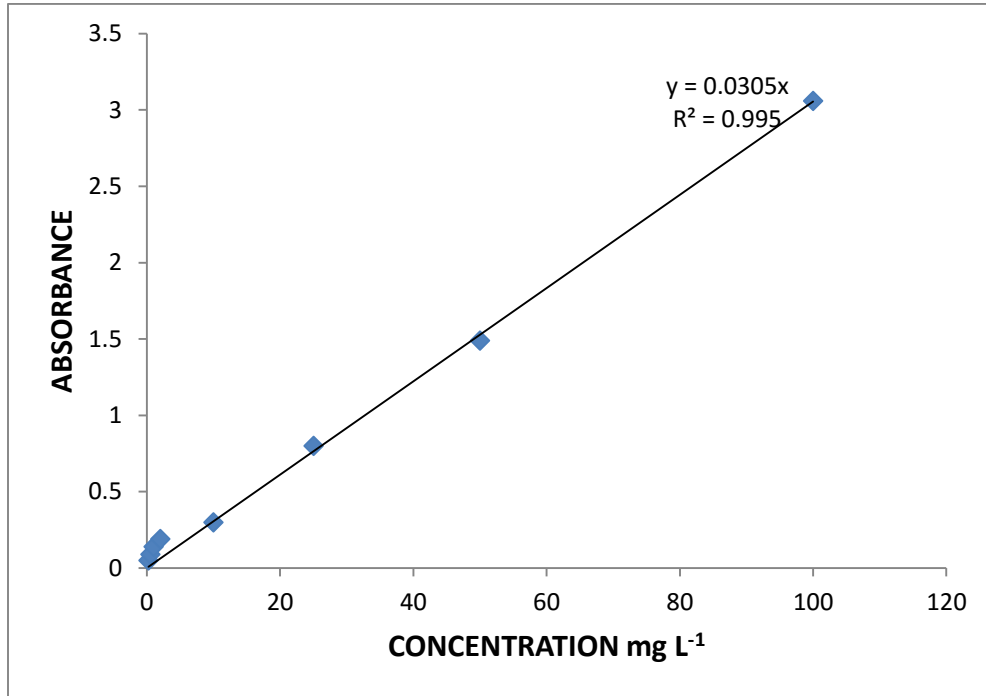
Appendix A 2.1- Calibration curve for Tetracycline

The graph shows Absorbance vs Concentration mg L^{-1} with $y = 0.0305x$ and $R^2 = 0.995$.
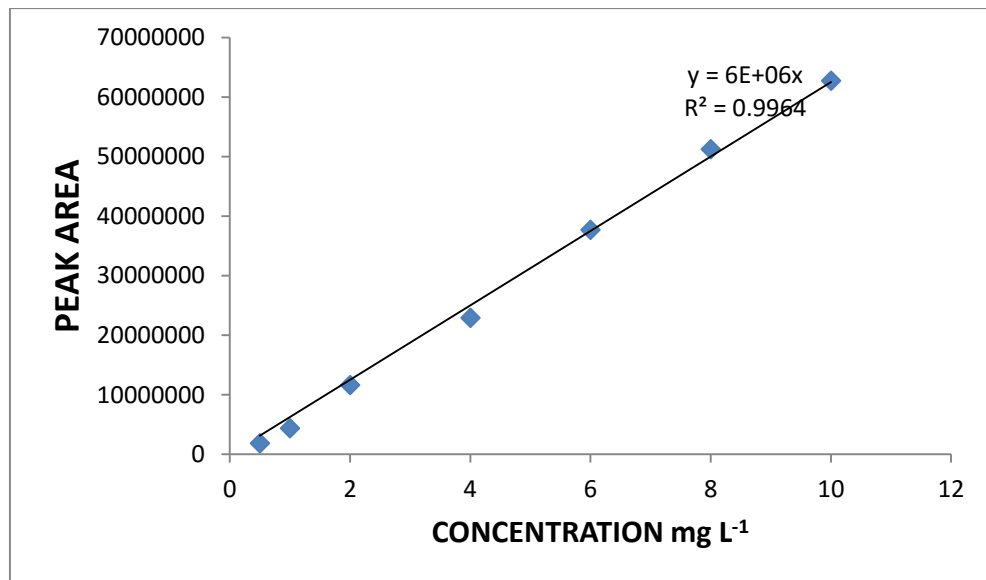
Appendix A 2.2- Calibration curve for chloramphenicol

The graph shows Peak Area vs Concentration mg L^{-1} with $y = 6E+06x$ and $R^2 = 0.9964$.
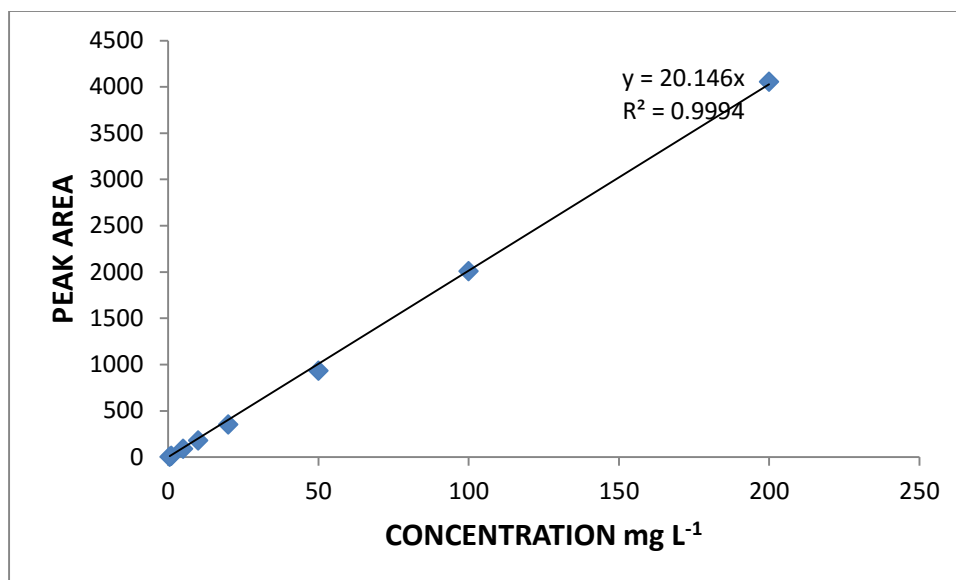
Appendix A 2.3- Calibration curve for diclofenac
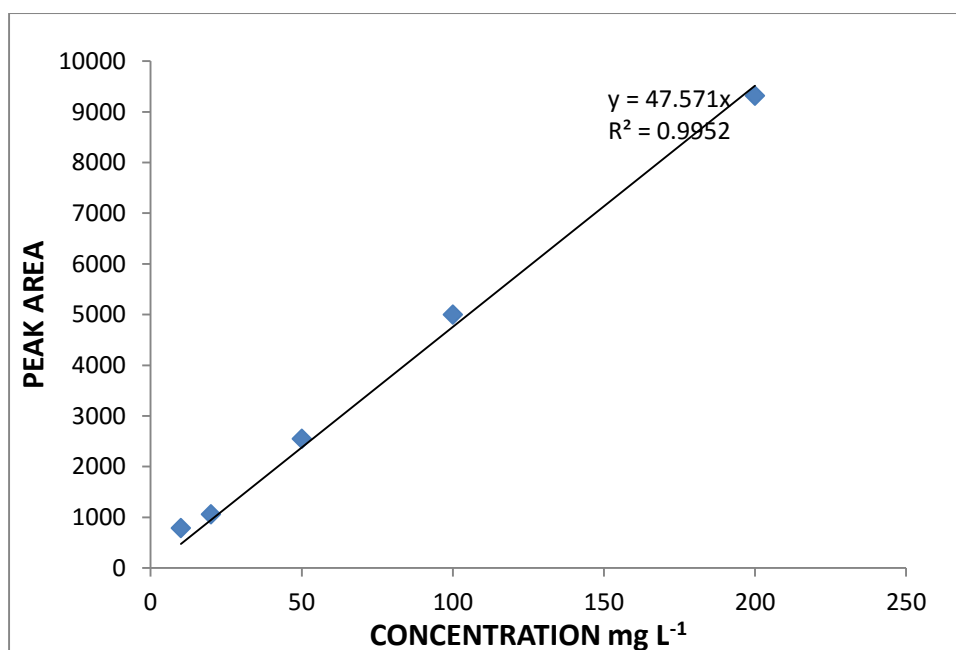
Appendix A 2.4- Calibration curve for ibuprofen
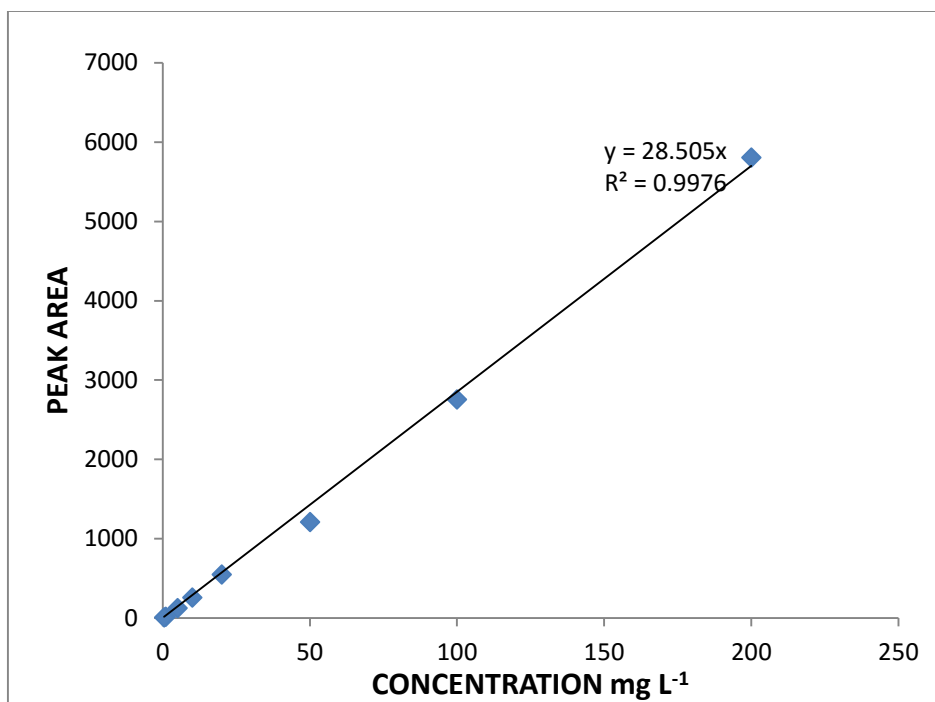
Appendix A 2.5- Calibration curve for ketoprofen
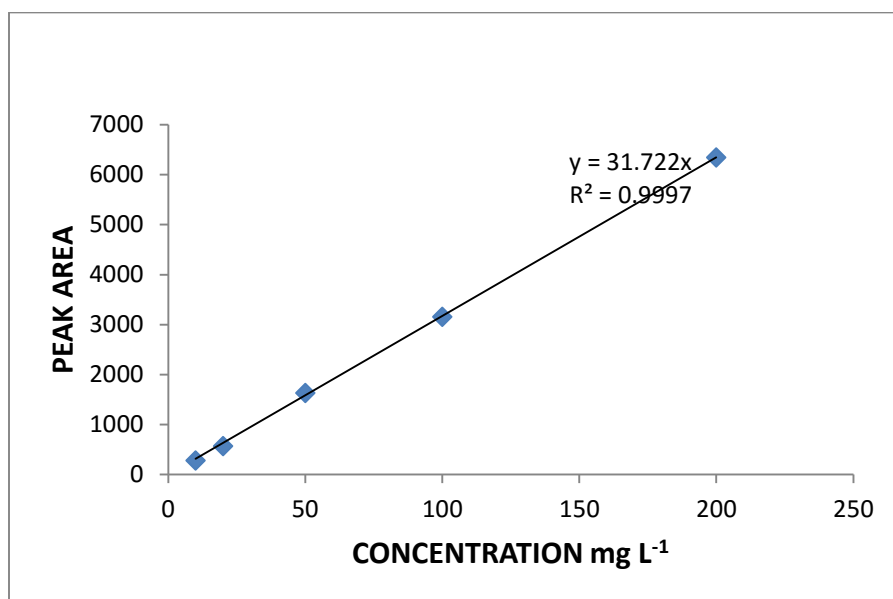
Appendix A 2.6- Calibration curve for sulfamethoxazole
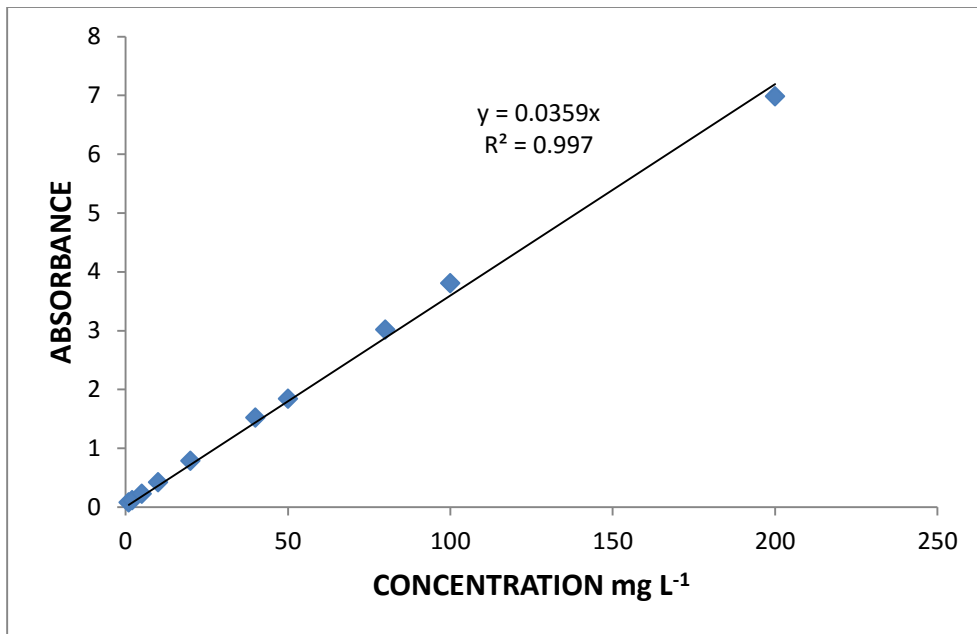
Appendix A 2.7- Calibration curve for nalidixic acid

Appendix A 3

Calibration curve for polyaromatic hydrocarbons
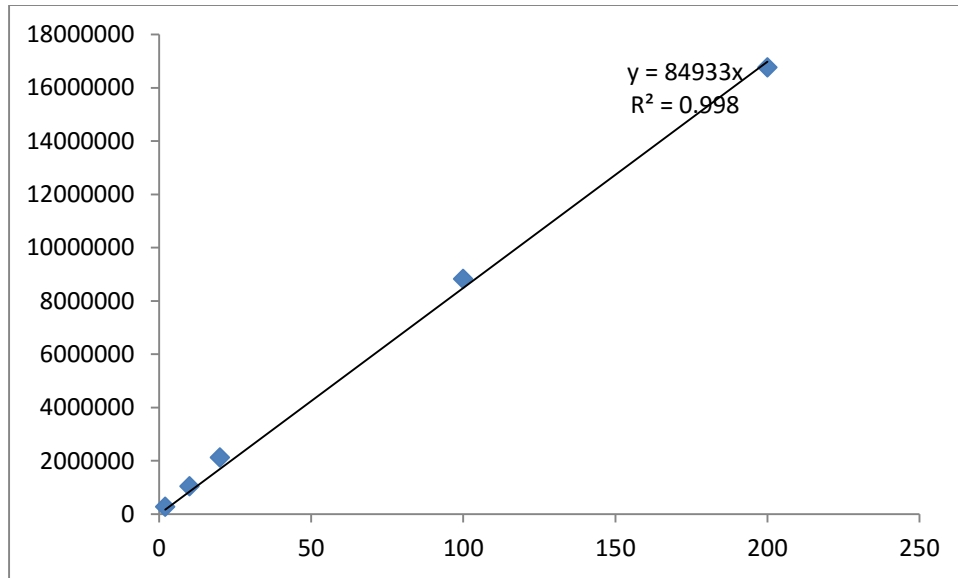
Appendix A 3.1- Calibration curve for phenanthrene

APPENDIX B: CHROMATOGRAPHS

Appendix B 1: Chromatographs for pharmaceuticals
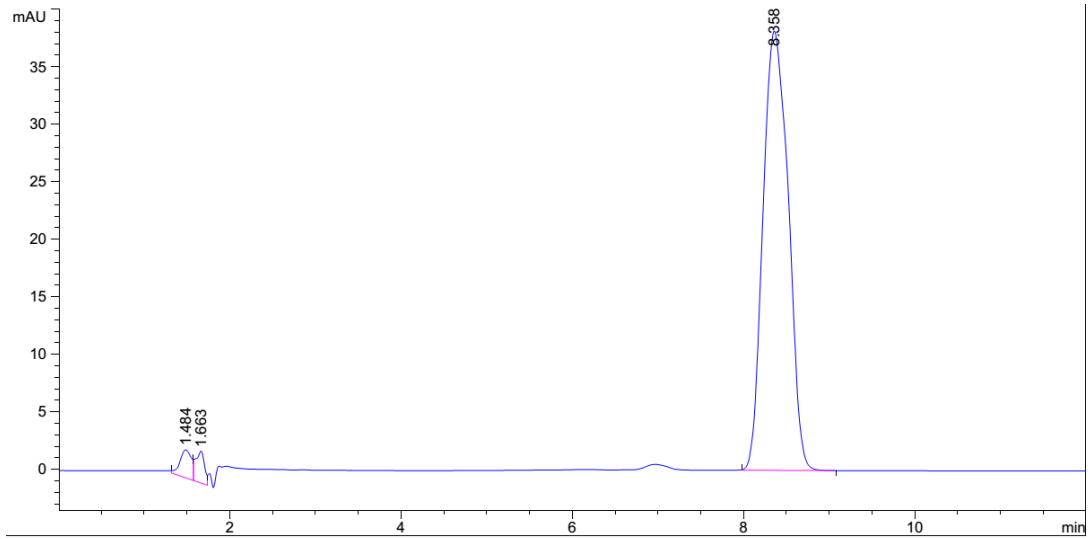
Appendix B 1.1- Chromatograph for Ketoprofen
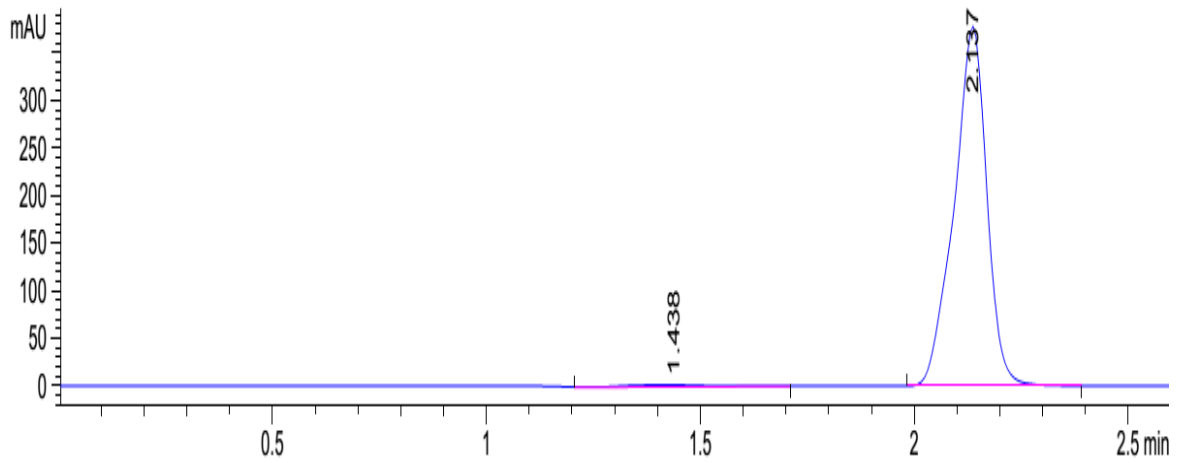
Appendix B 1.2- Chromatograph for Diclofenac
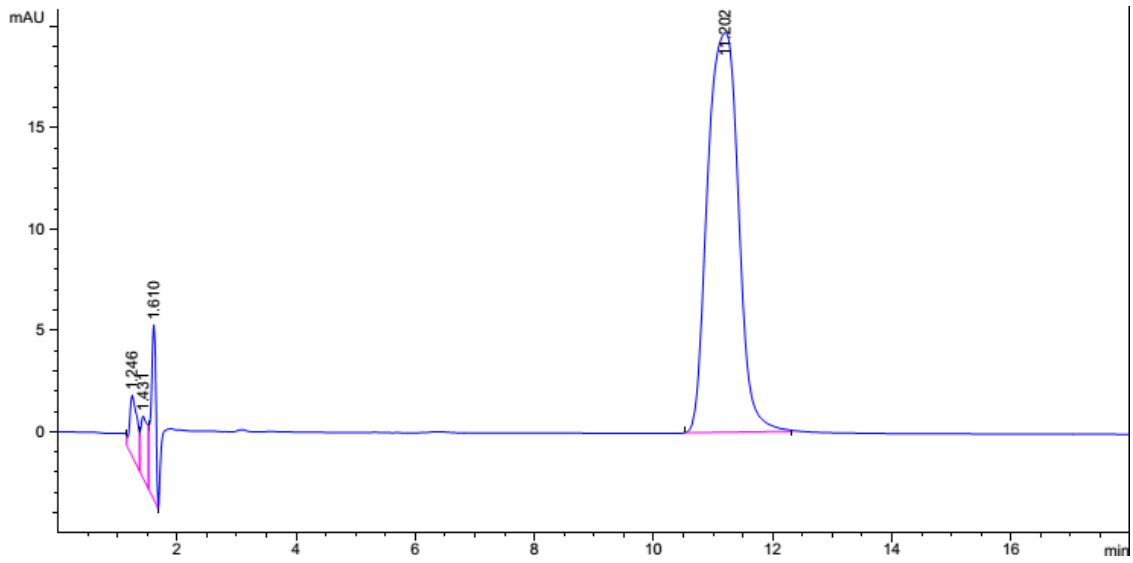
Appendix B 1.3- Chromatograph for Sulfamethoxazole
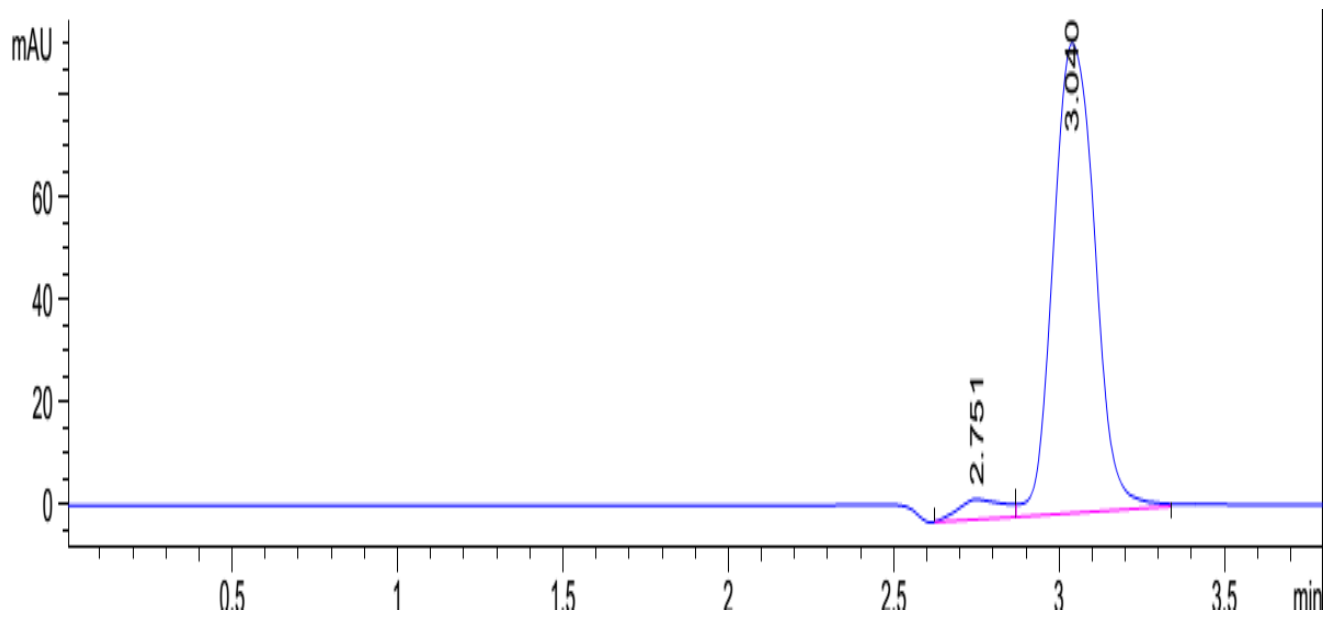
Appendix B 1.4- Chromatograph for Ampicillin
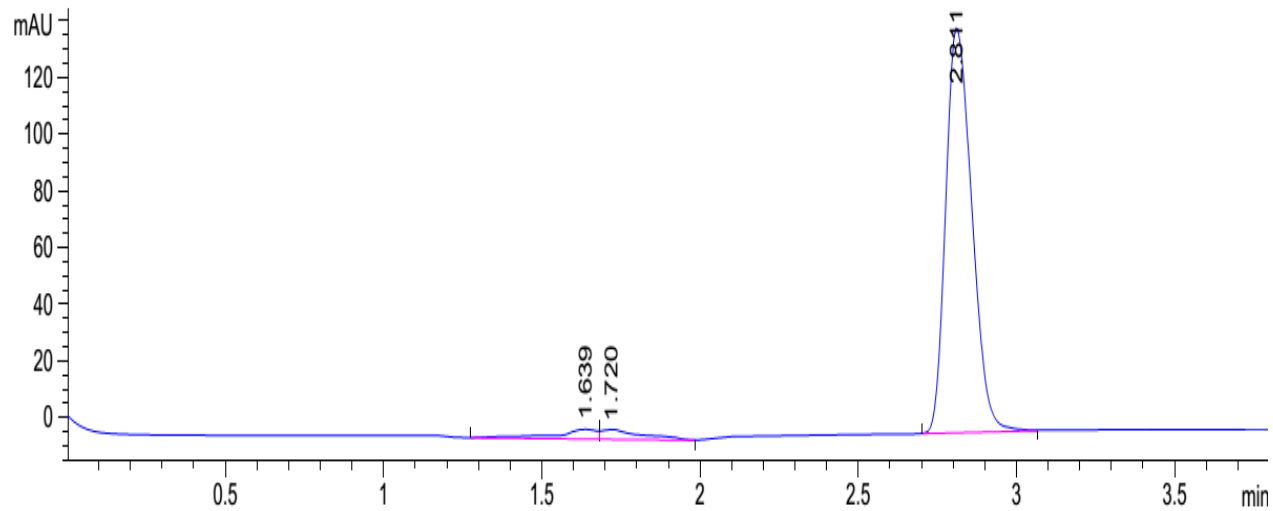
Appendix B 1.5- Chromatograph for Chloramphenicol
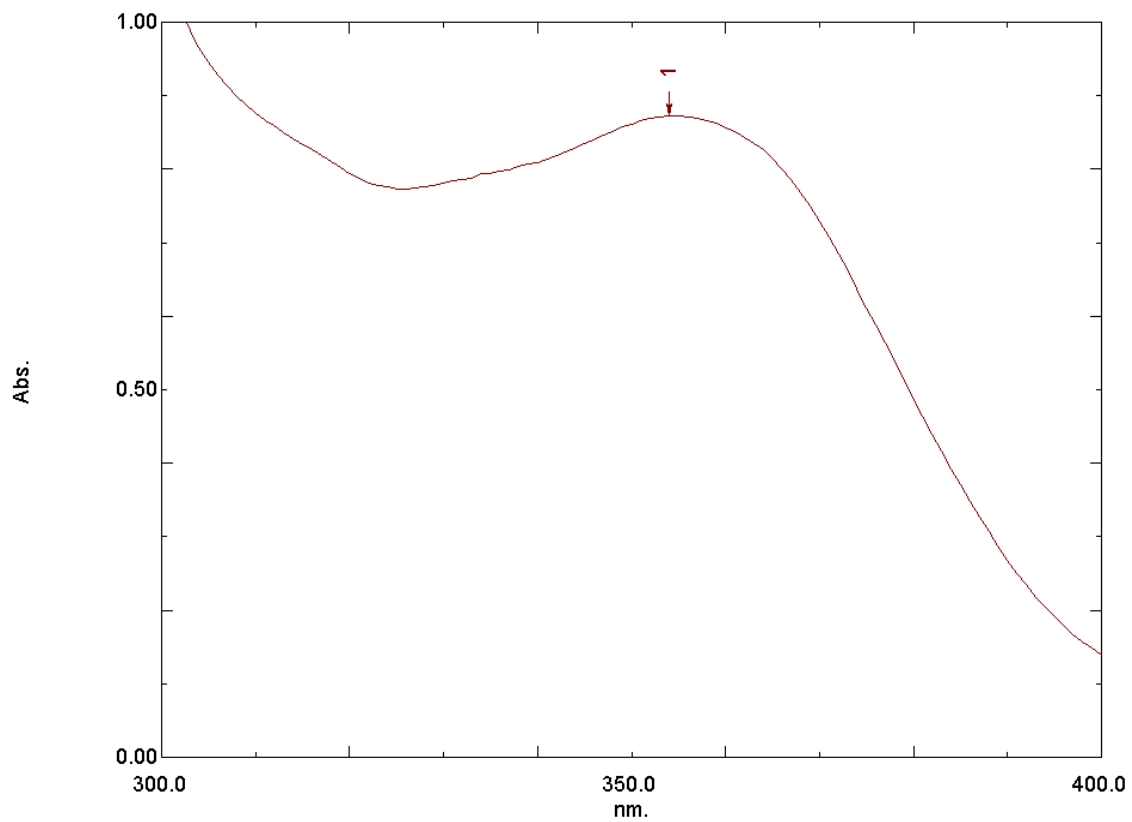
Appendix B 1.6- Chromatograph for Tetracycline

259
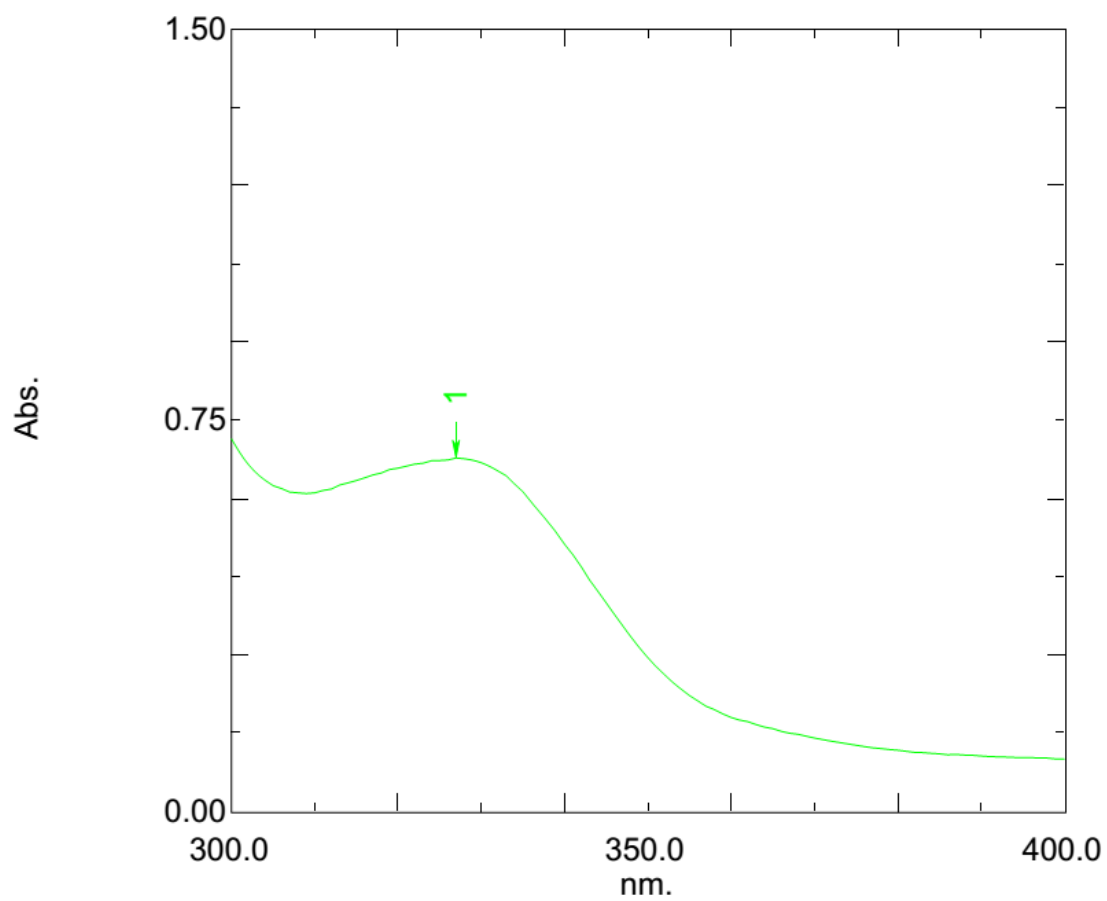
Appendix B 1.7- Chromatograph for Nalidixic acid

Appendix B 2 - Chromatograph for polyaromatic hydrocarbon
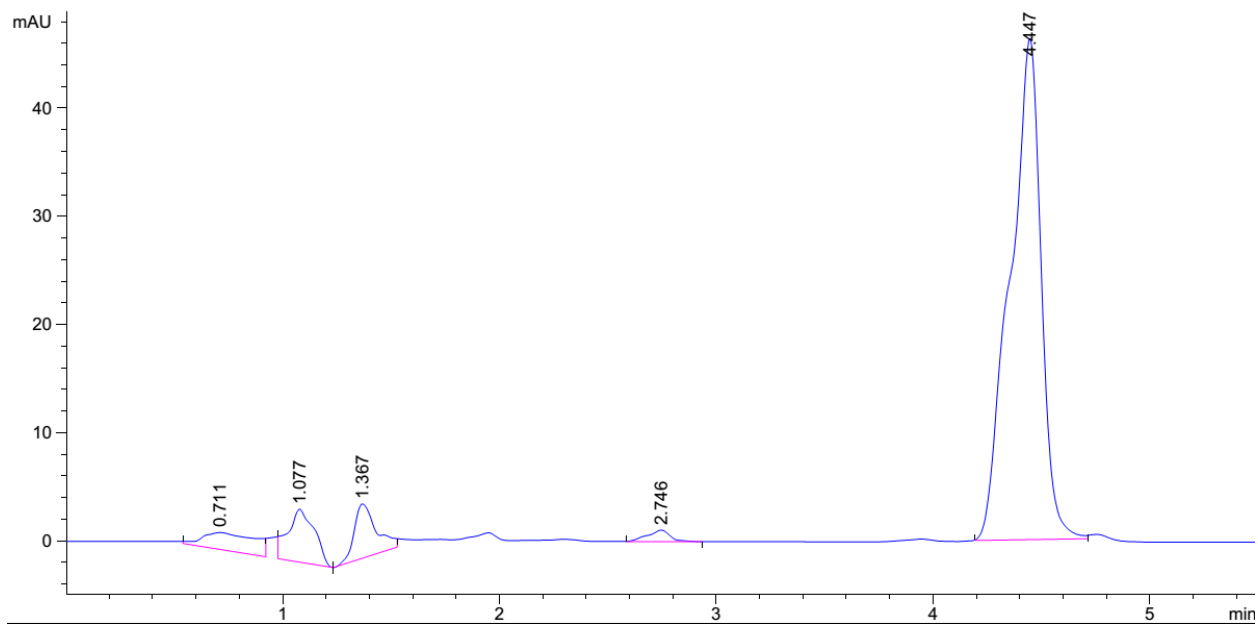
Appendix B 2.1 - Chromatograph for Phenanthrene

Appendix B 3 - Chromatographs for dye
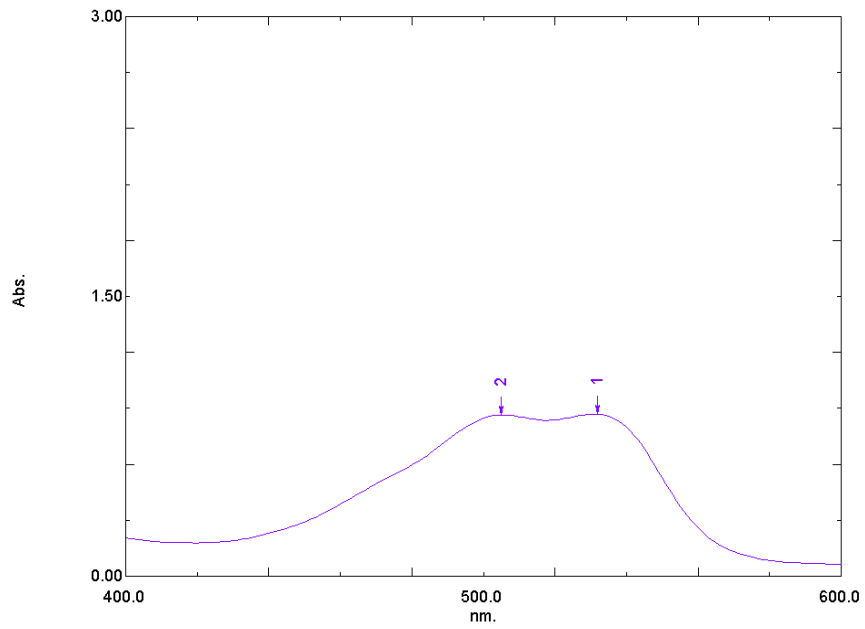
Appendix B 3.1 - Chromatograph for Acid red dye
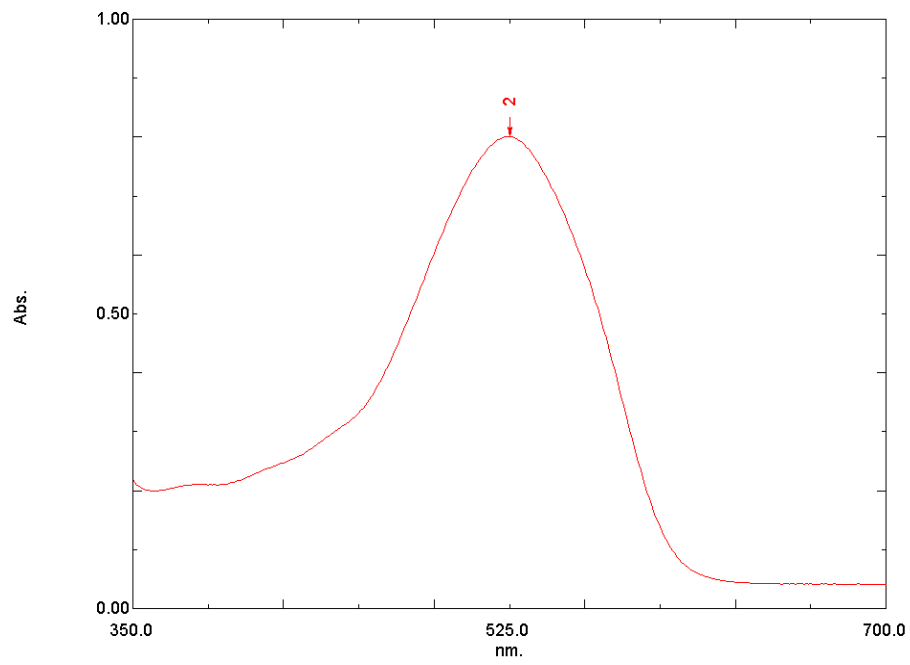
Appendix B 3.2 - Chromatograph for Amaranth
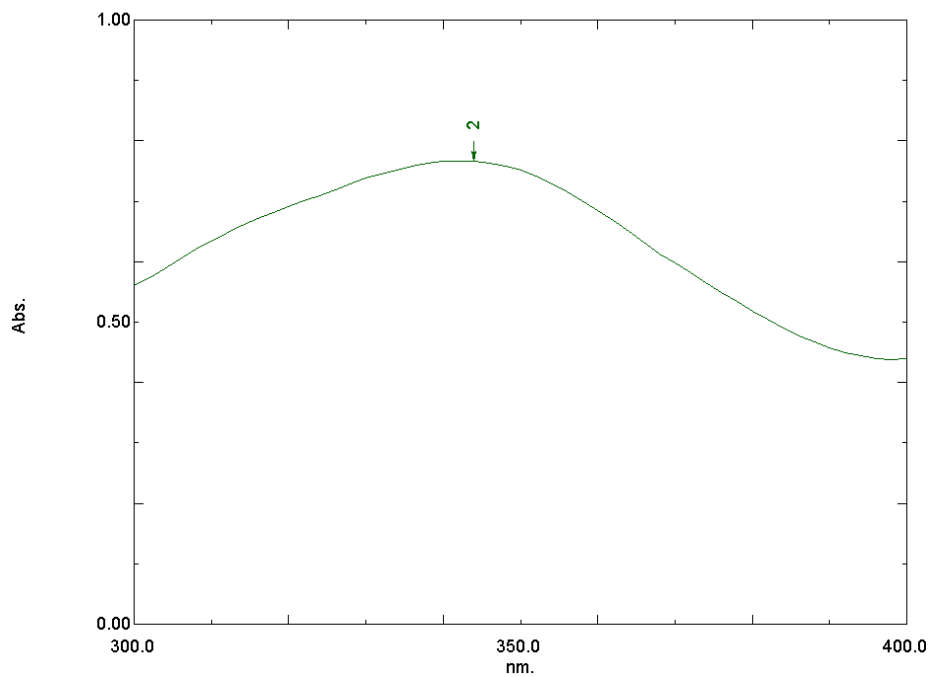
Appendix B 3.3 - Chromatograph Congo red
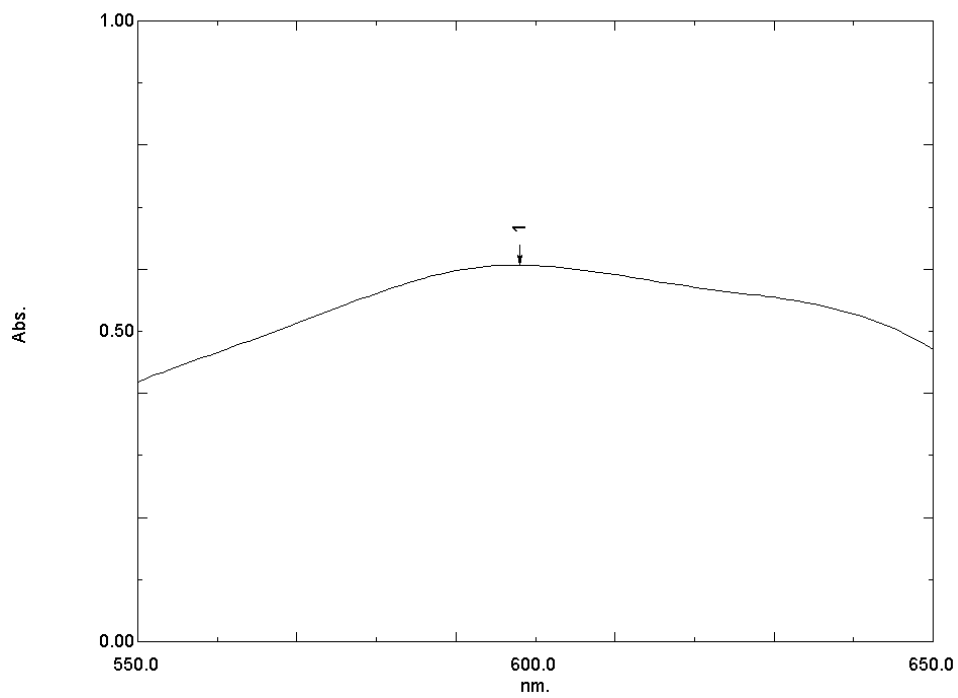
Appendix B 3.4 - Chromatograph reactive blue

263

APPENDIX C: NMR SPECTRA

Appendix C 1 – NMR spectra of 1- methyl, 3-decahexyl imidazolium
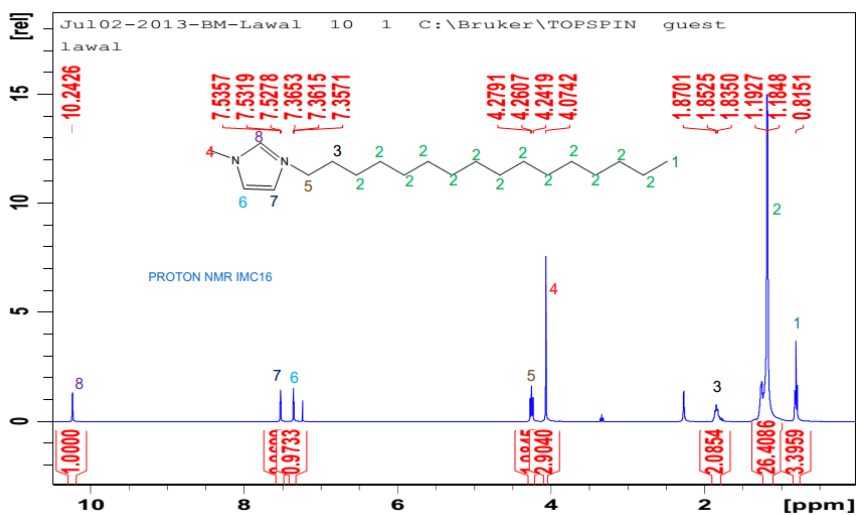
Appendix C 1.0 - Proton NMR of 1- methyl, 3-decahexyl imidazolium
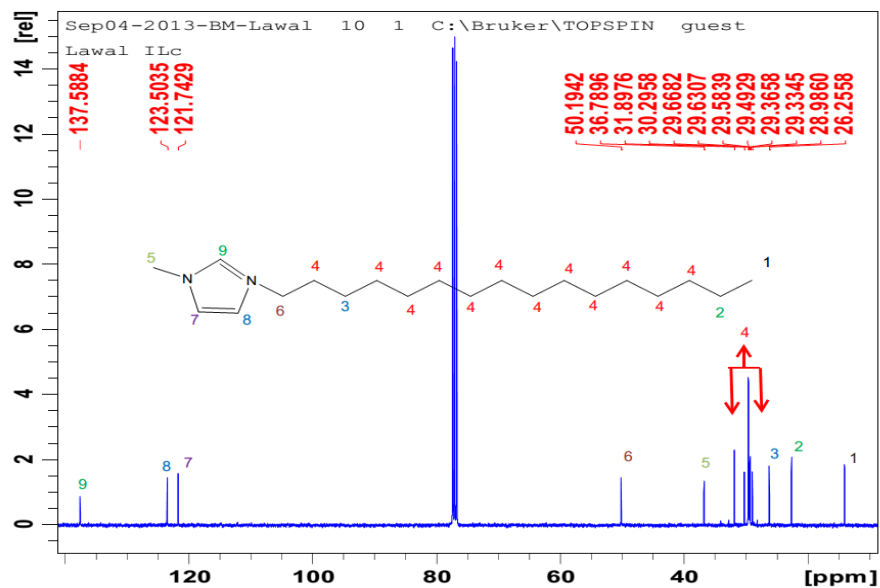
Appendix C 1.1 - Carbon NMR of 1- methyl, 3-decahexyl imidazolium

Appendix C 2 – NMR spectra of 1- hexyl, 3-decahexyl imidazolium
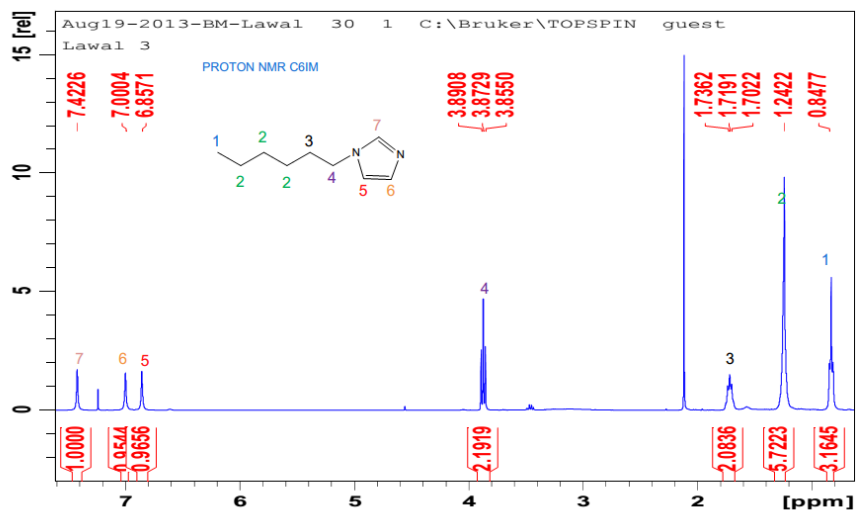
Appendix C 2.0 - Proton NMR of 1-hexyl imidazole
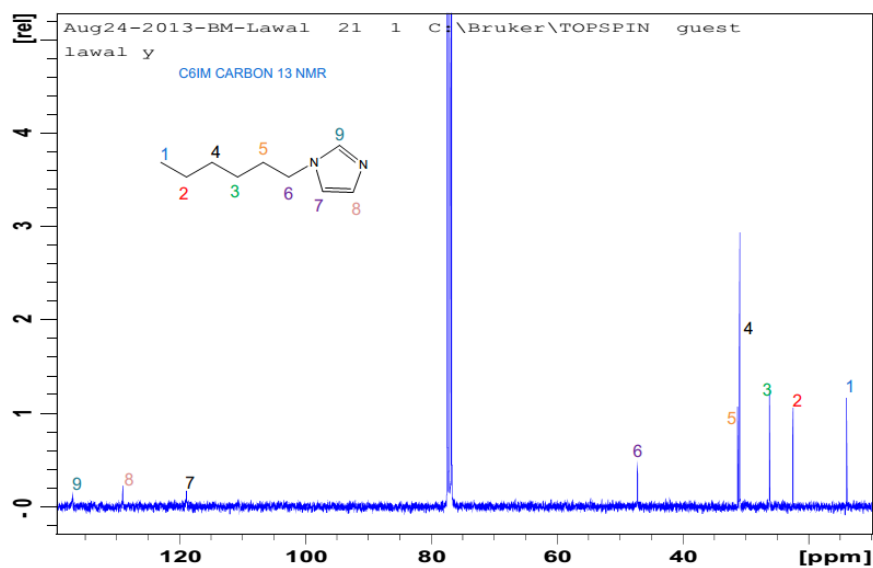
Appendix C 2.1 - Carbon NMR of 1-hexyl imidazole
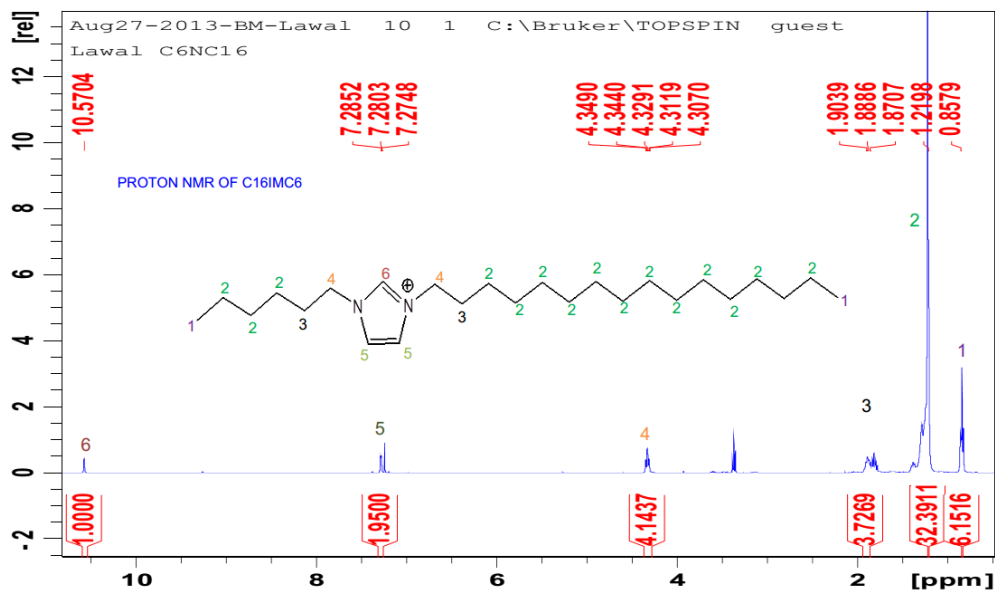
Appendix C 2.2 - Proton NMR of 1- hexyl, 3-decahexyl imidazolium
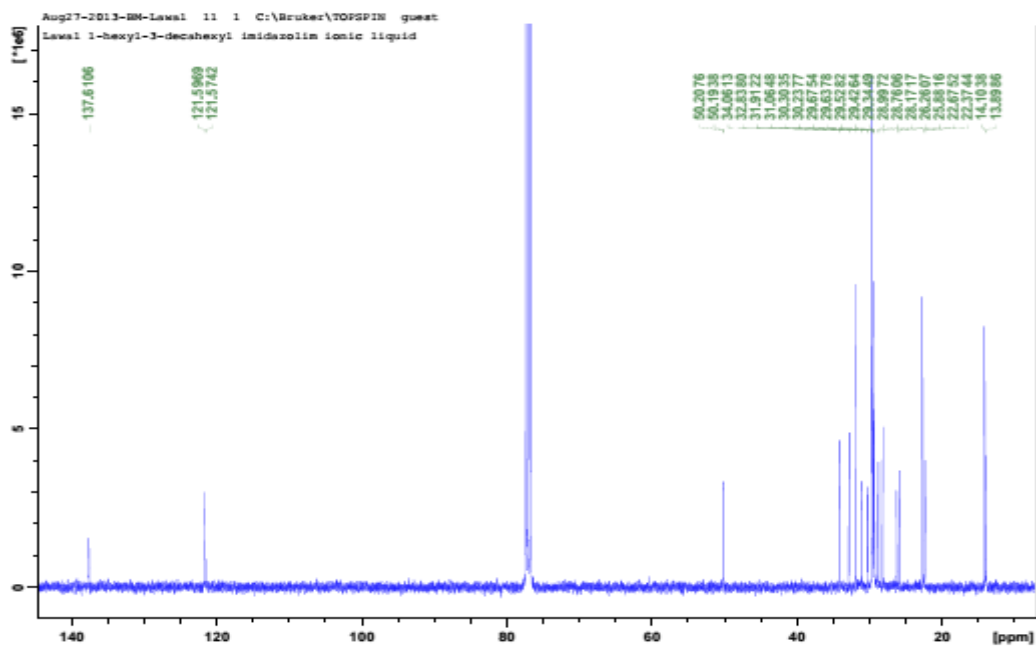
Appendix C 2.3 - Carbon NMR of 1- hexyl, 3-decahexyl imidazolium

Appendix D: FTIR of ionic liquid
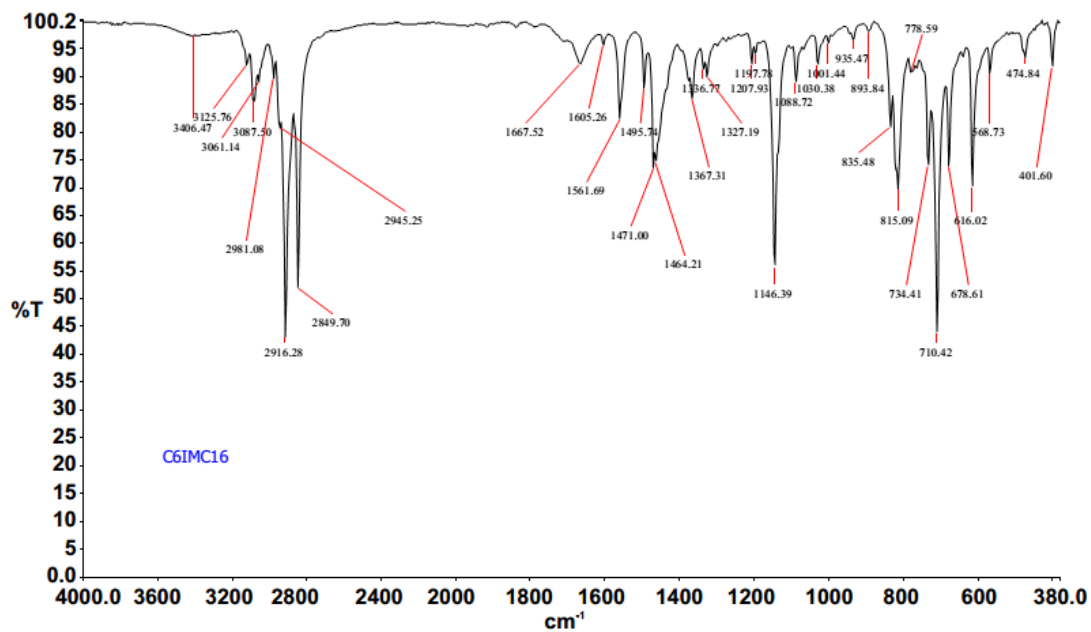
APPENDIX D 1.0 - FTIR of 1- hexyl, 3-decahexyl imidazolium

APPENDIX E: TGA

Appendix E: TGA-DSC of 1- methyl, 3-decahexyl imidazolium and MT-Na-IL
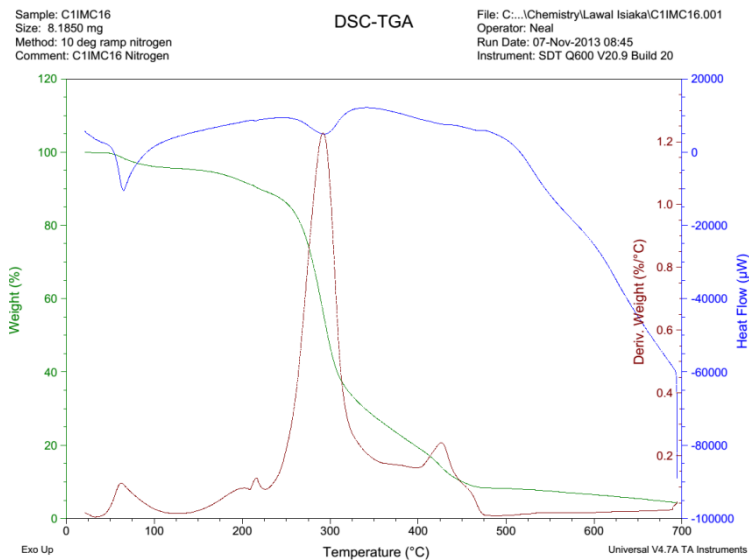

Appendix E 1.0 - TGA-DSC of 1- methyl, 3-decahexyl imidazolium
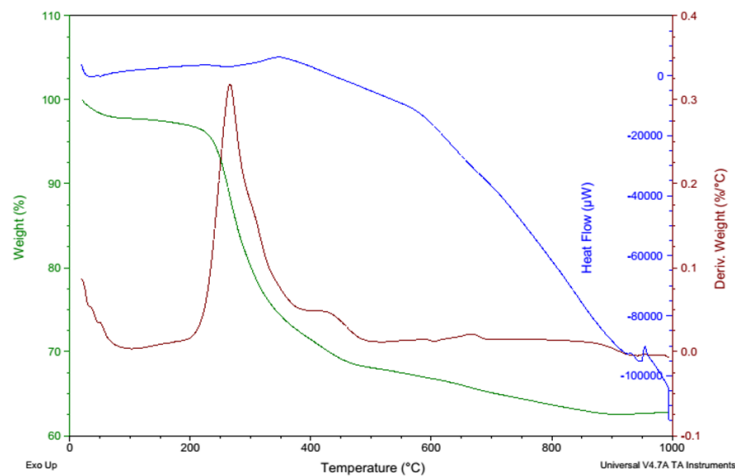
Appendix E 1.1 - TGA-DTA/DSC spectrum of MT-Na-IL

Appendix F 1.0 – Table showing the parameters for pseudo first order reaction of ILNS and ILAC on RB and CR

| Dyes	Conc. (mg g^{-1})	ILNS			ILAC		
		q_e,cal (mg g^{-1})	K_e (min^{-1})	R^2	q_e,cal (mg g^{-1})	K_e (min^{-1})	R^2
RB	200	8.80	-0.006	0.881	10.23	-0.214	0.258
	100	6.66	-0.003	0.215	25.14	-0.001	0.587
	50	7.92	-0.003	0.927	23.01	0.003	0.457
	20	3.41	0.037	0.884	12.03	0.213	0.547
CR	200	7.22	-0.004	0.868	21.36	-0.024	0.321
	100	5.23	-0.096	0.623	11.32	-0.002	0.582
	50	2.55	-0.002	0.002	8.23	-0.004	0.124
	20	1.99	-0.003	0.301	6.02	-0.201	0.597
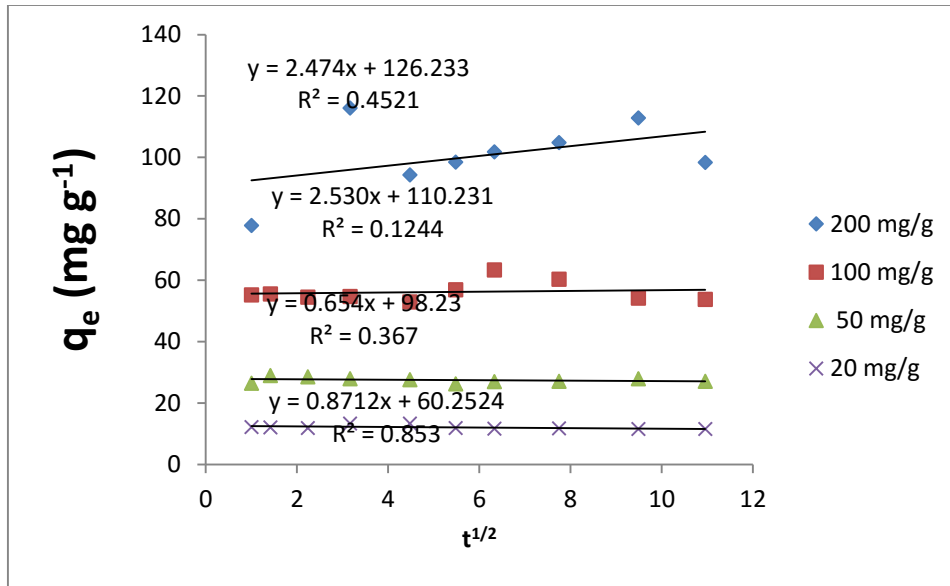
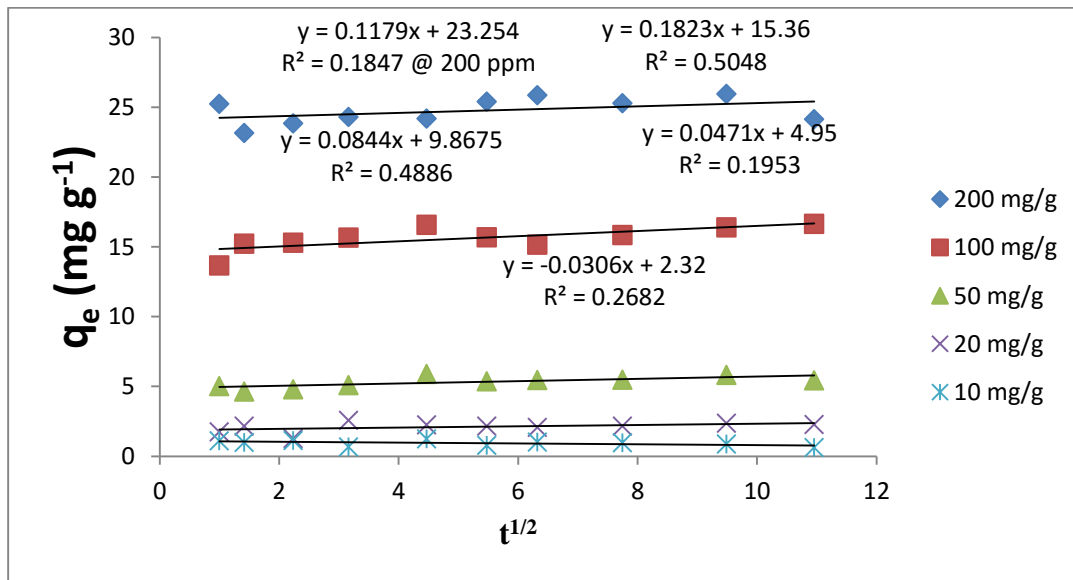Appendix F 1.1 - Intraparticle diffusion model for CR on ILAC
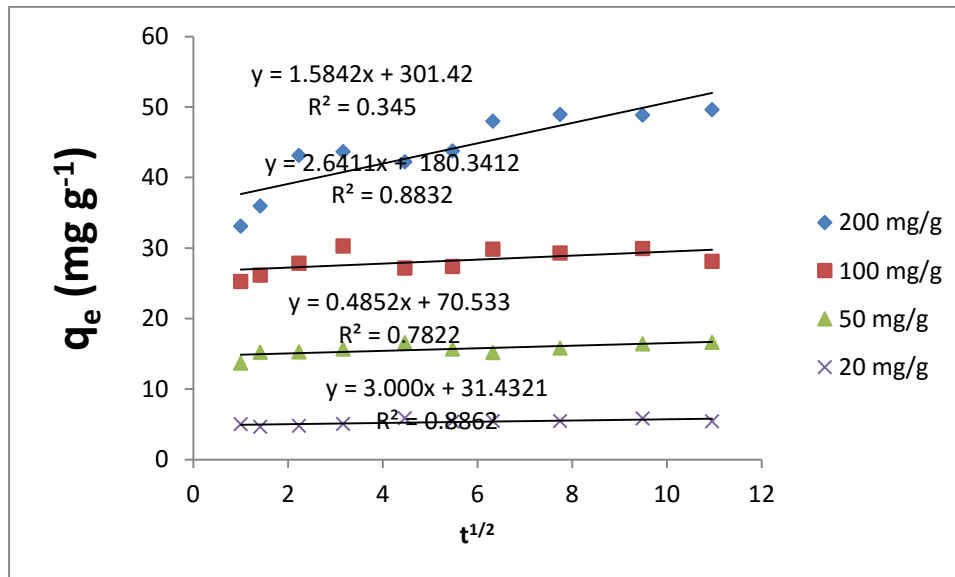
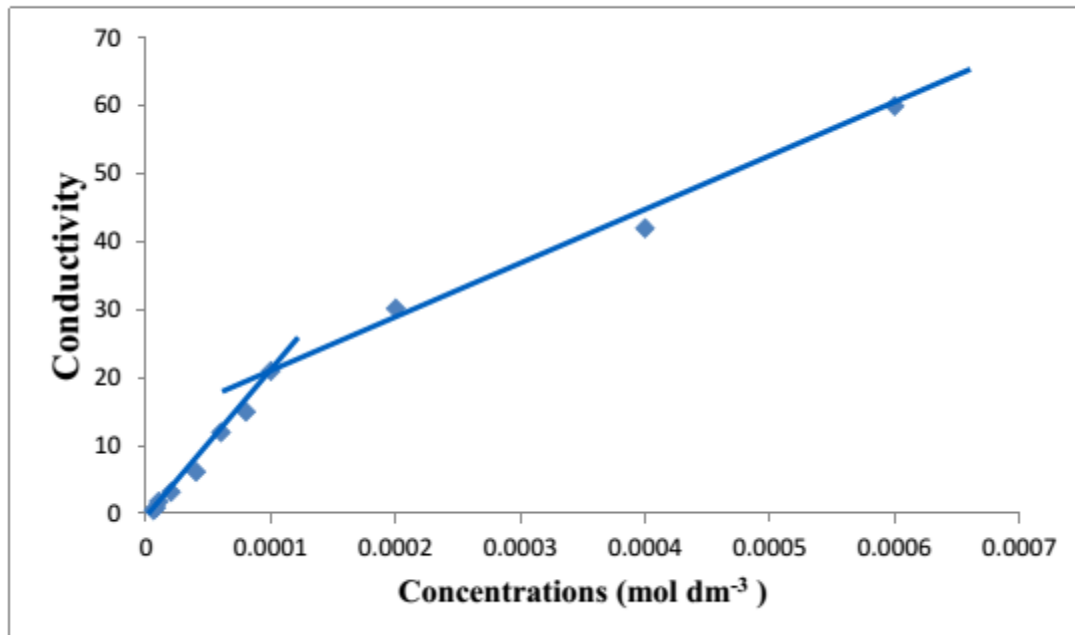Appendix F 1.2 - Intraparticle diffusion model for RB on ILAC

Appendix F 2
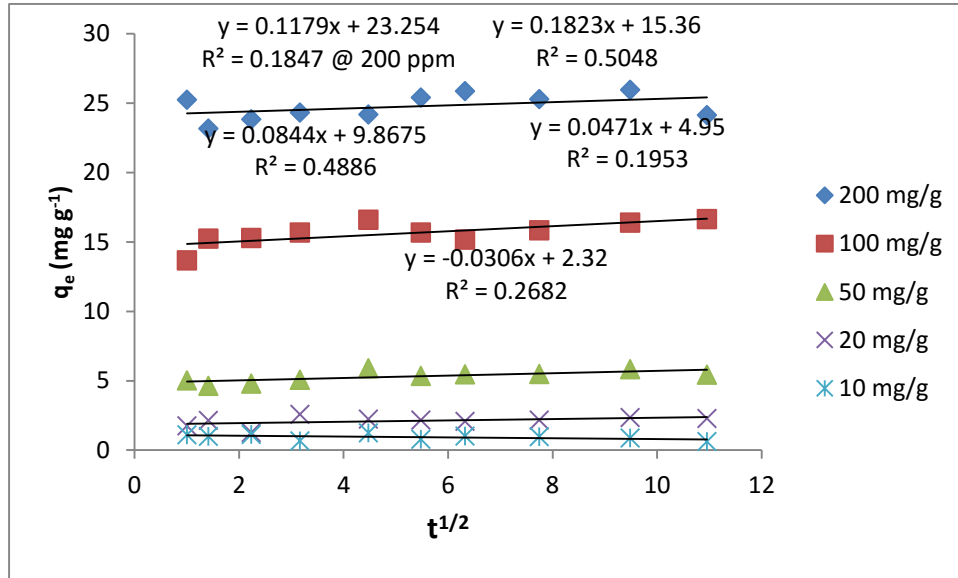
Appendix F 2.0 - Intraparticle diffusion plots of KP-IL on KET

Appendix F 2.1 - Intraparticle diffusion plots of KP-IL on AMP

Appendix F 2.2 - CMC